

/EVALUATION OF PROPOSED METHODS TO DETERMINE
FRACTURE PARAMETERS FOR CONCRETE IN BENDING/ *ms*

by

Sze-Ting Yap

B.S., Kansas State University, 1984

A MASTER'S THESIS

submitted in partial fulfillment of the
requirement for the degree of

MASTER OF SCIENCE

Department of Civil Engineering

Kansas State University

Manhattan, Kansas

1986

Approved:

Stuart E. Swartz
Major Professor

LD
2668
T4
1986
Y362
c. 2

TABLE OF CONTENTS

Al1202 971606

ACKNOWLEDGEMENTS	iii
LIST OF TABLES	iv
LIST OF FIGURES	vii
NOTATION	ix
CHAPTER 1 - INTRODUCTION	1
CHAPTER 2 - LITERATURE REVIEW	3
2.1 Proposed Methods	3
2.1.1 Proposed Methods for Beams Tested in Three-Point Bending	3
(a) RILEM Method	3
(b) Modified RILEM Method	4
(c) Direct Energy Method	4
(d) K _{IC} Methods	4
(i) Jenq/Shah Method	4
(ii) Go Method	5
(e) J _{IC} Method	5
(f) Bazant Size Effect Method	6
2.1.2 Proposed Method for Beams Tested in Four-Point Bending	6
2.2 Test Specimens Used at Kansas State University and Their Material Properties	7
2.2.1 Huang's Beams	8
2.2.2 Fartash's Beams	8
2.2.3 Go's Beams	9
2.2.4 Rood's Beams	9
2.3 Set Up and Testing Procedures	9
2.3.1 Compliance Measurement	10
2.3.2 Modified Compliance Measurement	11
2.3.3 Precracked Beams	11
2.3.4 Notched Beams with Teflon Insert or Sawcut	12
CHAPTER 3 - EXPERIMENTAL PROGRAM	39
3.1 Test Specimens	39
3.2 Set Up and Testing Procedure	40
CHAPTER 4 - EVALUATION OF METHODS	45
4.1 Notched Beams	45
4.1.1 Notched Beams Tested in Three-Point Bending	45
(a) RILEM Method	45
(b) Modified RILEM Method	46
(c) Direct Energy Method	46
(d) K _{IC} Methods	47
(i) Jenq/Shah Method	47
(ii) Go Method	47
(e) J _{IC} Method	47
(f) Bazant Size Effect Method	48
4.1.2 Notched Beams Tested in Four-Point Bending	48
4.2 Precracked Beams	49

TABLE OF CONTENTS (Continued)

4.2.1	Precracked Beams Tested in Three-Point Bending	.49
(a)	RILEM Method	.49
(b)	Modified RILEM Method	.49
(c)	Direct Energy Method	.49
(d)	K _{IC} Methods	.49
	(i) Jenq/Shah Method	.49
	(ii) Go Method	.50
(e)	J _{IC} Method	.50
(f)	Bazant Size Effect Method	.51
4.2.2	Precracked Beams Tested in Four-Point Bending	.51
CHAPTER 5	- CONCLUSIONS AND RECOMMENDATIONS	.52
APPENDIX I	- REFERENCES	.54
APPENDIX II	- TABLES AND FIGURES	.57
APPENDIX III	-P-LPD AND P-CMOD CURVES	.107

ACKNOWLEDGEMENTS

The writer wishes to thank Dr. Stuart E. Swartz, professor of Civil Engineering, for his assistance during research and preparation of this thesis.

Thanks are also extended to Dr. Robert Snell, Head, Department of Civil Engineering for his continual support during the entire duration of this research. Thanks also to Mr. Eric H. C. Siew, Mr. Randy Bernhardt, Mr. Ali Nikaeen, and Mr. Russell Gillespie for their encouragement and assistance during testing.

Finally special thanks and appreciation are extended to the writer's family for the valuable encouragement they provided during the course of graduate studies.

The work reported herein has been supported by the National Science Foundation on grants CEE-831736 and MSM-8317136. This support is greatly acknowledged.

LIST OF TABLES

Table 2.1	Huang's Mix Designs	13
Table 2.2	Fartash's Mix Designs	14
Table 2.3	Go's Mix Design	15
Table 2.4	Rood's Mix Designs	16
Table 2.5	Mix Design for Beams Tested in July 1985 and January 1986	17
Table II.1A	Notched Beams, Tested by Rood (12), RILEM Method (10), W = 4.00 in. (102 mm), B = 3.00 in. (76 mm), $E_c = 5.34 \times 10^6$ psi (36.8 GPa)	61
Table II.1B	Notched Beams, Tested July 1985, RILEM Method (10), W = 4.00 in. (102 mm), B = 3.00 in. (76 mm), $E_c = 5.02 \times 10^6$ psi (34.6 GPa)	62
Table II.1C	Notched Beams, Tested January 1986, RILEM Method (10), B = 3.00 in. (76 mm), $E_c = 6.60 \times 10^6$ psi (45.5 GPa)	63
Table II.2A	Notched Beams, Tested by Rood (12), Modified RILEM Method (14), W = 4.00 in. (102 mm), B = 3.00 in. (76 mm), $E_c = 5.34 \times 10^6$ psi (34.6 GPa)	64
Table II.2B	Notched Beams, Tested July 1985, Modified RILEM Method (14), W = 4.00 in. (102 mm), B = 3.00 in. (76 mm), $E_c = 5.02 \times 10^6$ psi (34.6 GPa)	65
Table II.2C	Notched Beams, Tested January 1986, Modified RILEM Method (14), B = 3.00 in. (76 mm), $E_c = 6.60 \times 10^6$ psi (45.5 GPa)	66
Table II.3A	Notched Beams, Tested by Rood (12), Direct Energy Method (4), W = 4.00 in. (102 mm), B = 3.00 in. (76 mm), $E_c = 5.34 \times 10^6$ psi (36.8 GPa)	67
Table II.4A	Notched Beams, Tested by Rood (12), Jenq/Shah Method (9), W = 4.00 in. (102 mm), B = 3.00 in. (76 mm), $E_c = 5.34 \times 10^6$ psi (36.8 GPa)	68
Table II.4B	Notched Beams, Tested July 1985, Jenq/Shah Method (9), W = 4.00 in. (102 mm), B = 3.00 in. (76 mm), $E_c = 5.02 \times 10^6$ psi (34.6 GPa)	69
Table II.4C	Notched Beams, Tested January 1986, Jenq/Shah Method (9), W = 8.00 in. (203 mm), B = 3.00 in. (76 mm), $E_c = 6.60 \times 10^6$ psi (45.5 GPa)	70
Table II.4D	Notched Beams, Tested by Go (4), Jenq/Shah Method (9), W = 4.00 in. (102 mm), B = 3.00 in. (76 mm), $E_c = 4.10 \times 10^6$ psi (28.2 GPa)	71
Table II.4E	Notched Beams, Tested by Fartash (11), Jenq/Shah Method (9), W = 4.00 in. (102 mm), B = 3.00 in. (76 mm), $E_c = 3.08 \times 10^6$ psi (21.1 GPa)	72
Table II.4F	Notched Beams, Tested by Fartash (11), Jenq/shah Method (9), W = 4.00 in. (102 mm), B = 3.00 in. (76 mm), $E_c = 3.30 \times 10^6$ psi (22.7 GPa)	73
Table II.5A	Notched Beams, Tested by Rood (12), Go Method (4), W = 4.00 in. (102 mm), B = 3.00 in. (76 mm), $E_c = 5.34 \times 10^6$ psi (36.8 GPa)	74

LIST OF TABLES (Continued)

Table II.5B Notched Beams, Tested by Go (4), Go Method (4), $W = 4.00$ in. (102 mm), $B = 3.00$ in. (76 mm), $E_C = 4.10 \times 10^6$ psi (28.2 GPa)75

Table II.5C Notched Beams, Tested by Fartash (11), Go Method (4), $W = 4.00$ in. (102 mm), $B = 3.00$ in. (76 mm), $E_C = 3.08 \times 10^6$ psi (21.1 GPa)76

Table II.5D Notched Beams, Tested by Fartash (11), Go Method (4), $W = 4.00$ in. (102 mm), $B = 3.00$ in. (76 mm), $E_C = 3.30 \times 10^6$ psi (22.7 GPa)77

Table II.6A Notched Beams, Tested by Fartash (11), K_{IC} Method (4, 8), $W = 4.00$ in. (102 mm), $B = 3.00$ in. (76 mm), $E_C = 4.63 \times 10^6$ psi (31.9 GPa)78

Table II.6B Notched Beams, Tested by Fartash (11), K_{IC} Method (4, 8), $W = 4.00$ in. (102 mm), $B = 3.00$ in. (76 mm), $E_C = 4.65 \times 10^6$ psi (32.0 GPa)79

Table II.7A Precracked Beams, Tested by Rood (12), RILEM Method (10), $W = 4.00$ in. (102 mm), $B = 3.00$ in. (76 mm), $E_C = 5.34 \times 10^6$ psi (36.8 GPa)80

Table II.8A Precracked Beams, Tested by Rood (12), Modified RILEM Method (10), $W = 4.00$ in. (102 mm), $B = 3.00$ in. (76 mm), $E_C = 5.34 \times 10^6$ psi (36.8 GPa)82

Table II.8B Precracked Beams, Tested by Go (4), Modified RILEM Method (10), $W = 4.00$ in. (102 mm), $B = 3.00$ in. (76 mm), $E_C = 4.10 \times 10^6$ psi (28.2 GPa)84

Table II.9A Precracked Beams, Tested by Rood (12), Direct Energy Method (4), $W = 4.00$ in. (102 mm), $B = 3.00$ in. (76 mm), $E_C = 5.34 \times 10^6$ psi (36.8 GPa)85

Table II.9B Precracked Beams, Tested by Go (4), Direct Energy Method (4), $W = 4.00$ in. (102 mm), $B = 3.00$ in. (76 mm), $E_C = 4.10 \times 10^6$ psi (28.2 GPa)86

Table II.10A Precracked Beams, Tested by Rood (12), Jenq/Shah Method (9), $W = 4.00$ in. (102 mm), $B = 3.00$ in. (76 mm), $E_C = 5.34 \times 10^6$ psi (36.8 GPa)87

Table II.10B Precracked Beams, Tested by Fartash (11), Jenq/Shah Method (9), $W = 4.00$ in. (102 mm), $B = 3.00$ in. (76 mm), $E_C = 3.08 \times 10^6$ psi (21.2 GPa)89

Table II.10C Precracked Beams, Tested by Fartash (11), Jenq/Shah Method (9), $W = 4.00$ in. (102 mm), $B = 3.00$ in. (76 mm), $E_C = 3.30 \times 10^6$ psi (22.7 GPa)90

Table II.10D Precracked Beams, Tested by Go (4), Jenq/Shah Method (9), $W = 4.00$ in. (102 mm), $B = 3.00$ in. (76 mm), $E_C = 4.10 \times 10^6$ psi (28.2 GPa)92

Table II.10E Precracked Beams, Tested by Huang (8), Jenq/Shah Method (9), $W = 4.00$ in. (102 mm), $B = 3.00$ in. (76 mm), $E_C = 3.21 \times 10^6$ psi (22.1 GPa) and $E_C = 4.93 \times 10^6$ psi (34.0 GPa)93

LIST OF TABLES (Continued)

Table II.10F	Precracked Beams, Tested by Huang (8), Jeng/Shah Method (9), $W = 8.00$ in. (203 mm), $B = 4.00$ in. (102 mm), $E_C = 3.41 \times 10^6$ psi (23.5 GPa) and $E_C = 5.05 \times 10^6$ psi (34.8 GPa)	94
Table II.11A	Precracked Beams, Tested by Rood (12), Go Method (4), $W = 4.00$ in. (102 mm), $B = 3.00$ in. (76 mm), $E_C = 5.34 \times 10^6$ psi (36.8 GPa)	96
Table II.11B	Precracked Beams, Tested by Fartash (11), Go Method (4), $W = 4.00$ in. (102 mm), $B = 3.00$ in. (76 mm), $E_C = 3.08 \times 10^6$ psi (21.2 GPa)	97
Table II.11C	Precracked Beams, Tested by Fartash (11), Go Method (4), $W = 4.00$ in. (102 mm), $B = 3.00$ in. (76 mm), $E_C = 3.08 \times 10^6$ psi (21.2 GPa)	98
Table II.11D	Precracked Beams, Tested by Go (4), Go Method (4), $W = 4.00$ in. (102 mm), $B = 3.00$ in. (76 mm), $E_C = 4.10 \times 10^6$ psi (28.2 GPa)	99
Table II.11E	Precracked Beams, Tested by Huang (8), Go Method (4), $W = 4.00$ in. (102 mm), $B = 3.00$ in. (76 mm), $E_C = 3.21 \times 10^6$ psi (22.1 GPa) and $E_C = 4.93 \times 10^6$ psi (34.0 GPa) ..	100
Table II.11F	Precracked Beams, Tested by Huang (8), Go Method (4), $W = 8.00$ in. (203 mm), $B = 4.00$ in. (102 mm), $E_C = 3.41 \times 10^6$ psi (23.5 GPa) and $E_C = 5.05 \times 10^6$ psi (22.1 GPa) ..	101
Table II.12A	Precracked Beams, Tested by Fartash (11), KIC Method (4, 8), $W = 4.00$ in. (102 mm), $B = 3.00$ in. (76 mm), $E_C = 4.63 \times 10^6$ psi (31.9 GPa)	102
Table II.12B	Precracked Beams, Tested by Fartash (11), KIC Method (4, 8), $W = 4.00$ in. (102 mm), $B = 3.00$ in. (76 mm), $E_C = 4.65 \times 10^6$ psi (32.0 GPa)	103
Table II.12C	Precracked Beams, Tested by Fartash (11), KIC Method (4, 8), $W = 4.00$ in. (102 mm), $B = 3.00$ in. (76 mm), $E_C = 4.42 \times 10^6$ psi (30.5 GPa)	104
Table II.12D	Precracked Beams, Tested by Huang (8), KIC Method (4, 8), $W = 4.00$ in. (102 mm), $B = 3.00$ in. (76 mm), $E_C = 3.39 \times 10^6$ psi (23.4 GPa) and $E_C = 5.14 \times 10^6$ psi (35.4 GPa)	105
Table II.12E	Precracked Beams, Tested by Huang (8), KIC Method (4, 8), $W = 8.00$ in. (102 mm), $B = 3.00$ in. (76 mm), $E_C = 3.63 \times 10^6$ psi (25.0 GPa) and $E_C = 5.12 \times 10^6$ psi (35.3 GPa)	106

LIST OF FIGURES

Fig. 2.1	Beam Dimensions, Three-Point Bending and Four-Point Bending	18
Fig. 2.2	P vs LPD, 4 in Deep Beam, Load Control, C-15, Tested by Rood (12)	19
Fig. 2.3	P vs CMDD, 4 in Deep Beam, Load Control, C-15, Tested by Rood (12)	19
Fig. 2.4	Compliance Variation for Notched Beams and Presumed Compliance Variation for Preracked Beams, Go (4)	20
Fig. 2.5	Compliance vs a/W, Large Beams, Mix No.1, Four-Point Bending, Huang (8)	21
Fig. 2.6	Compliance vs a/W, Small Beams, Mix No.1, Four-Point Bending, Huang (8)	22
Fig. 2.7	Compliance vs a/W, Large Beams, Mix No. 2, Four-Point Bending, Huang (8)	23
Fig. 2.8	Compliance vs a/W, Small Beams, Mix No. 2, Four-Point Bending, Huang (8)	24
Fig. 2.9	Compliance vs a/W, Large Beams, Mix No. 1, Three-Point Bending, Huang (8)	25
Fig. 2.10	Compliance vs a/W, Small Beams, Mix No. 1, Three-Point Bending, Huang (8)	26
Fig. 2.11	Compliance vs a/W, Large Beams, Mix No. 2, Three-Point Bending, Huang (8)	27
Fig. 2.12	Compliance vs a/W, Small Beams, Mix No. 2, Three-Point Bending, Huang (8)	28
Fig. 2.13	Compliance vs a/W, Group 1-A, Three-Point Bending, Fartash (11)	29
Fig. 2.14	Compliance vs a/W, Group 2-A, Three-Point Bending, Fartash (11)	30
Fig. 2.15	Compliance vs a/W, Group 3-A, Three-Point Bending, Fartash (11)	31
Fig. 2.16	Compliance vs a/W, Group 1-B, Four-Point Bending, Fartash (11)	32
Fig. 2.17	Compliance vs a/W, Group 2-B, Four-Point Bending, Fartash (11)	33
Fig. 2.18	Compliance vs a/W, Group 3-B, Four-Point Bending, Fartash (11)	34
Fig. 2.19	Compliance vs a/W, Teflon Beams, Three-Point Bending, Go (4)	35
Fig. 2.20	Compliance vs a/W, Precracked Beams, Three-Point Bending, Go (4)	36
Fig. 2.21	CMDD Compliance vs a/W, Three-Point Bending, Rood (12)	37
Fig. 2.22	LPD Compliance vs a/W, Three-Point Bending, Rood (12)	38
Fig. 3.1	f_c vs ϵ_c , Tested July 1985	42
Fig. 3.2	f_c vs ϵ_c , Tested January 1986	43
Fig. 3.3	Reverse Testing Configuration for Three-Point bending	44
Fig. II.1	J-Integral Method (4), Notched Beams, Rood (12), W = 4 in.	58

LIST OF FIGURES (Continued)

Fig. II.2	J-Integral Method (4), Notched Beams, Tested July 1985, W = 4 in.	58
Fig. II.3	Bazant Size Effect Method (1, 3), Notched Beams	59
Fig. II.4	J-Integral Method (4), Precracked Beams, Rood (12), W = 4 in.	59
Fig. II.5	J-Integral Method (4), Precracked Beams, Go (4), W = 4 in.	60

NOTATION

- a_0 - Initial Notch Depth
 a_i - Initial Crack Length
 a - Extended Crack Length
 a_e - Equivalent Elastic Crack Length
 B - Beam Width
 $CMOD$ - Crack Mouth Opening Displacement
 $\delta_0, \overline{\delta_0}$ - Vertical Displacement
 E_c - Young's Modulus
 f'_c - Concrete Strength
 $G_F, \overline{G_F}$ - Fracture Energy
 $G_{IC}, \overline{G_{IC}}$ - Critical Energy Release Rate
 J_{IC} - Critical J-Integral Value
 K_{IC} - Critical Stress Intensity Factor
 K_{IC}^G - Critical Stress Intensity Factor Using Go Method
 K_{IC}^S - Critical Stress Intensity Factor Using Jenq/Shah Method
 L - Total Beam Length
 LPD - Load Point Displacement
 M - Moment
 P_m - Maximum Load
 S - Supported Beam Span
 U, W_0 - Energy Consumption
 W - Beam Depth
 W/C - Water/Cement Ratio

CHAPTER 1

INTRODUCTION

Over the years, much effort has been devoted to the development of the experimental procedures, methods, techniques and analysis for the determination of fracture parameters for concrete - critical stress intensity factor (K_{IC}), fracture energy (G_F), critical energy release rate (G_{IC}) and critical J-integral (J_{IC}), using bending specimens of various sizes. Therefore, it is the time to propose standardized testing methods.

The group RILEM TC50-FMC, Fracture Mechanics of Concrete (10), has done the most work in the measurement of fracture energy - G_F , using notched beams in three-point bending.

Jenq and Shah (9) proposed a two-parameter fracture model to obtain the K_{IC} of bending specimens by estimating an equivalent elastic crack length. This concept is similar to Go's (4) approach, except that the extended crack length of the bending specimen is measured by a compliance calibration technique (4) and initial crack length is measured by a dye penetration technique (4).

Bazant (2, 3) has proposed an R-curve analysis method for the determination of fracture energy of different beam sizes. This method does not require the measurement of the specimen's crack length or the unloading compliance. The only test parameter required is the maximum load value.

In addition, the Modified RILEM Method (14) and Direct Energy

Method (4) were developed by Swartz and Go respectively. These two methods are very similar to the RILEM Method (10). However, the way of measuring energy consumption of the fractured specimen in the Modified RILEM Method (14) is unique and surface roughness is taken into account by the Direct Energy Method (4). The Modified RILEM Method is developed as an alternative for the RILEM Method (10).

A detailed description of these methods is found in Chapter 2.

An extensive evaluation of the validity of all these methods was done based on past data obtained from Huang (8), Fartash (11), Go (4), Rood (12) and recent data from beams tested in July 1985 and January 1986. The results (Appendix II) once again showed that concrete is a notch sensitive material, that is, it behaves differently when notched with teflon or a sawcut, then it does when it is orecracked. As a result, scatter and inconsistent results were obtained based on notched beams (except when the Bazant Size Effect Method (1, 3) was applied) as the results reported by Hillerborg in References 5, 6 and 7. However, consistent results (Appendix II) for K_{Ic} , G_F , G_{Ic} and J_{Ic} were obtained when precracked beams were used and crack extension was considered. The conclusions and recommendations are found in Chapter 5.

CHAPTER 2

LITERATURE REVIEW

Many methods have been proposed for the determination of fracture parameters of concrete using bending specimen in the recent years. A number of these proposed methods are presented in this chapter.

2.1 Proposed Methods

The methods described here use a beam bending specimen of the type shown in Fig. 2.1.

2.1.1 Proposed Methods for Beams Tested in Three-Point Bending

(a) RILEM Method (10)

Use of this method determines the fracture energy per unit surface area of real crack - G_f .

$$G_f = (W_0 \pm mg \delta_0) / (B (W - a_0)) \quad (1)$$

The energy consumption, W_0 , of the fracture specimen is represented by the total area ($A_1 + A_2$) under the full load-point-displacement (P-LPD) curve (Fig. 2.2). The weight of those portions of the bending specimen between the supports must be added or subtracted as in equation (1) depending on the load direction. The maximum vertical displacement at failure load δ_0 is obtained from the P-LPD curve. Initial notched length, a_0/W , or initial precracked length, a_i/W , should be applied for the fracture energy calculation.

(b) Modified RILEM Method (14)

As proposed by Swartz (14), the energy consumption U , of the bending specimen should be measured up to the point of instability from the P-LPD curve (Fig. 2.2), e.g. A1.

$$\overline{G_F} = (U \pm mg \overline{\delta_0}) / (B (W - a_0)) \quad (2)$$

Therefore, the vertical displacement should be taken at the point of instability. The point of instability is defined as the point where the maximum load begins to drop off on the P-LPD curve.

(c) Direct Energy Method (4)

Go (4) proposed that the fracture energy can also be calculated from the area under the P-LPD curve (area from point of origin up to the point of instability, Fig. 2.2) divided by the remaining uncracked area of the beam.

$$\overline{G_{IC}} = (U \pm mg \overline{\delta_0}) / (1.15 B (W - a)) \quad (3)$$

This method considered the effect of surface roughness on the crack front which is equal to 1.15 (4). In this approach, a/W can be determined from the initial crack length a_i or the extended crack length a .

(d) K_{IC} Methods

(i) Jenq/Shah Method (9)

In order to obtain the critical stress intensity factor, K_{IC} , a/W must be known. In this method, a/W can be estimated using $CMOD_e$ (Fig. 2.3) and LEFM, developed by Jenq and Shah.

$$CMOD_e = CMOD_{e1} + CMOD_{e2} \quad (4)$$

$$CMOD_e = (24 P A) / (B E_C) Z \quad (5)$$

$$Z = 0.76 - 2.28 A + 3.87 A^2 - 2.04 A^3 + 0.66 / (1 - A)^2$$

$$A = a/W = a_e/W$$

$CMOD_e$ is the equivalent elastic value of the crack-mouth-opening displacement (CMOD) associated with instability. However, in the determination of $CMOD_e$, in this report $CMOD_{e2}$ is neglected due to insufficient data. After a/W or a_e/W is obtained, $K_{IC} = K^S_{IC}$ and G_{IC} can be calculated using Go's (4) equations, see equations 6 and 7.

(ii) Go Method (4)

Using LEFM, K_{IC} is determined based on an extended crack length which is obtained by the compliance calibration technique.

$$K^G_{IC} = M / (B W^{1.5}) A \quad (6)$$

For $S/W = 3.75$,

$$A = -.065 Z^2 - 3.483 Z - .120 + 5.706 Z^{-1} + .166 Z^{-2}$$

$$Z = (1 - a/W)$$

Other expressions for different S/W are given in Reference 4.

$$G_{IC} = K_{IC}^2 / E_c \quad (7)$$

The moment is associated with the critical load, P_m , e.g.

$M = (P_m L) / 4$. The Poisson ratio is omitted from equation 7, to simplify the calculation.

(e) J_{IC} Method (4)

The J-integral concept was proposed by Go (4) for the calculation of J_{IC} for concrete.

$$J_{IC} = - (dU / d(a/W)) / (1.15 B W) \quad (8)$$

The slope, $dU / d(a/W)$, is obtained by plotting U versus a/W for initial (a_0/W for notched beam and a_i/W for precracked beam) or extended crack length (a/W). According to this approach, the slope of each data set plotted should be equal, see Appendix II, Figs. 3, 4 and 5.

(f) Bazant Size Effect Method (1, 3)

This method determines the fracture energy of beams with various depths.

$$GF = g(\alpha_0) / (E_c d (B W / P_0)^2 / d(W)) \quad (9)$$

$$P_0 = P \pm 1/2 mg$$

$$g(\alpha_0) = (S / W)^2 \pi \alpha_0 (1.5 F(\alpha_0))^2$$

For $S/W = 3.75$,

$$F(\alpha_0) = 1.089 - 1.746 \alpha_0 + 8.231 \alpha_0^2 - 14.22 \alpha_0^3 + 14.59 \alpha_0^4$$

$$\alpha_0 = a/W$$

Other functions $F(\alpha_0)$ are given in Reference 3.

For this approach, the only required data for the fracture energy calculation is the maximum load P_m . The beam self weight must also be taken into consideration. Notice that the negative sign is introduced into the calculation of the total load, P_0 , if the specimen is set up in a reverse configuration during testing. The slope is obtained from the best straight line fit through the three points from the plot of $(B W / P_0)^2$ versus W . In order to use this method effectively, it is necessary to test at least three beams, or three groups of beams, with various spans and depths, and the S/W ratio and the beam width B must be kept constant. The fracture energy obtained for each different set of sizes of beams should be equal.

2.1.2 Proposed Method for Beams Tested in Four-Point Bending

This method uses a combination of approaches by Huang (8) and Go (4), K_{Ic} Method. The procedure is as follows:

1. The compliance value must be determined first by taking the extended inverse slope of the straight line portion of the P-CMOD curve

(Fig. 2.3).

2. The extended a/W ratio of the cracked beam can be then determined from compliance versus a/W curves. If the compliance curve is obtained from sawcut beams, the a/W estimated is greater than the average interior a/W revealed by dye. Therefore, the a/W obtained by the sawcut beams needs to be modified by a correlation between a/W from the dye technique and a/W from compliance developed by Go (4) - equation (10), Fig. 2.4. In this report, only Huang's (8) and Fartash's (11) a/W were calculated using equation (10) because both of their compliance curves were obtained from sawcut beams.

$$(a/W)_{\text{dye}} = (a/W)_{\text{compliance}} - 0.14 \quad (10)$$

3. The K_{IC} value for each a/W ratio and load P_m can be determined by the finite element computer program developed by Huang (8).

4. The value of G_{IC} can be calculated using equation (7).

2.2 Test Specimens Used at Kansas State University and Their Material Properties

Two sizes of beams were used for the determination of the fracture parameters by the investigators at Kansas State University, Huang (8), Fartash (11), Go (4) and Rood (12). These two sizes of beams were constructed to the following dimensions (Fig. 2.1):

Group 1A: $L = 16$ in (406 mm)

$S = 15$ in (381 mm)

$W = 4$ in (102 mm)

$B = 3$ in (76 mm)

$S/W = 3.75$

Group 2A: $L = 25$ in (635 mm)
 $S = 24$ in (610 mm)
 $W = 8$ in (203 mm)
 $B = 4$ in (102 mm)
 $S/W = 3.125$

Fig. 2.3 shows typical beam dimensions.

2.2.1 Huang's Beams (8)

Huang (8) had two sizes of beams with two mix designs (Table 2.1). These two sizes of beams fall in the categories of group 1A and group 2A. Huang (8) called beams from group 1A as small beams and beams from group 2A as large beams. They were divided into two series of testing; beams with numbers S1S3, S2F3, L1S3 and L2F3 were tested in three-point bending (Fig. 2.1); beams with numbers S1S4, S2F4, L1S4 and L2S4 were tested in four-point bending (Fig. 2.1).

The primary difference between Huang's (8) two mix designs was the W/C ratio. Mix design number one (Table 2.1) had W/C of 0.78, average concrete strength of 3400 psi (23.1 MPa) and modulus of elasticity of 3.30×10^6 psi (22.7 GPa). The mix design number two had W/C of 0.50, average concrete strength of 7800 psi (53.8 MPa) and modulus of elasticity of 5.04×10^6 psi (34.7 GPa).

2.2.2 Fartash's Beams (11)

Fartash (11) had only one group of beams, group 1A, with two mix designs (Table 2.2). The two mix designs of Fartash (11) followed Huang's (8) mix designs very closely. The mix design A (Table 2.2) with W/C of 0.78 had an average concrete strength of 3200 psi (22.0 MPa) and

modulus of elasticity of 3.23×10^6 psi (22.2 MPa). The mix design B (Table 2.2) with W/C of 0.5 had a higher concrete strength as expected. The average strength was 6430 psi (44.3 MPa) and modulus of elasticity was 4.57×10^6 psi (31.5 GPa). Beams with mix design A were tested in three-point bending and beams with mix design B were tested in four-point bending.

2.2.3 Go's Beams (4)

Go (4) had only one mix design (Table 2.3) with W/C of 0.5 and one size of beams, group 1A. All these beams were tested in three-point bending. The average concrete strength was 5170 psi (35.6 MPa) and modulus of elasticity was 4.10×10^6 psi (28.2 GPa).

2.2.4 Rood's Beams (12)

Rood had only one size of beams, group 1A and one mix design (Table 2.4) with W/C of 0.5. The mix design followed Go's (4) mix design very closely. The average concrete strength was 8100 psi (55.8 MPa) and modulus of elasticity was 5.34×10^6 psi (35.8 GPa).

2.3 Set Up and Testing Procedures

All the testing that was performed by Huang (8), Fartash (11), Go (4) and Rood (12) at Kansas State University, was done using one set up (Fig. 2.1). For this set up the initial notch of the beam was on the bottom side of the specimen with one (three-point bending) or two (four-point bending) concentrated load(s) applied to the top of the specimen by an electro-hydraulic materials testing machine (MTS). During loading of the specimen, simultaneous traces of P-LPD and P-CMOD

were obtained. However, only Rood (12) collected all the P-LPD and P-CMOD traces of each beam. For Huang (8), Fartash (11) and Go (4), only P-CMOD or P-LPD was recorded. Huang (8) and Fartash (11) did not obtain P-LPD curves because of inadequate facilities available during testing.

Complete details of the various test setups and testing procedures used are contained in References 4, 8, 11, 12. In the following, this information is summarized briefly.

2.3.1 Compliance Measurement (8, 11)

Huang (8) and Fartash (11) did the compliance measurement in the following way:

Each beam was initially notched at mid-span with a sawcut to a desired crack length. No precracking of the notched beams was performed. The load was maintained low enough to ascertain that the crack did not begin at the end of the notch. The load was then applied (three-point bending or four-point bending) and a P-CMOD slope was obtained for each notch length. In order to obtain an average value of the compliance of each corresponding a_0/W , three consecutive plots were obtained. Then a curve of compliance versus a_0/W was plotted. The compliance value is the inverse slope of the straight portion of the P-CMOD curve. The compliance curves of Huang's (8) and Fartash (11) beams tested in four and three-point bending are shown in Figs. 2.5, 2.6, 2.7, 2.8, 2.9, 2.10, 2.11, 2.12, 2.13, 2.14, 2.15, 2.16, 2.17 and 2.18. Later, Go (4) discovered that using sawcut beams for compliance measurement somehow produced greater crack lengths than crack lengths revealed by dye. As a result, a modification of compliance measurement

was developed.

2.3.2 Modified Compliance Measurement (4, 12)

Go (4) and Rood (12) both did their compliance measurements using the following method. The procedure for determining the modified compliance value is almost the same as the compliance measurement mentioned in section 2.3.1, except that a dye penetration technique and precracking were applied. The dye was inserted into the crack after the last precracking load was applied. In order to assure the dye would penetrate to the tip of the crack, load recycling was used. Then the specimen was loaded to failure. The actual average crack depth was determined by finding the cracked surface area of the beam penetrated by the dye and dividing it by the width of the beam. The crack depth found by this method corresponds to the compliance measured from the initial slope of the P - $CMOD$ or P - LPD curve. This data provides one point on the compliance curve. The compliance curves for Go's (4) and Rood's (12) beams are presented in Figs. 2.19, 2.20, 2.21 and 2.22.

2.3.3 Precracked Beams (4, 8, 11, 12)

Each precracked beam was initially notched at mid-span similarly to the specimens prepared for compliance measurement. The starter notch was around 0.4 in. (10.2 mm) or smaller. The desired crack length of the specimen was obtained by loading the beam in the MTS machine until a compliance value corresponding to that of the compliance curve was found. Following precracking the specimen was then loaded to failure and P - LPD , P - $CMOD$ traces obtained.

2.3.4 Notched Beams with Teflon Insert or Sawcut (4, 11, 12)

Each specimen was previously notched to a desired crack depth by sawcut or insert and then loaded to failure under load control. These beams were tested without any precracking and dye insertion.

During the precracking and load to failure processes, P-LPD and P-CMOD traces were obtained, Figs. 2.2 and 2.3 are typical.

Table 2.1 Huang's Mix Designs

	<u>Mix No. 1</u>	<u>Mix No. 2</u>
Water/Cement	0.78	0.50
Cement Type	I	I
% Sand (Wt.)	31	31
Sand Dry Rodded Unit Wt.	109 pcf (1750 kg/m ³)	106 pcf (1700 kg/m ³)
S. G. Sand	2.49	2.49
Sand Moisture Content	0.5%	0.5%
Sand Finess Modulus	3.35	3.35
% Coarse Aggregate (Wt.)	45	45
Aggregate Dry Rodded Unit Wt.	94.5 pcf (1510 kg/m ³)	94.5 pcf (1510 kg/m ³)
S. G. Aggregate	2.50	2.50
Max. Size Aggregat	0.5 in (12.7 mm)	0.5 in (12.7 mm)
Aggregate Moisture Content	0.3%	0.3%
Aggregate Fineness Modulus	6.41	6.41
Sand/Aggregate	0.69	0.69
Air Content	2.8%	3.2%
Slump	7 in (178 mm)	1/8 in (3.18 mm)
Unit Wt. of Concrete	141.8 pcf (2270 kg/m ³)	148.4 pcf (2380 kg/m ³)
Water Cure	7 days	7 days
Air Cure Start	8 days (a) 23 days (b)	22 days (a) 51 days (b)
Air Cure Finish	16 days (a) 31 days (b)	50 days (a) 70 days (b)

Notes: (a) Three-point bending specimen
(b) Four-point bending specimen

Table 2.2 Fartash's Mix Designs

	<u>Mix A</u>	<u>Mix B</u>
Water/Cement	0.78	0.50
Cement Type	I	I
% Sand (Wt.)	31	31
Sand Dry Rodded Unit Wt.	106 pcf (1700 kg/m ³)	109 pcf (1750 kg/m ³)
S. G. Sand	2.62	2.62
Sand Moisture Content	0.50%	0.50%
Sand finess Modulus	3.35	3.35
% Coarse Aggregate (Wt.)	45	45
Aggregate Dry Rodded Rodded Unit Wt.	94.5 pcf (1510 kg/m ³)	94.5 pcf (1510 kg/m ³)
S. G. Aggregate	2.59	2.59
Max. Size Aggregate	0.5 in (12.7 mm)	0.5 in (12.7 mm)
Aggregate Moisture Content	0.3%	0.3%
Aggregate Fineness Modulus	6.41	6.41
Sand/Aggregate	0.69	0.69
Air Content	2.8%	3.2%
Slump	7 in (178 mm)	1/8 in (1.18 mm)
Unit Wt. of Concrete	141.8 pcf (2270 kg/m ³)	148.4 pcf (2380 kg/m ³)

Table 2.3 Go's Mix Design

Water/Cement	0.50
Cement Type	I
% Sand (Wt.)	31
% Aggregate by weight	45
S. G. Sand	2.49
S. G. Aggregate	2.50
Weight of Water*	9.31 lb (149 kg)
Weight of Cement*	18.6 lb (298 kg)
Weight of Sand*	46.0 (727 kg)
Weight of Aggregate*	66.8 (1070 kg)
Max. Size Aggregate	0.5 in (12.7 mm)
Unit Weight of Concrete.*	144 lb (2305 kg/m ³)
Curing Time	20 Days
Ultimate Strength	5200 psi (35.9 Mpa)

Note: * Proportions are for 1 ft³ (m³) of mix volume.

Table 2.4 Rood's Mix Designs

	<u>Batch 1</u>	<u>Batch 2</u>
Water/Cement	0.50	0.50
Cement Type	I	I
S. G. Sand	2.65	2.65
S. G. Aggregate	2.56	2.56
% Sand by Weight	32.7%	32.7%
% Aggregate by Weight	47.5%	47.5%
% Cement by Weight	13.2%	13.2%
% Water by Weight	6.62%	6.62%
Unit Weight of Concrete	149.7 pcf (2396 kg/m ³)	149.7 pcf (2396 kg/m ³)
Curing Time	145 days	138 days
Compressive strength	7950 psi (54.8 MPa)	8130 psi (56.0 MPa)
Tensile Strength	601 psi (4.14 MPa)	665 psi (4.58 MPa)
Superplasticizer	400 ml	300 ml
Slump	7.25 in (184 mm)	7.00 in (178 mm)
Sand Fineness Modulus	2.91	2.91
Maximum Aggregate Size	0.75 in (19.1 mm)	0.75 in (19.1 mm)

Table 2.5 Mix Design for Beams Tested in July 1985 and January 1986

Water/Cement	0.50
Cement Type	I
S. G. Sand	2.65
S. G. Aggregate	2.56
S. G. Cement	3.15
% Sand by Weight	32.64% (47.94 lb/ft ³)
% Aggregate by Weight	47.42% (69.65 lb/ft ³)
% Cement by Weight	13.22% (19.42 lb/ft ³)
% Water by Weight	6.03% (8.85 lb/ft ³)
% Super Plasticizer by Weight	0.70% (1.03 lb/ft ³)
Unit Weight of Concrete	146.89 pcf (2351 kg/m ³)
Curing Time	118 days
Slump	4.00 in (102 mm)
Sand Fineness Modulus	2.91
Maximum Aggregate Size	0.75 in (19.1 mm)

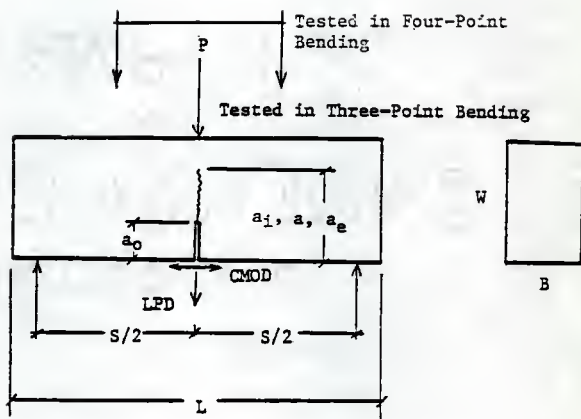


Fig. 2.1 Beam Dimensions, Three-Point Bending and Four-Point Bending

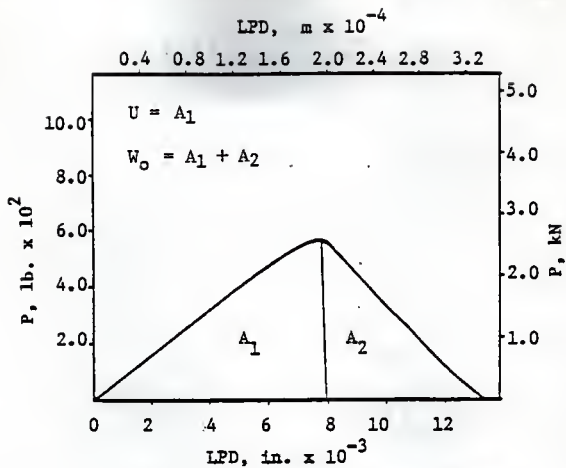


Fig. 2.2 P vs LPD, 4 in Deep Beam, Load Control, C-15, Tested by Rood (12)

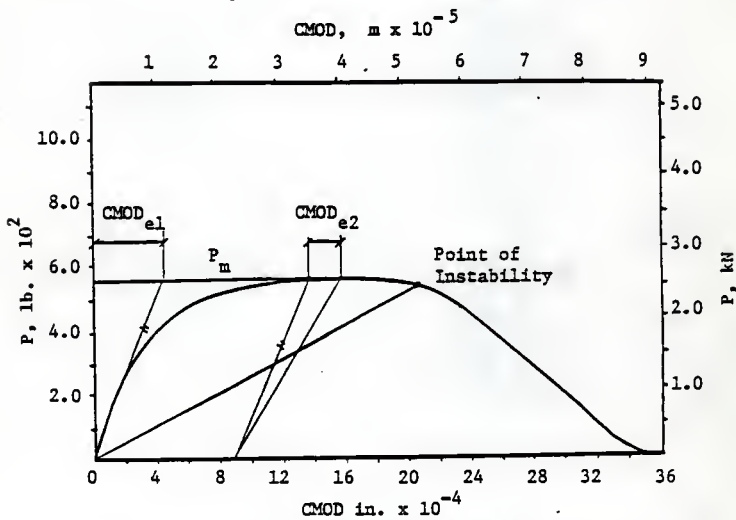


Fig. 2.3 P vs CMOD, 4 in Deep Beam, Load Control, C-15, Tested by Rood (12)

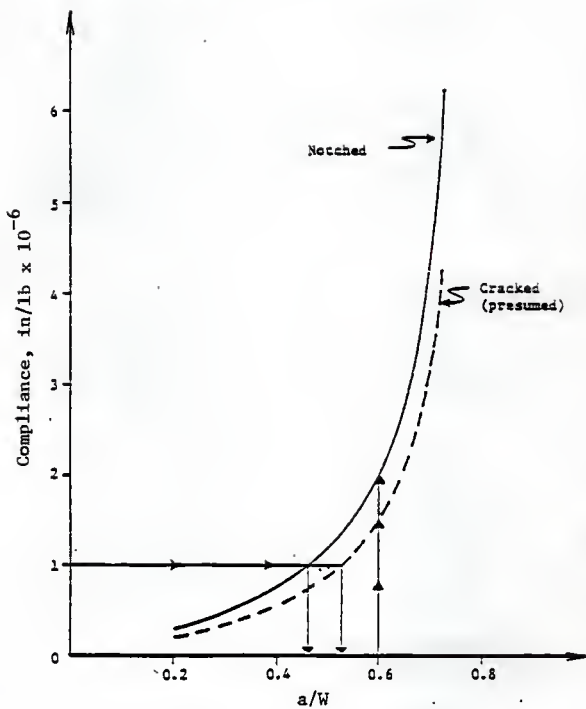


Fig. 2.4 Compliance Variation for Notched Beams and Presumed Compliance Variation for Pre-cracked Beams, Go (4)

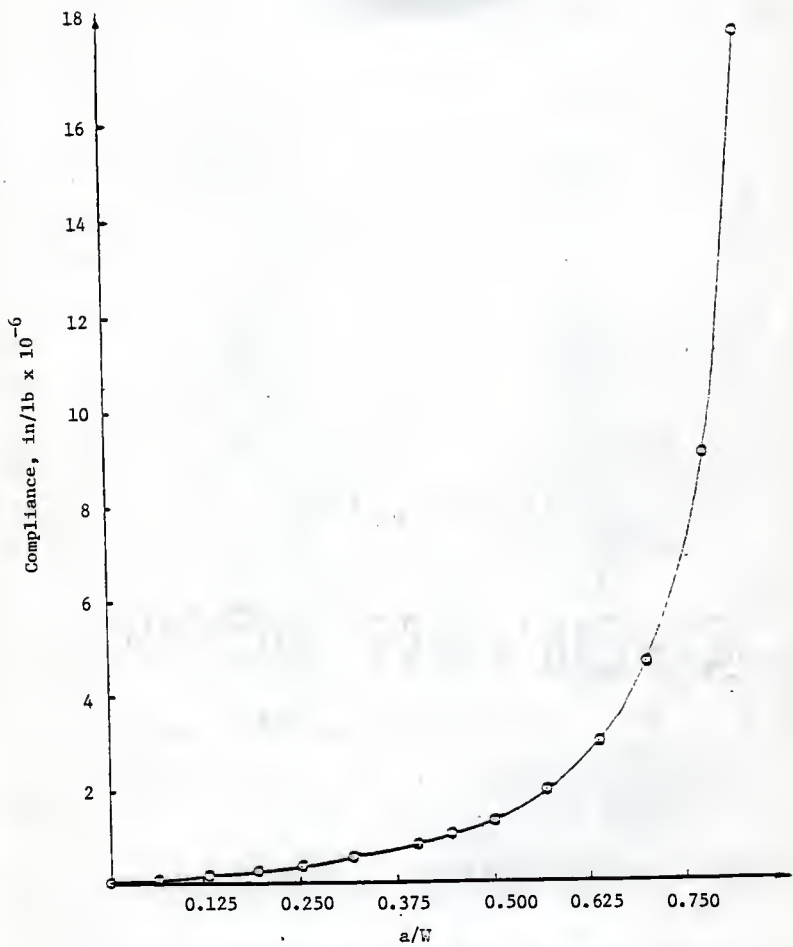


Fig. 2.5 Compliance vs a/W, Large Beams, Mix No. 1, Four-Point Bending, Huang (8)

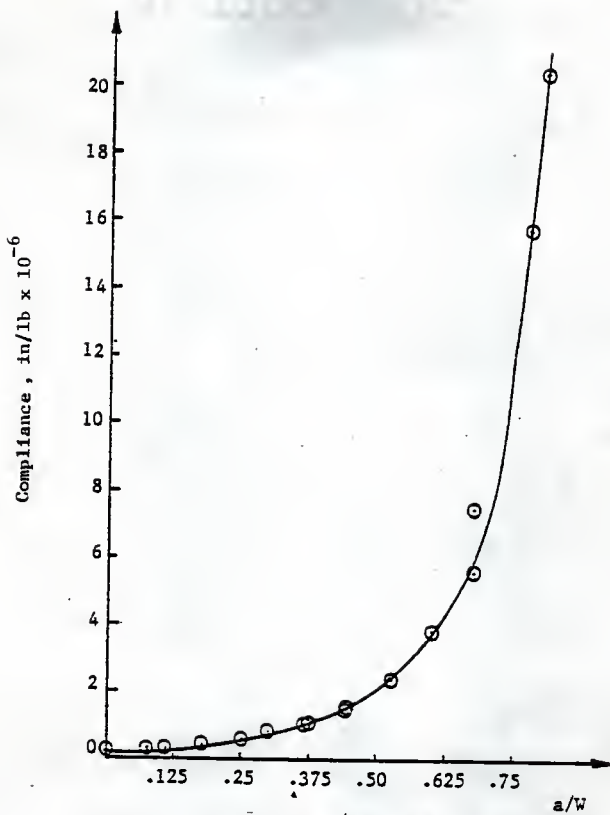


Fig. 2.6 Compliance vs a/W , Small Beams, Mix No.1, Four-Point Bending, Huang (8)

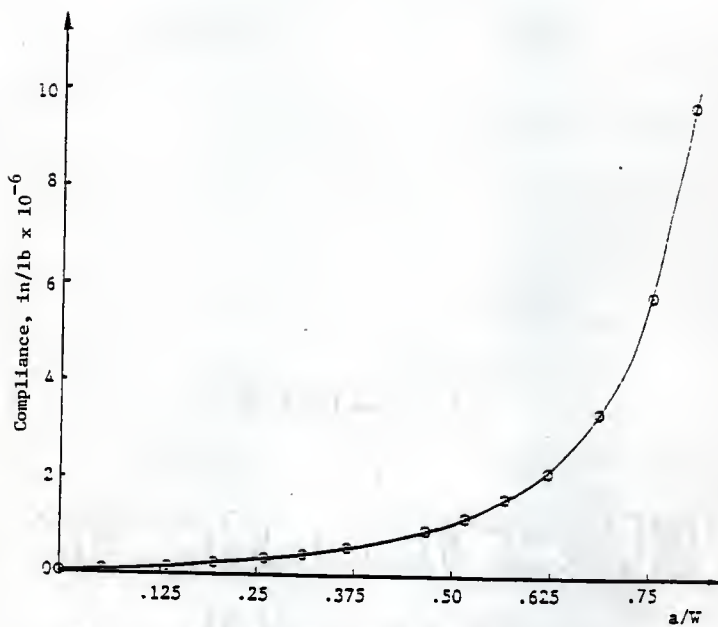


Fig. 2.7 Compliance vs a/W , Large Beams, Mix No. 2, Four-Point Bending, Huang (8)

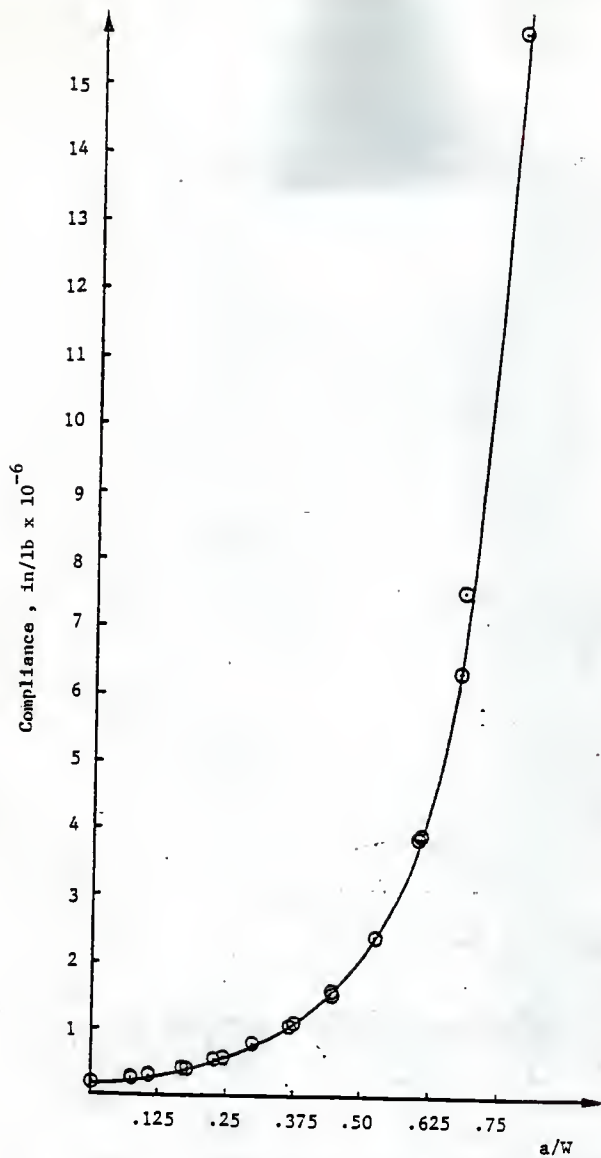


Fig. 2.8 Compliance vs a/W , Small Beams, Mix No. 2, Four-Point Bending, Huang (8)

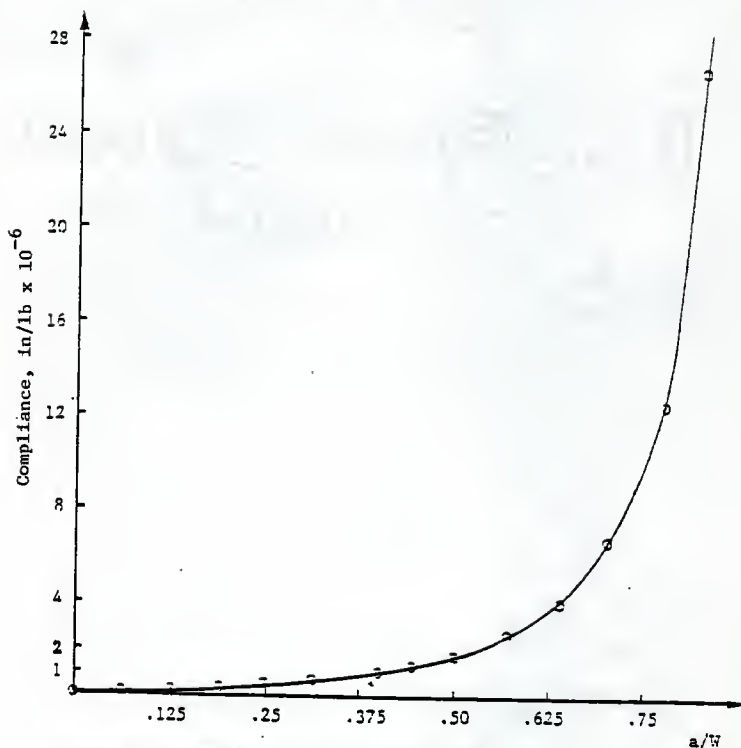


Fig- 2.9 Compliance vs a/W , Large Beams, Mix. No. 1, Three-Point Bending, Huang (8)

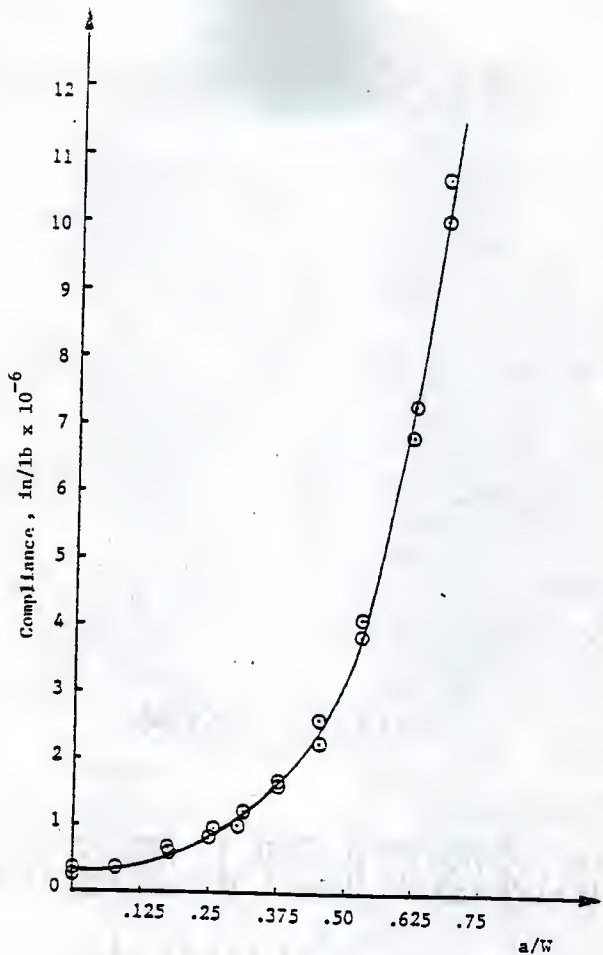


Fig. 2.10 Compliance vs a/W , Small Beams, Mix No. 1, Three-Point Bending, Huang (8)

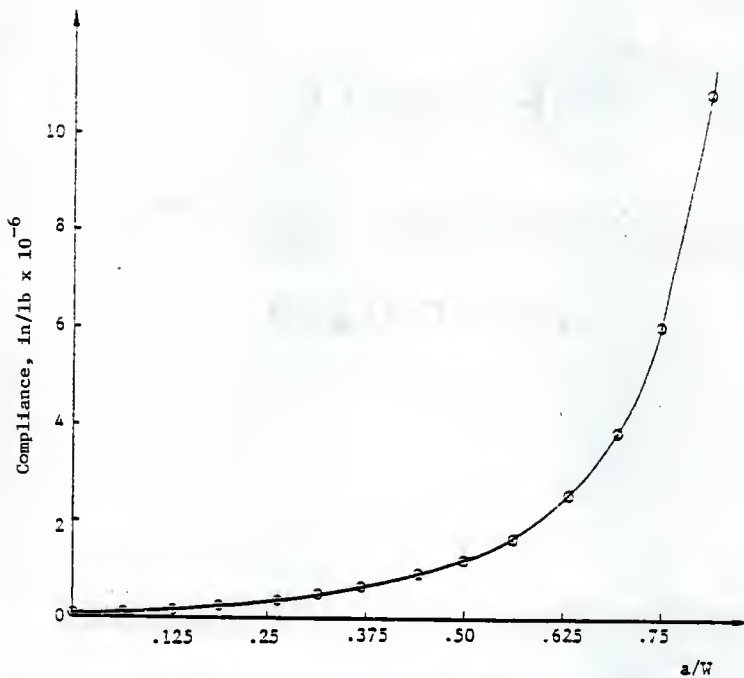


Fig. 2.11 Compliance vs a/W , Large Beams, Mix No. 2, Three-Point Bending, Euang (8)

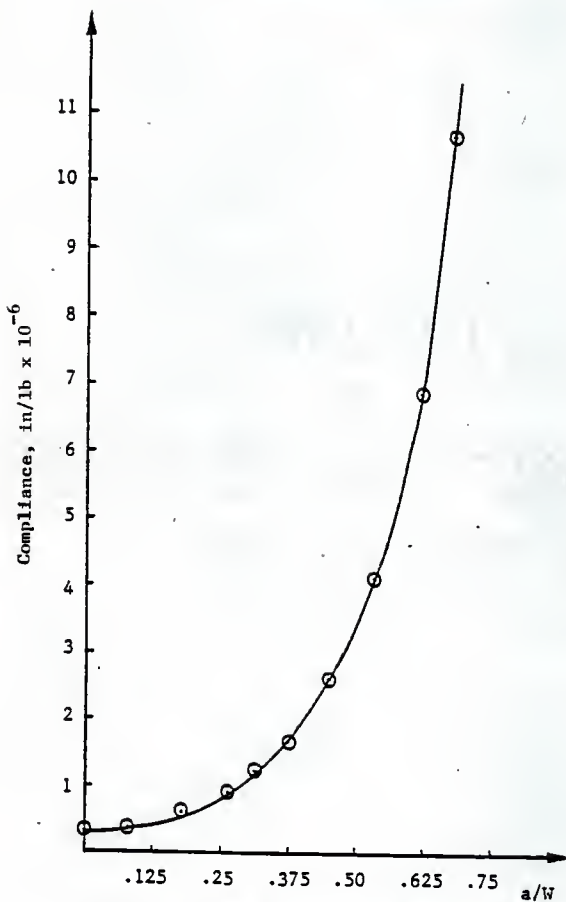


Fig. 2.12 Compliance vs a/W , Small Beams, Mix No. 2, Three-Point Bending, Huang (8)

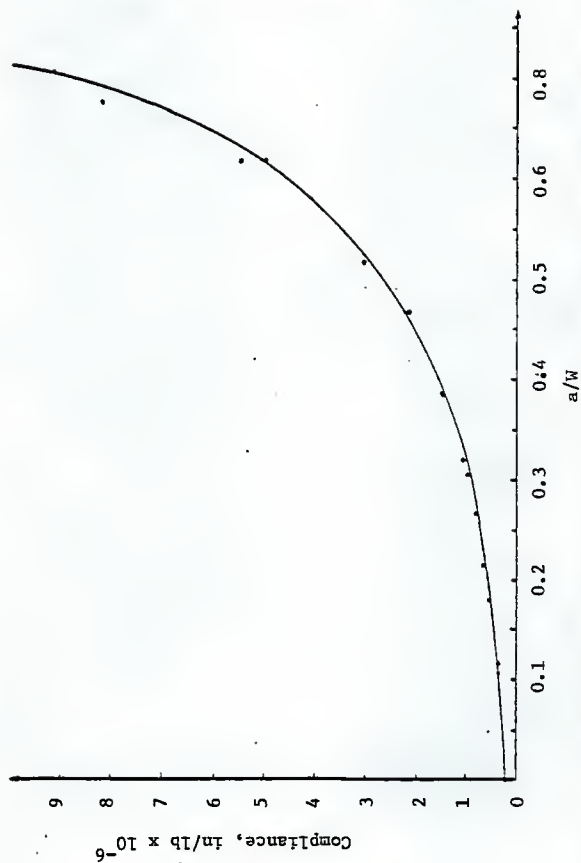


Fig. 2.13 Compliance vs a/w , Group 1-A, Three-Point Bending, Fartash (11)

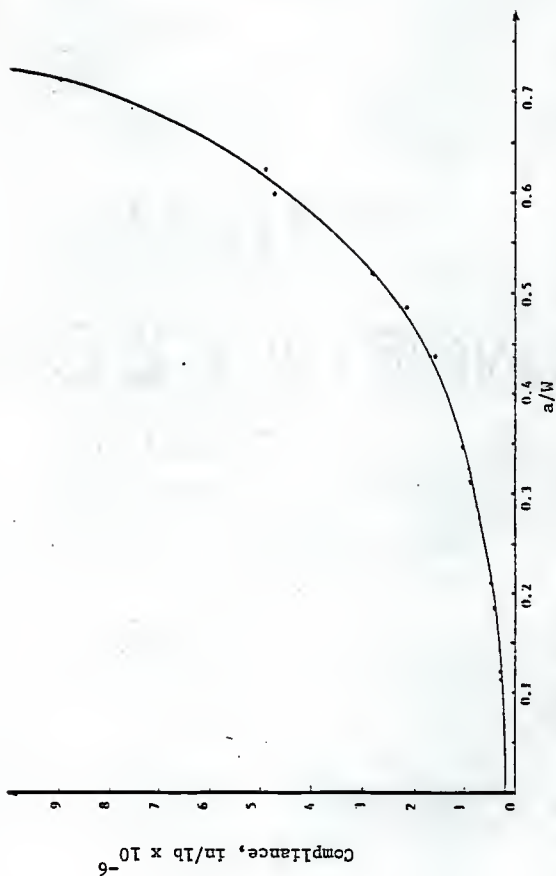


Fig. 2.14 Compliance vs a/W , Group 2-A, Three-Point Bending, Fartash (11)

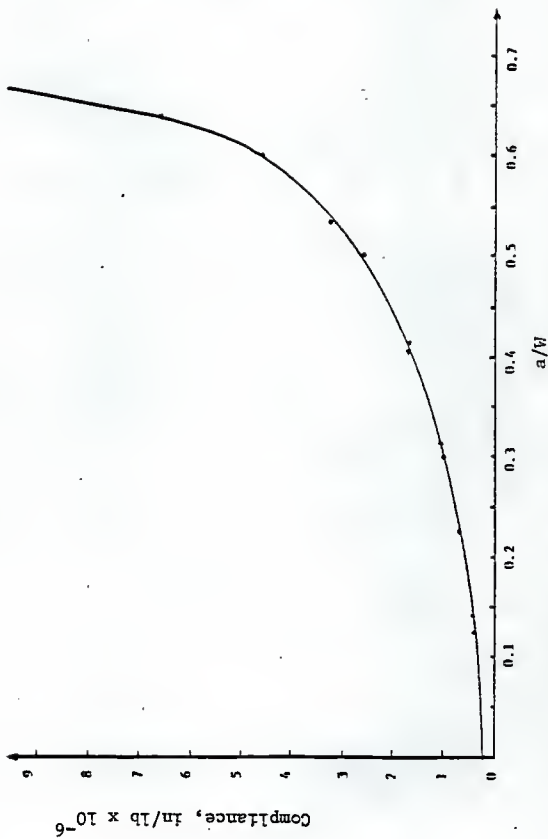


Fig. 2.15 Compliance vs a/W , Group 3-A, Three-Point Bending, Fartash (11)

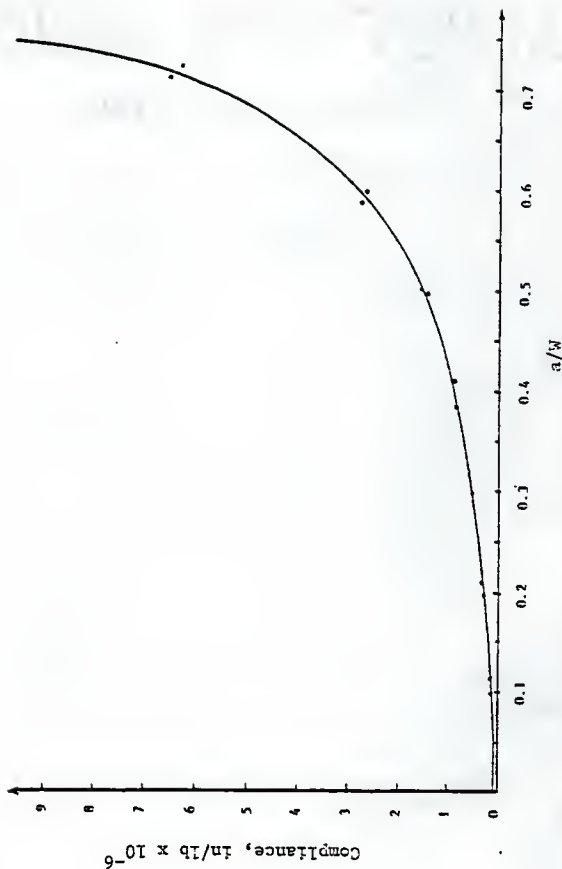


Fig. 2.16 Compliance vs a/W , Group 1-B, Four-Point Bending, Fartash (11)

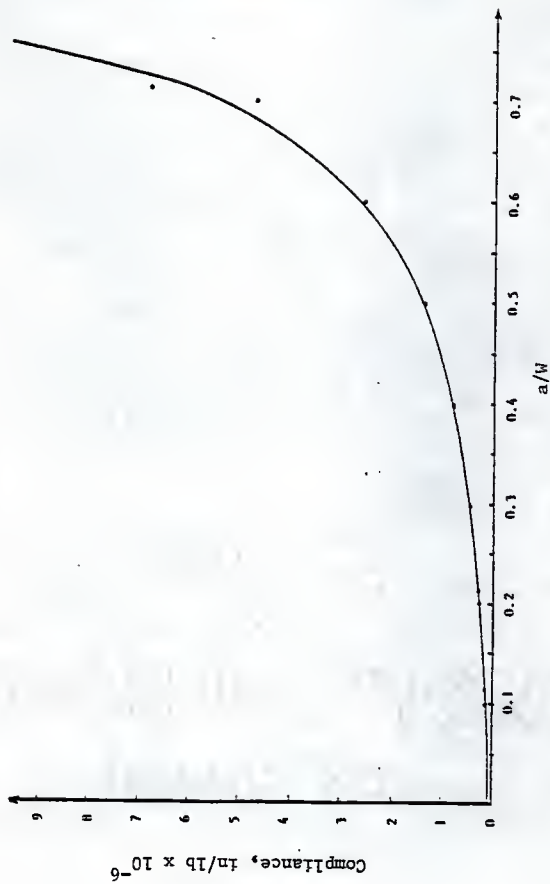


Fig. 2.17 Compliance vs a/W , Group 2-B, Four-Point Bending, Fartash (11)

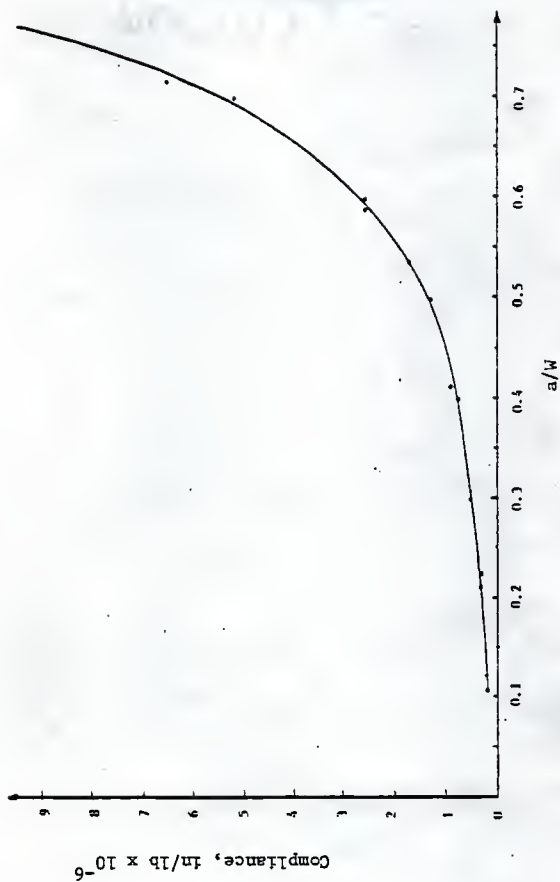


FIG. 2.18 Compliance vs a/W , Group 3-B, Four-Point Bending, Fartash (11)

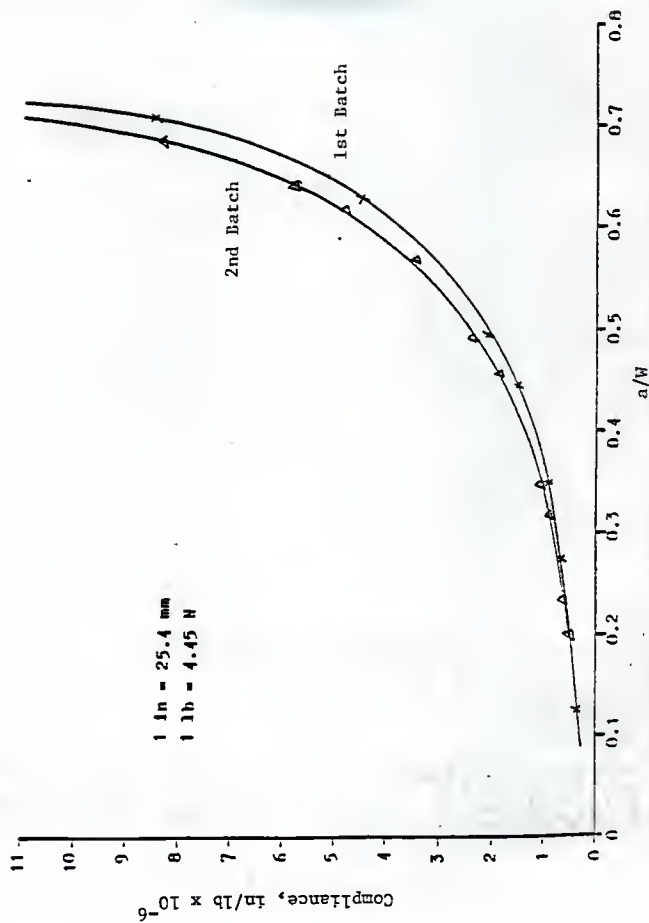


Fig. 2.19 Compliance vs a/W , Teflon Beams, Three-Point Bending, Co (4)

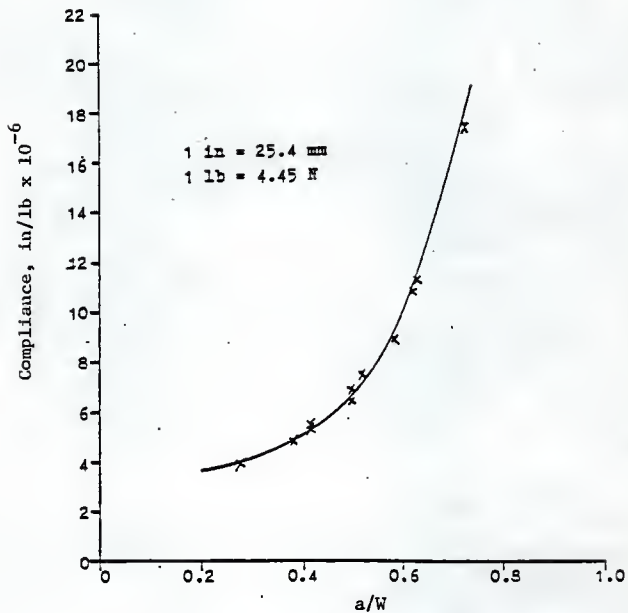
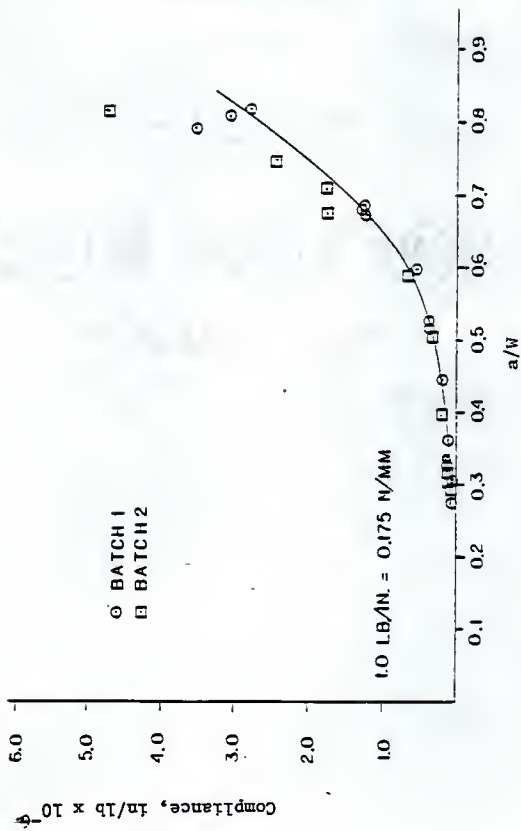


Fig. 2.20 Compliance vs a/W , Precracked Beams, Three-Point Bending, Go (4)

2.21 CMOD Compliance vs a/W , Three-Point Bending, Rod (12)

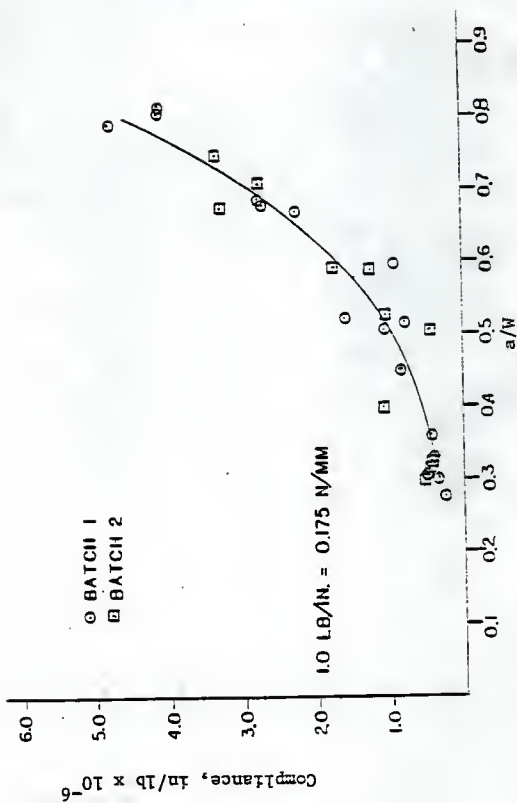


Fig. 2.22 LPD Compliance vs a/W , Three-Point Bending, Rod (12)

CHAPTER 3

EXPERIMENTAL PROGRAM

3.1 Test Specimens

For beams tested in July 1985 and January 1986, three sizes of beams were constructed with the following dimensions:

Group 1A: L = 16 in (406 mm)

S = 15 in (381 mm)

W = 4 in (102 mm)

B = 3 in (76 mm)

S/W = 3.75

Group 2B: L = 32 in (813 mm)

S = 30 in (762 mm)

W = 8 in (203 mm)

B = 3 in (76 mm)

S/W = 3.75

Group 3A: L = 48 in (1220 mm)

S = 45 in (1140 mm)

W = 12 in (305 mm)

B = 3 in (76 mm)

S/W = 3.75

(For the beam dimensions of Group 2A, refer to chapter 2.) For the schematic diagram of the beam dimensions, see Fig. 2.1. The mix design used was presented in Table 2.5. A total of sixteen beams of W = 4 in. (102 mm), two beams of W = 8 in. (203 mm) and three beams

of $W = 12$ (305 mm) in. were constructed. Beams of $W = 4$ in. (102 mm) were tested in July 1985 and beams with $W = 8$ in. (203 mm) and $W = 12$ in. (305 mm) were both tested in January 1986. Figures 3.1 and 3.2 show stress versus strain graphs of these beams. The average concrete strength of the beams with $W = 4$ in. (102 mm) was 6170 psi (42.5 MPa) and modulus of elasticity was 5.02×10^6 psi (34.6 GPa). The average concrete strength of beams with $W = 8$ in. (203 mm) and $W = 12$ in. (305 mm) was 8700 psi (59.9 MPa) and modulus of elasticity of 6.60×10^6 psi (45.5 GPa).

3.2 Set Up and Testing Procedure

The sixteen beams of $W = 4$ in. (102 mm) were all tested with the notches on the bottom sides of the specimens (Fig. 2.1). However, beams with $W = 8$ in. (203 mm) and $W = 12$ in. (305 mm) were all tested in the reverse configuration with the set up showed in Fig 3.3. The notch of the specimen was on the top side of the beam. The advantage of this reverse setup is that premature failure or cracking can be prevented during the process of transportation and setting up of the specimen on the MTS machine. Furthermore, the reverse set up eliminated the difficulties of turning the beams over for dye penetration.

All these beams were notched to a desired crack length at the mid-span. Of the sixteen beams with $W = 4$ in. (102 mm), six had nominal a_0/W of 0.3, six of the beams had nominal a_0/W of 0.5 and the remaining four beams had a_0/W of 0.7. The two $W = 8$ in. (203 mm) beams and $W = 12$ in. (305 mm) beams had a_0/W of 0.5.

The MTS machine was used throughout the testing. All these specimens were loaded to failure without precracking. Three of the six

beams with a_0/W of 0.3 were tested in strain control and the remaining three were tested in load control. Of the six beams with a_0/W of 0.5, three were tested in strain control and three were tested in load control. Of the last four of the beams with a_0/W of 0.7, half were tested in strain control and the other half were tested in load control. The P-LPD and P-CMOD traces were obtained simultaneously during testing.

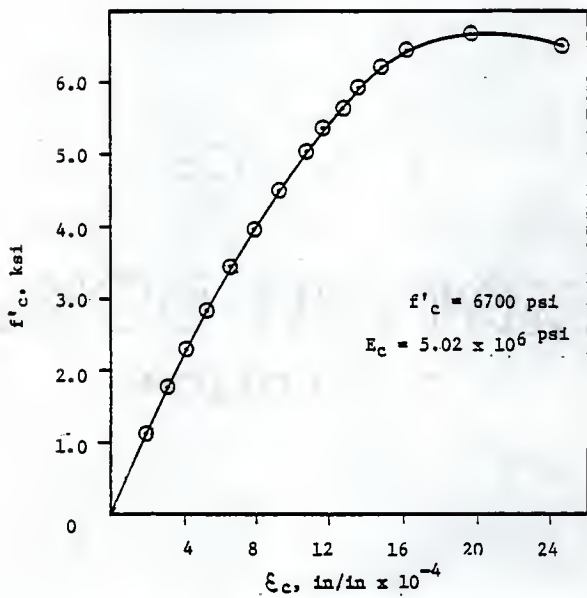


Fig. 3.1 f'_c versus ϵ_c , Tested July 1985

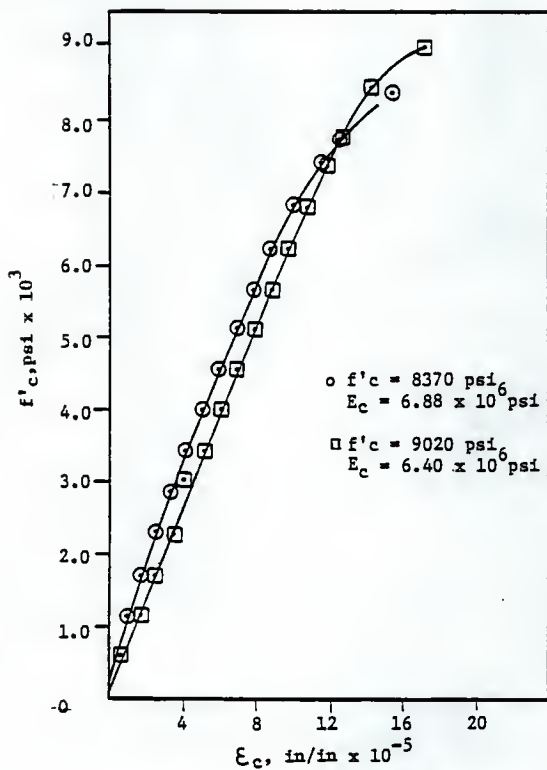


Fig. 3.2 f'_c versus ϵ_c , Tested January 1986

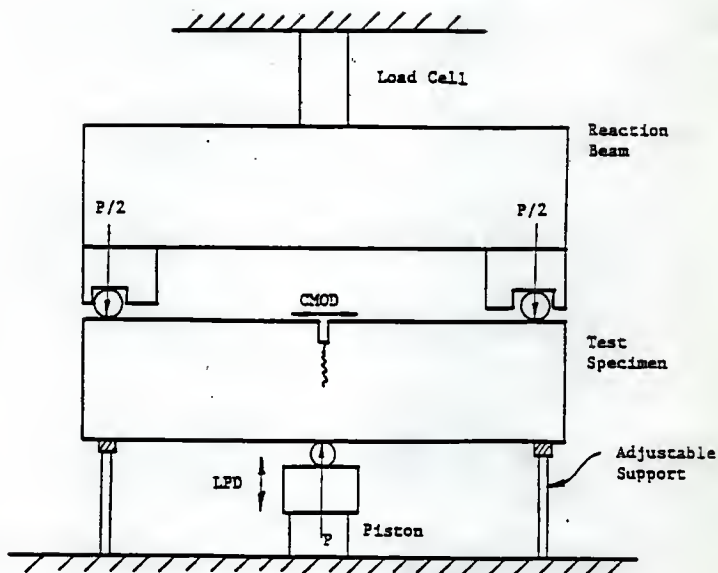


Fig. 3.3 Reverse Testing Configuration for Three-Point Bending

CHAPTER 4

EVALUATION OF METHODS

4.1 Notched Beams

4.1.1 Notched Beams Tested in Three-Point Bending

All the notched beams had $B = 3$ in. (76 mm) and S/W ratio of 3.75.

(a) RILEM Method (10)

Results of tests using the RILEM Method (10) on six beams tested by Rood (12) with $W = 4$ in. (102 mm), sixteen beams tested in July 1985 with $W = 4$ in. (102 mm), two beams with $W = 8$ in. (203 mm) and three beams with $W = 12$ in. (305 mm) which were both tested in January 1986 are presented in Appendix II, Tables 1A, 1B, 1C.

The results obtained using this method showed variation with a_0 and beam size. Swartz (14) and the writer had a fundamental disagreement in the use of the full P-LPD curve to determine the energy consumed by the crack propagation because the crack length changes rapidly after the point of instability. This also shows clearly that there should not be any correlation between the initial notch length a_0 and the full P-LPD curve. Furthermore, ambiguity arises in the determination of δ_0 . According to this method δ_0 is determined at the point of maximum vertical displacement on the P-LPD curve. However, the point of the maximum vertical displacement could be at the point where the trace of P-LPD ends or at the point of extension of the full P-LPD curve.

As a result of the above problems, an alternative to the RILEM

method is suggested the Modified RILEM Method (14).

(b) Modified RILEM Method (14)

Results of tests using Modified RILEM Method, equation 2, on the same beams mentioned in the above section (A) are presented in Appendix II, Tables 2A, 2B, 2C.

Notice that the results obtained in this method using A_1 (Fig.2.2), or U for the calculation of G_f exhibits scatter when $W = 4$ in. (102 mm) beams were used. However, with $W = 8$ in. (203 mm) and $W = 12$ in. (305 mm), the results obtained are consistent but smaller than the RILEM Method (10). For $W = 8$ in. (203 mm) and $W = 12$ in. (305 mm), G_f values obtained are smaller by approximately 38 percent and 40 percent respectively.

(c) Direct Energy Method (4)

The results of tests using the Direct Energy Method, equation 3, is presented in Appendix II, Table 3A. No measurement of the extended a/W were taken on the sixteen beams with $W = 4$ in. (102 mm) tested in July 1985 and the two beams with $W = 8$ in. (203 mm) and the three beams with $W = 12$ in. (305 mm), tested in January 1986. Therefore, only Rood's (12) six beams were used for the calculation of G_{IC} using this method, Appendix II, Table 3A.

The results obtained in this method showed consistency but were higher than the results of the Modified RILEM Method (14). For a/W approximately 0.5 and 0.65, the G_{IC} values are higher by 43 percent and 48 percent respectively. This is because cracked surface roughness was taken into consideration. Furthermore, the determination of the crack length is more reliable.

(d) K_{Ic} Methods

(i) Jenq/Shah Method (9)

The results of tests using the Jenq/Shah Method (9) on six beams with $W = 4$ in. (102 mm) tested by Rood (12), sixteen beams with $W = 4$ in. (102 mm) tested in July 1985, two beams with $W = 8$ in. (203 mm) and three beams with $W = 12$ in. (305 mm) which were both tested in January 1986, twelve teflon insert beams with $W = 4$ in. (102 mm) tested by Go (4), and the twenty-one teflon beams with $W = 4$ in. (102 mm) tested by Fartash (11) are presented in Appendix II, Tables 4A, 4B, 4C, 4D, 4E, 4F.

The results obtained showed scatter and inconsistency and G_{Ic} values are all much smaller than the corresponding values given in Tables 1A, 1B, 1C. However, it should be remembered that the $CMOD_{e2}$ was determined based on ignoring the effect of $CMOD_{e2}$.

(ii) Go Method (4)

The results of tests using the Go Method (4) with estimated extended crack length, on the six beams with $W = 4$ in. (102 mm) tested by Rood (12), twelve beams with $W = 4$ in. (102 mm) tested by Go (4) and twelve other beams with the same $W = 4$ in. (102 mm) tested by Fartash (11) are presented in Appendix II, Tables 5A, 5B, 5C, 5D.

Rood's (12) results, G_{Ic} were all at least twice greater than the results obtained by Jenq/Shah Method (9) with corresponding a/W . However, Fartash (11) results are compatible with the results obtained by the Jenq/Shah Method (9).

(e) J_{Ic} Method (4)

The plots of U versus a_0/W and (or) U versus extended a/W for Rood's (12) notched beams and the notched beams tested in July 1985 are

presented in Appendix II, Figs.1 and 2.

The J_{IC} values obtained for Rood's (12) beams was 0.472 lb-in/in^2 (82.7 N-m/m^2) when a_0/W is used and 0.436 lb-in/in^2 (76.4 N-m/m^2) when extended a/W is used. For the beams tested in July 1985, the J_{IC} value is 0.418 lb-in/in^2 (73.3 N-m/m^2). All these values showed agreement.

(f) Bazant Size Effect Method (1, 3)

Data obtained from Rood's $W = 4 \text{ in. (102 mm)}$ beams, the two $W = 8 \text{ in. (203 mm)}$ beams and the three $W = 12 \text{ in. (305 mm)}$ beams which were both tested in January 1986 were used for Bazant Three Beam Method (1, 3). The plot is shown in Appendix II Fig. 3. Notice that all the points fall on a straight line. The G_F values obtained by this method are lower than the results in Tables 1A and 1B. However, G_F values do agree fairly well with the Jend/Shah (9) results in Appendix II, Tables 4B and 4E, despite ignoring the effect of $CMOD_{e2}$.

4.1.2 Notched Beams Tested in Four-Point Bending

The only method suitable for the determination of G_{IC} is the K_{IC} Method developed by Huang (8) and Go (4) (this is not the K_{IC} Method used in the three-point bending beams).

The results of tests using this method on the fourteen beams with $W = 4 \text{ in. (102 mm)}$ tested by Fartash (11) are presented in Appendix II, Tables 6A and 6B.

The results of G_{IC} values obtained were smaller for Fartash's (11) beams, group 1-B; the average G_{IC} value for this group of beams was $0.0552 \text{ lb-in/in}^2$ (9.67 N-m/m^2) for average extended a/W of 0.335 and the average G_{IC} value for beams from group 2-B was 0.118 lb-in/in^2 (20.7 N-m/m^2) for average extended a/W of 0.575.

4.2 Precracked Beams

4.2.1 Precracked Beams Tested in Three-Point Bending

(a) RILEM Method (10)

The only data that was used for the determination of the G_f value with this method was the twenty-six beams from Rood (12) with $W = 4$ in. (102 mm), $B = 3$ in. (76 mm) and $S/W = 3.75$, Appendix II, Table 7A. The variation with a_1/W still exists.

(b) Modified RILEM Method (14)

The results of tests using this method on the same twenty-six beams and the sixteen beams tested by Go (4) are presented in Appendix II, Tables 8A and 8B. The results obtained are consistent.

(c) Direct Energy Method (4)

Two sets of data with $W = 4$ in. (102 mm), $B = 3$ in. (76 mm) and $S/W = 3.75$ were used in the determination of G_{fc} values. They are the thirteen beams tested by Rood (12) and the eleven beams tested by Go (4), Appendix II Tables 9A and 9B. The results not only show good consistency, but also agree very well with the results obtained by the Modified RILEM Method (14).

(d) K_{Ic} Methods

(i) Jenq/Shah Method (9)

The results obtained using this method for the twenty beams tested by Rood (12), the nine beams tested by Go (4), the twenty-one beams tested by Fartash (11), and the ten beams tested by Huang (8) - all beams had $W = 4$ in. (102 mm), $B = 3$ in. (76 mm) and $S/W = 3.75$. In addition, eleven beams tested by Huang (8) with $W = 8$ in. (203 mm), $B = 4$ in. (102 mm) and $S/W = 3.125$ are also used for the calculations. The

results are presented in Appendix 11, Tables 10A, 10B, 10C, 10D, 10E and 10F.

All these beams exhibit good consistency, even though the results are generally lower than the corresponding values on Tables 9A and 9B by at least 50 percent.

(ii) Go Method (4)

The results obtained using this method on the fourteen beams tested by Rood (12) with $W = 4$ in. (102 mm), the nine beams tested by Go (4) with $W = 4$ in. (102 mm), the fourteen beams tested by Fartash (11) with $W = 4$ in (102 mm), and the nine beams tested by Huang (8) with $W = 4$ in. (102 mm) and another ten beams tested by Huang (8) with $W = 8$ in. (203 mm), $B = 4$ in. (102 mm) and $S/W = 3.125$ (all these beams had $B = 3$ in. (76 mm) and $S/W = 3.75$ except Huang's (8) ten beams) are presented in Appendix II, Tables 11A, 11B, 11C, 11D, 11E, 11F.

The results of G_{IC} values obtained by using Huang's (8) beams showed inconsistency and scatter. However, the results using Fartash's (11), Go's (4) and Rood's (12) beams come very close to the results obtained by Jenq/Shah Method (9).

(e) J_{IC} Method (4)

The only data that were used with this method were Rood's (12) beams and Go's (4) sixteen beams. The plots of U versus a_1/W and U versus extended a/W are shown in Appendix 11 Figs. 4, 5. The J_{IC} value obtained for Rood's (12) beams is 0.270 lb-in/in² (47.3 N-m/m²) when a_1/W is considered and 0.239 lb-in/in² (41.9 N-m/m²) when extended a/W is considered. The average J_{IC} value is 0.255 lb-in/in² (44.7 N-m/m²). This value agrees very well with the results obtained by Modified RILEM Method (14) and Direct Energy Method (4). The J_{IC} values obtained for

Go's (4) beams is 0.299 lb-in/in^2 (52.4 N-m/m^2) when a_i/W is used and 0.346 lb-in/in^2 (60.6 N-m/m^2) when extended a/W is used. The average J_{IC} value for Go's (4) beams is 0.323 lb-in/in^2 (56.6 N-m/m^2). Once again, J_{IC} obtained agrees well with Modified RILEM (14) and Direct Energy methods (4).

(f) Bazant Size Effect Method (1, 3)

There is no adequate data to be used with this method.

4.2.2 Precracked Beams Tested in Four-Point Bending

The only method there is suitable for the determination of G_{IC} is the KIC Method developed by Huang (8) and Go (4).

The results of G_{IC} calculated based on modified extended a/W tested by Fartash (11) and Huang (8) are presented in Appendix II Tables 12A, 12B, 12C, 12D, 12E. (All the results of Fartash (11) and Huang (8) were separated in different tables based on the modulus of elasticity values and the mix designs.)

The results obtained using Fartash's (11) beams showed considerable scatter and inconsistency even though all these beams had similar mix design and concrete strength. The results obtained using Huang's (8) beams showed consistent results, however, the results are very low.

CHAPTER 5

CONCLUSIONS AND RECOMMENDATIONS

Conclusions are summarized in the following paragraphs based on the experimental results obtained in this thesis.

1. In all cases except one where notched beams were used for the evaluation of the fracture parameters scatter and inconsistency of results were obtained when compared to the results obtained by precracked beams. The only method that seemed to work well with notched beams is Bazant's Method (1, 3). Therefore, precracked beams tested in three-point bending are recommended in the experimental fracture testing of concrete in the future.
2. The Modified RILEM Method (14), Direct Energy Method (4) and J_{IC} Method using precracked beams in three-point bending and initial a/W and extended a/W exhibit equivalent results. The G_{IC} value appears to be a constant for different a/W values and concrete strengths. Swartz (14) and the writer prefer the latter two methods for the determination of fracture parameters where a/W values can be determined reliably.
3. Precracked beams using the K_{IC} methods may provide satisfactory and consistent results if strain control (13) is applied during testing especially when the Jenq/Shah Method (9) is used. In addition, results obtained by beams tested in four-point bending using the K_{IC} Method (some scatter and inconsistency still exist) appeared to be similar to the Jenq/Shah Method (9).

6. Swartz (14) and the writer recommend the use of beam size with at least $W = 4$ in. (102 mm) for experimental fracture testing in the future.

APPENDIX I

REFERENCES

1. Bazant, Zdenek P., "Fracture Energy of Concrete from Maximum Loads of Specimens of Various Sizes," Proposal for RILEM Recommendation, Northwestern University, Evanston, IL 1985.
2. Bazant, Zdenek P., and Cedolin, Luigi, "Approximate Linear Analysis of Concrete Fracture by R-Curves," Journal of Structural Engineering, ASCE, Vol. 110, No. 6, June 1984.
3. Bazant, Zdenek P., Kim, Jin-Keun and Pfeiffer, Phillip, "Nonlinear Fracture Properties from Size Effect Tests," Journal of Structural Engineering, ASCE, Vol. 112, No. 2, Feb. 1986.
4. Go, Cheer-Germ and Swartz, Stuart E., "Fracture Toughness Techniques to Predict Crack Growth and Tensile Failure in Concrete," report 154, Engineering Experiment Station, Kansas State University, Manhattan, KS, July 1983.
5. Hillerborg, Arne, "Concrete Energy Testes performed by Laboratories According to RILEM Recommendation," Report TVBM-3015, Lund Institute of Technology, Division of Building Materials, Lund, Sweden, 1983
6. Hillerborg, Arne, "Additional Concrete Fracture Energy Tests Performed by 6 Laboratories According to a draft RILEM Recommendation, " Report TVBM-3021, Lund Institute of Technology, Division of Building Materials, Lund, Sweden, 1984
7. Hillerborg, Arne, "Influence of Beams Size on Concrete Fracture Energy Determined According to a Draft RILEM Recommendation," Report TVBM-3021 Lund Institute of Technology, Division of Building Materials, Lund, Sweden, 1985.
8. Huang, C. M., "Finite Element and Experimental Studies of Stress-Intensity Factors for Concrete Beams," Doctor's Dissertation, Kansas State University, 1981.
9. Jenq, Y.S. and Shah, S. P., "Two Parameter Fracture Model for concrete," Journal of Engineering Mechanics, ASCE, Vol. 111, No. 10, Oct. 1985.
10. RILEM Technical Committee 50-FMC, "Determination of the Fracture Energy of Mortar and Concrete by Means of Three-Point Bend Tests on Notched Beams," proposed RILEM recommendation, January 1982, revised June 1982. Lund Institute of Technology of Building Materials, Lund, Sweden.

REFERENCES (Continued)

11. Fartash, M., "Stress Intensity Values for Pnotched and Precracked, Plain Concrete Beams," Master's Thesis, Kansas State University.
12. Rood, S., "Fracture Toughness Testing of Small Concrete Beams," Master's Thesis, Kansas State University, 1984.
13. Swartz, S. E. and Siew, H. C., "Time Effects in the Static Testing of Concrete to Determine Fracture Energy," Report 182, Engineering Experiment Station, Kansas State University, Manhattan, KS, June 1986.
14. Swartz, S. E., and Yap, S. T., "Evaluation of Recently Proposed Recommendations for the determination of Fracture Parameters for Concrete in Bending, " Proceedings, VIIIth International Conference on Experimental Stress Analysis, Amsterdam, May 12-16, 1986

APPENDIX II

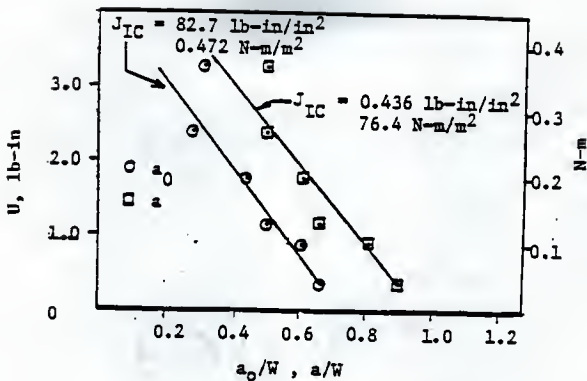


Fig. II.1 J-Integral Method (4), Notched Beams, Rood (12), $W = 4$ in

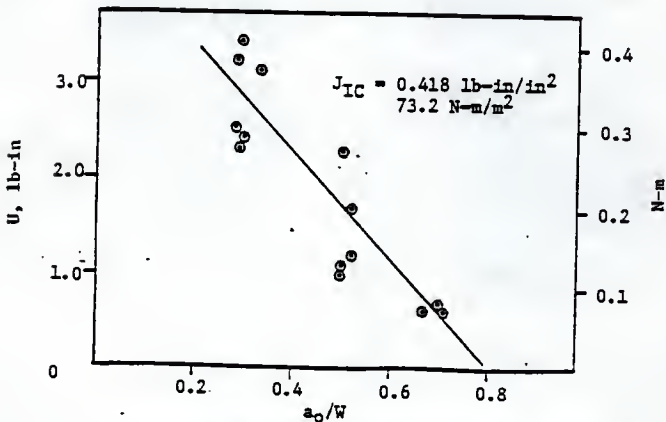


Fig. II.2 J-Integral Method (4), Notched Beams, Tested July 1985, $W = 4$ in

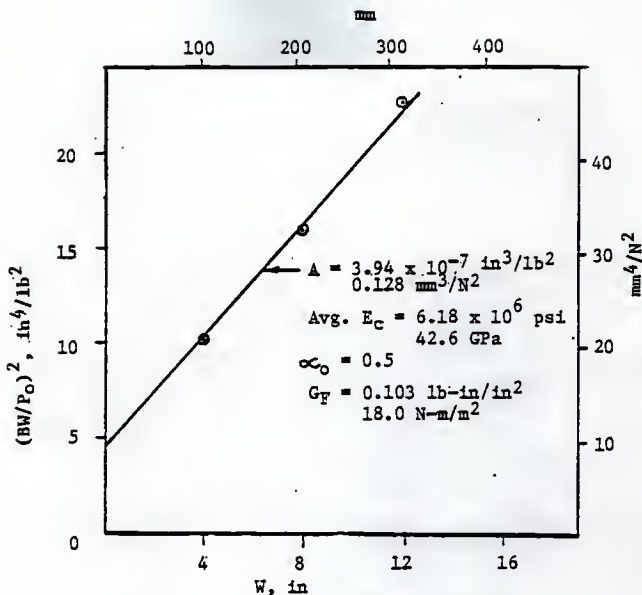


Fig. II.3 Bazant Size Effect Method (1, 3),
Notched Beams

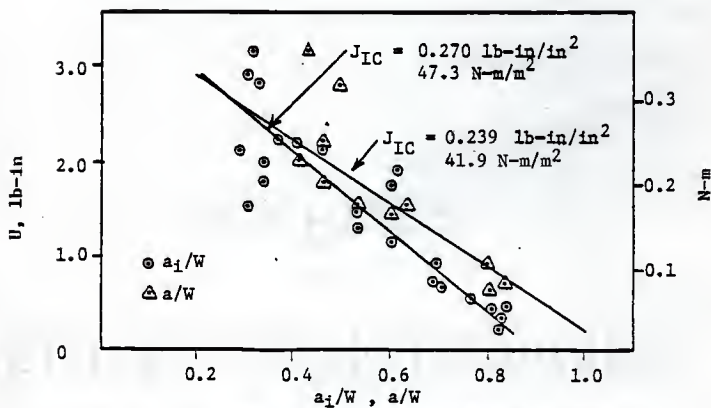


Fig. II.4 J-Integral Method (4), Precracked Beams,
Rood (12), $W = 4 \text{ in}$

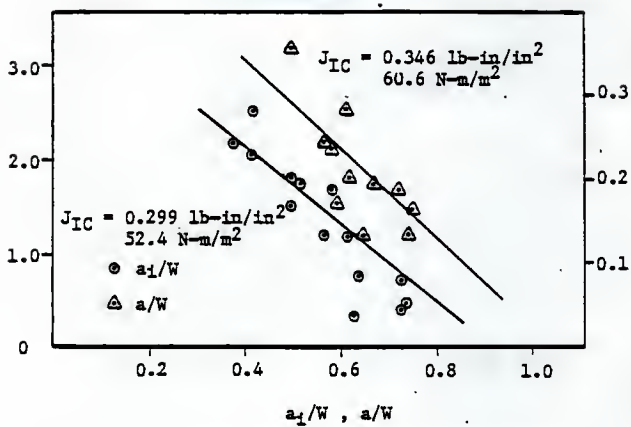


Fig. II.5 J-Integral Method (4), Precracked Beams,
Go (4), $W = 4 \text{ in}$

Table II.1A Notched Beams, Tested by Rood (12), RILEM Method (10), $W = 4.00$ in (102 mm), $B = 3.00$ in (76 mm), $E_c = 5.34 \times 10^6$ psi (36.8 GPa)

Fig. No.	Original No.	a_o in mm	Avg. a_o in mm	δ_o in $\times 10^{-3}$ mm	W_o lb-in N-m	G_F lb-in/in ² N-m/m ²	Avg. G_F lb-in/in ² N-m/m ²
222	C15	1.17	1.24	13.3	3.96	0.491	0.590
		29.7	31.4	0.340	0.450	86.0	103
224	C16	1.30		18.0	5.20	0.688	
		33.0		0.460	0.600	121	
226	C17	1.82	1.94	13.5	2.54	0.421	0.387
		46.2	49.3	0.340	0.290	74.0	67.8
228	C18	2.06		13.0	1.85	0.353	
		52.3		0.330	0.200	62.0	
230	C19	2.50	2.59	13.0	1.11	0.292	0.248
		63.5	65.8	0.330	0.130	51.0	43.4
232	C20	2.68		11.3	0.630	0.204	
		68.1		0.290	0.0700	36.0	

Notes: 1. $W/C = 0.50$, For complete mix design see Table 2.4.

2. $S = 15$ in (381 mm), $L = 16$ in (406 mm), $m_g = 15.6$ lb (7.08 Kg), $f'_c = 8100$ psi (55.8 MPa)

Table II.1B Notched Beams, Tested July 1985, RILEM Method (10), $W = 4.00$ in (102 mm), $B = 3.00$ in (76 mm), $E_c = 5.02 \times 10^6$ psi (34.6 GPa)

Fig. No.	Original No.	a_0 in mm	Avg. a_0 in mm	δ_0 in $\times 10^{-3}$ mm	W_0 lb-in N-m	GF lb-in/in ² N-m/m ²	Avg. GF lb-in/in ² N-m/m ²
236	2S.3	1.12		8.90	2.43	0.297	
		28.4		0.226	0.276	52.1	
238	3S.3	1.12		10.1	3.11	0.378	
		28.4		0.257	0.352	66.3	
234	1S.3	1.16	1.18	10.2	2.27	0.285	0.348
		29.5	30.0	0.259	0.257	50.0	61.0
244	3L.3	1.16		14.3	3.33	0.417	
		29.5		0.363	0.376	73.1	
242	2L.3	1.20		13.9	2.30	0.300	
		30.5		0.353	0.260	52.5	
240	1L.3	1.32		13.9	3.10	0.413	
		33.5		0.353	0.350	72.4	
246	1S.5	2.00		9.30	1.10	0.208	
		50.8		0.236	0.124	36.4	
248	2S.5	2.00		7.70	0.960	0.180	
		50.8		0.196	0.108	31.5	
254	2L.5	2.00	2.02	15.1	2.25	0.414	0.278
		50.8	51.3	0.384	0.254	72.6	48.7
250	3S.5	2.04		8.50	1.20	0.227	
		51.8		0.216	0.136	39.7	
252	1L.5	2.04		14.2	1.68	0.323	
		51.8		0.361	0.189	56.6	
256	3L.5	2.04		12.9	1.66	0.317	
		51.8		0.328	0.187	55.5	
262	2L.7	2.68		8.20	0.621	0.189	
		68.1		0.208	0.0701	33.1	
260	3S.7	2.76	2.76	8.10	0.620	0.200	0.205
		70.1	70.1	0.206	0.0701	35.2	35.9
258	1S.7	2.80		8.60	0.547	0.189	
		71.1		0.218	0.0618	33.1	
264	3L.7	2.80		11.1	0.700	0.243	
		71.1		0.282	0.0791	42.6	

Notes 1. $W/C = 0.50$, for complete mix design see Table 2.5.

2. $S = 15$ in (381 mm), $L = 16$ in (406 mm), $m_g = 15.6$ lb (7.08 Kg), $f'_c = 6170$ psi (42.5 MPa)

Table II.1C Notched Beams, Tested January 1986, RILEM Method (10), B = 3.00 in (76 mm), $E_c = 6.60 \times 10^6$ psi (45.5 GPa)

Fig. No.	Original No.	W in mm	a_o in mm	δ_o in mm	W_o lb-in N-m	G_F lb-in/in ² N-m/m ²	Avg. G_F lb-in/in ² N-m/m ²
266	N-2-8	8	4.00	31.6	7.95	0.498	
		203	102.0	0.803	0.898	87.2	0.506
268	W-1-8	8	4.00	27.0	7.86	0.514	88.6
		203	102.0	0.685	0.888	90.1	
272	PW12	12	6.00	25.8	10.3	0.372	
		305	152.0	0.655	1.16	65.2	
270	CB12	12	6.00	35.6	12.7	0.429	0.388
		305	152.0	0.904	1.47	78.0	68.0
274	W12	12	6.00	28.8	10.6	0.364	
		305	152.0	0.732	1.30	73.0	

- Notes:
1. W/C = 0.50, for complete mix design see Table 2.5.
 2. For W = 8 in (203 mm), S = 30 in (762 mm), L = 32 in (813 mm), mg = 62.5 lb (28.4 Kg)
 3. For W = 12 in (305 mm), S = 45 in (1143 mm), L = 48 in (1219 mm), mg = 140.6 lb (63.8 Kg)
 4. Average $f'_c = 8700$ psi

Table II.2A Notched Beams, Tested by Rood (12), Modified RILEM Method (14), $W = 4.00$ in (102 mm), $B = 3.00$ in (76 mm), $E_c = 5.34 \times 10^6$ psi (36.8 GPa)

Fig. No.	Original No.	a_0 in mm	Avg. a_0 in mm	$\bar{\delta}_0$ in $\times 10^{-3}$ mm	U lb-in N-m	\bar{G}_F lb-in/in ² N-m/m ²	Avg. \bar{G}_F lb-in/in ² N-m/m ²
222	C15	1.17	1.24	7.90	2.40	0.297	0.366
		29.7	31.4	0.201	0.271	52.0	63.6
224	C16	1.30		13.8	3.30	0.434	
		33.0		0.351	0.373	76.0	
226	C17	1.82	1.82	8.10	1.75	0.287	0.256
		46.2	46.2	0.206	0.198	50.3	44.8
228	C18	2.06	2.06	8.10	1.18	0.224	
		52.3	52.3	0.206	0.133	39.2	
230	C19	2.50	2.59	7.70	0.860	0.218	0.170
		63.5	65.8	0.196	0.0972	38.2	29.8
232	C20	2.68		5.70	0.390	0.121	
		68.1		0.145	0.0441	21.2	

- Notes: 1. For dimensions and material properties see Table II.1A.
2. $J_{IC} = 0.472$ lb-in/in² (82.7 N-m/m²) - based on a_0 (4).

Table II.2B Notched Beams, Tested July 1985, Modified RILEM Method (14)
 , W = 4.00 in (102mm), B = 3.00 in (76 mm), $E_c = 5.02 \times 10^6$
 psi (34.6 GPa)

Fig. No.	Original No.	a_0 in mm	Avg. a_0 in mm	$\bar{\delta}_0$ in $\times 10^{-3}$ mm	U lb-in N-m	\bar{G}_F lb-in/in ² N-m/m ²	Avg. \bar{G}_F lb-in/in ² N-m/m ²
236	2S.3	1.12 28.4		3.67 0.0932	1.46 0.166	0.176 30.8	
238	3S.3	1.12 28.4		5.00 0.127	1.75 0.197	0.212 37.1	
234	1S.3	1.16 26.5	1.18 30.0	4.82 0.122	1.78 0.200	0.218 38.1	0.179 31.4
244	3L.3	1.16 26.5		2.65 0.0673	1.47 0.166	0.177 31.1	
242	2L.3	1.20 30.5		3.38 0.0859	1.06 0.119	0.133 23.2	
240	1L.3	1.32 33.5		2.77 0.0704	1.20 0.136	0.155 27.2	
246	1S.5	2.00 50.8		4.33 0.110	0.650 0.0735	0.120 21.0	
248	2S.5	2.00 50.8		2.10 0.0533	0.490 0.0553	0.0870 15.3	
254	2L.5	2.00 50.8	2.02 51.3	3.19 0.0810	0.752 0.0849	0.134 23.4	0.106 18.6
250	3S.5	2.04 51.8		3.31 0.0841	0.640 0.0723	0.118 20.7	
252	1L.5	2.04 51.8		2.46 0.0625	0.443 0.0502	0.0820 14.3	
256	3L.5	2.04 51.8		2.55 0.0648	0.527 0.0595	0.0960 16.9	
262	2L.7	2.68 68.1		2.10 0.0533	0.272 0.0306	0.0770 13.5	
260	3S.7	2.76 70.1	2.76 70.1	2.48 0.0630	0.200 0.0226	0.0640 11.2	0.0685 12.0
258	1S.7	2.80 71.1		2.67 0.0678	0.179 0.0203	0.0610 10.7	
264	3L.7	2.80 71.1		2.41 0.0612	0.220 0.0249	0.0720 12.6	

Notes: 1. For dimensions and material properties see Table II.1B.

2. $J_{IC} = 0.418$ lb-in/in² (73.2 N-m/m²) - based on a_0 (4).

Table II.2C Notched Beams, Tested January 1986, Modified RILEM Method (14), B = 3.00 in (76 mm), $E_c = 6.60 \times 10^6$ psi (45.5 GPa)

Fig. No.	Original No.	W in mm	a_0 in mm	$\bar{\delta}_0$ in $\times 10^{-3}$ mm	U lb-in N-m	\bar{G}_F lb-in/in ² N-m/m ²	Avg. \bar{G}_F lb-in/in ² N-m/m ²
266	N-2-8	8	4.00	13.0	4.46	0.304	
		203	102	0.330	0.504	53.6	0.314
268	W-1-8	8	4.00	11.8	4.61	0.323	55.0
		203	102	0.300	0.521	56.6	
272	PW12	12	6.00	9.8	5.17	0.211	
		305	152	0.249	0.584	37.0	
270	CB12	12	6.00	13.0	6.20	0.243	0.233
		305	152	0.330	0.750	46.8	40.8
274	W12	12	6.00	13.4	6.27	0.244	
		305	152	0.340	0.770	48.0	

Note: For dimensions and material properties see Table II.1C.

Table II.3A Notched Beams, Tested by Rood (12), Direct Energy Method (4), $W = 4.00$ in (102 mm), $B = 3.00$ in (76 mm), $E_C = 5.34 \times 10^6$ psi (36.8 GPa)

Fig. No.	Original No.	Ext. a/W	Avg. a/W	$\bar{\delta}_0$ in $\times 10^{-3}$ mm	U lb-in N-m	\bar{GIC} lb-in/in ² _n N-m/m ²	Avg. \bar{GIC} lb-in/in ² N-m/m ²
222	C15	0.510	0.510	7.90 0.201	2.40 0.271	0.373 65.3	0.447
224	C16	0.510		13.8 0.351	3.30 0.373	0.520 91.1	78.2
226	C17	0.620	0.645	8.10 0.206	1.75 0.198	0.358 62.7	0.325
228	C18	0.670		8.10 0.206	1.18 0.133	0.287 50.2	56.5
230	C19	0.820	0.820	7.70 0.196	0.860 0.0972	0.395 69.2	0.395 69.2
232	C20	0.910	0.910	5.70 0.145	0.390 0.0441	0.386 67.6	0.386 67.6

- Notes:
1. For dimensions and material properties see Table II.1A.
 2. Ext. a/W = Extended a/W; measured by compliance technique.
 3. $JIC = 0.436$ lb-in/in² (76.4 N-m/m²) - based on extended a (4).

Table II.4A Notched Beams, Tested by Rood (12), Jenq/Shah Method (9), $W = 4.00$ in (102 mm), $B = 3.00$ in (76 mm), $E_c = 5.34 \times 10^6$ psi (36.8 GPa)

Fig. No.	Original No.	P_m lb in $\times 10^{-4}$ N	CMOD _e mm	a_e/W	K^2_{IC} lb-in ^{-3/2} kN-m ^{-3/2}	G _{IC} lb-in/in ² N-m/m ²
221	C15	570	4.60	0.308	536	0.0540
		2540	0.0117		590	9.46
223	C16	570	6.00	0.360	619	0.0720
		2540	0.0152		681	12.6
229	C19	165	3.60	0.698	261	0.0130
		734	0.00914		287	2.28
227	C18	290	8.20	0.542	523	0.0510
		1290	0.0208		575	8.94
225	C17	370	12.2	0.568	719	0.097
		1650	0.0310		791	17.0
231	C20	95	9.00	0.720	318	0.0190
		423	0.0229		350	3.33

Note: For dimensions and material properties see Table II.1A.

Table II.4B Notched Beams, Tested July 1985, Jend/Shah Method (9), $W = 4.00$ in (102 mm), $B = 3.00$ in (76 mm), $E_c = 5.02 \times 10^6$ psi (34.6 GPa)

Fig. No.	Original No.	P_m lb N	$CMOD_e$ in $\times 10^{-3}$ mm	a_e/w	Avg. a_e/W	K^S_{GIC} lb-in $^{-3/2}$ kN-m $^{-3/2}$	G_{IC} lb-in/in 2 N-m/m 2	Avg. G_{IC} lb-in/in 2 N-m/m 2
243	3L.3	692	0.602	0.311		657	0.0861	
		3080	0.0153			723	15.1	
241	2L.3	712	0.650	0.320		693	0.0957	
		3170	0.0165			762	16.8	
239	1L.3	634	0.630	0.337	0.343	647	0.0833	
		2820	0.0160			712	14.6	
237	3S.3	685	0.740	0.353		729	0.106	0.104
		3050	0.0188			802	18.6	18.2
233	1S.3	704	0.770	0.355		754	0.113	
		3130	0.0196			829	19.8	
235	2S.3	738	0.920	0.380		845	0.142	
		3280	0.0234			930	24.9	
255	3L.5	400	1.23	0.546		729	0.106	
		1780	0.0321			802	18.6	
247	2S.5	354	1.12	0.551		655	0.0854	
		1580	0.0284			721	15.0	
251	1L.5	335	1.08	0.554	0.560	625	0.0778	0.0980
		1490	0.0274			688	13.6	17.2
253	2L.5	408	1.28	0.554		761	0.115	
		1820	0.0325			837	20.1	
249	3S.5	358	1.32	0.576		714	0.102	
		1590	0.0335			785	17.9	
245	1S.5	358	1.17	0.576		714	0.102	
		1590	0.0297			785	17.9	
259	3S.7	157	1.18	0.683		452	0.0452	
		700	0.0300			497	7.92	
257	1S.7	173	1.68	0.716	0.714	569	0.0644	0.0496
		770	0.0427			626	11.3	8.69
263	3L.7	145	1.55	0.727		500	0.0497	
		650	0.0394			550	8.71	
261	2L.7	127	1.39	0.730		443	0.0392	
		570	0.0353			487	6.87	

Note: For dimensions and material properties see Table II.1B.

Table II.4C Notched Beams, Tested January 1986, Jend/Shan Method (9),
 $W = 8.00$ in (203 mm), $B = 3.00$ in (76 mm), $E_c = 6.60 \times 10^6$
 psi (45.5 GPa)

Fig. No.	Original No.	P_m lb N	$CMOD_e$ in $\times 10^{-4}$ mm	a_e/w	Avg. a_e/W	$K_{SIC}^{3/2}$ lb-in $^{-3/2}$ kN-m $^{-3/2}$	GIC lb-in/in 2 N-m/m 2	Avg. GIC lb-in/in 2 N-m/m 2
265	N-2-8	640	10.6	0.475	0.475	672	0.0680	0.0680
		2850	0.0269			739	11.9	11.9
267	W-1-8	660	20.6	0.595	0.595	989	0.147	0.147
		2940	0.0523			1090	25.8	25.8
$W = 12.00$ in (305 mm)								
269	CB12	900	21.0	0.547	0.547	948	0.135	0.135
		4010	0.0533			1040	23.7	23.7
271	PW12	810	24.4	0.589	0.591	973	0.143	0.151
		3600	0.0620			1070	25.0	25.5
273	W12	850	26.1	0.592	0.592	1029	0.159	
		3780	0.0663			1130	27.9	

Note: For dimensions and material properties see Table II.1C.

Table II.4D Notched Beams, Tested by Go (4), Jenq/Shah Method (9), $W = 4.00$ in (102 mm), $B = 3.00$ in (76 mm), $E_c = 4.10 \times 10^6$ psi (28.2 GPa)

Fig. No.	Original No.	P_m lb N	CMOD _e in $\times 10^{-3}$ mm	a_e/W	Avg. a_e/W	K_{IC}^S lb-in ^{-3/2} kN-m ^{-3/2}	GIC lb-in/in ² N-m/m ²	Avg. GIC lb-in/in ² N-m/m ²
128	T1	450 2000	0.458	0.310	0.310	426 469	0.0443 7.76	0.0443 7.76
134	T8	450 2000	0.615	0.360	0.360	488 537	0.0582 10.2	0.0582 10.2
133	T7	348 1550	1.06	0.510	0.510	571 628	0.0794 13.9	0.0794 13.9
136	T10	300 1340	1.08	0.540		537 591	0.0703 12.3	
137	T11	300 1340	1.22	0.560	0.560	570 627	0.0793 13.9	0.0600 10.5
130	T4	240 1070	0.965	0.560		456 502	0.0507 8.88	
135	T9	180 801	0.940	0.580		404 444	0.0398 7.00	
129	T3	250 1110	1.97	0.680	0.680	711 782	0.123 21.5	0.123 21.5
131	T5	94 418	1.28	0.720	0.720	314 345	0.0241 4.22	0.0241 4.22
132	T6	99 735	1.99	0.774	0.774	427 470	0.0444 7.78	0.0444 7.78
139	T13	95 423	1.63	0.790	0.795	447 492	0.0486 8.51	0.0400 7.01
138	T12	72 320	2.08	0.800		358 394	0.0313 5.48	

- Notes: 1. $W/C = 0.50$, for complete mix design see Table 2.3.
2. $S = 15$ in (762 mm), $L = 16$ in (406 mm), $m_g = 15.0$ lb (7.08 Kg), $f'_c = 5200$ psi (35.6 MPa)

Table II.4E Notched Beams, Tested by Fartash (11), Jenq/Shah Method (9)
 , $W = 4.00$ in (102 mm), $B = 3.00$ in (76 mm), $E_c = 3.08 \times 10^6$ psi (21.1 GPa)

Fig. No.	Original No.	P_m lb N	$CMOD_e$ in $\times 10^3$ mm	a_e/W	K^{SIC} lb-in ^{-3/2} kN-m ^{-3/2}	GIC lb-in/in ² N-m/m ²
50	1-A5	670	0.560	0.150	399	0.0518
		2980	0.0152		439	9.08
51	1-A6	674	0.630	0.230	511	0.0847
		3000	0.0160		562	14.8
46	1-A1	685	0.670	0.240	536	0.0932
		3050	0.0170		590	16.3
48	1-A3	635	0.650	0.250	509	0.0843
		2830	0.0165		560	14.8
49	1-A4	698	0.750	0.260	576	0.108
		3100	0.0191		634	18.9
52	1-A7	603	0.670	0.270	512	0.0850
		2680	0.0170		563	14.9
47	1-A2	648	0.820	0.290	581	0.110
		2880	0.0208		639	19.3

- Notes: 1. $W/C = 0.78$, for complete mix design see Table 2.2.
 2. $S = 15$ in (381 mm), $L = 16$ in (406 mm), $f'_c = 2920$ psi (20.1 MPa)

Table II.4F Notched Beams, Tested by Fartash (11), Jend/Shah Method (9)
 , $W = 4.00$ in (102 mm), $B = 3.00$ in (76 mm), $E_c = 3.30 \times 10^6$ psi (22.7 GPa)

Fig. No.	Original No.	P_m lb N	$CMOD_E$ in $\times 10^{-3}$ mm	a_e/W	Avg. a_e/W	K^S_{GIC} lb-in $^{-3/2}$ kN-m $^{-3/2}$	GIC lb-in/in 2 N-m/m 2	Avg. GIC lb-in/in 2 N-m/m 2
61	2-A2	300 1340	0.630	0.400		363 399	0.0399 6.99	
60	2-A1	330 1470	0.730	0.410		410 45	0.0509 8.92	
64	2-A5	294 1310	0.690	0.420		375 413	0.0427 7.48	
63	2-A4	368 1640	0.910	0.430	0.426	483 531	0.0706 12.4	0.0526 9.21
65	2-A6	300 1340	0.740	0.430		394 433	0.0469 8.22	
66	2-A7	265 1180	0.690	0.440		357 393	0.0387 6.78	
62	2-A3	368 1640	1.00	0.450		510 561	0.0788 12.8	
76	3-A3	105 467	0.950	0.650	0.650	268 295	0.0217 3.81	0.0203 3.56
79	3-A6	98 436	0.890	0.650		250 275	0.0189 3.31	
74	3-A1	85 378	1.00	0.690		251 276	0.0195 3.42	
75	3-A2	85 378	1.00	0.690		251 276	0.0195 3.42	
77	3-A4	83 369	1.00	0.690	0.690	245 270	0.0183 3.21	0.0197 3.45
78	3-A5	100 445	1.20	0.690		296 326	0.0265 4.64	
80	3-A7	74 329	0.890	0.690		219 241	0.0145 2.54	

Notes: 1. $W/C = 0.78$, for complete mix design see Table 2.2, for dimensions see Table II.4E.

2. $f'_c = 3340$ psi (23.0 MPa)

Table II.5A Notched Beams, Tested by Rood (12), Go Method (4), $W = 4.00$ in (102 mm), $B = 3.00$ in (76 mm), $E_c = 5.34 \times 10^6$ psi (36.8 GPa)

Fig. No.	Original No.	P_m lb N	Ext. a/W	Avg. Ext. a/W	K_{GIC} lb-in ^{-3/2} kN-m ^{-3/2}	G_{IC} lb-in/in ² N-m/m ²	Avg. G_{IC} lb-in/in ² N-m/m ²
221	C15	570	0.510	0.510	935	0.157	0.159
		2540			1030		
223	C16	570	0.510		943	0.160	
		2540			1040		
225	C17	370	0.620	0.620	876	0.138	0.138
		1650			964		
227	C18	290	0.670	0.670	795	0.114	0.114
		1290			875		
229	C19	165	0.820	0.820	932	0.157	0.157
		730			1030		
231	C20	95	0.910	0.910	1239	0.276	0.276
		420			1360		

- Notes: 1. For dimensions and material properties see Table II.1A.
 2. Ext. a/W = Extended a/W; measured by compliance technique.

Table II.5B Notched Beams, Tested by Go (4), Go Method (4), $W = 4.00$ in (102 mm), $B = 3.00$ in (76 mm), $E_c = 4.10 \times 10^6$ psi (28.2 GPa)

Fig. No.	Original No.	P_m lb N	a_i/W	Avg. a_i/W	K^GIC lb-in ^{-3/2} kN-m ^{-3/2}	GIC lb-in/in ² N-m/m ²	Avg. GIC lb-in/in ² N-m/m ²
133	T7	348	0.320	0.335	339	0.0280	0.0421
		1550			373	4.91	
128	T1	450	0.350		475	0.0551	7.29
		2000			523	9.65	
134	T8	450	0.410	0.410	559	0.0762	0.0762
		2000			615	13.4	
130	T4	240	0.490		372	0.0337	
		1070			409	5.90	
129	T3	250	0.510	0.507	410	0.0410	0.0324
		1110			397	7.18	
135	T9	180	0.520		304	0.0225	5.67
		801			334	4.47	
137	T11	300	0.540	0.565	537	0.0703	0.0829
		1340			591	12.3	
136	T10	300	0.590		626	0.0955	14.5
		1340			689	16.7	
131	T5	94	0.650	0.665	240	0.0140	0.0167
		418			264	2.45	
132	T6	99	0.680		282	0.0194	2.93
		440			310	3.40	
139	T13	95	0.700	0.710	292	0.0208	0.0175
		423			257	3.64	
138	T12	72	0.720		241	0.0141	3.07
		320			264	2.47	

Note: For dimensions and material properties see Table II.4D.

Table II.5C Notched Beams, Tested by Fartash (11), Go Method (4), $W = 4.00$ in (102 mm), $B = 3.00$ in (76 mm), $E_c = 3.08 \times 10^6$ psi (21.1 GPa)

Fig. No.	Original No.	P_m lb N	Ext. a/W	Avg. Ext. a/W	K^{GIC} lb-in ^{-3/2} kN-m ^{-3/2}	GIC lb-in/in ² N-m/m ²	Avg. GIC lb-in/in ² N-m/m ²
51	1-A6	674	0.191	0.191	456	0.0674	0.0674
		3000			502	11.8	11.8
49	1-A4	698	0.234	0.234	535	0.0925	0.0925
		3100			589	16.2	16.2
50	1-A5	670	0.334	0.336	678	0.149	0.154
		2980			746	26.1	27.0
46	1-A1	685	0.338		700	0.159	
		2050			770	27.9	
48	1-A3	635	0.353	0.353	676	0.148	0.148
		2830			744	25.9	25.9
47	1-A2	648	0.366	0.366	759	0.187	0.187
		2880			835	32.8	32.8
52	1-A7	603	0.373	0.373	678	0.149	0.149
		3100			746	26.1	26.1

Notes: 1. For dimensions and material properties see Table II.4E.

2. Ext. a/W = (a/W)compliance - 0.14

Table II.5D Notched Beams, Tested by Fartash (11), Go Method (4), $W = 4.00$ in (102 mm), $B = 3.00$ in (76 mm), $E_c = 3.30 \times 10^6$ psi (22.7 GPa)

Fig. No.	Original No.	P_m lb N	Ext. a/W	Avg. Ext. a/W	K^{GIC} lb-in ^{-3/2} kN-m ^{-3/2}	GIC lb-in/in ² N-m/m ²	Avg. GIC lb-in/in ² N-m/m ²
60	2-A1	330	0.488	0.488	508	0.0783	0.0783
		1470			559		
63	2-A4	368	0.521	0.524	629	0.118	0.0979
		1640			692		
64	2-A5	294	0.527		506	0.0777	
		1310		557	13.6		
65	2-A6	300	0.534	0.534	527	0.0843	0.0843
		1340			580		
61	2-A2	300	0.541	0.543	538	0.0879	0.111
		1340			592		
62	2-A3	368	0.545		668	0.135	
		1640		735	237		
66	2-A7	265	0.564	0.564	510	0.0787	0.0787
		1180			561		

Notes: 1. For dimensions and material properties see Tables II.4E, II.4F.

2. Ext. a/W = (a/W)compliance - 0.14

Table II.6A Notched Beams Tested by Fartash (11), K_{IC} Method (4, 8), $W = 4.00$ in (102 mm), $B = 3.00$ in (76 mm), $E_c = 4.63 \times 10^6$ psi (31.9 GPa)

Fig. No.	Original No.	P_m lb N	Ext. a/W	Avg. Ext. a/W	K_{IC} lb-in ^{-3/2} kN-m ^{-3/2}	G_{IC} lb-in/in ² N-m/m ²	Avg. G_{IC} lb-in/in ² N-m/m ²
90	1-B3	1240	0.305	0.306	448	0.0433	0.0467
		5520			493		
94	1-B7	1300	0.306		481	0.0500	8.18
		5790			529		
88	1-B1	1150	0.317		426	0.0392	
		5120			469		
92	1-B5	1230	0.332	0.333	501	0.0542	0.0505
		5470			551		
93	1-B6	1120	0.340		477	0.0491	8.85
		4980			524		
91	1-B4	1230	0.341		524	0.0593	
		5470			576		
89	1-B2	1170	0.367	0.367	563	0.0685	0.0685
		5210			619		

- Notes: 1. $W/C = 0.50$, for complete mix design see Table 2.2.
2. $S = 15$ in (381 mm), $L = 16$ in (406 mm), $f'_c = 6610$ psi (45.5 MPa)
3. Ext. a/W = (a/W)compliance - 0.14

Table II.6B Notched Beams, Tested by Fartash (11), K_{IC} Method (4, 8). $W = 4.00$ in (102 mm), $B = 3.00$ in (76 mm), $E_c = 4.65 \times 10^6$ psi (32.0 GPa)

Fig. No.	Original No.	P_m lb N	Ext. a/W	Avg. Ext. a/W	K_{IC} lb-in ^{-3/2} kN-m ^{-3/2}	G_{IC} lb-in/in ² N-m/m ²	Avg. G_{IC} lb-in/in ² N-m/m ²
102	2-B1	515	0.480		679	0.0991	
		2290			747	17.4	
104	2-B3	470	0.510		669	0.0962	
		2090			736	16.9	
106	2-B5	580	0.510	0.510	806	0.140	0.116
		2580			887	24.5	20.3
108	2-B7	595	0.514		832	0.149	
		2650			915	26.1	
103	2-B2	480	0.518		683	0.100	
		2140			751	17.5	
107	2-B6	498	0.527		719	0.111	
		2220			791	19.4	
105	2-B4	550	0.640	0.640	743	0.119	0.119
		2450			817	20.8	20.8

Notes: 1. For dimensions and material properties see Table II.6A.

2. $f'_c = 6650$ psi (45.8 MPa)

Table II.7A Precracked Beams, Tested by Rood (12), RILEM Method (10), $W = 4.00$ in (102 mm), $B = 3.00$ in (76 mm), $E_c = 5.34 \times 10^6$ psi (36.8 GPa)

Fig. No.	Original No.	a_i/W	Avg. a_i/W	δ_0 in $\times 10^{-3}$ mm	W_0 lb-in N-m	G_f lb-in/in ² N-m/m ²	Avg. G_f lb-in/in ² N-m/m ²
180	B9	0.276		14.2	5.89	0.703	
				0.361	0.666	123	
166	B1	0.301		12.0	4.72	0.585	
				0.305	0.533	102	
210	C7	0.296		14.0	6.00	0.736	
				0.356	0.678	129	
184	B11	0.307		16.2	7.76	0.964	
				0.411	0.877	169	
198	C1	0.314	0.336	15.8	6.56	0.827	0.714
				0.401	0.741	145	125
182	B10	0.330		13.3	5.86	0.755	
				0.338	0.662	132	
200	C2	0.326		14.0	4.69	0.607	
				0.356	0.530	106	
168	B2	0.362		12.0	4.85	0.658	
				0.305	0.548	115	
212	C8	0.398		12.2	4.13	0.598	
				0.310	0.467	105	
170	B3	0.448		11.9	4.47	0.703	
				0.302	0.505	123	
186	B14	0.506		10.2	2.47	0.444	
				0.259	0.279	77.8	
188	B16	0.514		15.3	3.37	0.619	
				0.389	0.381	108	
190	B17	0.521		11.6	2.27	0.426	
				0.295	0.257	74.6	
204	C4	0.525	0.549	11.8	2.43	0.459	0.497
				0.300	0.275	80.4	87.1
214	C9	0.593		11.6	2.60	0.569	
				0.295	0.294	99.7	
216	C10	0.587		14.3	2.07	0.463	
				0.363	0.234	81.1	
172	B4	0.597		10.5	2.26	0.501	
				0.26	0.250	87.8	
196	B20	0.671		13.3	1.49	0.430	
				0.338	0.168	75.3	
208	C6	0.673	0.705	13.7	1.41	0.414	0.502
				0.348	0.159	72.5	87.9
192	B18	0.790		13.8	1.48	0.673	
				0.351	0.167	118	
194	B19	0.685		11.8	1.23	0.490	
				0.300	0.139	85.8	

Table II.7A (Continued)

Fig. No.	Original No.	a_i/W	Avg. a_i/W	δ_0 in $\times 10^{-3}$	W_0 lb-in	G_F lb-in/in ²	Avg. G_F lb-in/in ²
218	C11	0.746		13.6	0.940	0.378	
				0.345	0.106	66.2	
178	B8	0.790		15.3	0.730	0.384	
				0.390	0.0825	67.3	
175	B7	0.808	0.794	11.0	0.590	0.331	0.386
				0.279	0.0677	58.0	67.6
220	C12	0.812		19.7	0.560	0.384	
				0.500	0.0633	67.3	
174	B6	0.816		14.4	0.780	0.455	
				0.366	0.0881	79.7	

Note : For dimension and material properties see Table II.1A.

Table II.8A Precracked Beams, Tested by Rood (12), Modified RILEM Method (14), $W = 4.00$ in (102 mm), $B = 3.00$ in (76 mm), $E_c = 5.34 \times 10^6$ psi (38.6 GPa)

Fig. No.	Original No.	a_i/W	Avg. a_i/W	$\bar{\delta}_0$ in $\times 10^{-3}$ mm	U lb-in N-m	\bar{G}_F lb-in/in ² N-m/m ²	Avg. \bar{G}_F lb-in/in ² N-m/m ²
180	B9	0.28		5.50	2.18	0.260	
				0.140	0.246	45.6	
166	B1	0.30		4.30	1.52	0.189	
				0.109	0.172	33.1	
210	C7	0.30		6.30	2.86	0.350	
				0.160	0.323	61.3	
184	B11	0.31		7.20	3.12	0.389	
				0.183	0.353	68.2	
198	C1	0.32	0.368	7.80	2.77	0.350	0.296
				0.198	0.313	61.7	51.9
182	B10	0.33		5.10	1.96	0.255	
				0.130	0.221	44.7	
200	C2	0.33		6.90	1.76	0.231	
				0.175	0.200	40.5	
168	B2	0.36		4.40	2.16	0.291	
				0.112	0.240	51.0	
212	C8	0.40		7.10	2.19	0.318	
				0.180	0.247	55.7	
170	B3	0.45		5.40	2.09	0.328	
				0.137	0.236	57.5	
186	B14	0.50		5.80	1.51	0.269	
				0.147	0.171	47.1	
188	B16	0.52		8.40	1.44	0.270	
				0.213	0.163	47.3	
190	B17	0.52		6.20	1.51	0.279	
				0.157	0.171	48.9	
204	C4	0.52	0.55	6.20	1.25	0.236	0.296
				0.157	0.141	41.3	51.9
214	C9	0.59		8.00	1.73	0.379	
				0.203	0.195	66.4	
216	C10	0.59		6.00	1.11	0.243	
				0.152	0.125	42.6	
172	B4	0.60		4.00	1.86	0.393	
				0.102	0.210	69.7	
196	B20	0.67		5.70	0.730	0.207	
				0.145	0.0825	36.3	
208	C6	0.67	0.68	0.690	0.720	0.211	0.217
				0.0184	0.0814	37.0	38.0
192	B18	0.68		7.30	0.890	0.261	
				0.185	0.101	45.7	

Table II.8A (Continued)

Fig. No.	Original No.	a_i/W	Avg. a_i/W	$\bar{\delta}_0$ in $\times 10^{-3}$ mm	U lb-in N-m	\bar{G}_F lb-in/in ² N-m/m ²	Avg. \bar{G}_F lb-in/in ² N-m/m ²
194	B19	0.69		6.00 0.152	0.610 0.0690	0.189 33.1	
218	C11	0.75		6.00 0.152	0.520 0.0588	0.203 35.6	
178	B8	0.79		4.80 0.122	0.390 0.0441	0.184 32.2	
176	B7	0.81	0.80	3.50 0.0889	0.210 0.0237	0.115 20.1	0.185 32.4
220	C12	0.81		6.80 0.173	0.32 0.0362	0.189 33.1	
174	B6	0.82		6.10 0.155	0.420 0.0475	0.232 40.6	

- Notes: 1. For dimensions and material properties see Table II.1A.
2. a_i/W = initial a_i/W ; measured by dye.
3. $J_{IC} = 0.270$ lb-in/in² (47.3 N-m/m²) - based on initial a (4).

Table II.8B Precracked Beams, Tested by Go (4), Modified RILEM Method (14), $W = 4.00$ in (102 mm), $B = 3.00$ in (76 mm), $E_C = 4.10 \times 10^6$ psi (28.2 GPa)

Fig. No.	Original No.	a_i/W	Avg. a_i/W	δ_0 in $\times 10^{-3}$ mm	U lb-in N-m	G_F lb-in/in ² N-m/m ²	Avg. G_F lb-in/in ² N-m/m ²
157	N9	0.276	0.276	6.00 0.152	3.13 0.354	0.371 65.0	0.232 65.0
158	N10	0.374		6.15 0.156	2.17 0.245	0.301 52.7	
149	N1	0.412	0.400	5.50 0.140	2.06 0.233	0.304 53.3	0.324 56.8
159	N11	0.413		6.70 0.170	2.48 0.280	0.366 64.1	
150	N2	0.490		5.30 0.135	1.78 0.201	0.304 53.3	
160	N12	0.490	0.497	4.73 0.167	1.48 44.5	0.254 44.5	0.290 50.8
151	N3	0.512		6.60	1.72	0.311	
161	N13	0.561	0.561	4.45 0.113	1.17 0.132	0.235 41.1	0.235 41.1
162	N14	0.575	0.575	6.65 0.169	1.65 0.186	0.343 60.1	0.343 60.1
153	N5	0.610	0.610	5.26 0.134	1.16 0.131	0.265 46.4	0.265 46.4
152	N4	0.620	0.620	6.65 0.169	1.45 0.164	0.340 59.6	0.340 59.6
163	N15	0.633	0.633	3.65 0.0927	0.74 0.0836	0.180 31.5	0.180 31.5
164	N16	0.640	0.640	3.90 0.0991	0.880 0.0994	0.217 38.0	0.217 38.0
154	N6	0.719		4.91 0.125	0.740 0.0836	0.241 38.0	
155	N7	0.725	0.724	2.30 0.0580	0.400 0.0452	0.132 23.1	0.175 30.7
156	N8	0.728		2.83 0.0719	0.460 0.0520	0.154 27.0	

Notes: 1. For dimensions and material properties see Table II.4D.

2. $J_{IC} = 0.299$ lb-in/in² (52.4 N-m/m²) - based on initial a (4).

Table II.9A Precracked Beams, Tested by Rood (12), Direct Energy Method (4), $W = 4.00$ in (102 mm), $B = 3.00$ in (76 mm), $E_c = 5.34 \times 10^6$ psi (36.8 GPa)

Fig. No.	Original No.	Ext. a/W	Avg. Ext. a/W	$\bar{\delta}_0$ in $\times 10^{-3}$ mm	U lb-in N-m	\bar{G}_I lb-in/in ² N-m/m ²	Avg. \bar{G}_I lb-in/in ² N-m/m ²
182	B10	0.400		5.10	1.96	0.246	
				0.133	0.221	43.1	
184	B11	0.430		7.20	3.12	0.411	
				0.183	0.353	72.0	
180	B9	0.450	0.442	5.50	2.18	0.299	0.311
				0.140	0.246	52.4	54.5
200	C2	0.450		6.90	1.76	0.246	
				0.175	0.200	43.1	
198	C1	0.480		7.80	2.77	0.352	
				0.198	0.313	61.7	
186	B14	0.580		5.80	1.51	0.269	
				0.147	0.171	47.1	
204	C4	0.580	0.593	6.20	1.25	0.232	0.217
				0.157	0.141	40.6	47.5
188	B16	0.590		8.40	1.44	0.278	
				0.213	0.163	48.7	
190	B17	0.620		6.20	1.51	0.306	
				0.157	0.171	53.6	
192	B18	0.770		7.30	0.890	0.316	
				0.185	0.101	55.4	
208	C6	0.780	0.790	6.90	0.720	0.273	0.291
				0.175	0.0814	47.8	51.0
194	B19	0.790		6.00	0.610	0.243	
				0.152	0.0689	42.6	
196	B20	0.820		5.70	0.730	0.330	
				0.145	0.0825	57.8	

- Notes:
1. For dimensions and material properties see Table II.1A.
 2. Ext. a/W = Extended a/W; measured by compliance technique.
 3. $J_{IC} = 0.239$ lb-in/in² (41.9 N-m/m²) - based on extended a (4).

Table II.9B Precracked Beams, Tested by Go (4), Direct Energy Method (4), $W = 4.00$ in (102 mm), $B = 3.00$ in (76 mm), $E_C = 4.10 \times 10^6$ psi (28.2 GPa)

Fig. No.	Original No.	Ext. a/W	Avg. Ext. a/W	\bar{S}_0 in $\times 10^{-3}$ mm	U lb-in N-m	\bar{G}_{IC} lb-in/in ² N-m/m ²	Avg. \bar{G}_{IC} lb-in/in ² N-m/m ²
157	N9	0.490	0.490	6.00 0.152	3.13 0.354	0.458 80.2	0.450 80.2
158	N10	0.571	0.571	6.15 0.156	2.17 0.245	0.383 67.1	0.383 67.1
149	N1	0.574	0.577	5.50 0.140	2.06 0.233	0.365 63.9	0.318 55.7
160	N12	0.585		4.73 0.120	1.48 0.167	0.271 47.5	
159	N11	0.605	0.609	6.70 0.170	2.48 0.280	0.474 83.0	0.411 72.0
150	N2	0.612		5.30 0.135	1.78 0.201	0.348 61.0	
161	N13	0.640	0.652	4.50 0.114	1.18 0.133	0.252 44.1	0.323 56.6
151	N3	0.663		6.60 0.168	1.72 0.194	0.392 68.7	
162	N14	0.716		6.70 0.170	1.65 0.186	0.448 78.5	
153	N5	0.731	0.729	5.28 0.134	1.16 0.131	0.335 58.7	0.405 71.0
152	N4	0.740		6.65 0.169	1.45 0.164	0.433 75.9	

- Notes:
1. For dimensions and material properties see Table II.4D.
 2. Ext. a/W = Extended a/W; measured by compliance technique.
 3. $J_{IC} = 0.346$ lb-in/in² (60.6 N-m/m²) - based on extended a (4).

Table II.10A Precracked Beams, Tested by Rood (12), Jenq/Shah Method (9), $W = 4.00$ in (102 mm), $B = 3.00$ in (76 mm), $E_c = 5.34 \times 10^6$ psi (36.8 GPa)

Fig. No.	Original No.	P_m lb N	$CMOD_e$ in mm	a_e/W	Avg. a_e/W	K^S_{IC} lb-in ^{-3/2} kN-m ^{-3/2}	G_{IC} lb-in/in ² N-m/m ²	Avg. G_{IC} lb-in/in ² N-m/m ²
179	B9	905	6.55	0.290		812	0.123	
		4030	0.0166			893	21.5	
209	C7	865	6.25	0.290		776	0.113	
		3850	0.0159			854	19.8	
165	B1	870	6.25	0.290		780	0.114	
		3870	0.0159			858	20.0	
183	B11	960	8.20	0.320	0.321	935	0.164	0.137
		4270	0.0208			1030	28.7	24.0
167	B2	780	7.55	0.340		802	0.120	
		3470	0.0192			882	21.0	
199	C2	780	7.50	0.340		802	0.120	
		3470	0.0191			882	21.0	
181	B10	910	9.00	0.350		961	0.173	
		4050	0.0229			1060	30.3	
197	C1	890	8.80	0.350		940	0.165	
		3960	0.0224			1030	28.9	
201	C3	460	12.6	0.540		823	0.127	
		2050	0.0320			905	22.3	
203	C4	425	12.2	0.540		761	0.108	
		1890	0.0310			837	18.9	
185	B14	480	15.5	0.560	0.560	912	0.156	0.145
		2140	0.0394			1000	27.3	25.4
187	B16	520	16.2	0.560		988	0.183	
		2310	0.0411			1090	32.1	
171	B4	490	17.8	0.580		990	0.184	
		2180	0.0452			1090	32.2	
189	B17	380	13.8	0.580		768	0.110	
		1690	0.0351			845	19.3	
193	B19	220	23.6	0.730		768	0.110	
		979	0.0599			845	19.3	
191	B18	190	21.9	0.740		694	0.0902	
		846	0.0556			763	15.8	
195	B20	220	23.8	0.740	0.757	803	0.121	0.106
		980	0.0605			883	21.2	18.6
205	C5	165	24.1	0.770		697	0.0909	
		735	0.0612			767	15.9	
207	C6	190	27.2	0.770		802	0.120	
		846	0.0691			882	21.0	
217	C11	160	28.4	0.790		752	0.106	
		712	0.0721			827	18.6	

Note: For dimensions and material properties see Table II.1A.

Table II.10B Precracked Beams, Tested by Fartash (11), Jenq/Shah Method (9), $W = 4.00$ in (102 mm), $B = 3.00$ in (76 mm), $E_c = 3.08 \times 10^6$ psi (21.2 GPa)

Fig. No.	Original No.	P_m lb in $\times 10^{-4}$ N	$CMOD_e$ mm $\times 10^{-2}$	a_e/W	Avg. a_e/W	K^SIC lb-in $^{-3/2}$ kN-m $^{-3/2}$	GIC lb-in/in 2 N-m/m 2	Avg. GIC lb-in/in 2 N-m/m 2
59	1-A16	928	6.30	0.180		607	0.120	
		4130	1.60			668	21.0	
58	1-A15	890	6.40	0.190	0.187	600	0.117	0.187
		3960	1.63			660	20.5	
57	1-A14	862	6.20	0.190		581	0.110	
		3840	1.57			639	19.3	
55	1-A12	895	6.90	0.200		621	0.125	
		3980	1.75			683	21.9	
54	1-A11	848	6.50	0.200	0.203	589	0.113	0.126
		3770	1.65			648	19.8	
53	1-A10	918	7.50	0.210		656	0.140	
		4090	1.91			722	24.5	
56	1-A13	752	8.60	0.270	0.270	638	0.132	0.132
		3350	2.18			702	23.1	

- Notes: 1. $C/W = 0.78$, for complete mix design see Table 2.2.
2. $S = 15$ in (381 mm), $L = 16$ in (406 mm), $m_g = 15.6$ lb (7.08 Kg), $f'_c = 2920$ psi (20.1 MPa)

Table II.10C Precracked Beams, Tested by Fartash (11), Jenq/Shah Method (9), $W = 4.00$ in (102 mm), $B = 3.00$ in (76 mm), $E_c = 3.30 \times 10^6$ psi (22.7 GPa)

Fig. No.	Original No.	Pm lb in x 10 ⁻⁴ N mm x 10 ⁻²	CMOD _e	a _e /W	Avg. a _e /W	K ^S _{IC} lb-in ^{-3/2} kN-m ^{-3/2}	GIC lb-in/in ² N-m/m ²	Avg. GIC lb-in/in ² N-m/m ²
70	2-A13	675	1.00	0.340	0.340	694	0.146	0.146
		3000	0.254			763	25.6	
68	2-A11	585	1.10	0.380		670	0.136	
		2600	0.279			737	23.8	
72	2-A15	548	1.10	0.390	0.393	645	0.126	0.139
		2440	0.279			710	22.1	
71	2-A14	575	1.20	0.400		695	0.147	24.4
		2560	0.305			765	25.8	
69	2-A12	572	1.20	0.400		692	0.145	
		2550	0.305			761	25.4	
73	2-A16	445	1.00	0.420	0.420	568	0.0978	0.0978
		1980	0.254			625	17.1	
67	2-A10	490	1.40	0.460	0.460	698	0.148	0.148
		2180	0.356			768	25.9	
84	3-A13	338	16.0	0.550	0.550	623	0.118	0.118
		1500	0.406			685	20.7	
85	3-A14	270	16.0	0.590	0.590	563	0.0961	0.0961
		1200	0.406			619	16.8	
87	3-A16	180	17.0	0.660	0.660	475	0.0685	0.0685
		801	0.432			523	12.0	
82	3-A11	155	24.0	0.720	0.720	518	0.0814	0.0814
		690	0.610			570	14.3	
81	3-A10	150	27.0	0.740		548	0.0909	
		668	0.686			603	15.9	
86	3-A15	157	31.0	0.750	0.750	601	0.109	0.106
		699	0.788			661	19.1	
83	3-A12	155	34.0	0.760		622	0.117	18.6
		690	0.864			684	20.5	

Notes: 1. $C/W = 0.78$, for complete mix design see Table 2.2.

2. $S = 15$ in (381 mm), $L = 16$ in (406 mm), $m_g = 15.6$ lb (7.08 Kg)

Table II.10C (Continued)

3. For beams no. 2-A10 to 2-A16, $f'_c = 3340$ psi (23.0 MPa)
4. for beams no. 3-A10 to 3-A16, $f'_c = 3330$ psi (23.0 MPa)

Table II.10D Precracked Beams, Tested by Go (4), Jend/Shah Method (9),
 $W = 4.00$ in (102 mm), $B = 3.00$ in (76 mm), $E_c = 4.10 \times 10^6$
 psi (28.2 GPa)

Fig. No.	Original No.	P_m lb N	$CMOD_e$ in $\times 10^{-3}$ mm	a_e/W	Avg. a_e/W	K_{SIC}^{SIC} lb-in ^{-3/2} kN-m ^{-3/2}	G_{IC} lb-in/in ² N-m/m ²	Avg. G_{IC} lb-in/in ² N-m/m ²
144	P7	1095 4870	0.710 0.0180	0.220		806 887	0.159 27.9	
145	P8	1090 4850	0.725 0.0184	0.220	0.223	803 883	0.157 27.5	0.178 31.2
140	P2	1250 5560	0.855 0.0217	0.230		947 1040	0.219 38.4	
141	P3	765 3400	1.19 0.0302	0.380		876 964	0.187 32.8	
147	P10	795 3540	1.35 0.0343	0.400	0.393	961 1060	0.225 39.4	0.223 39.1
142	P4	800 3560	1.34 0.0340	0.400		967 1060	0.228 39.9	
146	P9	800 3560	2.71 0.0688	0.530	0.530	1390 1530	0.471 82.5	0.471 82.5
143	P5	505 2250	1.96 0.0498	0.550	0.560	931 1020	0.211 37.0	0.194 34.0
148	P11	435 1940	1.91 0.0485	0.570		852 937	0.177 31.0	

Note: For dimensions and material properties see Table II.4D.

Table II.10E Precracked Beams, Tested by Huang (8), Jenq/Shah Method (9), $W = 4.00$ in (102 mm), $B = 3.00$ in (76 mm), $E_c = 3.21 \times 10^6$ psi (22.1 GPa) and $E_c = 4.93 \times 10^6$ psi (34.0 GPa)

$E_c = 3.21 \times 10^6$ psi (22.1 GPa)									
Fig. No.	Original No.	P_m lb N	$CMOD_e$ in $\times 10^{-3}$ mm	a_e/W	Avg. a_e/W	K_{IC}^B lb-in ^{-3/2} kN-m ^{-3/2}	G_{IC} lb-in/in ² N-m/m ²	Avg. G_{IC} lb-in/in ² N-m/m ²	
1	S1S3-1	820	0.475	0.160	0.160	504	0.0793	0.0793	
		3650	0.0121			554	13.8	13.8	
2	S1S3-2	565	1.23	0.330	0.330	565	0.100	0.100	
		2510	0.0312			662	17.5	17.5	
4	S1S3-4	180	0.650	0.500	0.500	287	0.0256	0.0256	
		801	0.0165			316	4.56	4.56	
3	S1S3-3	248	2.25	0.650	0.650	632	0.125	0.125	
		1100	0.0577			695	21.9	21.9	
$E_c = 4.93 \times 10^6$ psi (34.0 GPa)									
26	S2F3-1	1020	0.490	0.200	0.210	708	0.102	0.119	
		4540	0.0124			779	17.9	20.8	
23	S2S3-1	1110	0.610	0.220		817	0.136		
		4940	0.0155			899	23.8		
27	S2F3-2	432	0.84	0.460	0.465	615	0.0768	0.0831	
		1920	0.0213			677	13.5	14.6	
24	S2S3-2	453	0.95	0.470		663	0.0893		
		2020	0.0241			729	15.6		
25	S2S3-3	520	1.61	0.540	0.550	931	0.176	0.167	
		2310	0.0409			1020	30.8	29.3	
28	S2F3-3	464	1.59	0.560		882	0.158		
		2060	0.0404			970	27.7		

- Notes:
1. For beams no. S1S3, $W/C = 0.78$, for complete mix design see Table 2.1, $f'_c = 3170$ psi (21.8 MPa)
 2. For beams no. S2S3 and S2F3, $W/C = 0.50$, for complete mix design see Table 2.1, $f'_c = 7480$ psi (21.8 MPa)
 3. For all beams, $S = 15$ in (381 mm), $L = 16.3$ in (413 mm)

Table II.10F Precracked Beams, Tested by Huang (8), Jenq/Shah Method (9), $W = 8.00$ in (203 mm), $B = 4$ in (102 mm), $E_c = 3.41 \times 10^6$ psi (23.5 GPa) and $E_c = 5.05 \times 10^6$ psi (34.8 GPa)

$E_c = 3.41 \times 10^6$ psi (23.5 GPa)

Fig. No.	Original No.	P_m lb in x 10^{-3} N	$CMOD_e$ mm	a_e/W	Avg. a_e/W	K^{SIC} lb-in $^{-3/2}$ N-m $^{-3/2}$	GIC lb-in/in 2 N-m/m 2	Avg. GIC lb-in/in 2 N-m/m 2
10	L1S3-1	3080 13710	0.650 0.0165	0.0650	0.0685	584 642	0.0999 17.5	0.0928 16.3
13	L1F3-1	2780 12370	0.650 0.0165	0.0720		541 595	0.0857 15.0	
11	L1S3-2	1310 5830	2.05 0.0521	0.350	0.350	587 646	0.101 17.7	0.0988 17.3
14	L1F3-2	1280 5700	1.86 0.0472	0.350		574 631	0.0965 16.9	
15	L1F3-3	1100 4910	1.98 0.0503	0.380	0.380	536 590	0.0844 14.8	0.0844 14.8
12	L1S3-3	460 2050	4.52 0.115	0.670	0.670	535 589	0.0839 14.7	0.0839 14.7

$E_c = 5.05 \times 10^6$ psi (34.8 GPa)

37	L2F3-1	2550 11350	1.45 0.0368	0.230	0.230	820 902	0.133 23.3	0.133 23.3
35	L2S3-1	2300 10240	1.75 0.0445	0.290	0.290	875 963	0.152 26.6	0.152 26.6
38	L2F3-2	880 3900	3.44 0.0874	0.590	0.590	779 857	0.120 21.0	0.120 21.0
36	L2S3-2	900 4010	3.39 0.0861	0.760	0.760	1533 1710	0.465 81.5	0.465 81.5
39	L2F3-3	240 1070	3.90 0.0991	0.770	0.770	1010 1110	0.203 35.6	0.203 35.6

- Notes: 1. For beams no. L1S3 and L1F3, $W/C = 0.78$, for complete mix design see Table 2.1, $f'_c = 3570$ psi (24.6 MPa)
2. For beams no. L2S3 and L2F3, $W/C = 0.50$, for complete mix design see Table 2.1, $f'_c = 7980$ psi (52.9 MPa)

Table II.10F (Continued)

3. For all beams, $S = 24$ (610 mm), $L = 25$ in (635 mm)

Table II.11A Precracked Beams, Tested by Rood (12), Go Method (4), $W = 4.00$ in (102 mm), $B = 3.00$ in (76 mm), $E_c = 5.34 \times 10^6$ psi (36.8 GPa)

Fig. No.	Original No.	P_m lb N	Ext. a/W	Avg. Ext. a/W	K^{GIC} lb-in ^{-3/2} kN-m ^{-3/2}	GIC lb-in/in ² N-m/m ²	Avg. GIC lb-in/in ² N-m/m ²
181	B10	905 4030	0.400		1109 1220	0.230 40.3	
183	B11	955 4250	0.430		1253 1390	0.294 51.5	
179	B9	915 4070	0.450	0.442	1268 1400	0.301 52.7	0.273 47.8
199	C2	770 3430	0.450		1067 1170	0.213 37.3	
197	C1	890 3960	0.480		1325 1460	0.329 57.6	
201	C3	470 2090	0.560		893 983	0.149 26.1	
185	B14	480 2140	0.580		985 1080	0.182 31.9	
203	C4	445 1980	0.580	0.586	885 974	0.147 25.8	0.168 29.4
187	B16	525 2340	0.590		1088 1190	0.222 38.9	
189	B17	390 1740	0.620		868 955	0.141 24.7	
191	B18	225 1000	0.770		965 1060	0.174 30.5	
207	C6	190 846	0.780	0.790	845 930	0.134 23.5	0.186 32.6
193	B19	190 846	0.790		893 982	0.149 26.1	
195	B20	220 979	0.820		1240 1360	0.288 50.5	

- Notes: 1. For dimensions and material properties see Table II.1A.
 2. Ext. a/W = Extended a/W; measured by compliance technique.

Table II.11B Precracked Beams, Tested by Fartash (11), Go Method (4), $W = 4.00$ in (102 mm), $B = 3.00$ in (76 mm), $E_c = 3.08 \times 10^6$ psi (21.2 GPa)

Fig. No.	Original No.	P_m lb N	Ext. a/W	Avg. a/W	K_{IC} lb-in ^{-3/2} kN-m ^{-3/2}	GIC lb-in/in ² N-m/m ²	Avg. GIC lb-in/in ² N-m/m ²
57	1-A14	862 3840	0.238		668 735	0.145 25.4	
53	1-A10	918 4090	0.245	0.243	726 799	0.171 30.0	0.164 28.7
59	1-A16	928 4130	0.245		734 807	0.175 30.7	
55	1-A12	895 3980	0.256		794 873	0.205 35.9	
58	1-A15	890 3960	0.264	0.263	743 817	0.179 31.4	0.184 32.2
54	1-A11	848 3770	0.269		718 873	0.167 35.9	
56	1-A13	752 3350	0.325	0.325	742 816	0.179 31.4	0.179 31.4

Notes: 1. For dimensions and material properties see Table II.10B.

2. Ext. a/W = (a/W)compliance - 0.14

Table II.11C Precracked Beams, Tested by Fartash (11), Go Method (4), $W = 4.00$ in (102 mm), $B = 3.00$ in (76 mm), $E_c = 3.08 \times 10^6$ psi (21.2 GPa)

Fig. No.	Original No.	P_m lb N	Ext. a/W	Avg. a/W	K_{IC}^{GIC} lb-in ^{-3/2} kN-m ^{-3/2}	GIC lb-in/in ² N-m/m ²	Avg. GIC lb-in/in ² N-m/m ²
70	2-A13	675 3000	0.395	0.405	805 889	0.210 36.8	0.193 33.8
68	2-A11	585 2600	0.414		735 809	0.175 30.7	
71	2-A14	575 2560	0.423	0.423	740 814	0.178 31.2	0.170 29.8
72	2-A15	548 2440	0.423		705 776	0.161 28.2	
69	2-A12	572 2550	0.434	0.434	759 835	0.187 32.8	0.187 32.8
73	2-A16	445 980	0.453	0.453	766 843	0.190 33.3	0.190 33.3
67	2-A10	490 2180	0.471	0.471	720 792	0.168 29.4	0.168 29.4

- Notes: 1. For dimensions and material properties see Table II.10C.
 2. Ext. a/W = (a/W)compliance - 0.14

Table II.11D Precracked Beams, Tested by Go (4), Go Method (4), $W = 4.00$ in (102 mm), $B = 3.00$ in (76 mm), $E_c = 4.10 \times 10^6$ psi (28.2 GPa)

Fig. No.	Original No.	P_m lb N	Ext. a/W	Avg. Ext. a/W	K_{GIC} lb-in ^{-3/2} kN-m ^{-3/2}	G_{IC} lb-in/in ² N-m/m ²	Avg. G_{IC} lb-in/in ² N-m/m ²
145	P8	1080 4810	0.140		624 686	0.0949 16.6	
140	P2	1250 5560	0.160	0.153	769 846	0.144 25.2	0.116 20.3
144	P7	1080 4810	0.160		664 730	0.108 18.9	
141	P3	768 3420	0.320		748 823	0.136 23.8	
146	P9	810 3600	0.320	0.335	789 867	0.152 26.6	0.158 27.7
142	P4	800 3560	0.350		845 930	0.174 30.5	
147	P10	790 3520	0.350		834 917	0.170 29.8	
143	P5	490 2180	0.510	0.510	803 883	0.157 27.5	0.121 21.2
148	P11	360 1600	0.510		590 649	0.0850 14.9	

- Notes. 1. For dimensions and material properties see Table II.4D.
 2. Ext. a/W = (a/W)compliance - 0.14

Table II.11E Precracked Beams, Tested by Huang (8), Go Method (4), $W = 4.00$ in (102 mm), $B = 3.00$ in (76 mm), $E_c = 3.21 \times 10^6$ psi (22.1 GPa) and $E_c = 4.93 \times 10^6$ psi (34.0 GPa)

$E_c = 4.93 \times 10^6$ psi (34.0 GPa)							
Fig. No.	Original No.	P_m lb N	Ext. a/W	Avg. a/W	K^G_{IC} lb-in ^{-3/2} kN-m ^{-3/2}	GIC lb-in/in ² N-m/m ²	Avg. GIC lb-in/in ² N-m/m ²
1	S1S3-1	820 3650	0.135	0.135	466 513	0.0676 11.8	0.0676 11.8
2	S1S3-2	565 2510	0.360	0.360	613 674	0.117 20.5	0.117 20.5
3	S1S3-3	248 1100	0.597	0.597	530 583	0.0874 15.3	0.0874 15.3
$E_c = 4.93 \times 10^6$ psi (34.0 GPa)							
23	S2S3-1	1110 4940	0.123	0.123	606 667	0.0744 13.0	0.0744 13.0
26	S2F3-1	1020 4540	0.166	0.166	639 703	0.0829 14.5	0.0829
27	S2F3-2	432 1920	0.329	0.342	431 474	0.0377 6.60	0.0426 7.46
24	S2S3-2	453 2020	0.354		484 532	0.0475 8.32	
28	S2F3-3	464 2060	0.429	0.435	607 668	0.0747 13.1	0.0874 15.3
25	S2S3-3	520 2310	0.441		703 773	0.100 17.5	

- Notes:
1. For beams no. S1S3, $W/C = 0.78$, for complete mix design see Table 2.1, $f'_c = 3170$ psi (21.8 MPa)
 2. For beams no. S2F3 and S2S3, $W/C = 0.50$, for complete mix design see Table 2.1, $f'_c = 7480$ psi (51.5 MPa)
 3. For all beams, $S = 15$ in (381 mm), $L = 16.3$ in (413 mm)

Table II.11F. Precracked Beams, Tested by Huang (8), Go Method (4), $W = 8.00$ in (203 mm), $B = 4.00$ in (102 mm), $E_c = 3.41 \times 10^6$ psi (23.5 GPa) and $E_c = 5.05 \times 10^6$ psi (22.1 GPa)

$E_c = 3.41 \times 10^6$ psi (23.5 GPa)							
Fig. No.	Original No.	P_m lb N	Ext. a/W	Avg. a/W	K^{GIC} $lb\text{-in}^{-3/2}$ $kN\text{-m}^{-3/2}$	GIC $lb\text{-in}/in^2$ $N\text{-m}/m^2$	Avg. GIC $lb\text{-in}/in^2$ $N\text{-m}/m^2$
13	L1F3-1	2780 12400	0.085	0.085	755 831	0.167 29.3	0.167 29.3
10	L1S3-1	3080 1370	0.123	0.123	951 1050	0.265 46.4	0.265 46.4
14	L1F3-2	1280 5700	0.394		861 947	0.218 38.2	
11	L1S3-2	1310 5830	0.401	0.404	898 988	0.237 41.5	0.212 37.1
15	L1F3-3	1104 4910	0.416		789 867	0.182 31.9	
12	L1S3-3	460 2050	0.641	0.641	643 707	0.121 21.2	0.121 21.2
$E_c = 5.05 \times 10^6$ psi (22.1 GPa)							
37	L2F3-1	2550 11340	0.298	0.292	1321 1450	0.345 60.4	0.345 60.4
35	L2S3-1	2300 10200	0.391	0.391	1535 1690	0.467 81.8	0.467 81.8
36	L2S3-2	910 4050	0.601	0.601	1112 1220	0.245 42.9	0.237 41.5
38	L2F3-2	880 3920	0.601		1075 1183	0.229 40.1	

- Notes.
1. For beams no. L1F3 and L1S3, $W/C = 0.78$, for complete mix design see Table 2.1, $f'_c = 3570$ psi (24.6 MPa)
 2. For beams no. L2F3 and L2S3, $W/C = 0.50$, for complete mix design see Table 2.1, $f'_c = 7680$ psi (52.9 MPa)
 3. For all beams, $S = 24$ in (610 mm), $L = 25$ in (635 mm)

Table II.12A Precracked Beams, Tested by Fartash (11), KIC Method (4, 8), $W = 4.00$ in (102 mm), $B = 3.00$ in (76 mm), $E_c = 4.63 \times 10^6$ psi (31.9 GPa)

Fig. No.	Original No.	P_m lb N	Ext. a/W	Avg. Ext. a/W	K _{IC} lb-in ^{-3/2} kN-m ^{-3/2}	G _{IC} lb-in/in ² N-m/m ²	Avg. G _{IC} lb-in/in ² N-m/m ²
97	1-B12	1520	0.234	0.234	253	0.0138	0.0144
		6740			278	2.42	2.52
98	1-B13	1580	0.234		263	0.0149	
		7030			289	2.61	
95	1-B10	1710	0.241	0.241	459	0.0455	0.0403
		7610			505	7.97	7.06
100	1-B15	1470	0.241		403	0.0351	
		6680			443	6.15	
96	1-B11	1565	0.242		420	0.0381	
99	1-B14	6960	0.242	0.242	462	6.68	
		1610			447	0.0432	0.0402
101	1-B16	7160	0.242		492	7.57	7.04
		1540			426	0.0392	
		6830			469	6.87	

- Notes:
1. $W/C = 0.50$, for complete mix design see Table 2.2.
 2. $S = 15$ in (381 mm), $L = 16$ in (406 mm), $f'_c = 6605$ psi (45.5 MPa)
 3. Ext. $a/W = (a/W)_{\text{compliance}} - 0.14$

Table II.12B Precracked Beams, Tested by Fartash (11), K_{IC} Method (4, 8), W = 4.00 in (102 mm), B = 3.00 in (76 mm), E_c = 4.65 x 10⁶ psi (32.0 GPa)

Fig. No.	Original No.	P _m lb N	Ext. a/W	Avg. Ext. a/W	K _{IC} lb-in ^{-3/2} kN-m ^{-3/2}	G _{IC} lb-in/in ² N-m/m ²	Avg. G _{IC} lb-in/in ² N-m/m ²
111	2-B12	1090	0.412	0.412	1190	0.305	0.305
		4850			1310		
114	2-B15	820	0.430	0.401	957	0.197	0.202
		3650			1050		
115	2-B16	840	0.431		980	0.207	
		3740			1080		
112	2-B13	940	0.437	0.438	1100	0.259	0.256
		4180			1210		
109	2-B10	930	0.438		1090	0.253	
		4140			1190		
113	2-B14	920	0.453	0.453	1120	0.272	0.272
		4090			1240		
110	2-B11	860	0.464	0.464	1070	0.245	0.245
		3830			1170		

Note: For dimensions and material properties see Table II.6B.

Table II.12C Precracked Beams, Tested by Fartash (9), K_{IC} Method (4, 8), W = 4.00 in (102 mm), B = 3.00 in (76 mm), E_c = 4.42 x 10⁶ psi (30.5 MPa)

Fig. No.	Original No.	P _m lb N	Ext. a/W	Avg. Ext. a/W	K _{IC} lb-in ^{-3/2} kN-m ^{-3/2}	G _{IC} lb-in/in ² N-m/m ²	Avg. G _{IC} lb-in/in ² N-m/m ²	
127	3-B16	460	0.601	0.601	792	0.142	0.118	
		2050			871			24.9
125	3-B14	420	0.619		647	0.0947	20.7	
		1870			712			16.6
126	3-B15	380	0.627	0.628	697	0.110	0.104	
		1700			767			19.3
123	3-B12	360	0.628		660	0.0986	18.2	
		1500			726			17.3

Notes: 1. f'_c = 6020 psi (41.5 MPa)

2. For dimensions and material properties see Table II.12A.

Table II.12D Precracked Beams, Tested by Huang (8), KIC Method (4, 8),
 $W = 4.00$ in (102 mm), $B = 3.00$ in (76 mm), $E_C = 3.39 \times 10^6$
 psi (23.4 GPa) and $E_C = 5.14 \times 10^6$ psi (35.4 GPa)

$E_C = 3.39 \times 10^6$ psi (23.4 GPa)

Fig. No.	Original No.	P_m lb N	Ext. a/W	Avg. Ext. a/W	KIC $lb\text{-in}^{-3/2}$ $kN\text{-m}^{-3/2}$	GIC $lb\text{-in}/in^2$ $N\text{-m}/m^2$	Avg. GIC $lb\text{-in}/in^2$ $N\text{-m}/m^2$
5	S1S4-1	1210	0.173	0.173	174	0.0895	0.0895
		5380			192	1.57	1.57
6	S1S4-2	1000	0.298	0.298	200	0.0118	0.0118
		4450			220	2.07	2.07
7	S1S4-3	880	0.339	0.339	197	0.0114	0.0114
		3920			217	2.00	2.00
8	S1S4-5	255	0.654	0.0654	180	0.00956	0.00956
		1140			198	1.67	1.67

$E_C = 5.14 \times 10^6$ psi (35.4 GPa)

29	S2S4-1	1740	0.110	0.123	223	0.00965	0.00965
		7740			245	1.69	1.69
32	S2F4-1	1740	0.135		223	0.00965	
		7740			245	1.69	
30	S2S4-2	1190	0.329	0.339	266	0.0137	0.0130
		5280			292	2.40	2.28
33	S2F4-2	1040	0.348		251	0.0122	
		4630			276	2.14	
31	S2S4-3	1020	0.381	0.383	261	0.0133	0.0108
		4540			287	2.33	1.89
34	S2F4-3	778	0.385		205	0.00821	
		3460			226	1.44	

- Notes: 1. For beams no. S1S4, $W/C = 0.78$, for complete mix design see Table 2.1, $f'_c = 3540$ psi (24.4 MPa)
2. For beams no. S2S4 and S2F4, $W/C = 0.50$, for complete mix design see Table 2.1, $f'_c = 8130$ psi (56.0 MPa)
3. For all beams, $S = 15$ in (381 mm), $L = 16.3$ in (413 mm)
4. Ext. a/W = (a/W)compliance - 0.14

Table II.12E Precracked Beams, Tested by Huang (8), K_{IC} Method (4, 8),
 $W = 8.00$ in (102 mm), $B = 3.00$ in (76 mm), $E_C = 3.63 \times 10^6$
 psi (25.0 GPa) and $E_C = 5.12 \times 10^6$ psi (35.3 GPa)

$E_C = 3.63 \times 10^6$ psi (25.0 GPa)

Fig. No.	Original No.	P_m lb N	Ext. a/W	Avg. Ext. a/W	K_{IC} lb-in ^{-3/2} kN-m ^{-3/2}	G_{IC} lb-in/in ² N-m/m ²	Avg. G_{IC} lb-in/in ² N-m/m ²
16	L1S4-1	2730 12130	0.191	0.204	441 485	0.0536 9.39	0.0561 9.83
20	L1F4-1	2550 11350	0.216		461 508	0.0586 10.3	
21	L1F4-2	1460 6500	0.438	0.456	528 581	0.0769 13.5	0.0985 17.3
17	L1S4-2	1540 6850	0.473		660 726	0.120 20.0	
22	L1F4-3	1290 5740	0.529	0.539	688 757	0.130 22.8	0.107 18.7
19	L1S4-4	984 4380	0.548		553 608	0.0842 14.8	
18	L1S4-3	736 3280	0.604	0.604	726 571	0.0741 13.0	0.0741 13.0

$E_C = 5.12 \times 10^6$ psi (35.3 GPa)

43	L2F4-1	5180 23100	0.129	0.151	691 760	0.0932 16.3	0.112 19.6
40	L2S4-1	5050 22500	0.173		818 899	0.131 23.0	
44	L2F4-2	2625 11700	0.382	0.382	750 825	0.110 19.3	0.110 19.3
41	L2S4-2	2510 11170	0.441	0.441	908 999	0.161 28.2	0.161 28.2
45	L2F4-3	1680 7480	0.523	0.523	848 933	0.140 24.5	0.140 24.5
42	L2S4-3	1260 5610	0.601	0.601	864 950	0.146 25.6	0.146 25.6

Notes: 1. For beams no. L1S4 and L1F4, $W/c = 0.78$, for complete mix design see Table 2.1, $f'_C = 4060$ psi (28.0 MPa)

Table II. 12E (Continued)

2. For beams no. L2S4 and L2F4, W/C = 0.50, for complete mix design see Table 2.1, $f'_c = 8070$ psi (55.6 MPa)
3. For all beams, S = 24 in (610 mm), L = 25 in (25 mm)

APPENDIX III

THE UNIVERSITY OF CHICAGO
CHICAGO, ILL. 60637

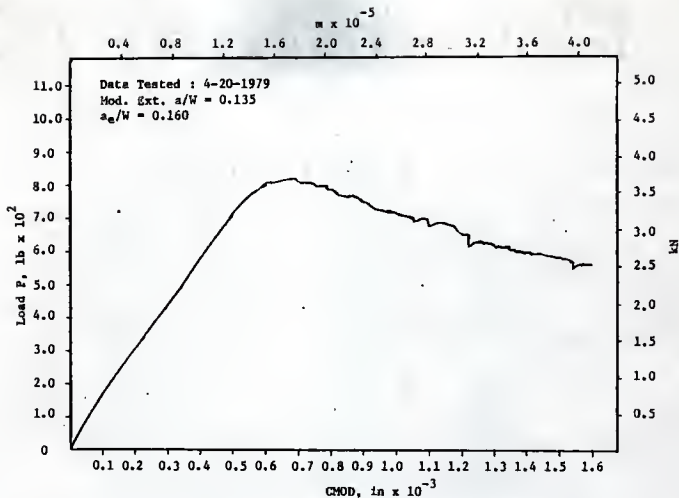


Fig. 1 P vs CMOD, 4 in Deep Beam (SIS3-1), Load Control, Huang (8)

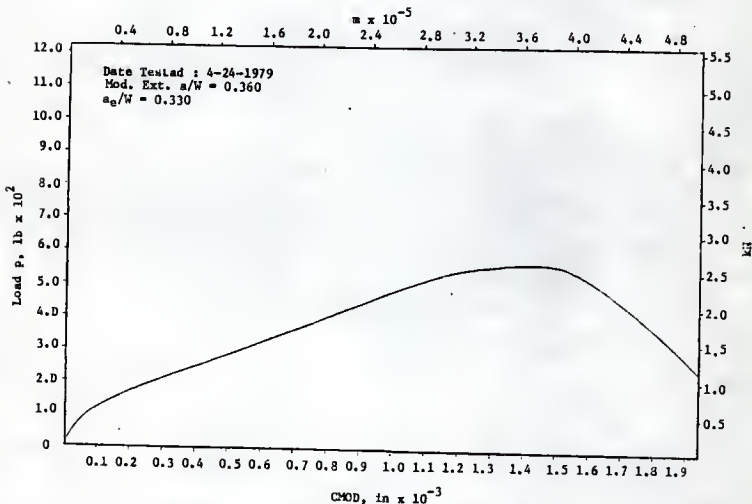


Fig. 2 P vs CMOD, 4 in Deep Beam (SIS3-2), Load Control, Huang (8)

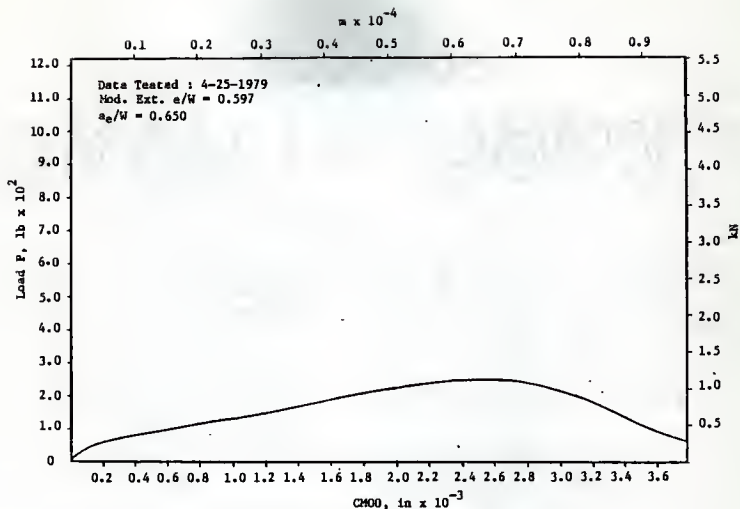


Fig. 3 P vs CM00, 4 in Deep Beam (SIS3-3), Load Control, Huang (8)

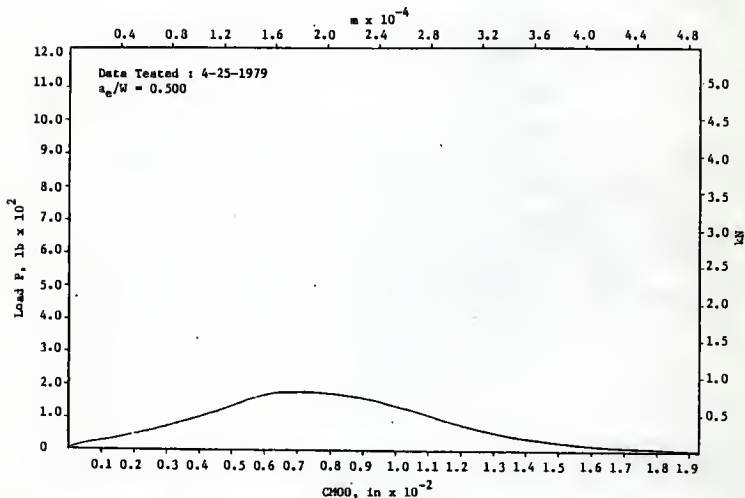


Fig. 4 P vs CM00, 4 in Deep Beam (SIS3-4), Load Control, Huang (8)

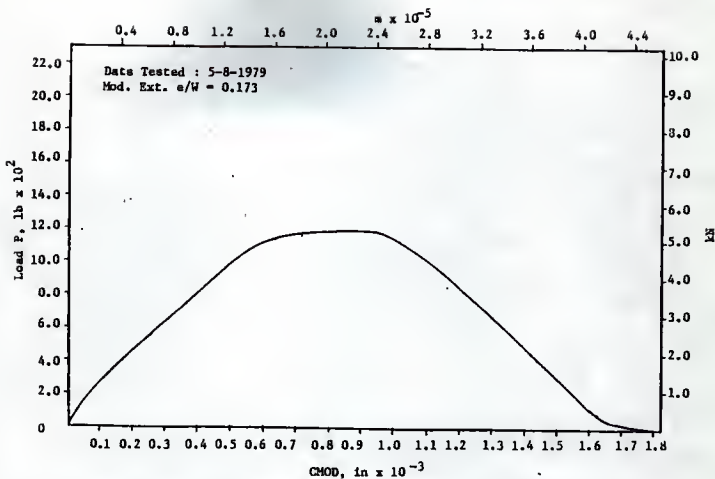


Fig. 5 P vs CHOD, 4 in Deep Beam (S1S4-1), Load Control, Suang (8)

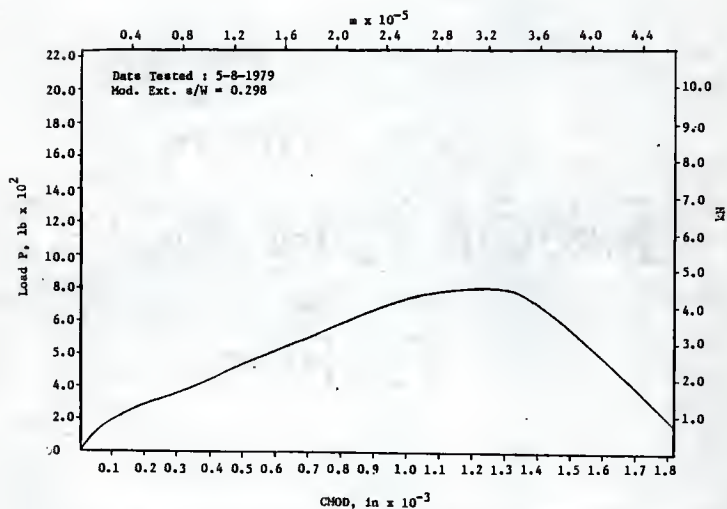


Fig. 6 P vs CHOD, 4 in Deep Beam (S1S4-2), Load Control, Huang (8)

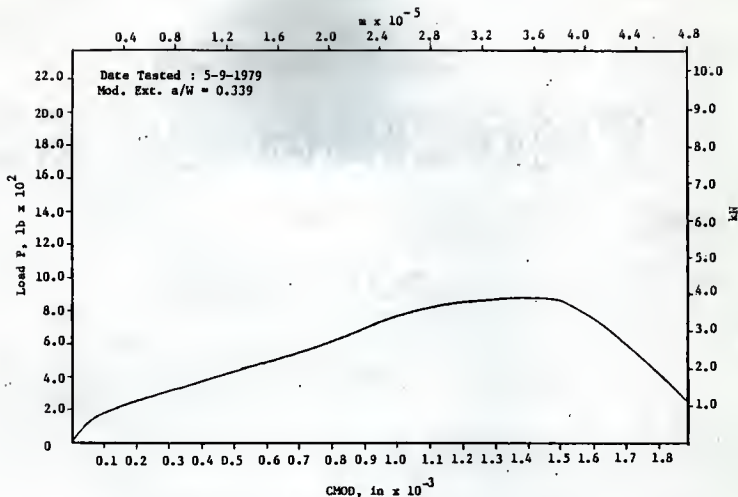


Fig. 7 P vs CHOD, 4 in Deep Beam (SLS4-3), Load Control, Huang (8)

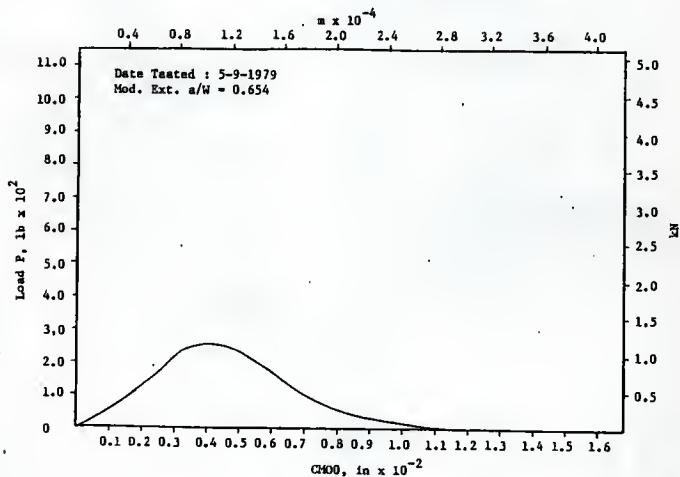


Fig. 8 P vs CHOD, 4 in Deep Beam (SLS4-5), Load Control, Huang (8)

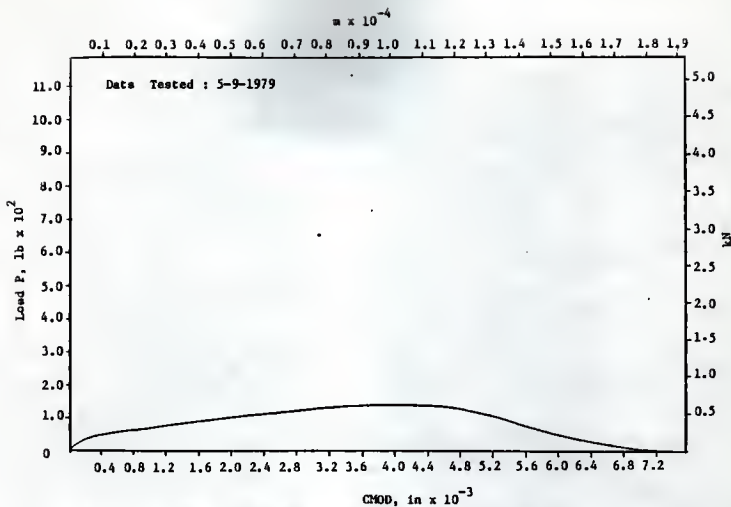


Fig. 9 P vs CMOD, 4 in Deep Beam (SIS4-6), Load Control, Huang (8)

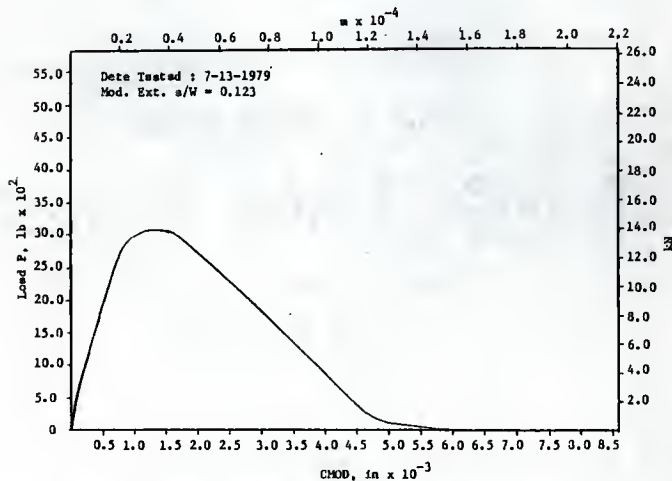


Fig. 10 P vs CMOD, 8 in Deep Beam (LIS3-1), Load Control, Huang (8)

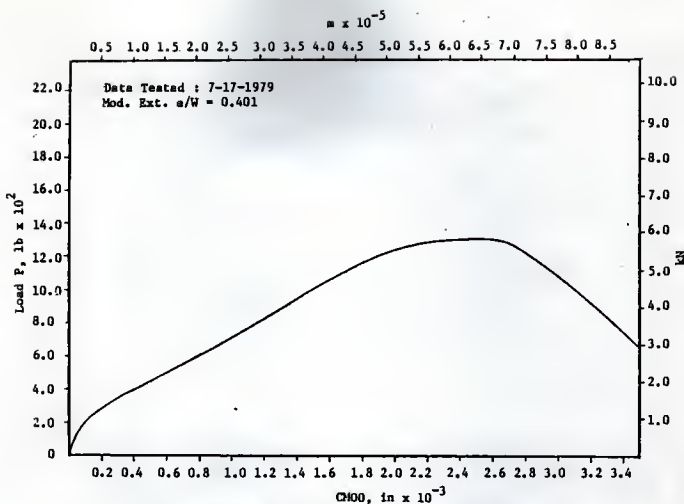


Fig. 11 P vs CHOD, 8 in Deep Beam (L1S3-2), Load Control, Huang (8)

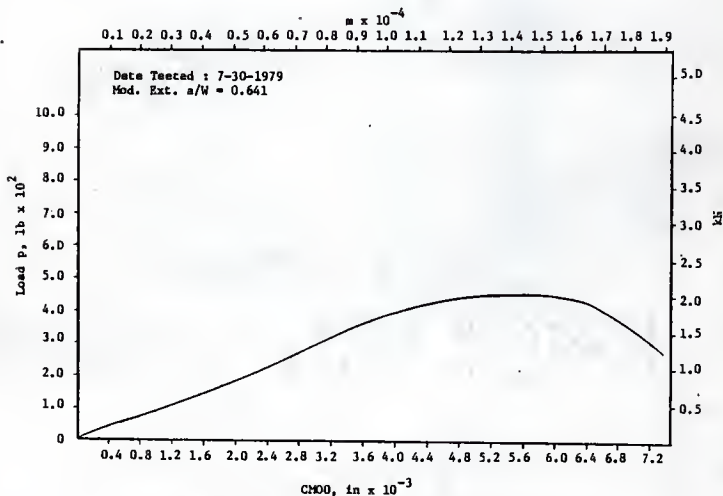


Fig. 12 P vs CHOD, 8 in Deep Beam (L1S3-3), Load Control, Huang (8)

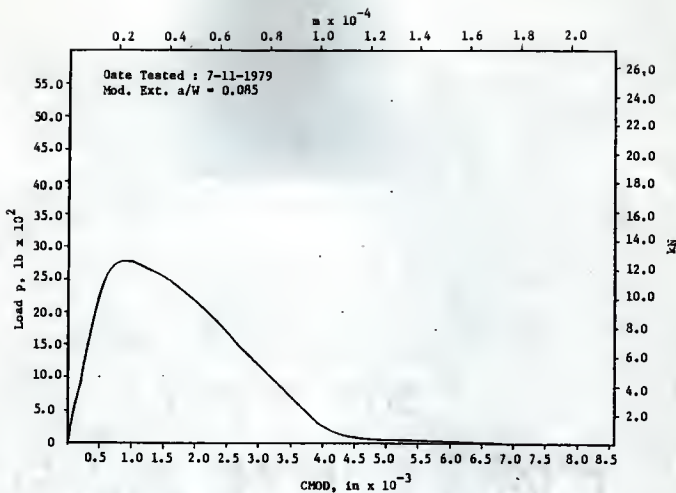


Fig. 13 P vs CHOD, 8 in Deep Beam (LIF3-1), Load Control, Huang (8)

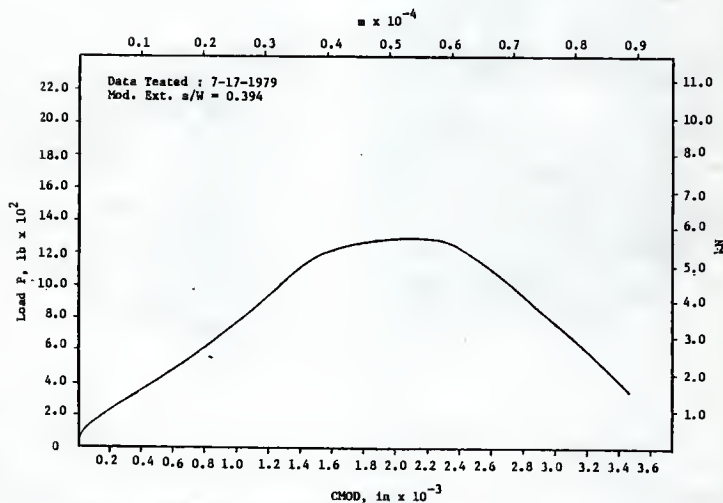


Fig. 14 P vs CHOD, 8 in Deep Beam (LIF3-2), Load Control, Huang (8)

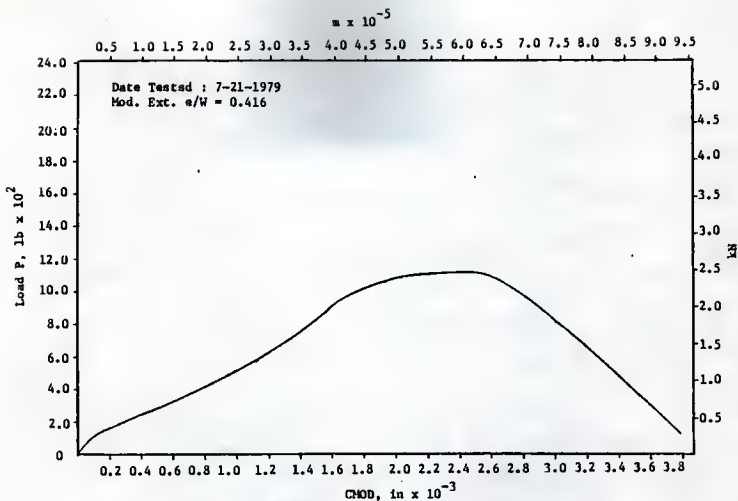


Fig. 15 P vs CHOD, 8 in Deep Beam (L1F3-3), Load Control, Huang (8)

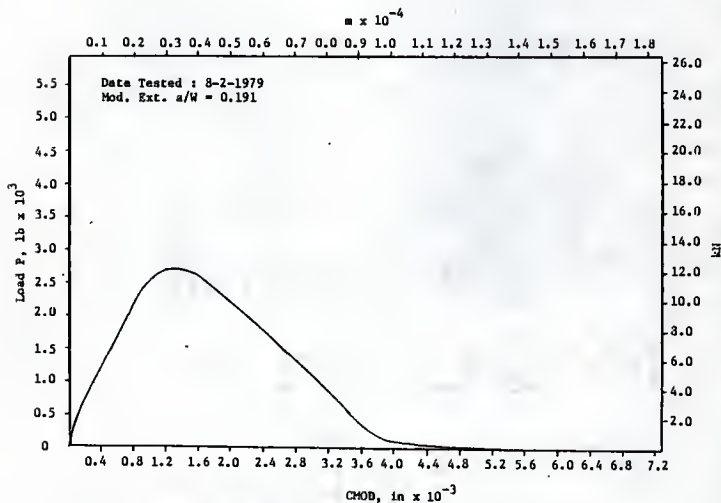


Fig. 16 P vs CHOD, 8 in Deep Beam (L1S4-1), Load Control, Huang (8)

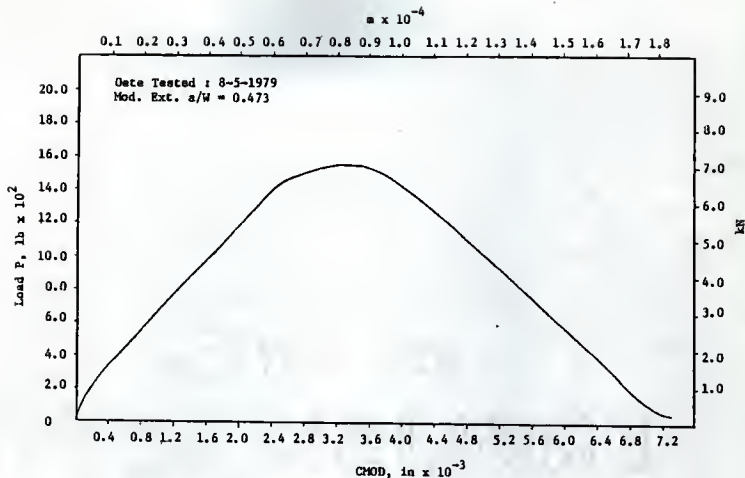


Fig. 17 P vs CHOD, 8 in Deep Beam (LIS4-2), Load Control, Huang (8)

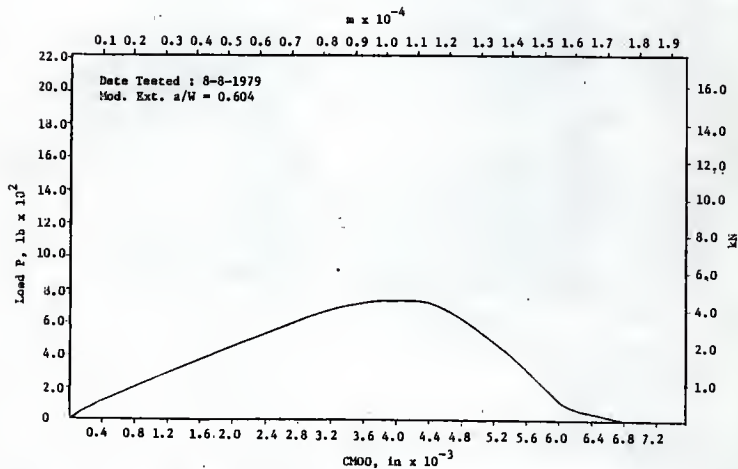
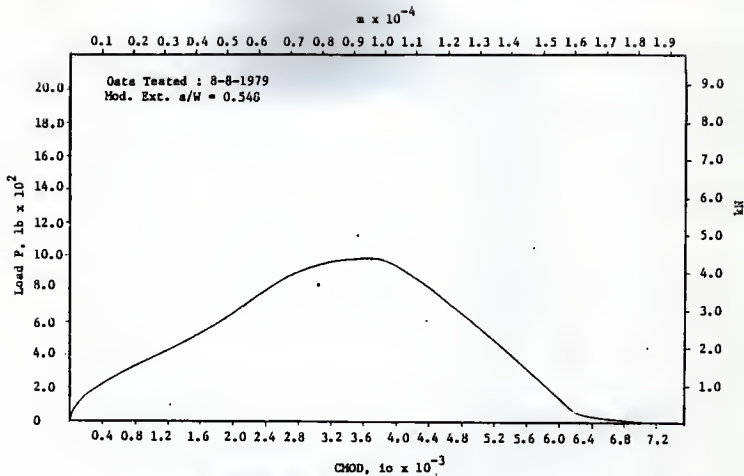
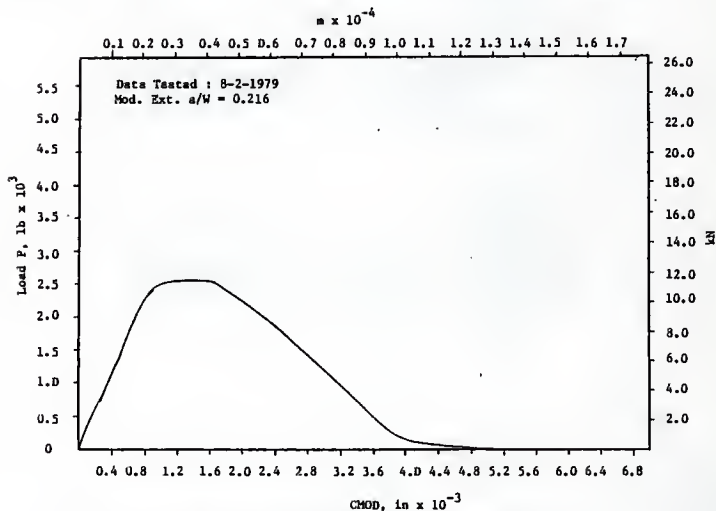


Fig. 18 P vs CHOD, 8 in Deep Beam (LIS4-3), Load Control, Huang (8)

Fig. 19 P vs CHOD, 8 in Deep Beam (LIS4-4), Load Control, Husog (8)Fig. 20 P vs CHOD, 8 in Deep Beam (LIF4-1), Load Control, Huang (8)

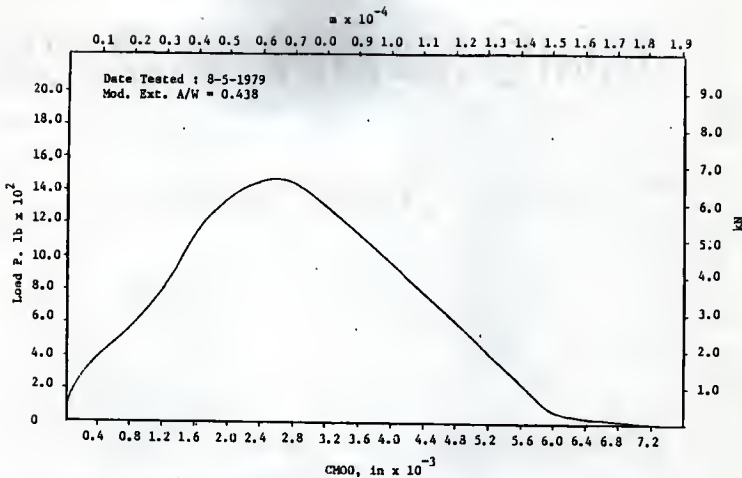


Fig. 21 P vs CMOD, 8 in Deep Beam (LIF4-2), Load Control, Huang (8)

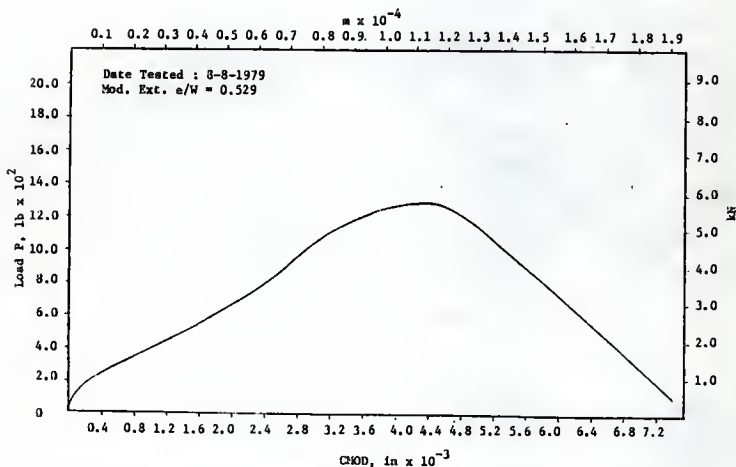


Fig. 22 P vs CMOD, 8 in Deep Beam (LIF4-3), Load Control, Huang (8)

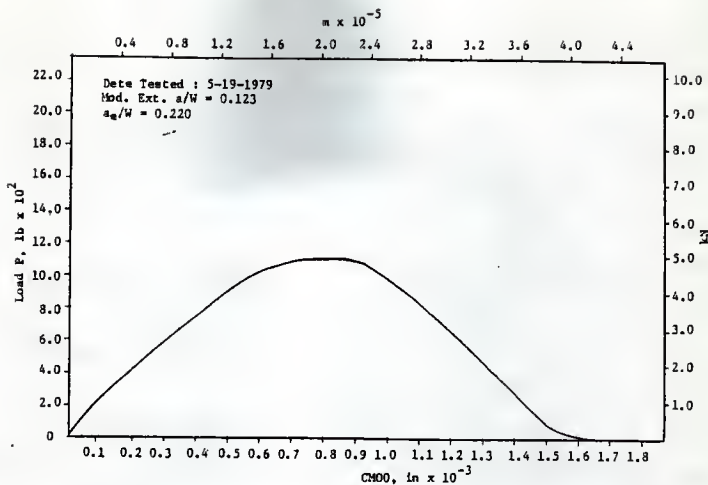


Fig. 23 P vs CMOD, 4 in Deep Beam (S2S3-1), Load Control, Huang (8)

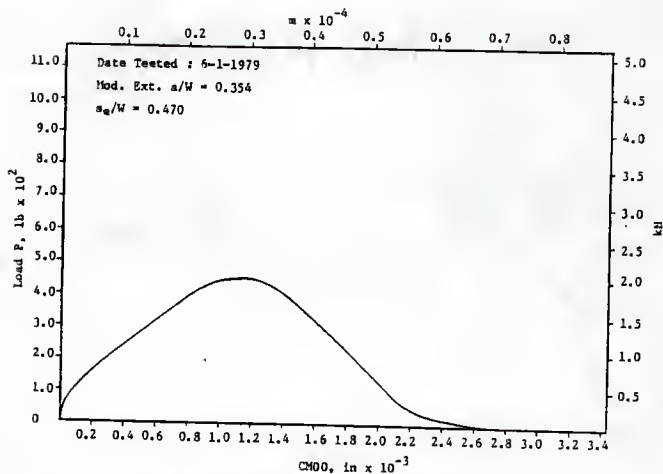
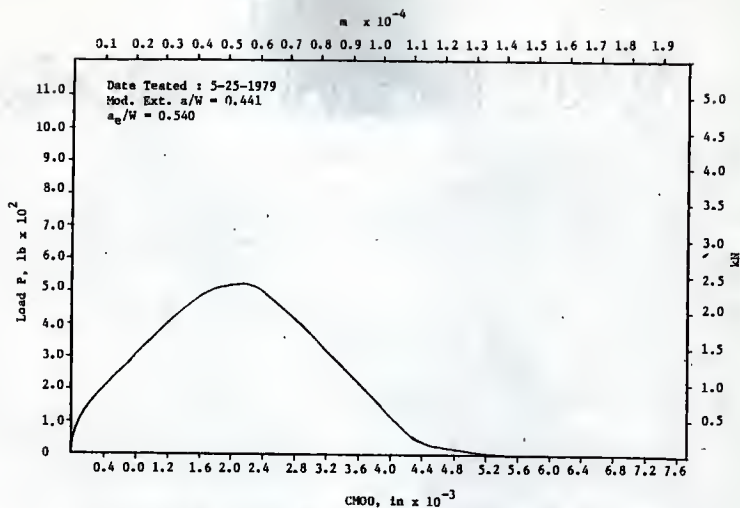
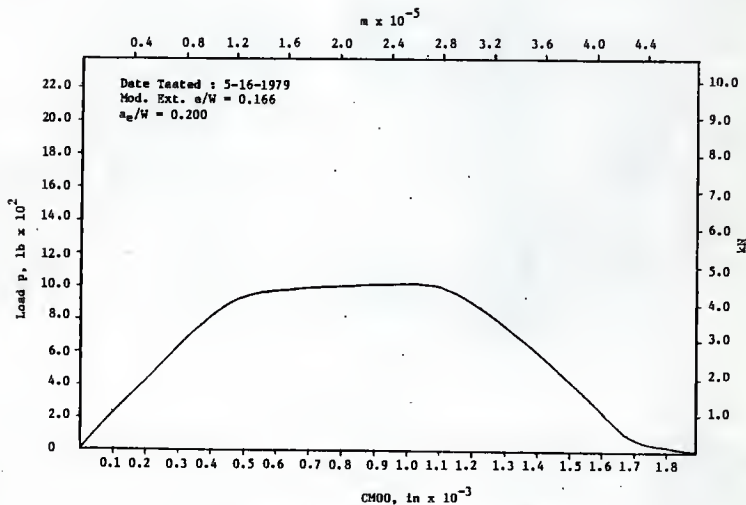


Fig. 24 P vs CMOD, 4 in Deep Beam (S2S3-2), Load Control, Huang (8)

Fig. 25 P vs $CM00$, 4 in Deep Beam (S2S3-3), Load Control, Huang (8)Fig. 26 P vs $CM00$, 4 in Deep Beam (S2F3-1), Load Control, Huang (8)

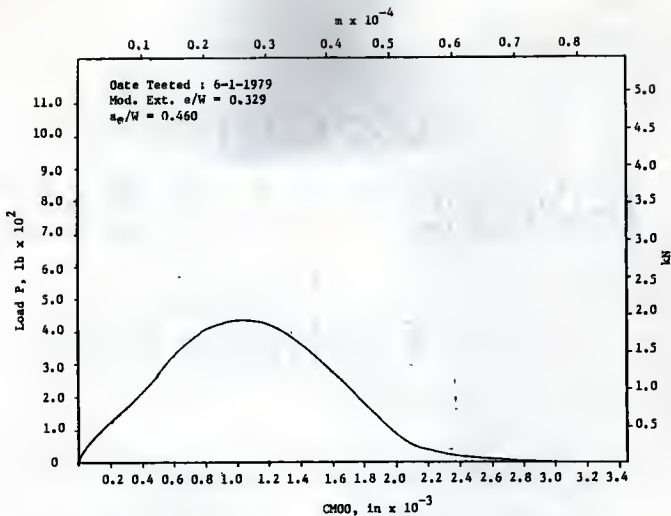


Fig. 27 P vs CHOD, 4 in Deep Beam (SZF3-2), Load Control, Huang (8)

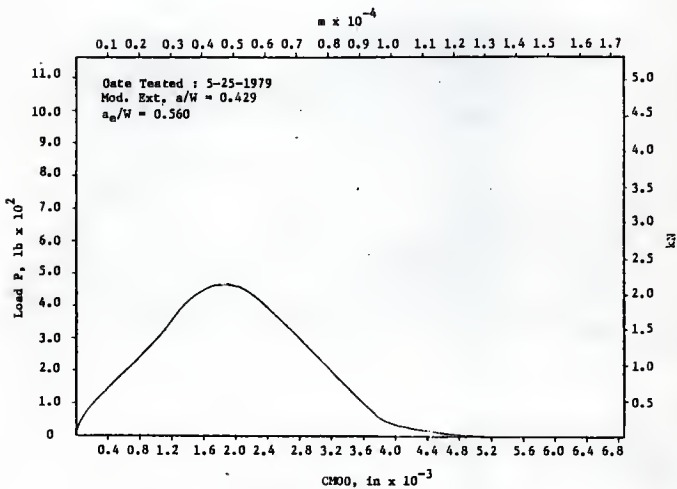


Fig. 28 P vs CHOD, 4 in Deep Beam (SZF3-3), Load Control, Suang (8)

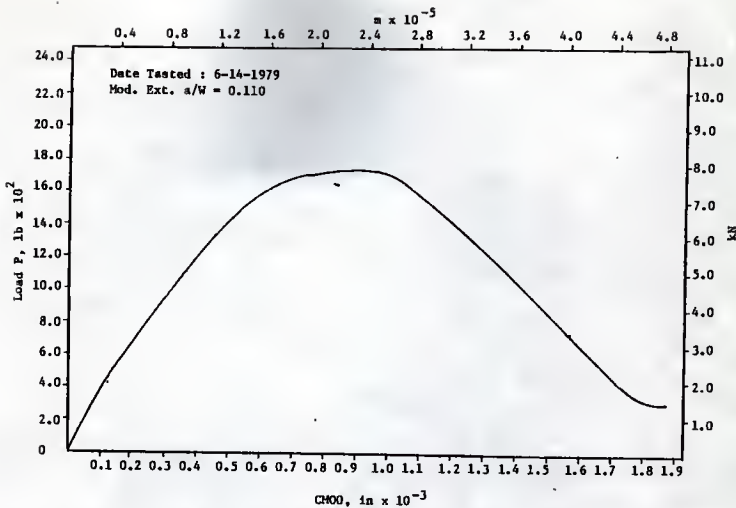


Fig. 29 P vs CM00, 4 in Deep Beam (S2S4-1), Load Control, Huang (8)

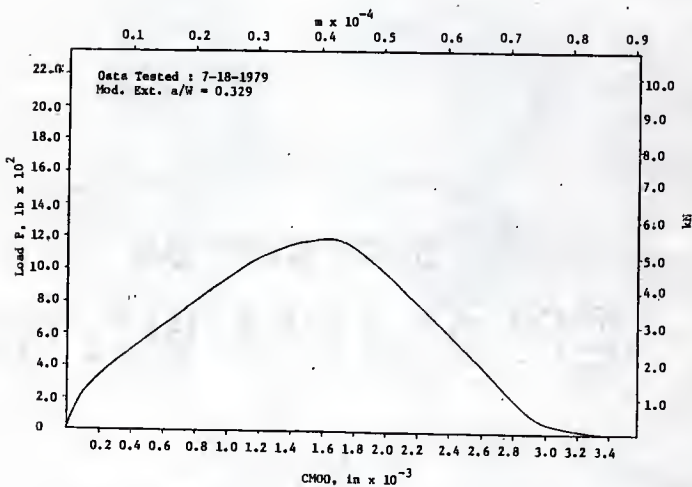


Fig. 30 P vs CM00, 4 in Deep Beam (S2S4-2), Load Control, Huang (8)

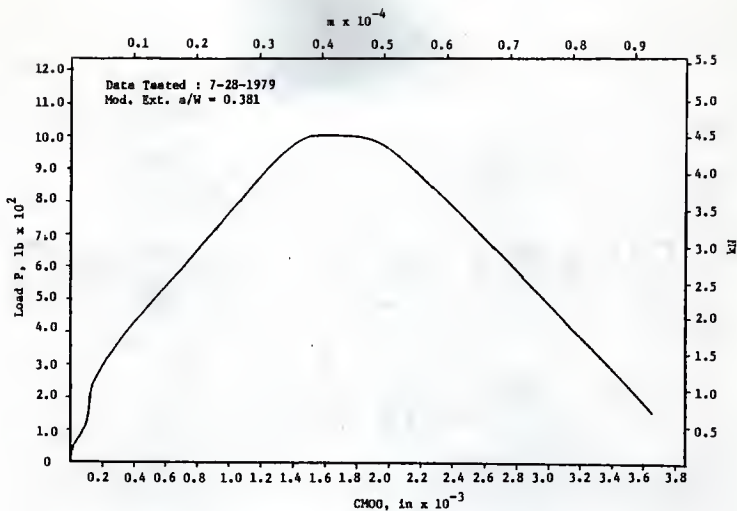


Fig. 31 P vs CHOO, 4 in Deep Beam (S2S4-3), Load Control, Huang (8)

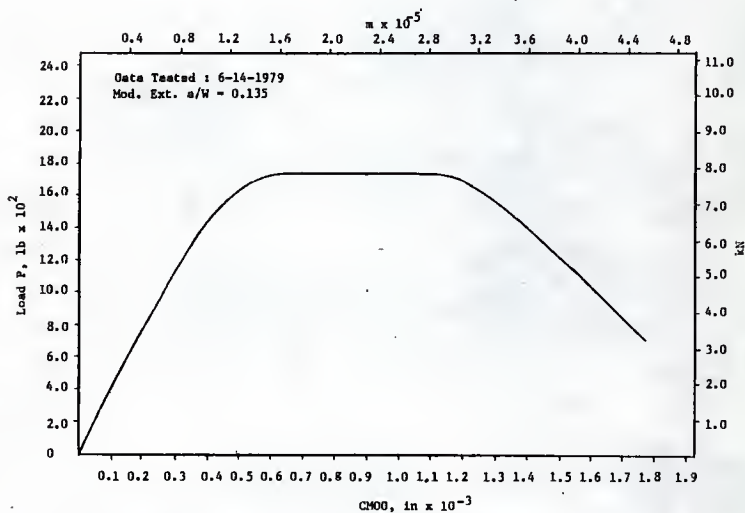


Fig. 32 P vs CHOO, 4 in Deep Beam (S2F4-1), Load Control, Huang (8)

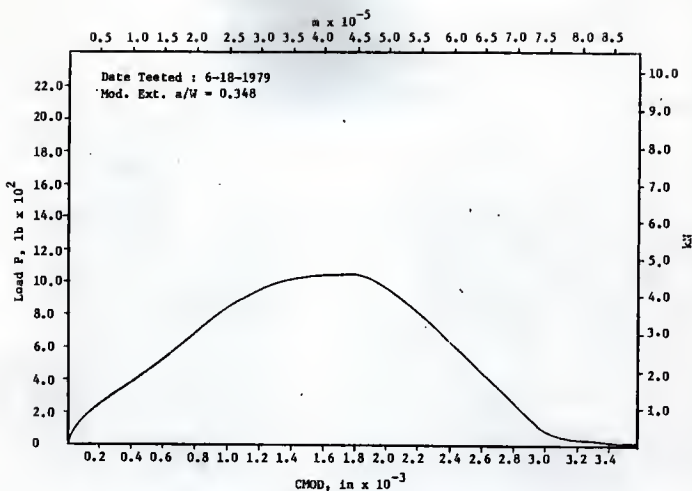


Fig. 33 P vs CMOD, 4 in Deep Beam (S2F4-2), Load Control, Huang (8)

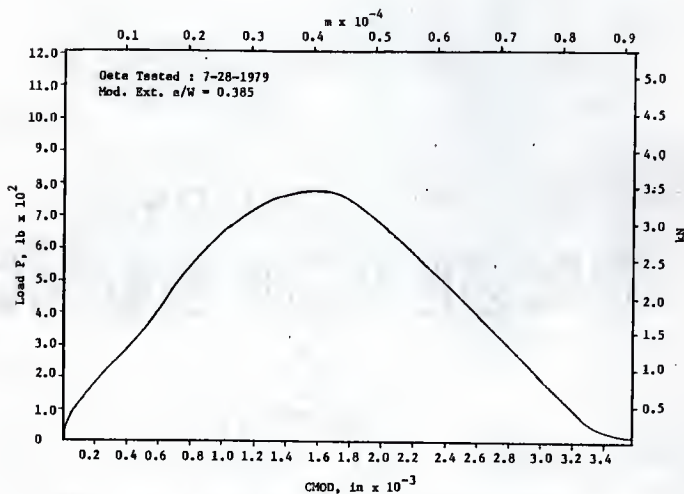


Fig. 34 P vs CMOD, 4 in Deep Beam (S2F4-3), Load Control, Huang (8)

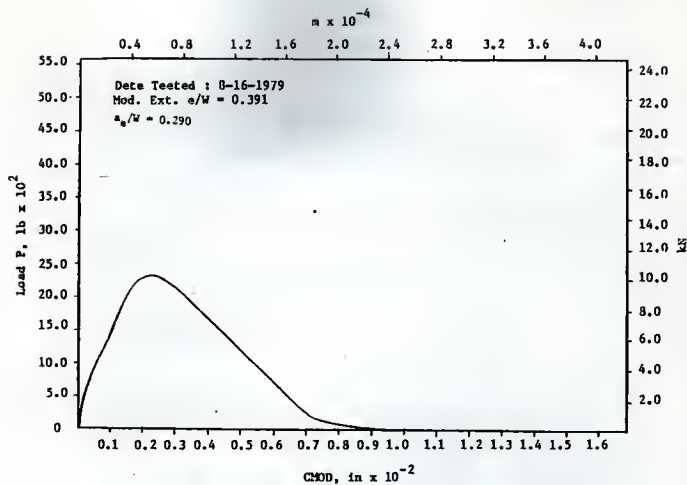


Fig. 35 P vs CMOD, 8 in Deep Beam (L2S3-1), Load Control, Huang (8)

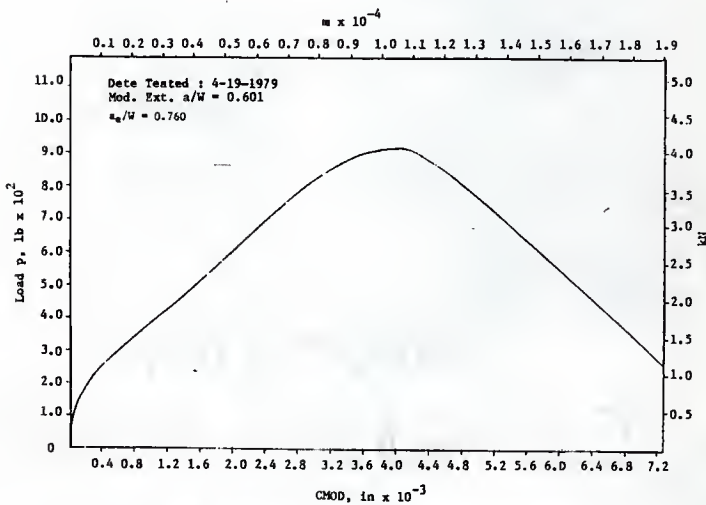


Fig. 36 P vs CMOD, 8 in Deep Beam (L2S3-2), Load Control, Huang (8)

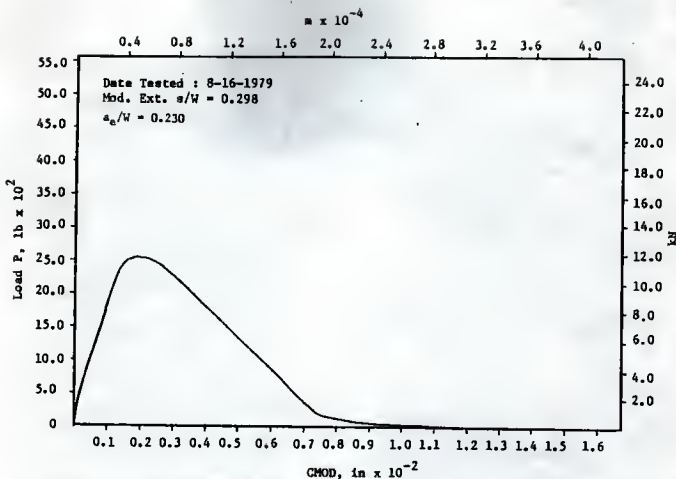


Fig. 37 P vs CHOD, 8 in Deep Beam (L2F3-1), Load Control, Huang (8)

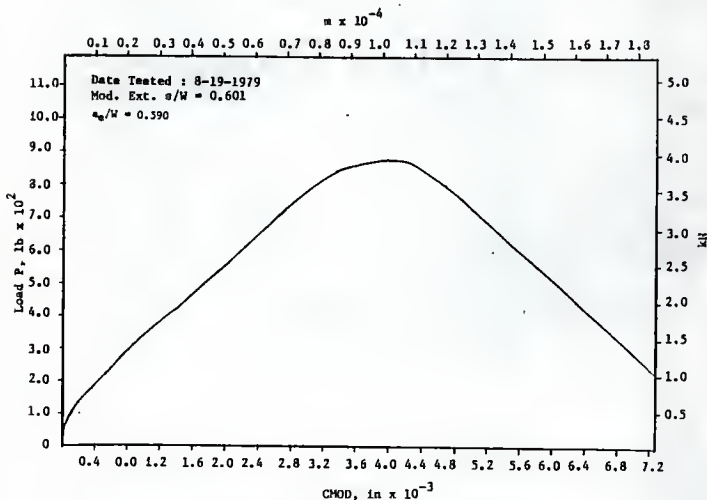


Fig. 38 P vs CHOD, 8 in Deep Beam (L2F3-2), Load Control, Huang (8)

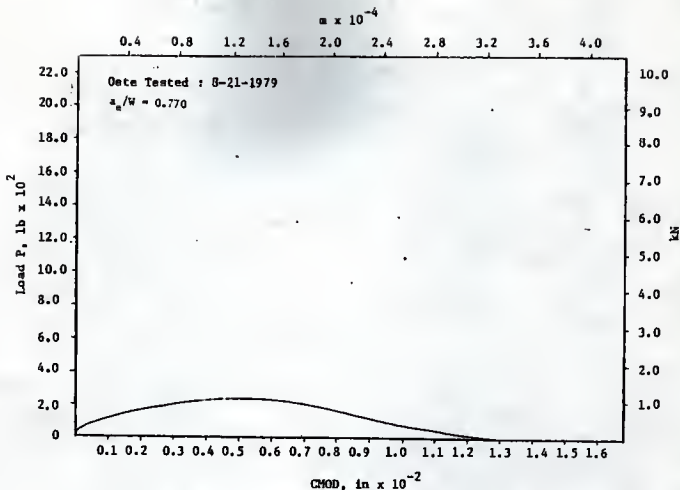


Fig. 39 P vs CHOD, 8 in Deep Beam (L2F3-3), Load Control, Huang (8)

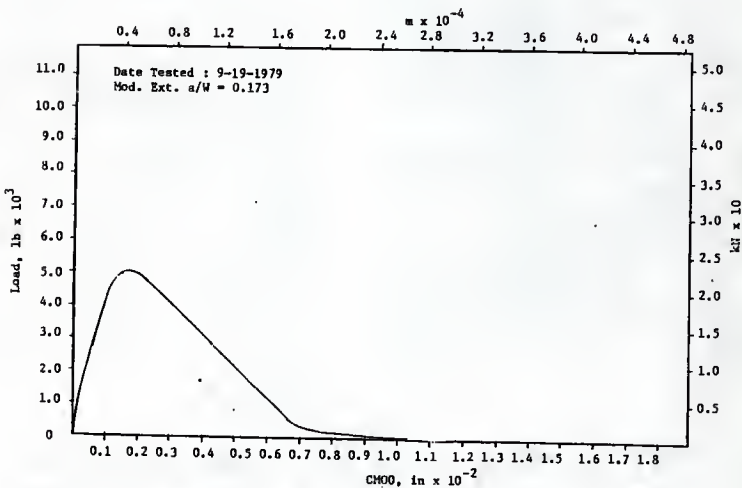


Fig. 40 P vs CHOD, 8 in Deep Beam (L2S4-1), Load Control, Huang (8)

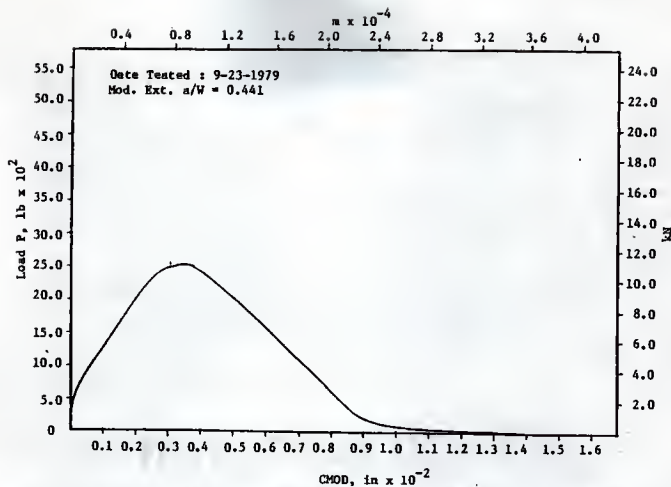


Fig. 41 P vs CHOD, 8 in Deep Beam (L2S4-2), Load Control, Huang (8)

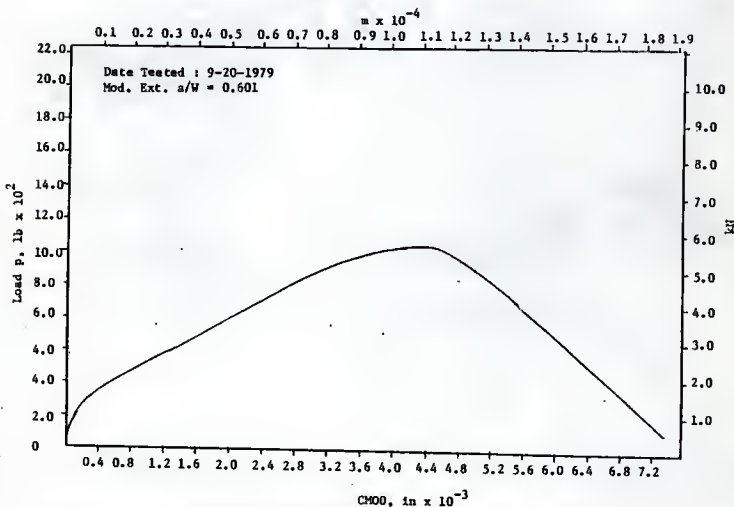


Fig. 42 P vs CHOD, 8 in Deep Beam (L2S4-3), Load Control, Huang (8)

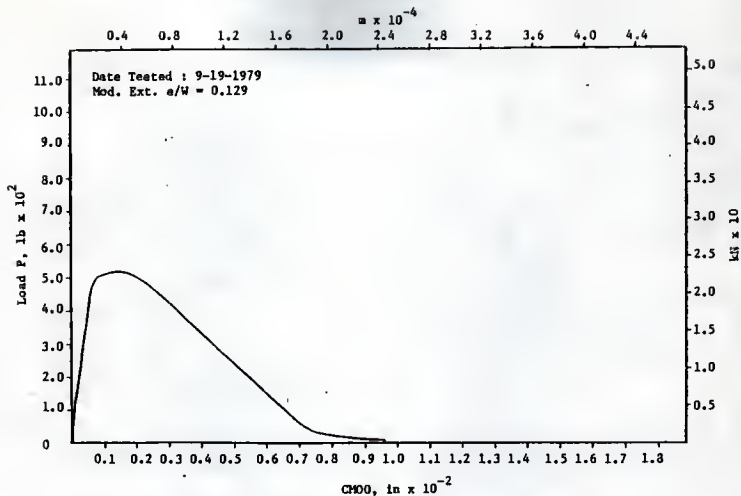


Fig. 43 P vs CMOD, δ in Deep Beam (L2F4-1), Load Control, Huang (8)

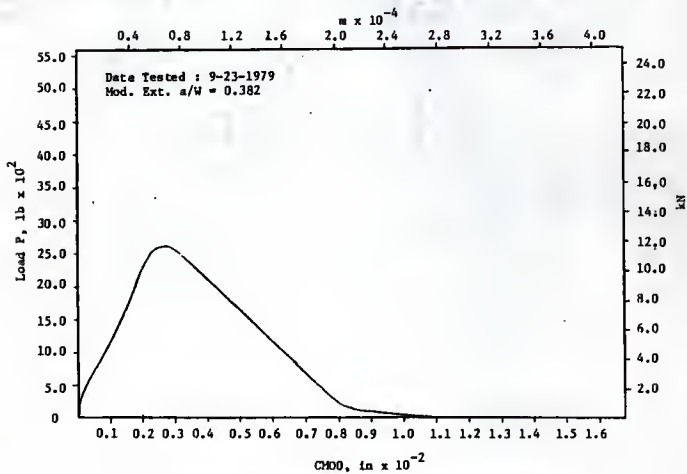


Fig. 44 P vs CMOD, δ in Deep Beam (L2F4-2), Load Control, Huang (8)

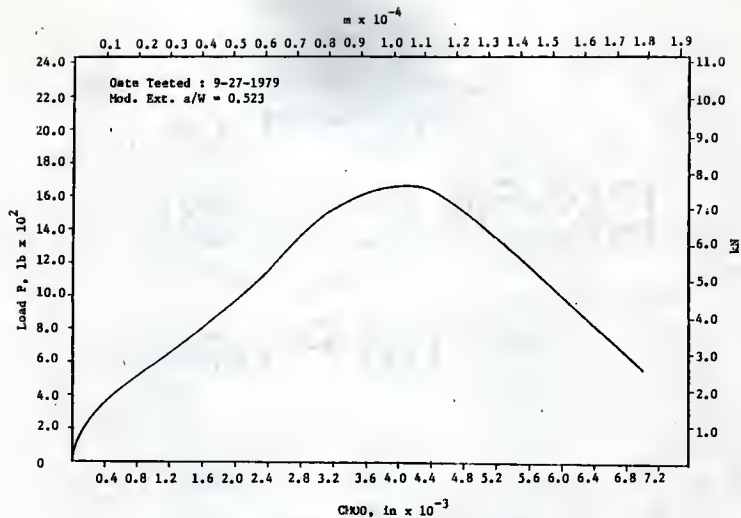


Fig. 45 P vs CMOD, 8 in Deep Beam (L2F4-3), Load Control, Huang (8)

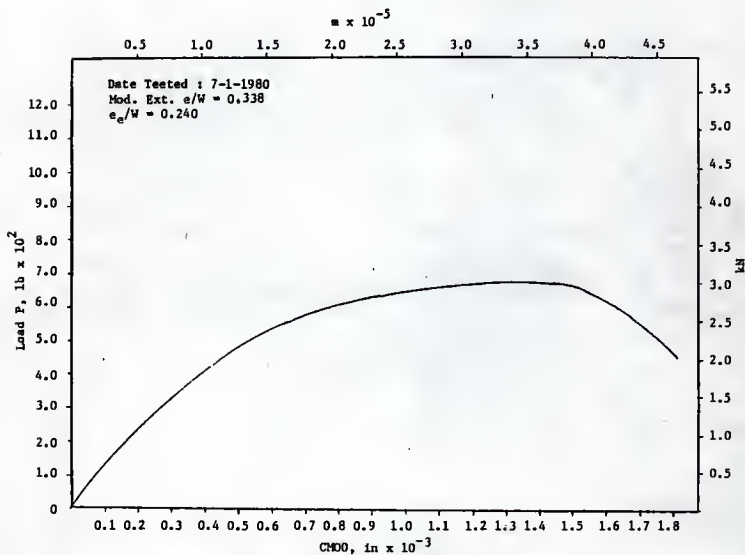


Fig. 46 P vs CMOD, 4 in Deep Beam (1-A1), Load Control, Fartash (11)

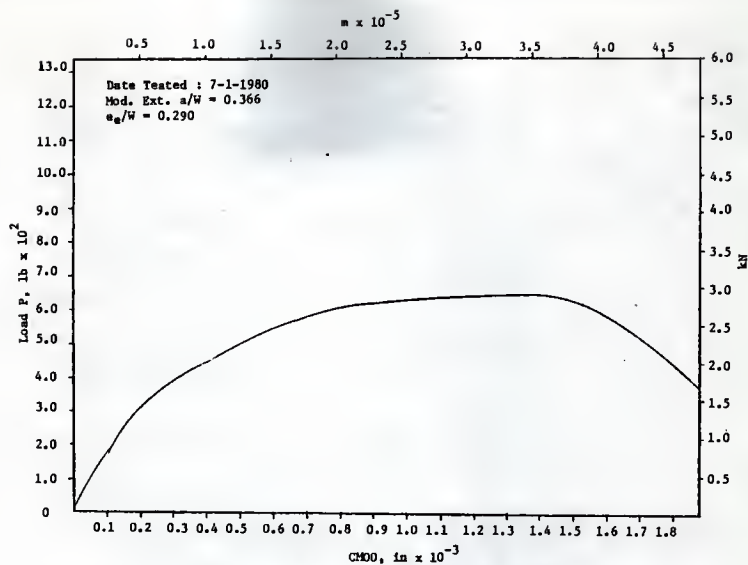


Fig. 47 P vs CMDO, 4 in Deep Beam (1-A2), Load Control, Fartash (11)

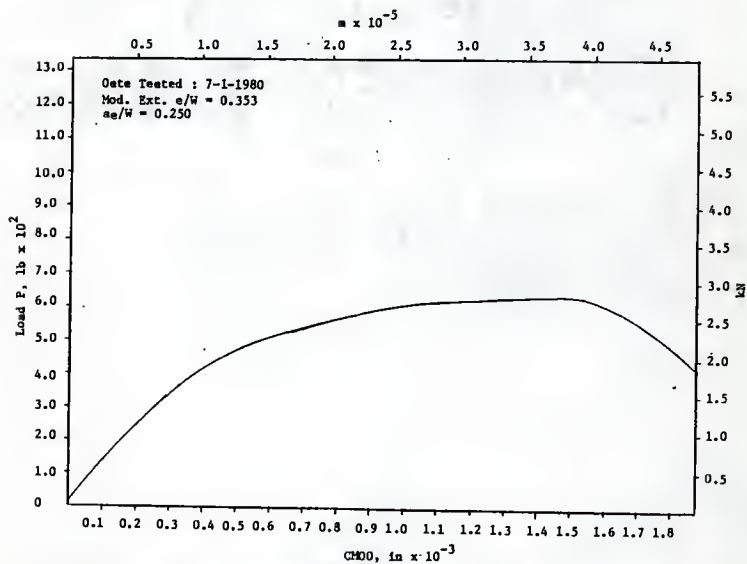
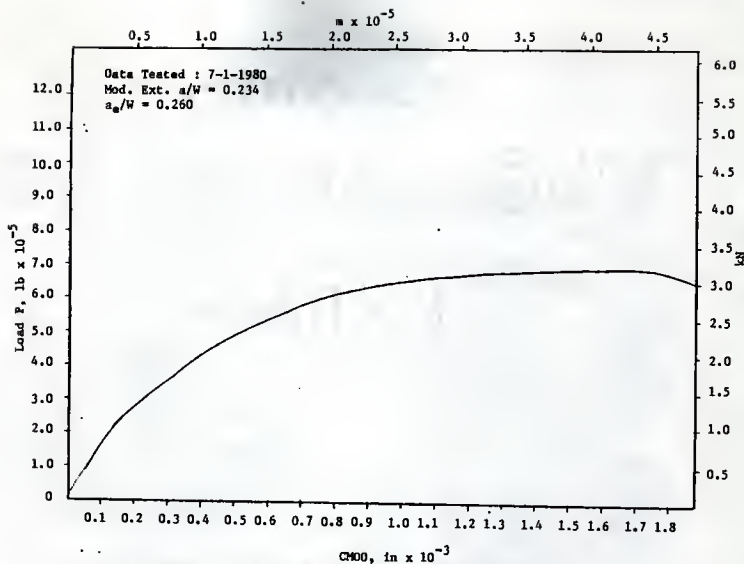
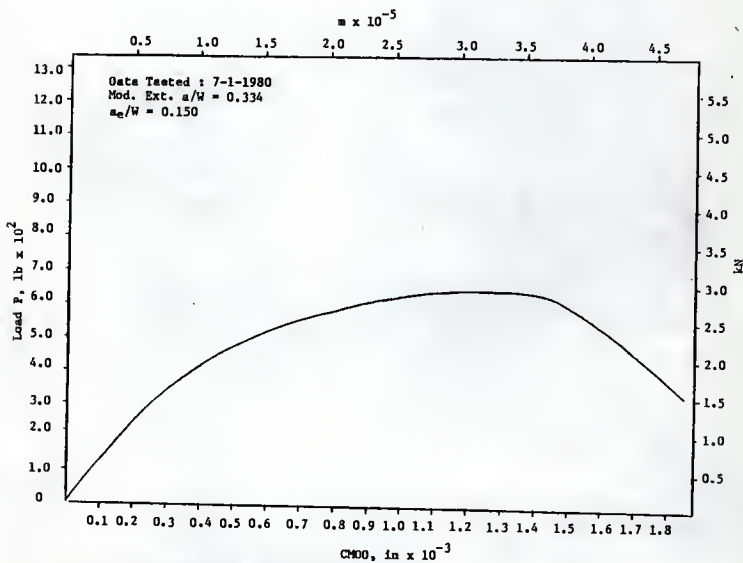


Fig. 48 P vs CMDO, 4 in Deep Beam (1-A3), Load Control, Fartash (11)

Fig. 49 F vs CMDO, 4 in Deep Beam (1-A4), Load Control, Fartash (11)Fig. 50 F vs CMDO, 4 in Deep Beam (1-A5), Load Control, Fartash (11)

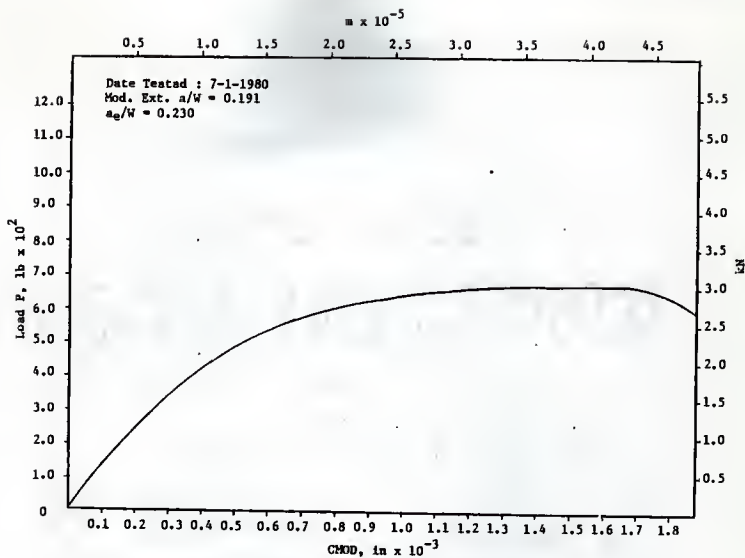


Fig. S1 P vs CMOD, 4 in Deep Beam (1-A6), Load Control, Fartash (11)

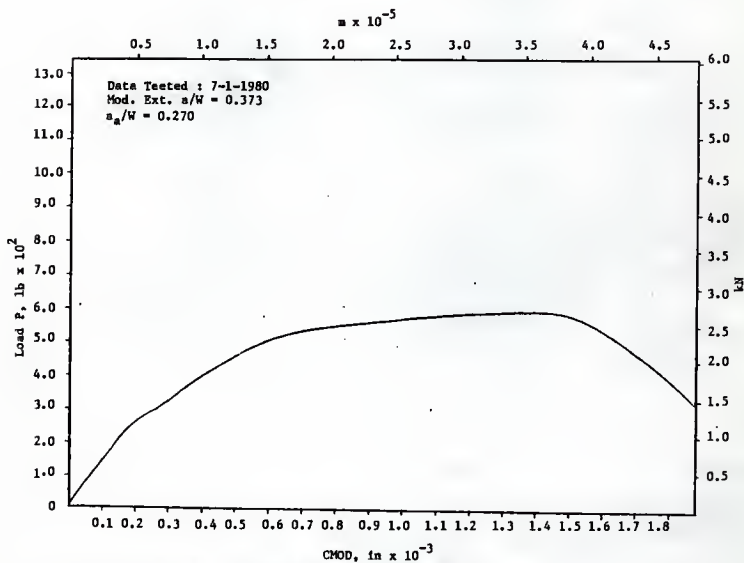


Fig. S2 P vs CMOD, 4 in Deep Beam (1-A7), Load Control, Fartash (11)

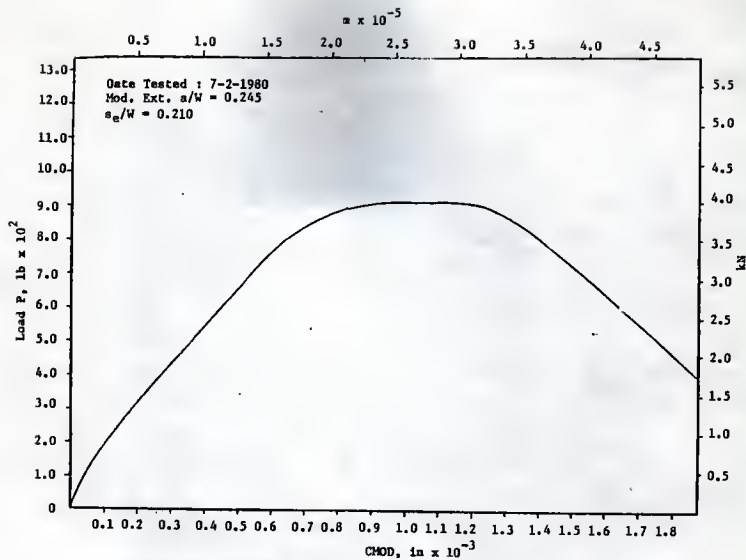


Fig. 53 P vs CHOD, 4 in Deep Beam (1-A10), Load Control, Fartash (11)

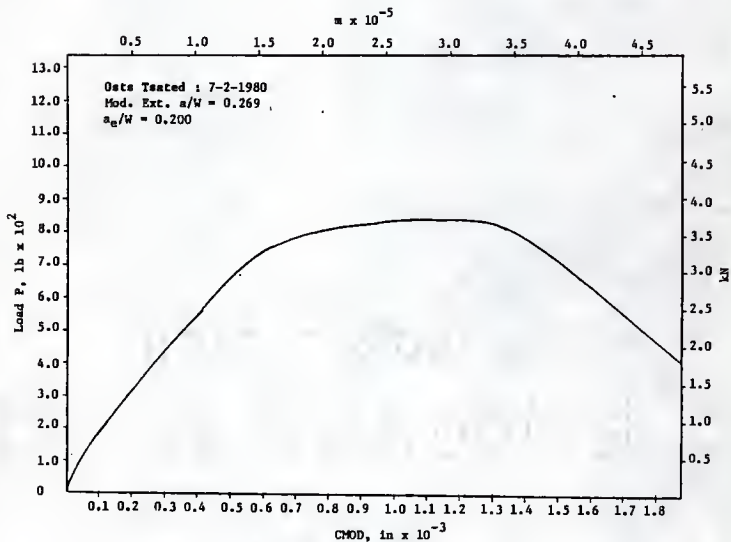


Fig. 54 P vs CHOD, 4 in Deep Beam (1-A11), Load Control, Fartash (11)

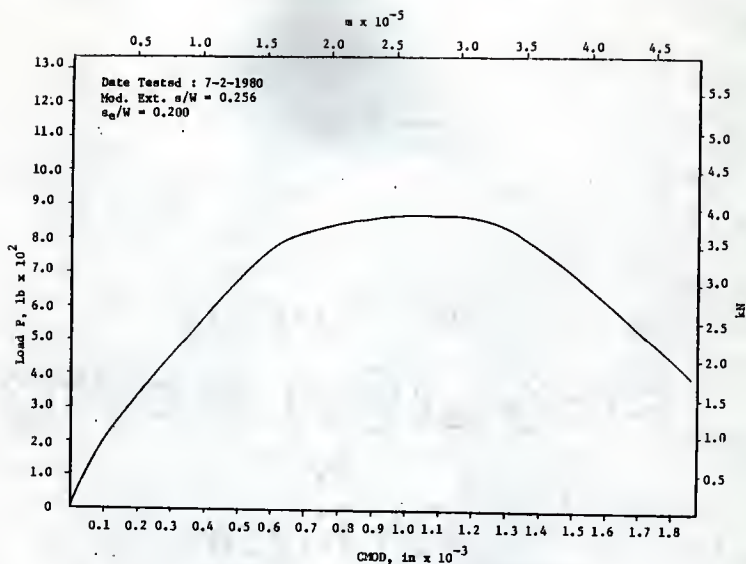


Fig. 55 P vs CMDD, 4in Deep Beam (1-A12), Load Control, Fartash (11)

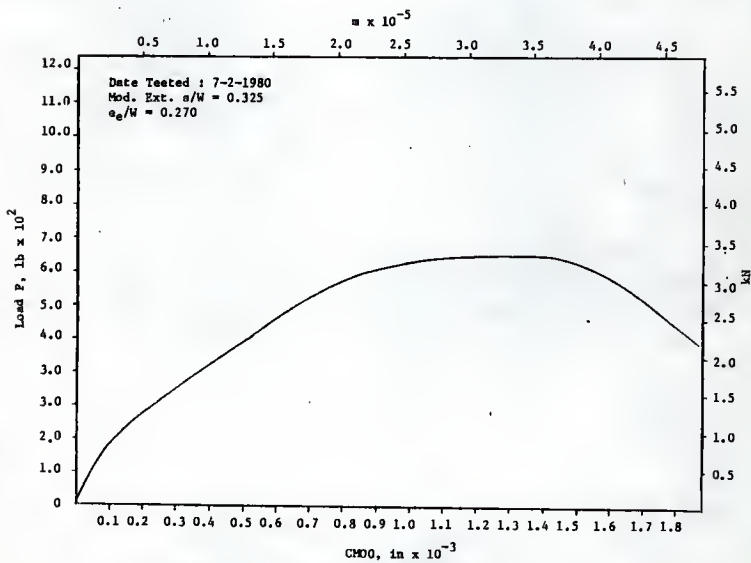


Fig. 56 P vs CMDD, 4 in Deep Beam (1-A13), Load Control, Fartash (11)

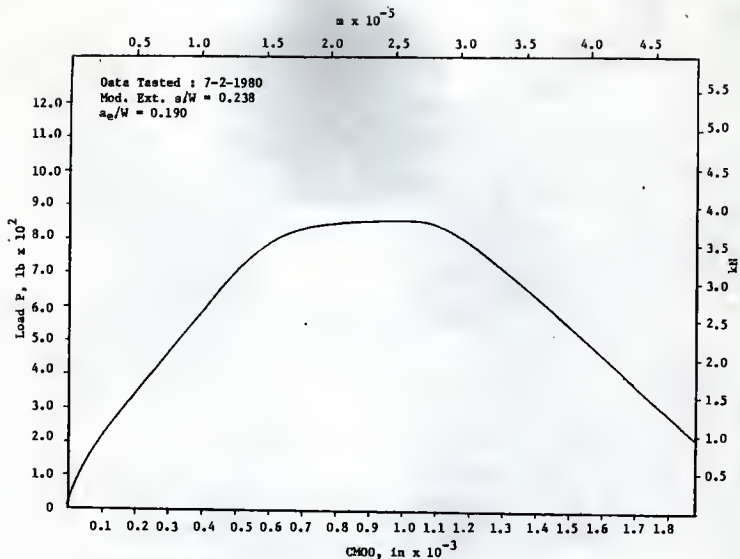


Fig. 57 P vs CMOD, 4 in Deep Beam (1-A14), Load Control, Fartash (11)

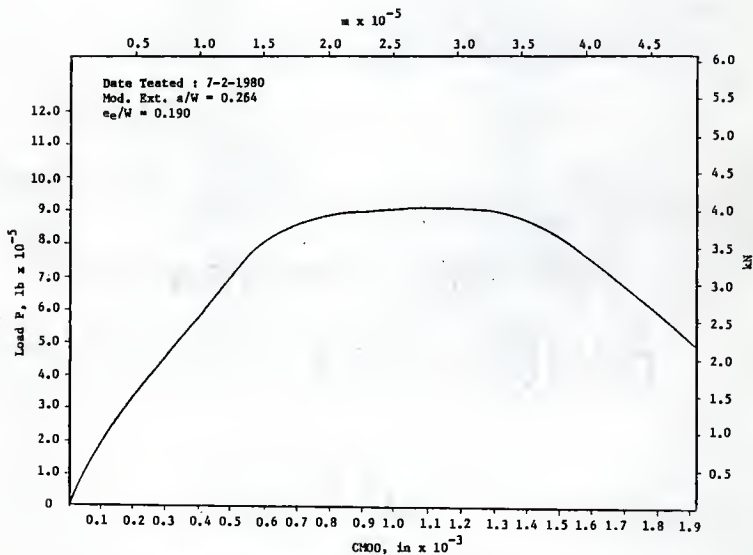


Fig. 58 P vs CMOD, 4 in Deep Beam (1-A15), Load Control, Fartash (11)

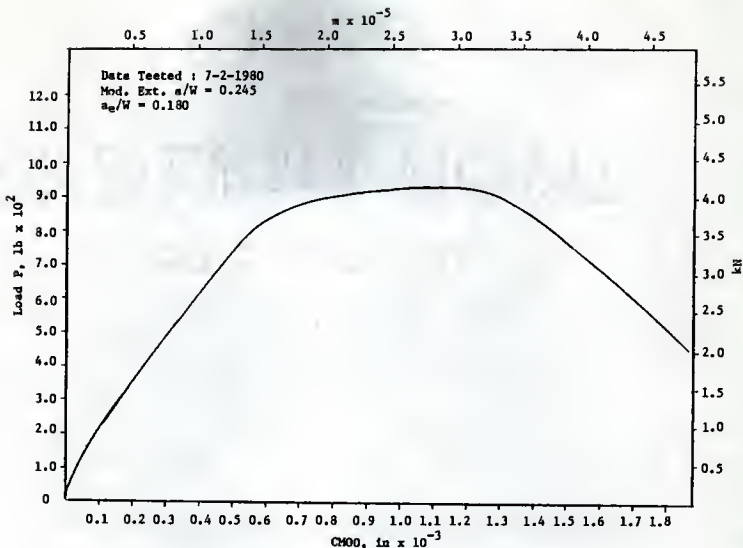


Fig. 59 P vs CMOD, 4 in Deep Beam (1-A16), Load Control, Fartash (11)

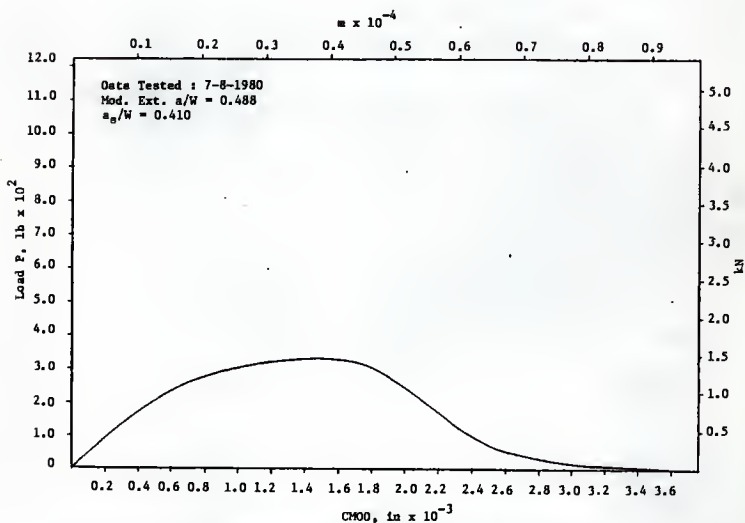


Fig. 60 P vs CMOD, 4 in Deep Beam (2-A1), Load Control, Fartash (11)

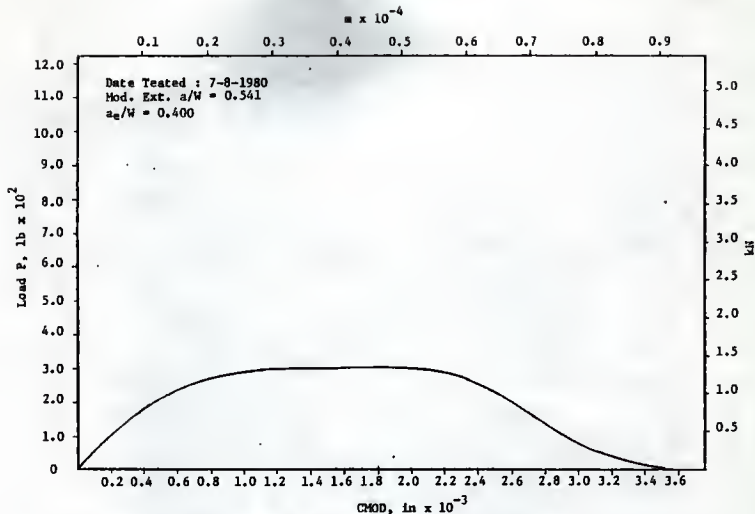


Fig. 61 P vs CMOD, 4in Deep Beam (2-A2), Load Control, Fartash (11)

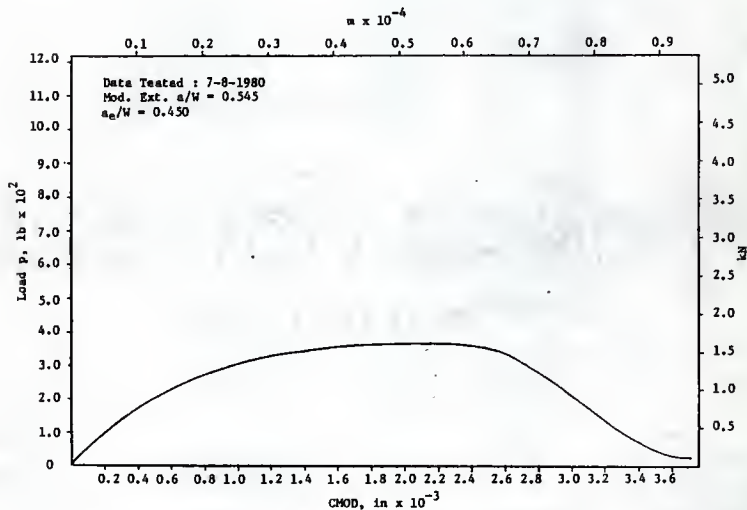


Fig. 62 P vs CMOD, 4 in Deep Beam (2-A3), Load Control, Fartash (11)

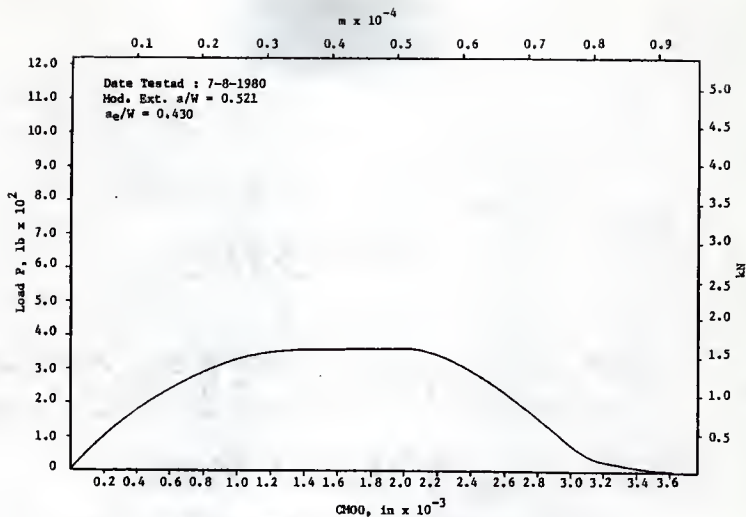


Fig. 63 P vs CMOD, 4 in Deep Beam (2-A4), Load Control, Fartash (11)

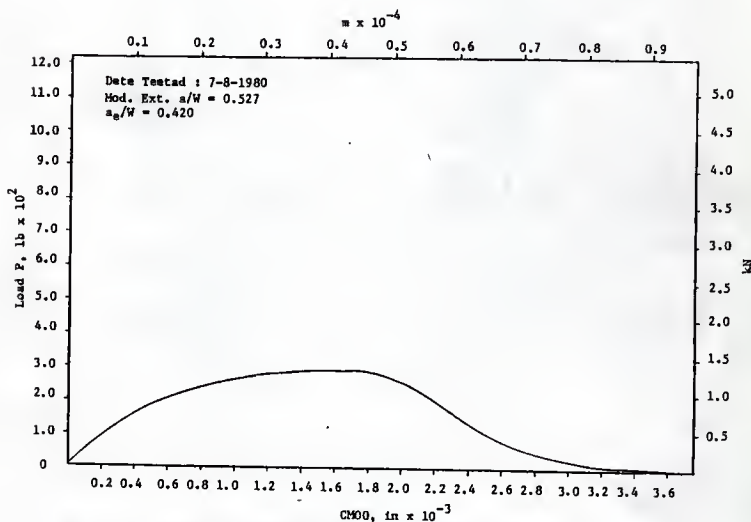


Fig. 64 P vs CMOD, 4 in Deep Beam (2-A5), Load Control, Fartash (11)

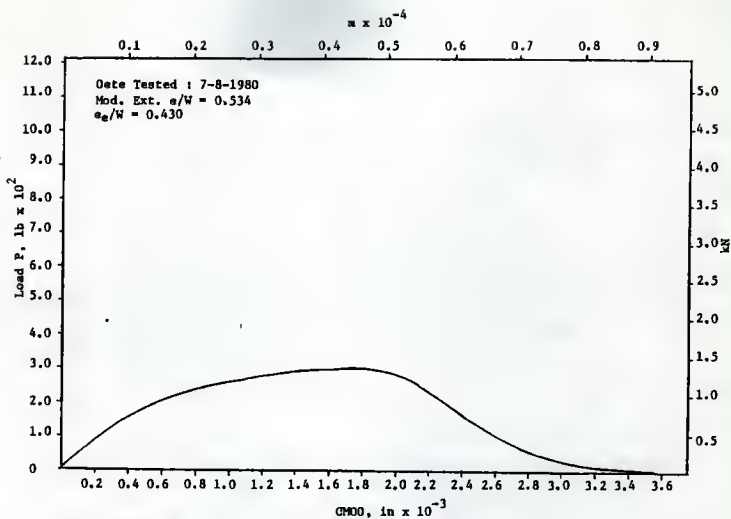


Fig. 65 P vs CMOD, 4 in Deep Beam (2-A6), Load Control, Fartash (11)

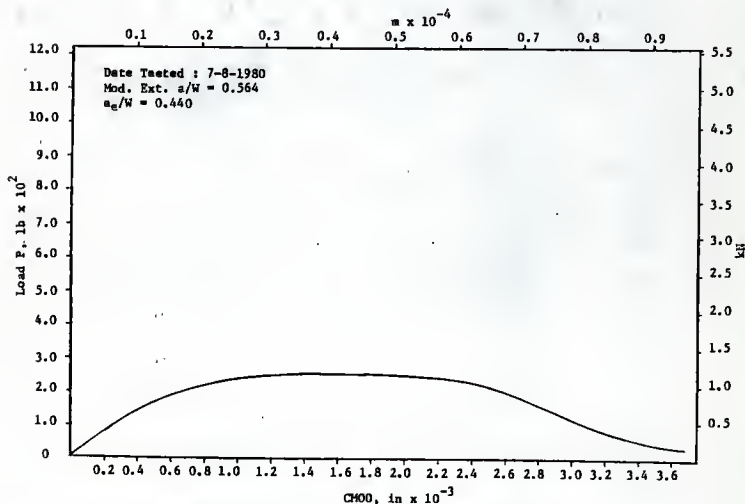


Fig. 66 P vs CMOD, 4 in Deep Beam (2-A7), Load Control, Fartash (11)

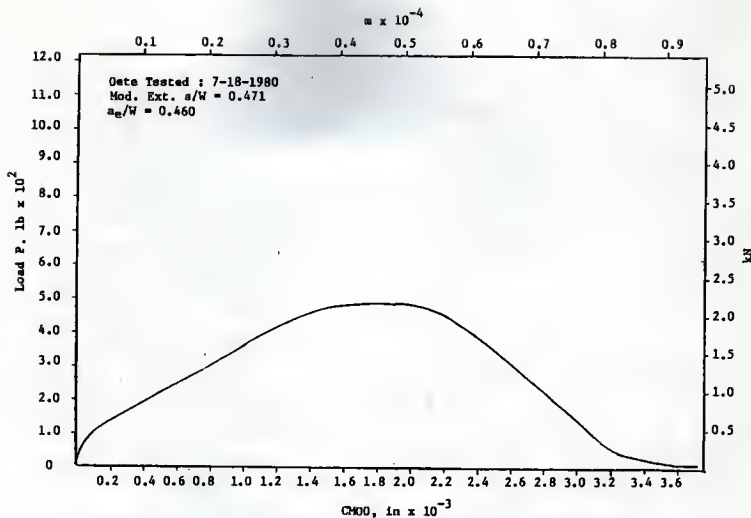


Fig. 67 P vs CMOD, 4 in Deep Beam (2-A10), Load Control, Fortash (11)

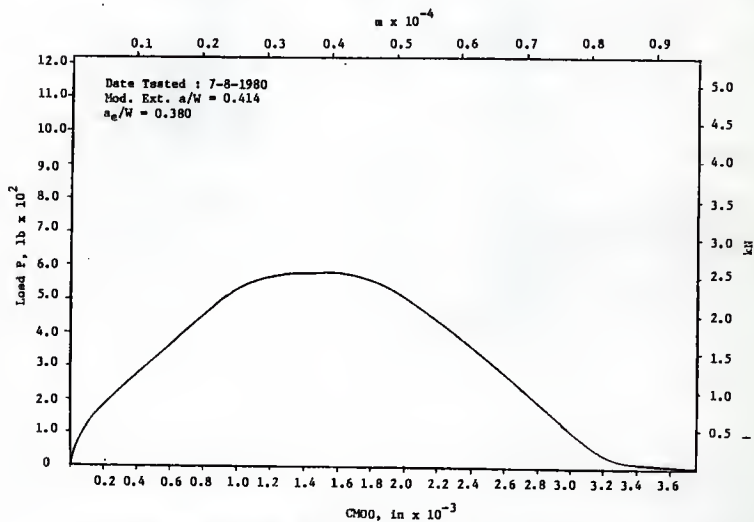
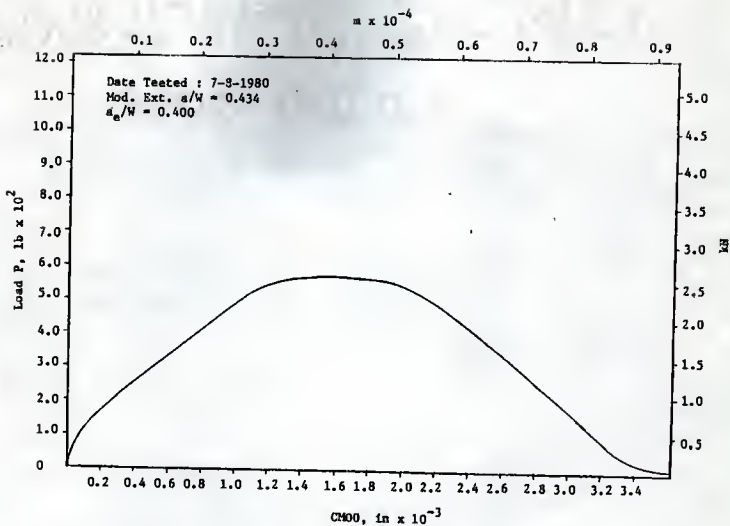
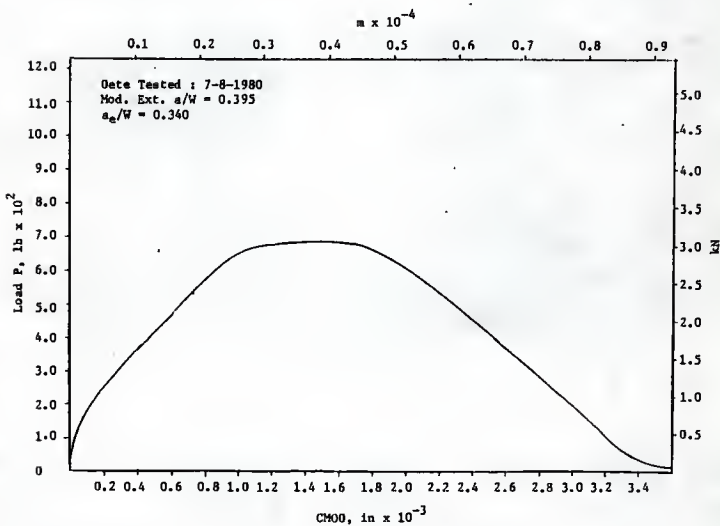


Fig. 68 P vs CMOD, 4 in Deep Beam (2-A11), Load Control, Fortash (11)

Fig. 69 P vs CMOD, 4 in Deep Beam (2-A12), Load Control, Fartash (11)Fig. 70 P vs CMOD, 4 in Deep Beam (2-A13), Load Control, Fartash (11)

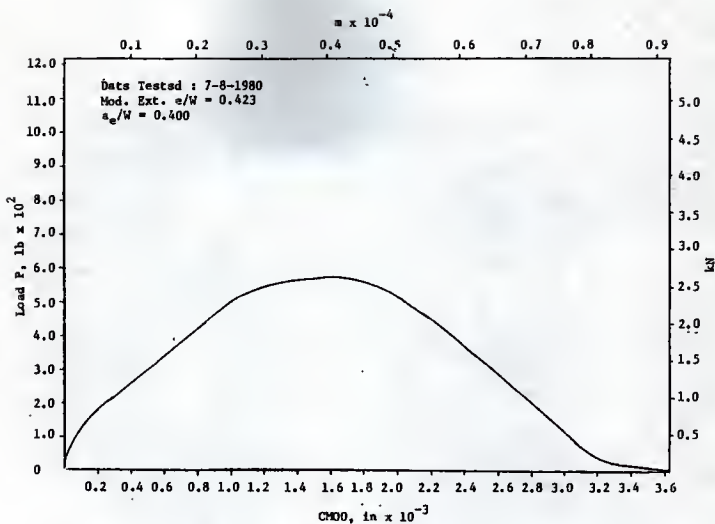


Fig. 71 P vs CMOD, 4 in Deep Beam (2-A14), Load Control, Fartash (11)

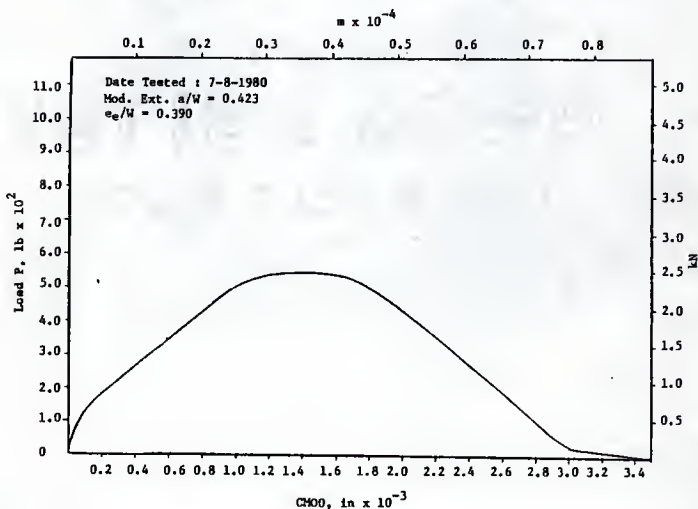


Fig. 72 P vs CMOD, 4 in Deep Beam (2-A15), Load Control, Fartash (11)

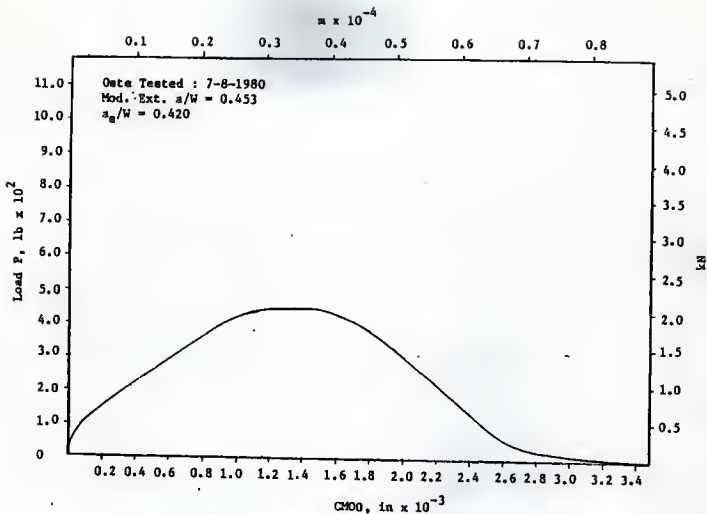


Fig. 73 P vs CM00, 4 in Deep Beam (2-A16), Load Control, Fartash (11)

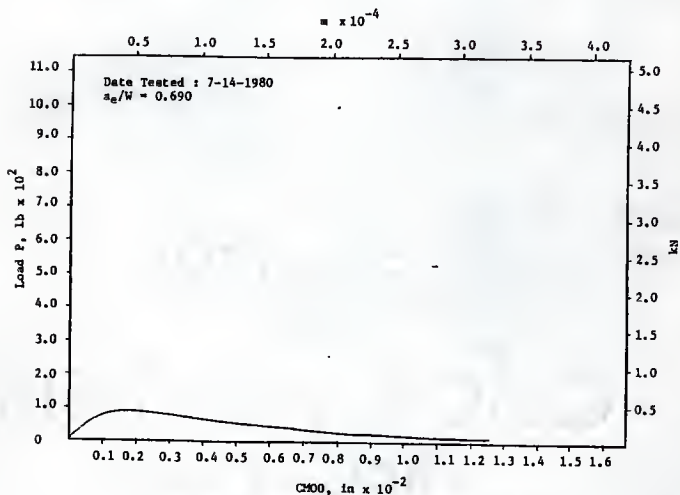


Fig. 74 P vs CM00, 4 in Deep Beam (3-A1), Load Control, Fartash (11)

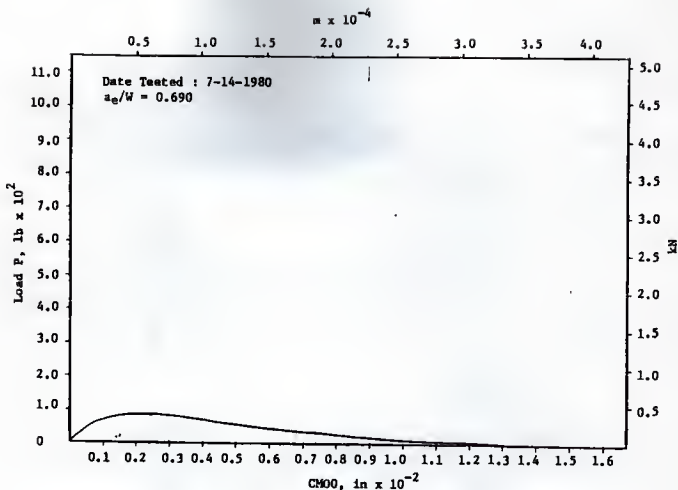


Fig. 75 P vs $CHOO$, 4 in Deep Beam (3-A2), Load Control, Fartash (11)

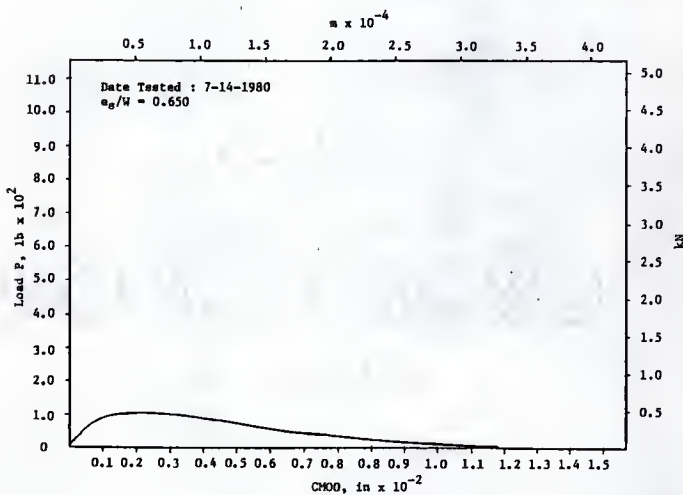


Fig. 76 P vs $CHOO$, 4 in Deep Beam (3-A3), Load Control, Fartash (11)

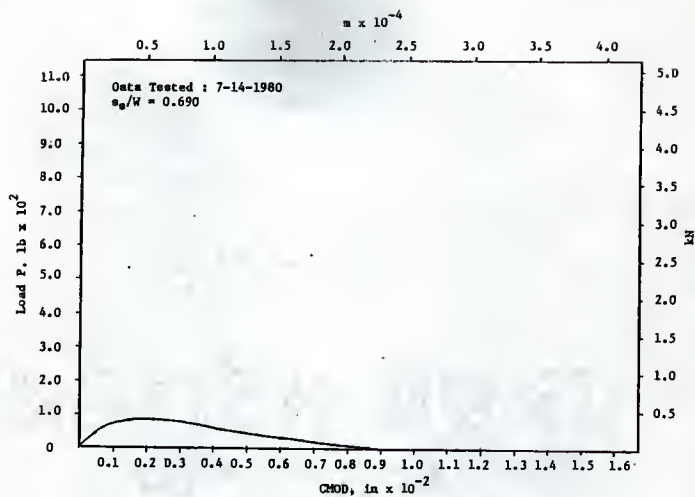


Fig. 77 P vs CHOD, 4 in Deep Beam (3-A4), Load Control, Fartash (11)

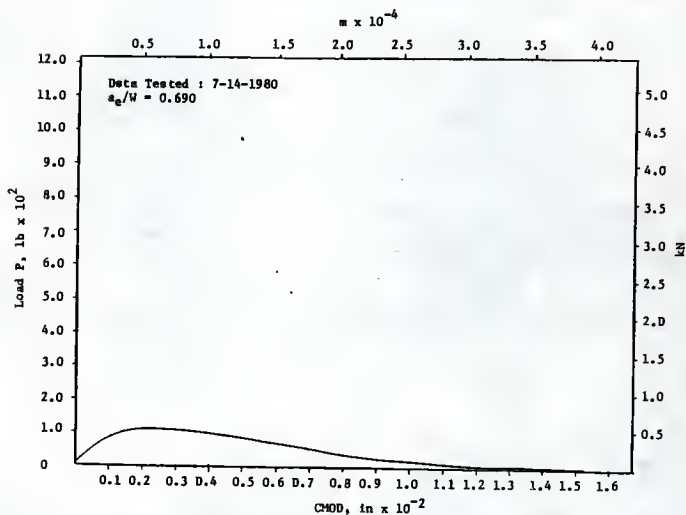


Fig. 78 P vs CHOD, 4 in Deep Beam (3-A5), Load Control, Fartash (11)

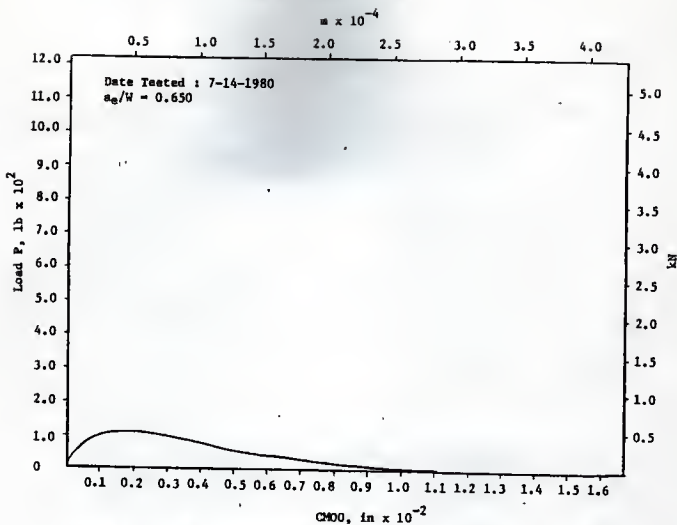


Fig. 79 P vs CMDO, 4 in Deep Beam (3-A6), Load Control, Fartash (11)

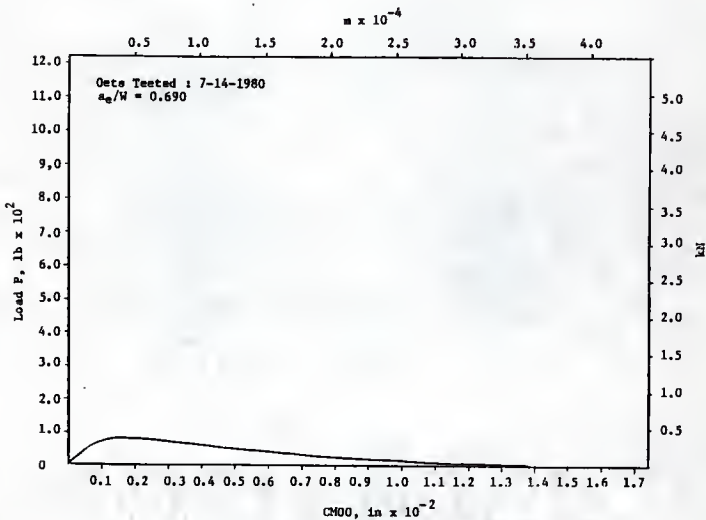


Fig. 80 P vs CMDO, 4 in Deep Beam (3-A7), Load Control, Fartash (11)

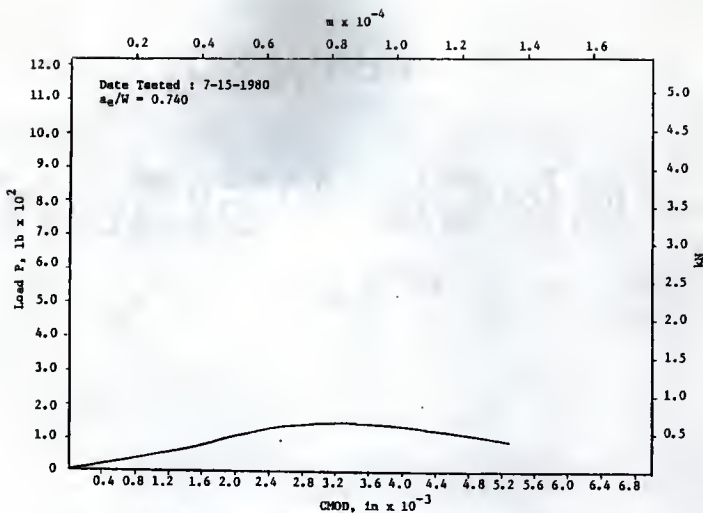


Fig. 81 P vs CMOD, 4 in Deep Beam (3-A10), Load Control, Fartash (11)

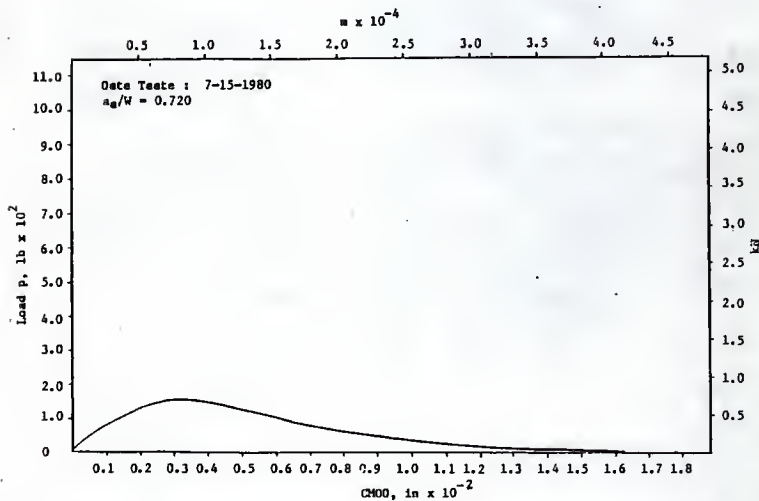


Fig. 82 P vs CMOD, 4 in Deep Beam (3-A11), Load Control, Fartash (11)

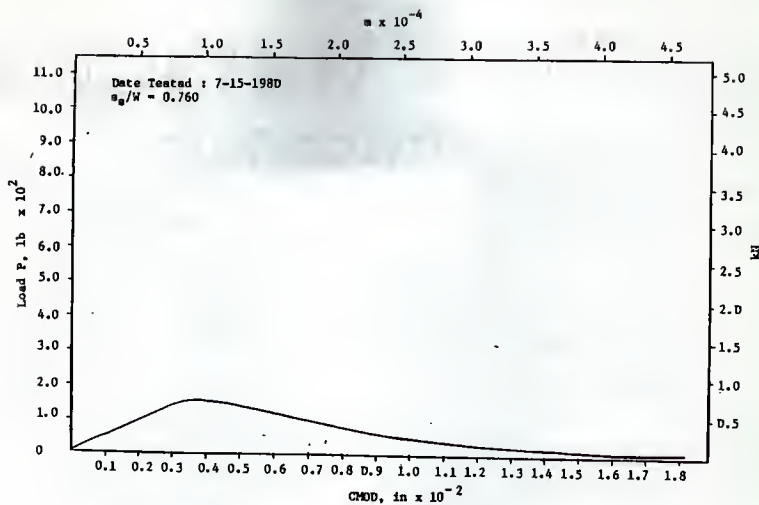


Fig. 83 P vs CHOD, 4 in Deep Beam (3-A12), Load Control, Fartash (11)

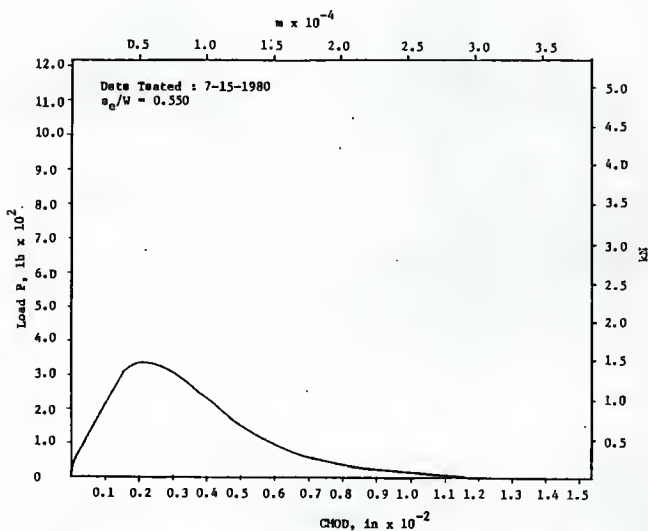


Fig. 84 P vs CHOD, 4 in Deep Beam (3-A13), Load Control, Fartash (11)

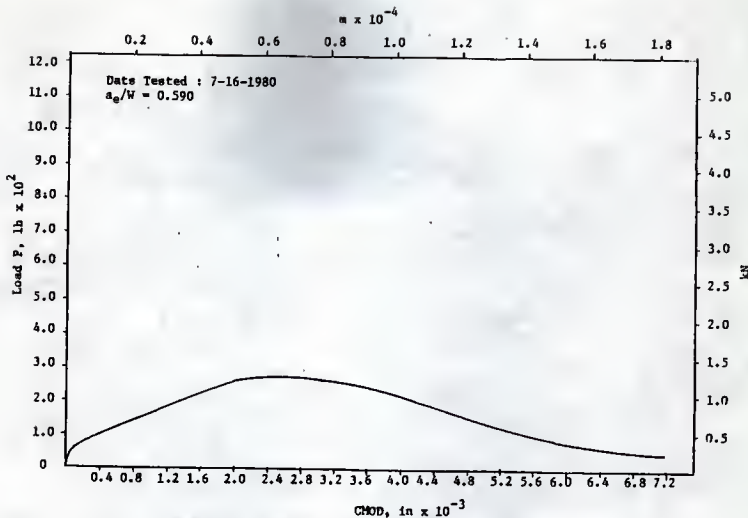


Fig. 85 P vs CMOD, 4 in Deep Beam (J-A14), Load Control, Fartash (11)

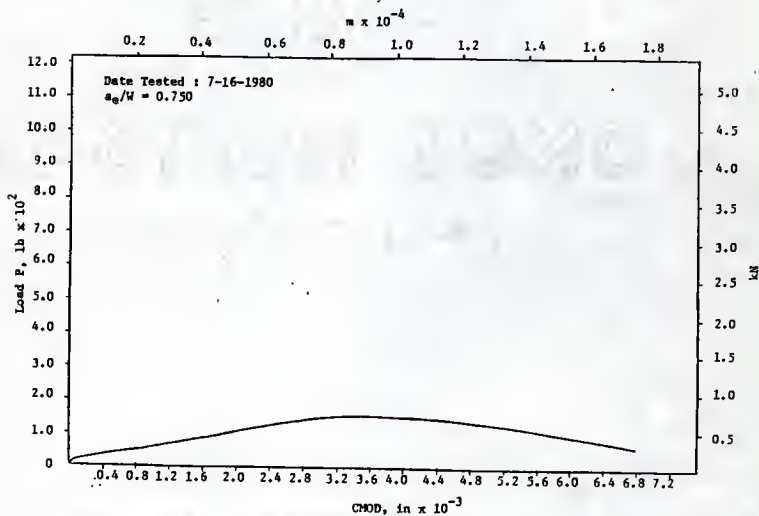


Fig. 86 P vs CMOD, 4 in Deep Beam (J-A15), Load Control, Fartash (11)

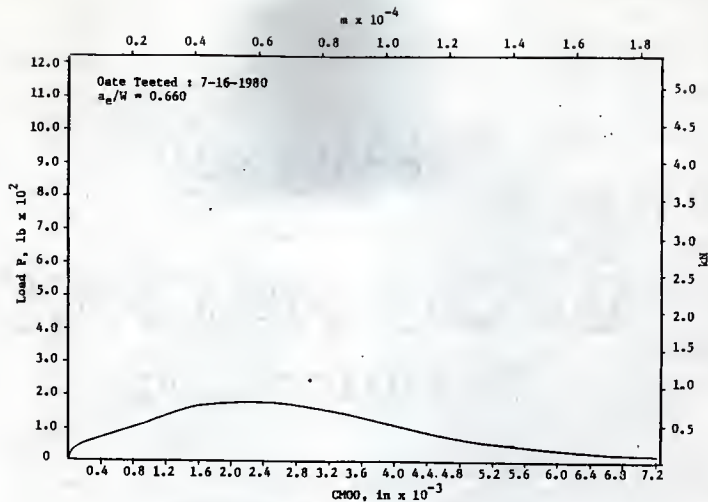


Fig. 87 P vs CM00, 4 in Deep Beam (3-A16) Load Control, Fartash (11)

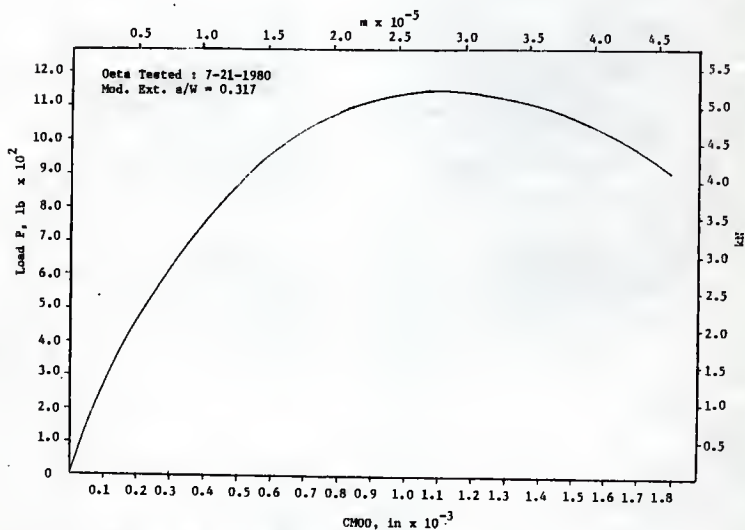


Fig. 88 P vs CM00, 4 in Deep Beam (1-B1), Load Control, Fartash (11)

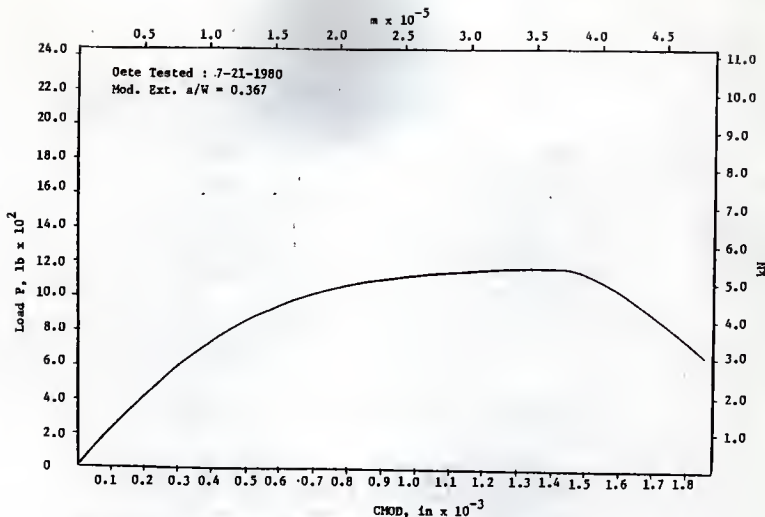


Fig. 89 P vs CHOD, 4 in Deep Beam (I-B2), Load Control, Fartash (11)

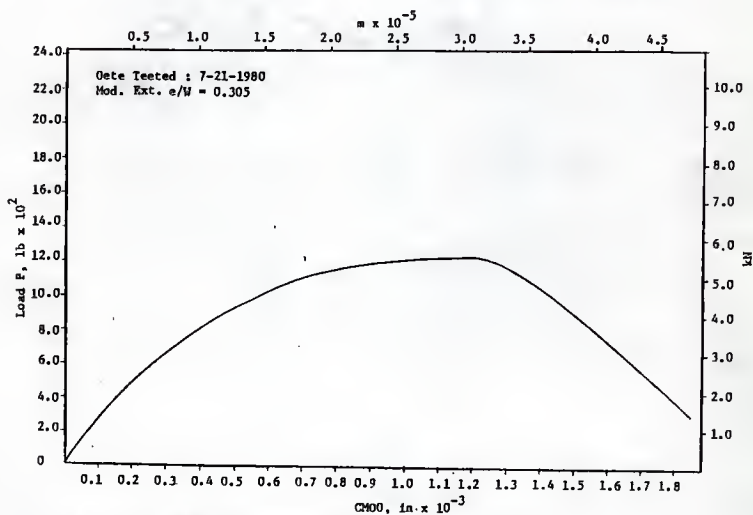


Fig. 90 P vs CHOD, 4 in Deep Beam (I-B3), Load Control, Fartash (11)

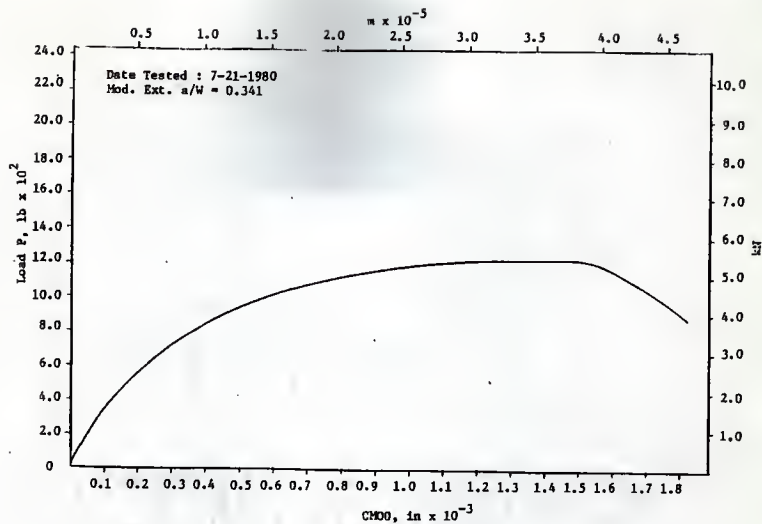


Fig. 91 P vs CMOD, 4 in Deep Beam (1-B4), Load Control, Fartash (11)

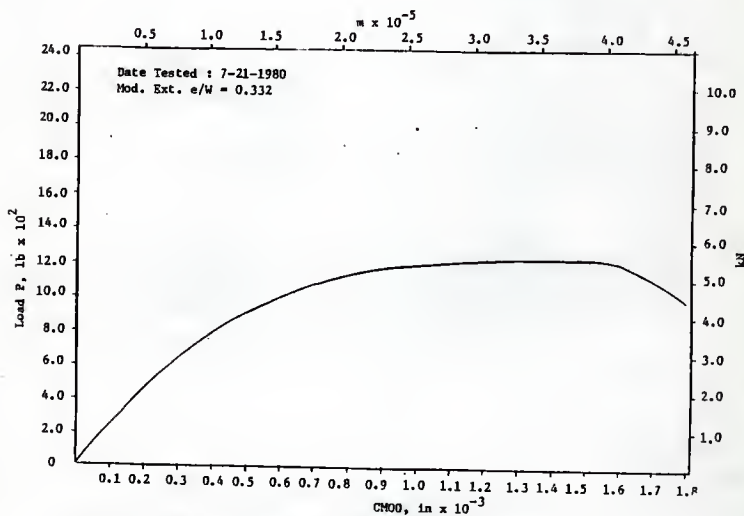
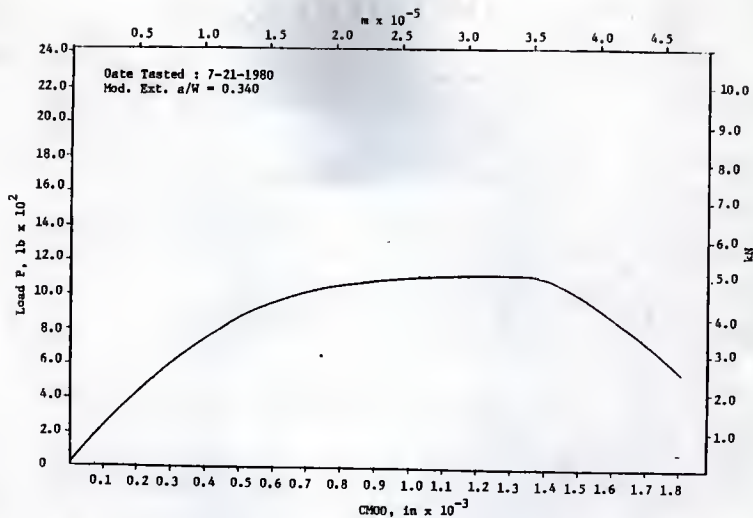
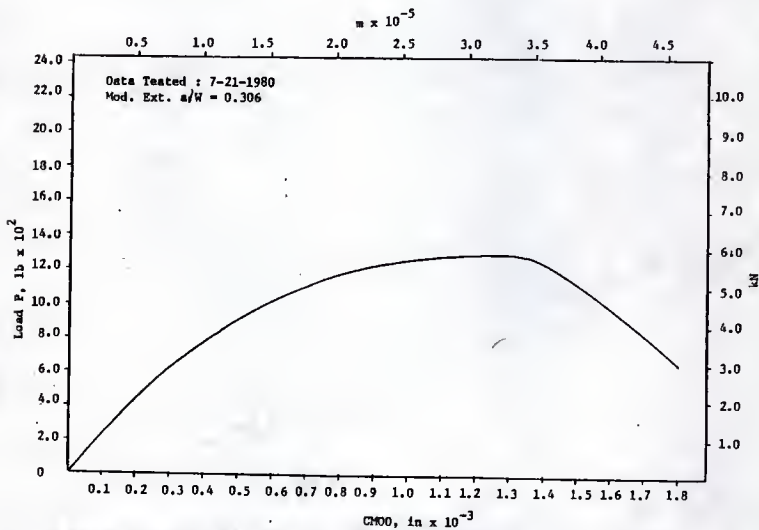
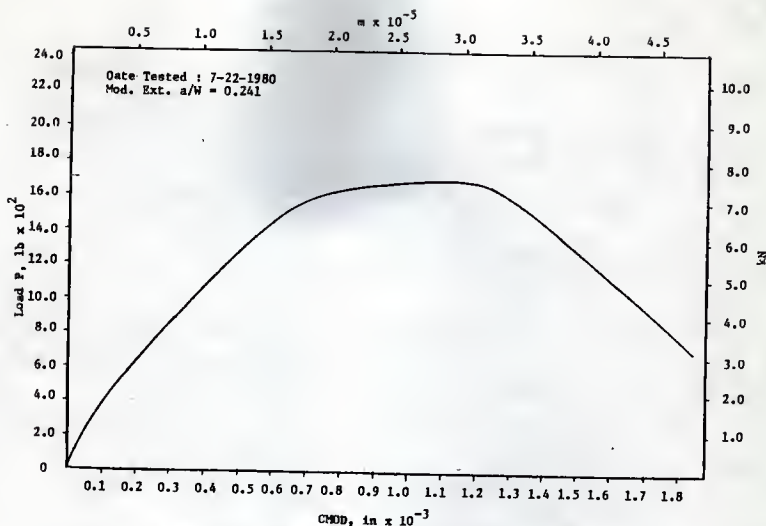
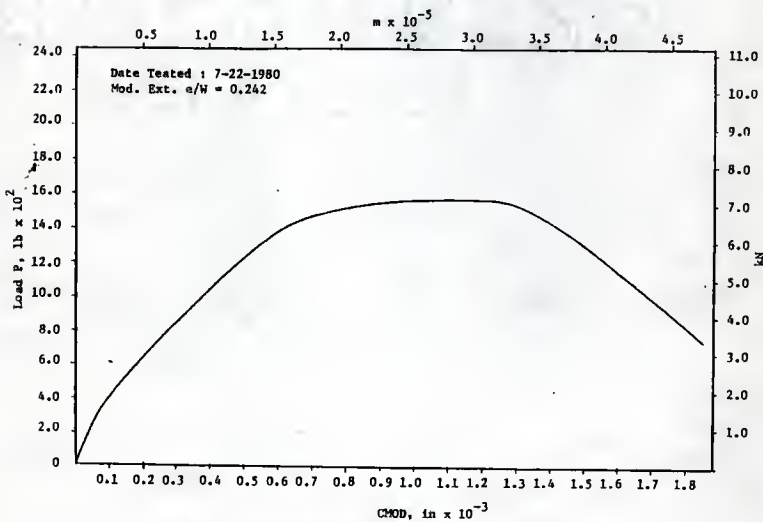


Fig. 92 P vs CMOD, 4 in Deep Beam (1-B5), Load Control, Fartash (11)

Fig. 93 P vs $CM00$, 4 in Deep Beam (1-86), Load Control, Fartash (11)Fig. 94 P vs $CM00$, 4 in Deep Beam (1-87), Load Control, Fartash (11)

Fig. 95 P vs CMOD, 4 in Deep Beam (1-B10), Load Control, Fartash (11)Fig. 96 P vs CMOD, 4 in Deep Beam (1-B11), Load Control, Fartash (11)

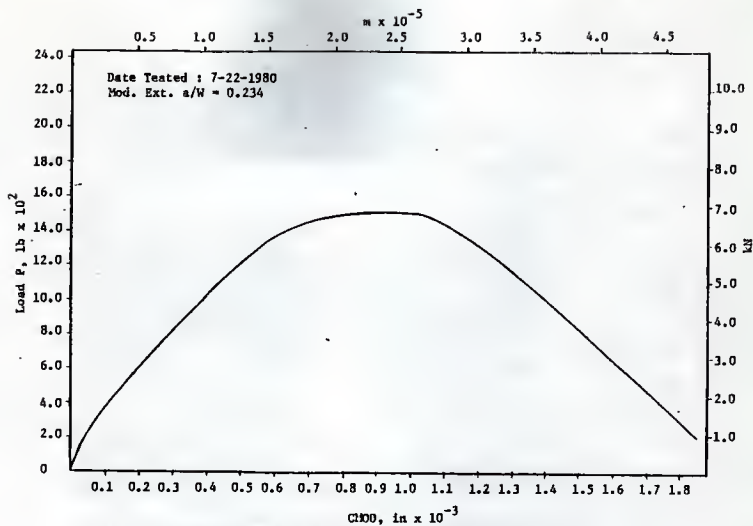


Fig. 97 P vs CMDO, 4 in Deep Beam (1-B12), Load Control, Fartash (11)

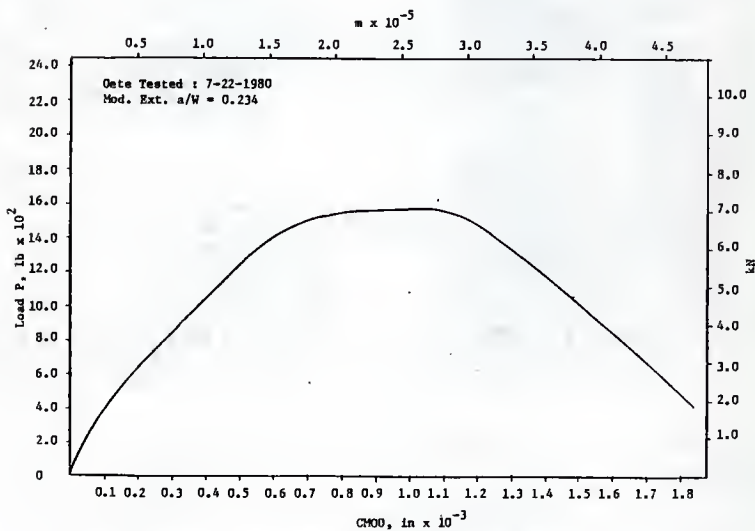


Fig. 98 P vs CMDO, 4 in Deep Beam (1-B13), Load Control, Fartash (11)

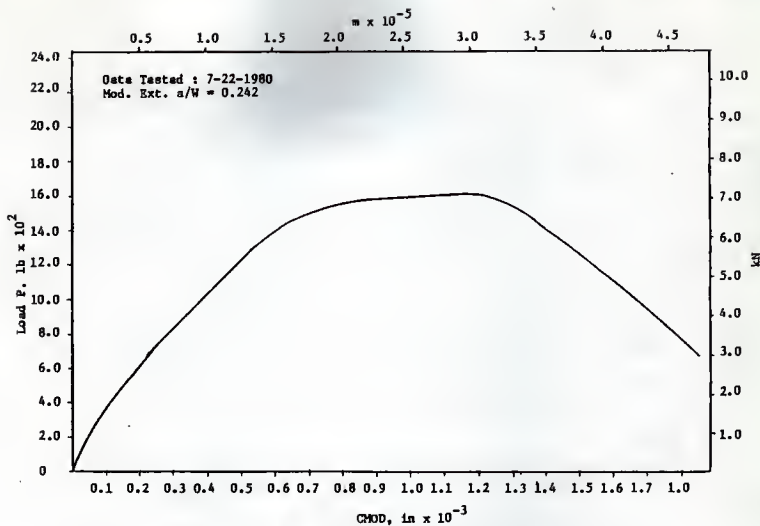


Fig. 99 P vs CHOD, 4 in Deep Beam (1-B14), Load Control, Fartash (11)

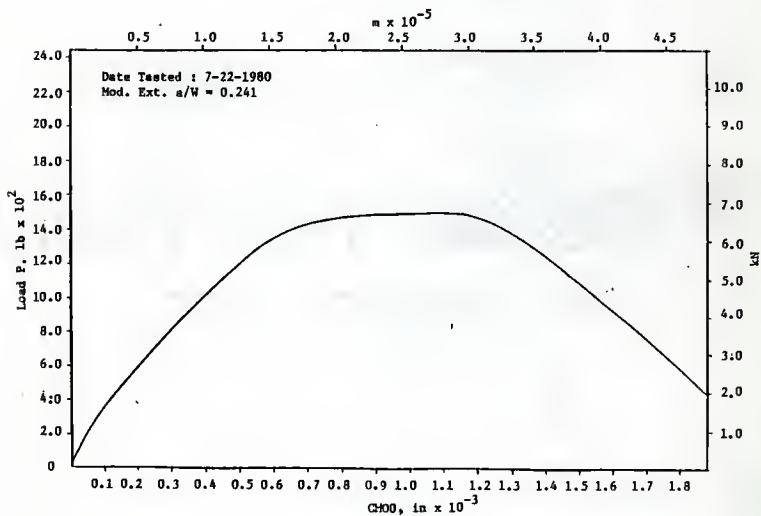
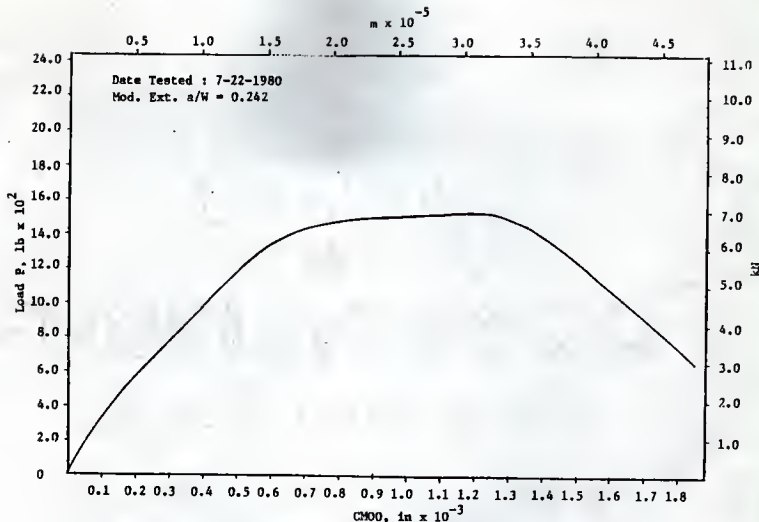
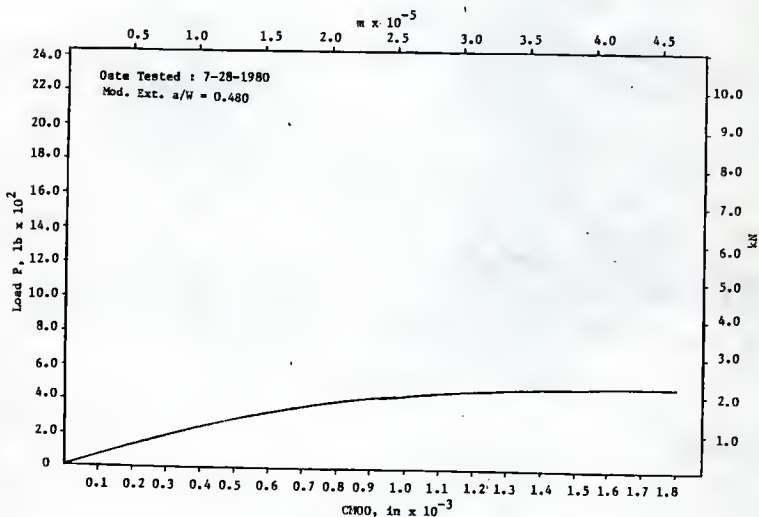


Fig. 100 P vs CHOD, 4 in Deep Beam (1-B15), Load Control, Fartash (11)

Fig. 101 P vs CMOD, δ in Deep Beam (1-816), Load Control, Fartash (11)Fig. 102 P vs CMOD, δ in Deep Beam (2-B1), Load Control, Fartash (11)

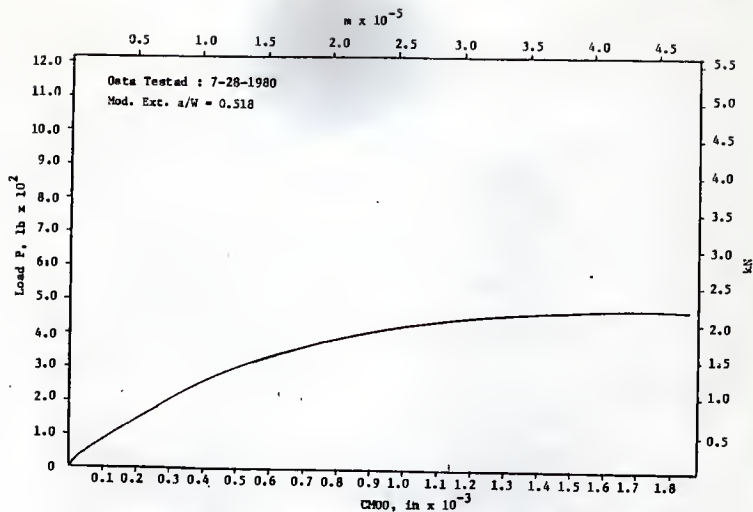


Fig. 103 P vs $CM00$, 4 in Deep Beam (2-B2), Load Control, Fartash (11)

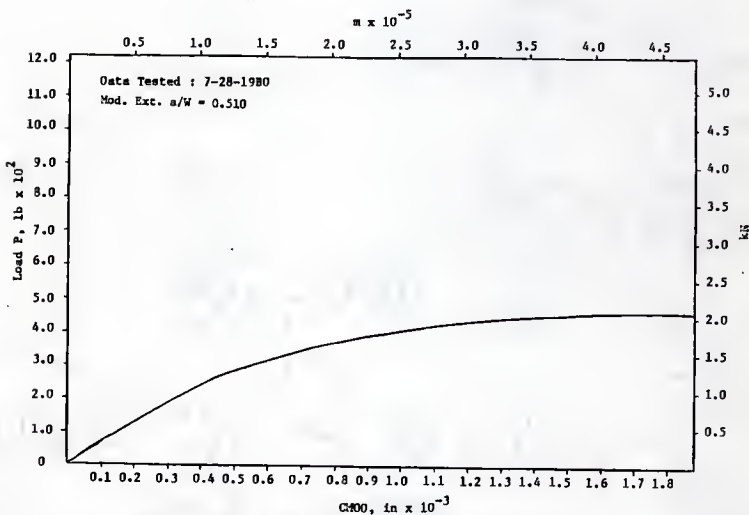


Fig. 104 P vs $CM00$, 4 in Deep Beam (2-B3), Load Control, Fartash (11)

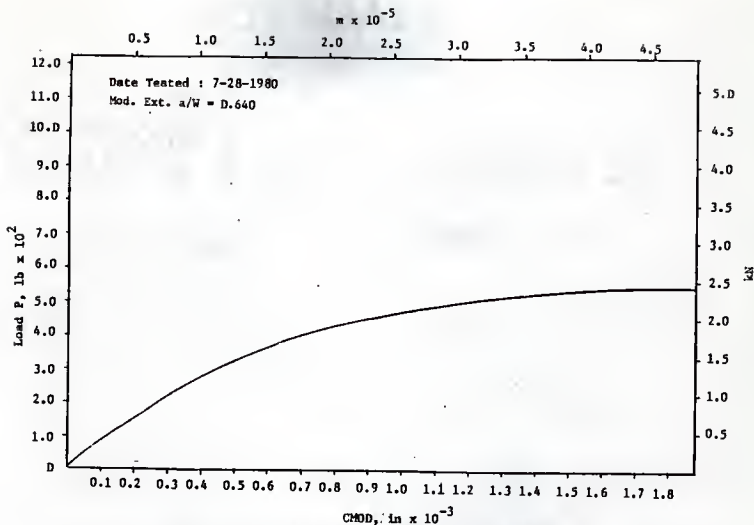


Fig. 105 P vs CMOD, 4 in Deep Beam (2-B4), Load Control, Fartash (11)

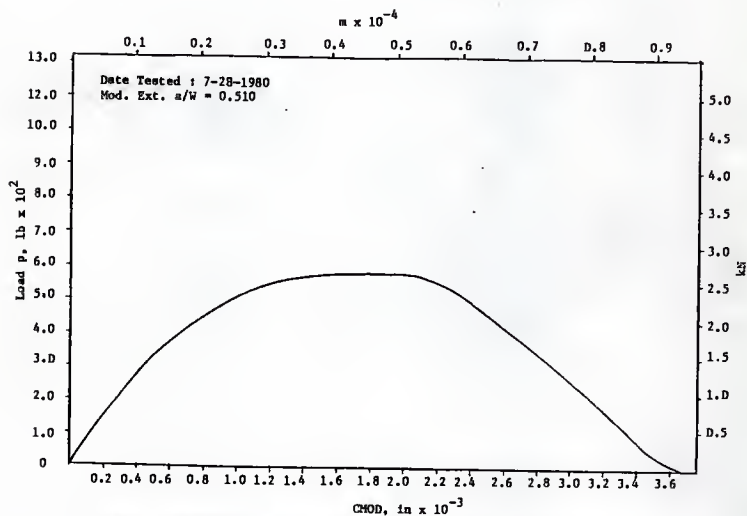


Fig. 106 P vs CMOD, 4 in Deep Beam (2-B5), Load Control, Fartash (11)

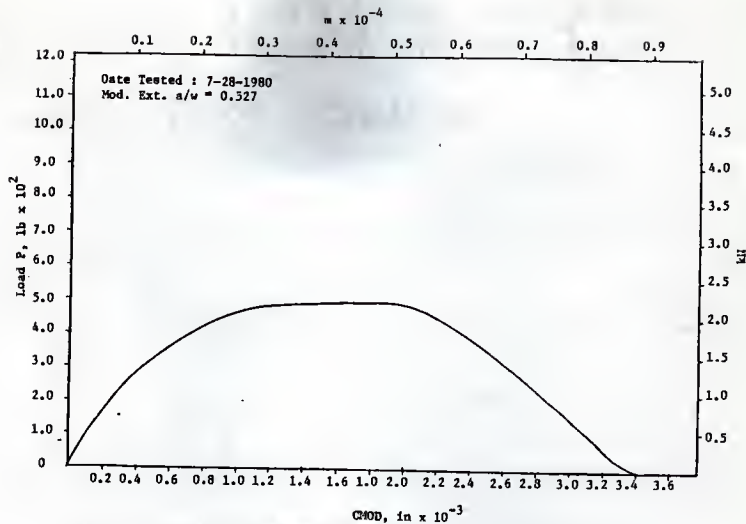


Fig. 107 P vs $CHOD$, 4 in Deep Beam (2-B6), Load Control, Fartash (11)

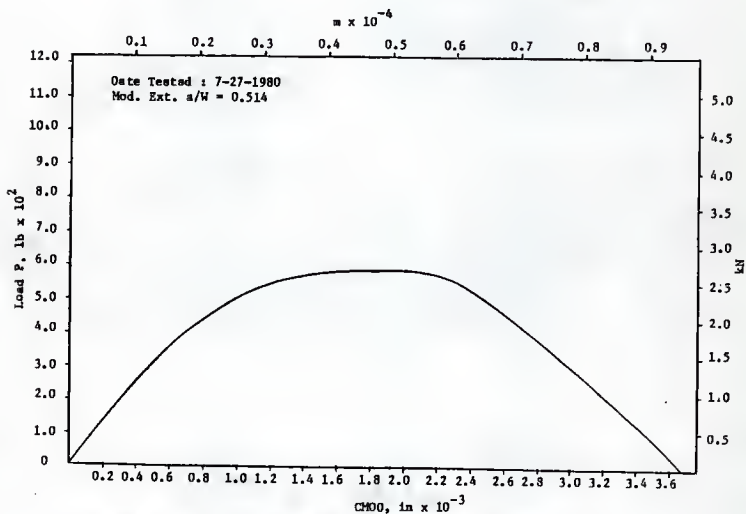


Fig. 108 P vs $CHOD$, 4 in Deep Beam (2-B7), Load Control, Fartash (11)

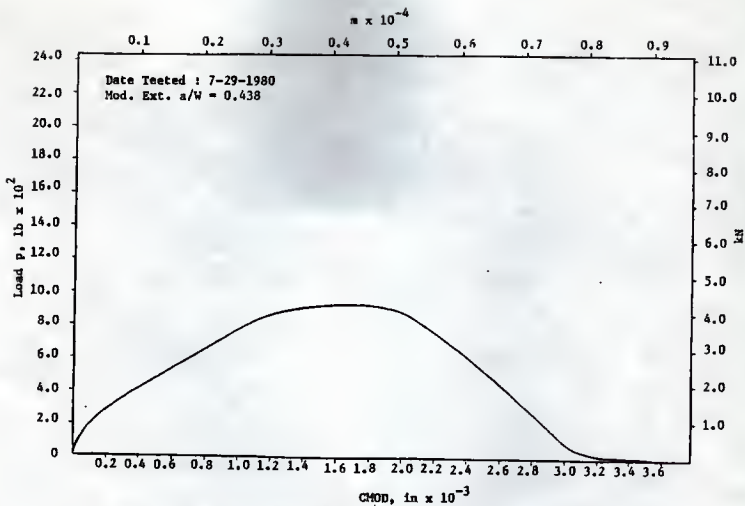


Fig. 109: P vs CMOD, 4 in Deep Beam (2-B10), Load Control, Fartash (11)

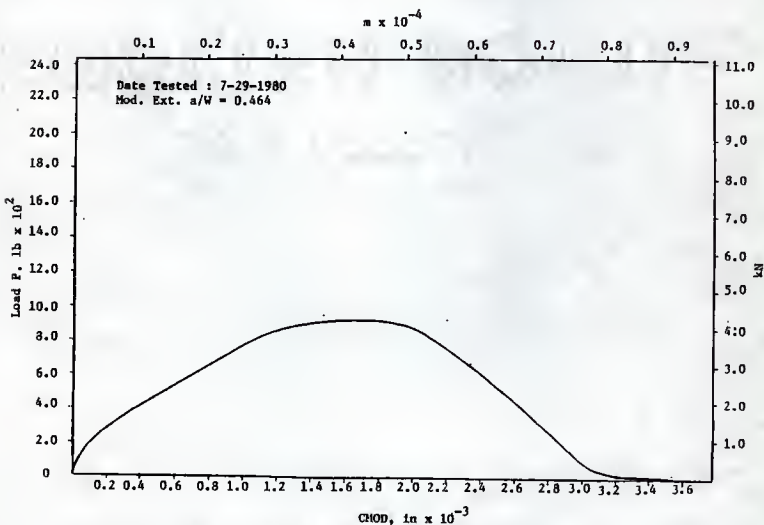


Fig. 110: P vs CMOD, 4 in Deep Beam (2-B11), Load Control, Fartash (11)

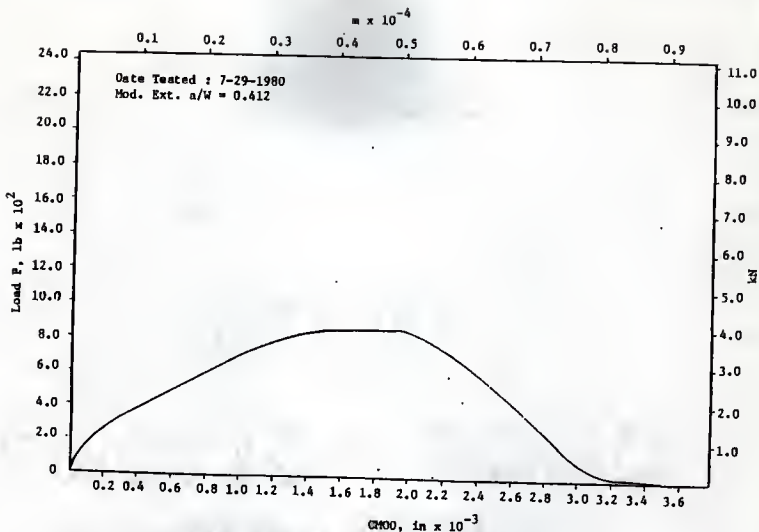


Fig. 111 P vs CMOD, 4 in Deep Beam (2-B12), Load Control, Fartash (11)

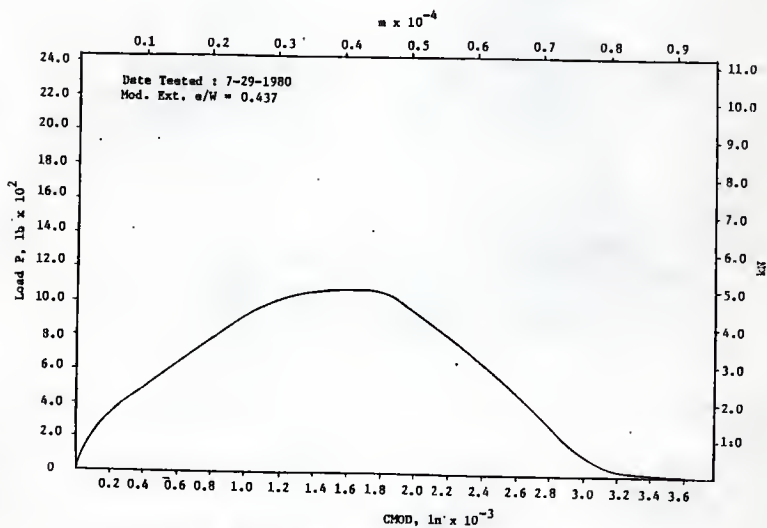


Fig. 112 P vs CMOD, 4 in Deep Beam (2-B13), Load Control, Fartash (11)

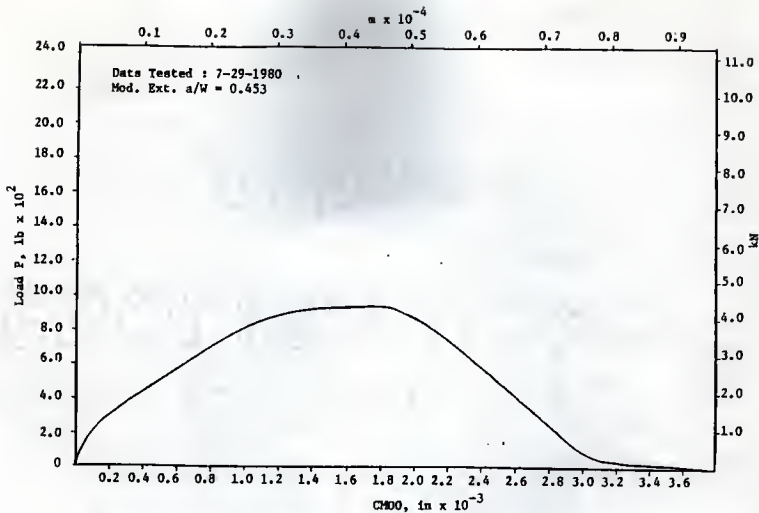


Fig. 113 P vs CMDO, 4 in Deep Beam (2-B14), Load Control, Fartash (11)

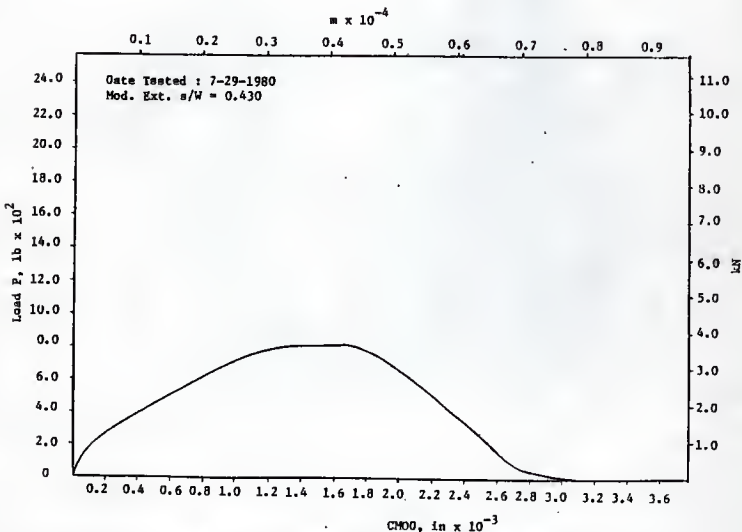


Fig. 114 P vs CMDO, 4 in Deep Beam (2-B15), Load Control, Fartash (11)

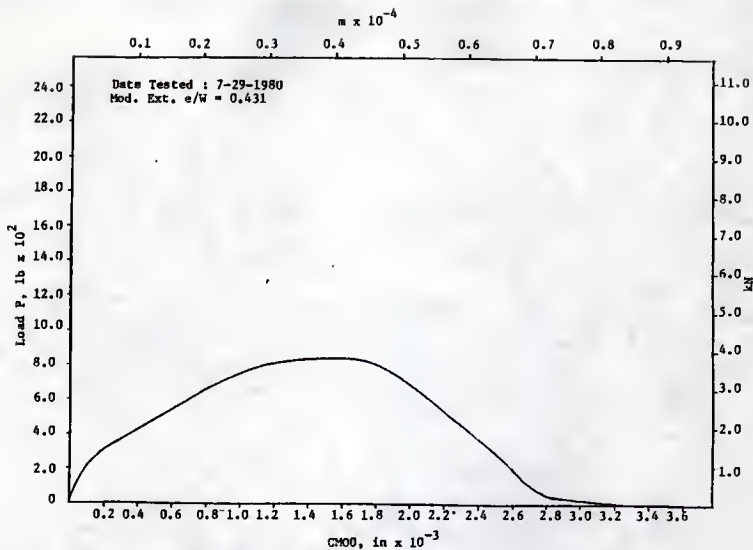


Fig. 115 P vs CMOD, 4 in Deep Beam (2-B16), Load Control, Fertash (11)

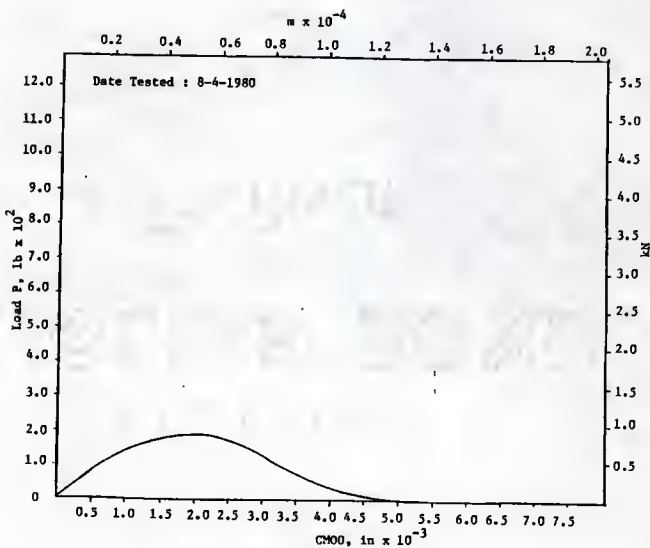


Fig. 116 P vs CMOD, 4 in Deep Beam (3-B1), Load Control, Fertash (11)

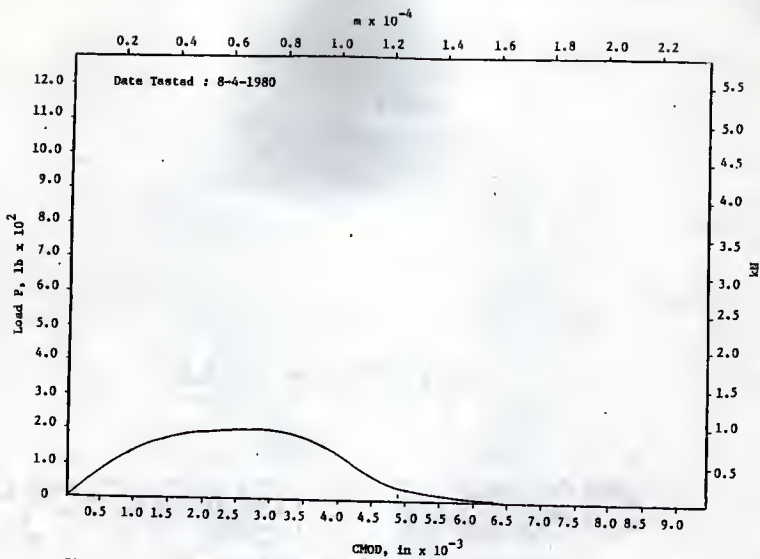


Fig. 117 P vs CHOD, 4 in Deep Beam (3-B2), Load Control, Fartash (11)

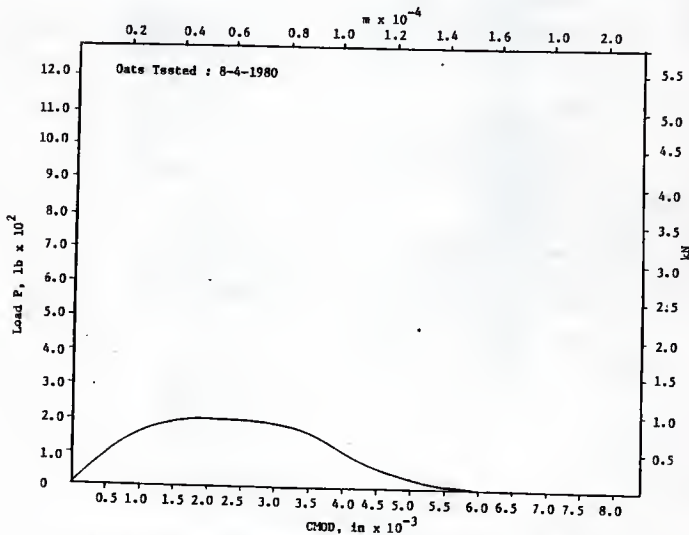


Fig. 118 P vs CHOD, 4 in Deep Beam (3-B3), Load Control, Fartash (11)

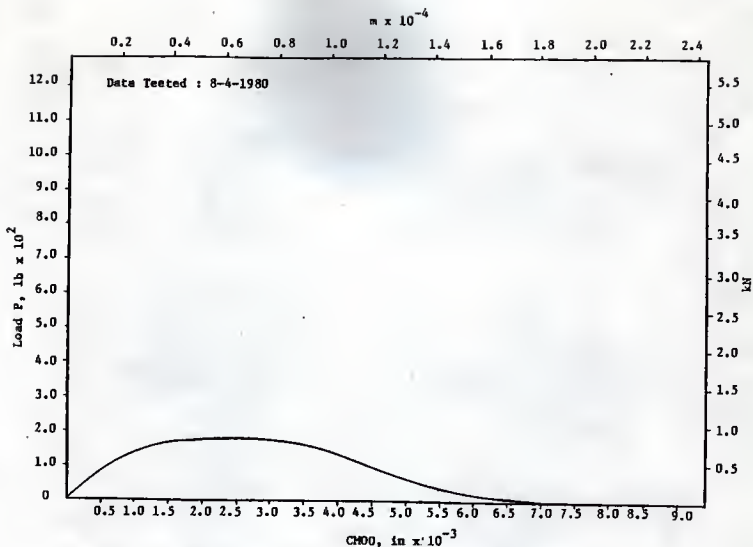


Fig. 119 P vs CMOD, 4 in Deep Beam (3-B4), Load Control, Fartash (11)

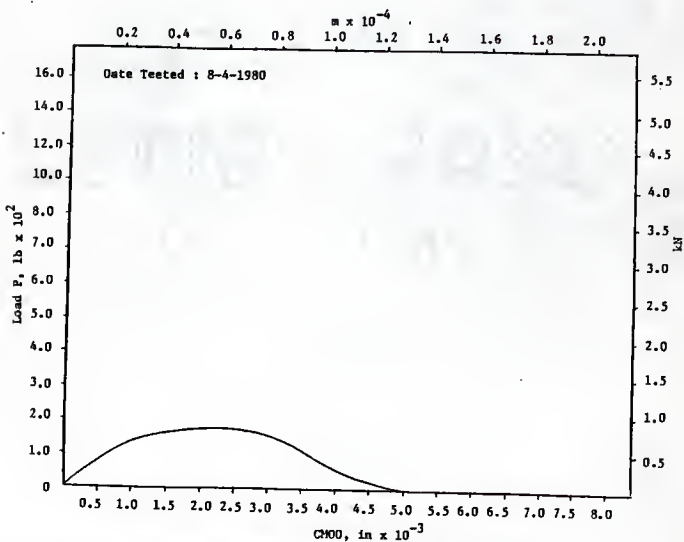


Fig. 120 P vs CMOD, 4 in Deep Beam (3-B5), Load Control, Fartash (11)

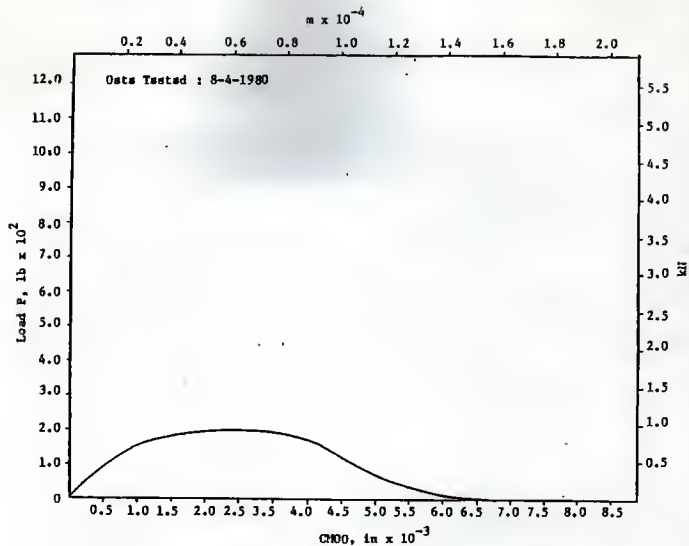


Fig. 121 P vs $CHOO$, 4 in Deep Beam (3-B6), Load Control, Fartash (11)

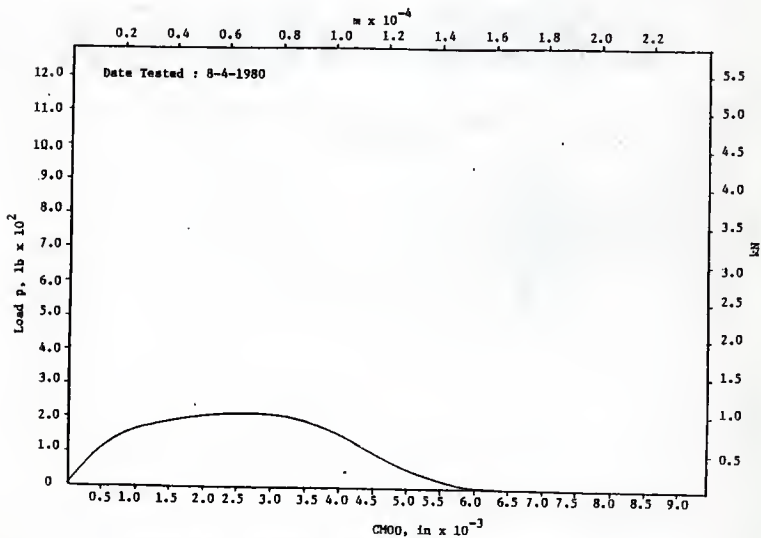


Fig. 122 P vs $CHOO$, 4 in Deep Beam (3-B7), Load Control, Fartash (11)

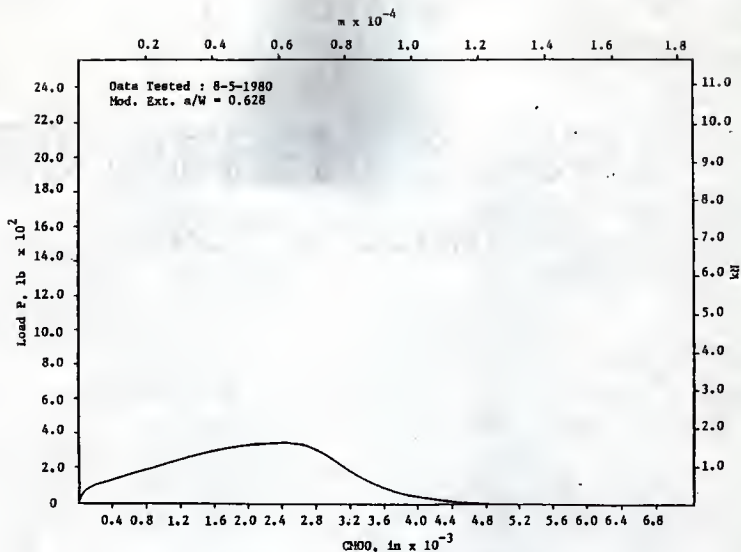


Fig. 123 P vs CHOO, 4 in Deep Beam (3-B12), Load Control, Fartash (11)

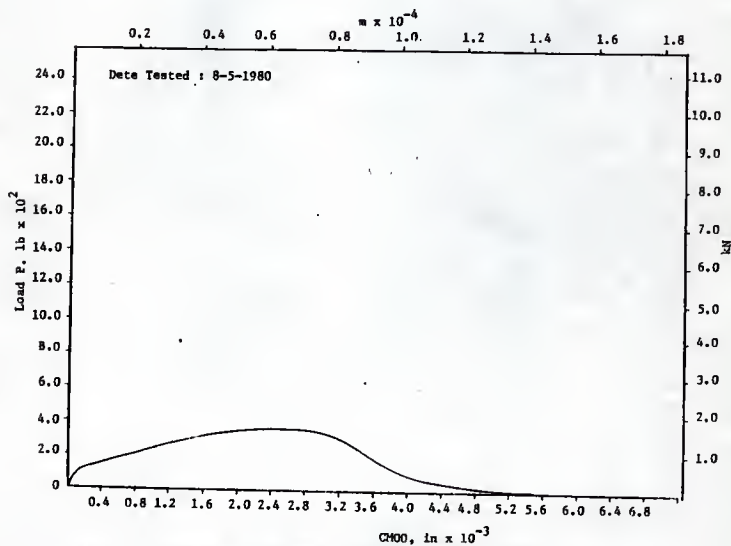


Fig. 124 P vs CHOO, 4 in Deep Beam (3-B13), Load Control, Fartash (11)

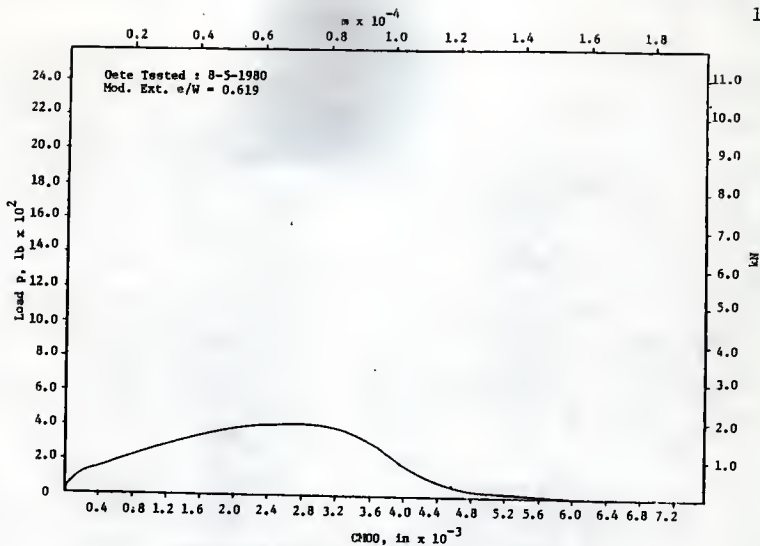


Fig. 125 P vs $CH00$, 4 in Deep Beam (3-B14), Load Control, Fartash (11)

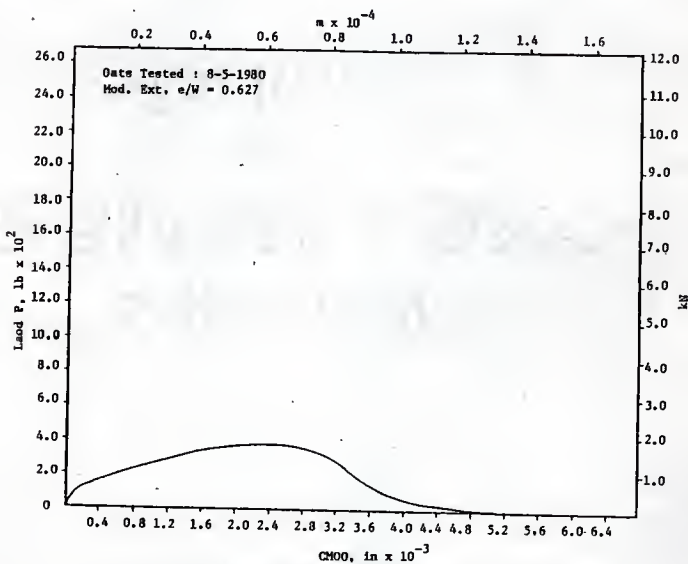


Fig. 126 P vs $CH00$, 4 in Deep Beam (3-B15), Load Control, Fartash (11)

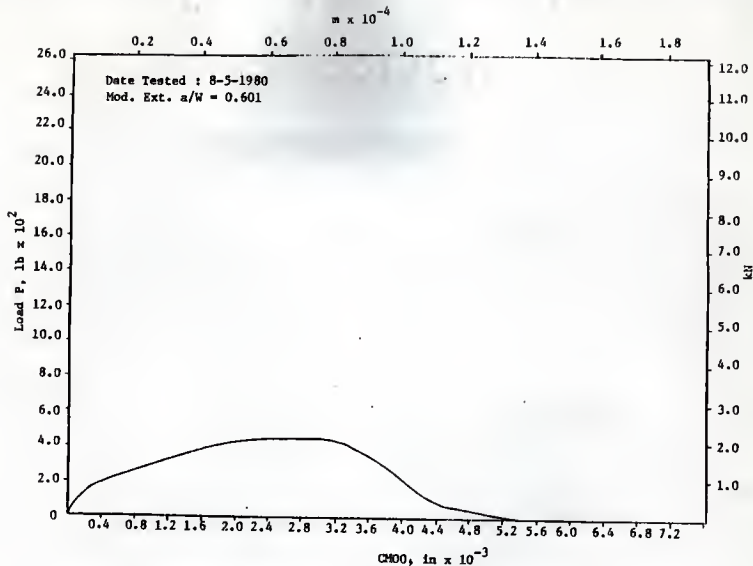


Fig. 127 P vs CMOD, 4 in Deep Beam (3-B16), Load Control, Fartash (11)

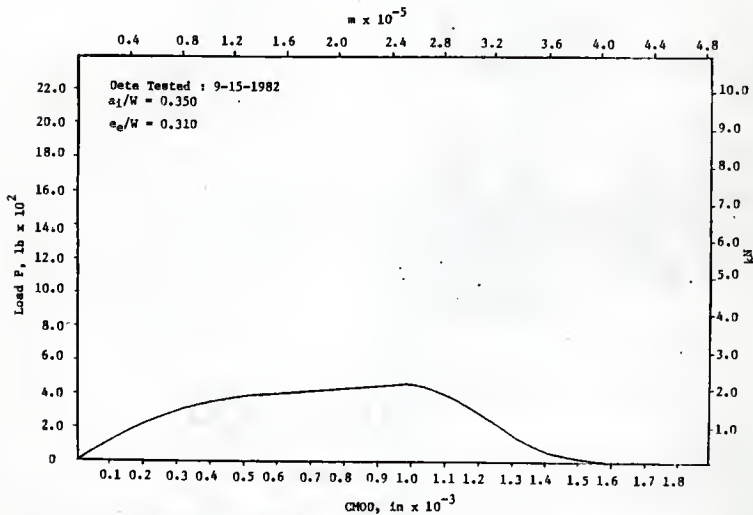


Fig. 128 P vs CMOD, 4 in Deep Beam (T1), Load Control, Co (4)

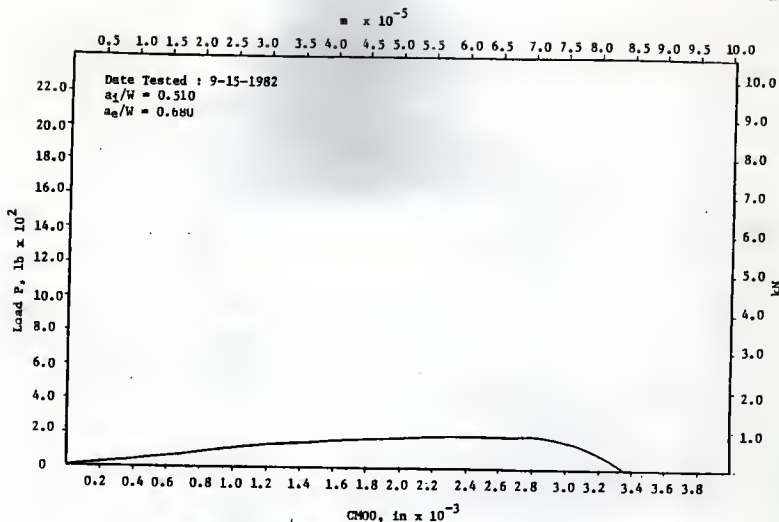


Fig. 129 P vs CHOD, 4 in Deep Beam (T3), Load Control, Co (4)

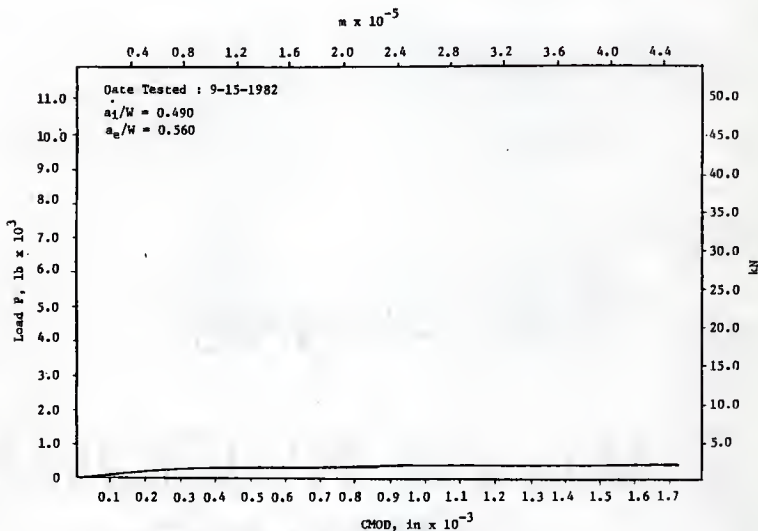


Fig. 130 P vs CHOD, 4 in Deep Beam (T4), Load Control, Co (4)

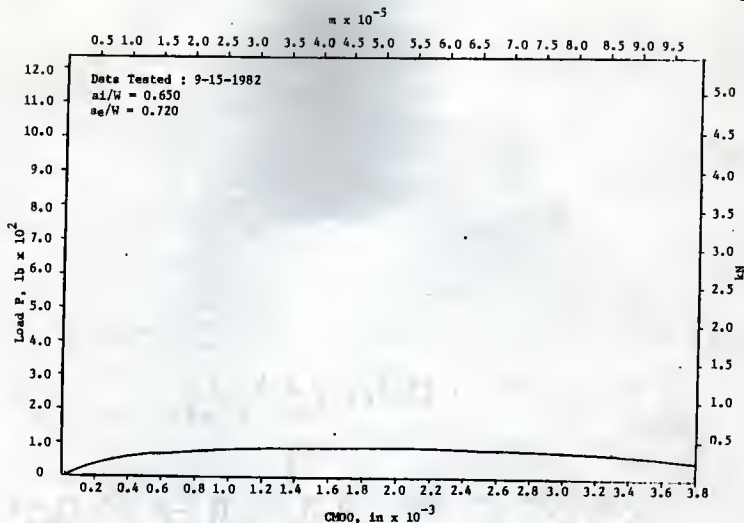


Fig. 131 P vs CMDO, 4 in Deep Beam (T5), Load Control, Go (4)

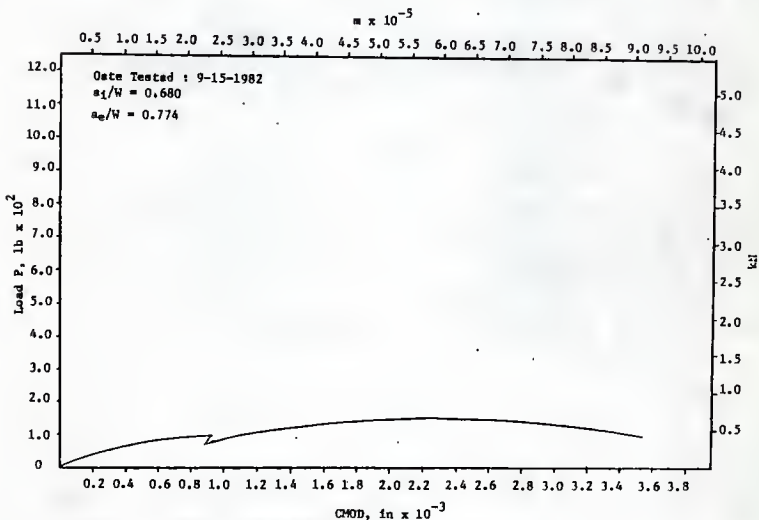


Fig. 132 P vs CMDO, 4 in Deep Beam (T6), Load Control, Go (4)

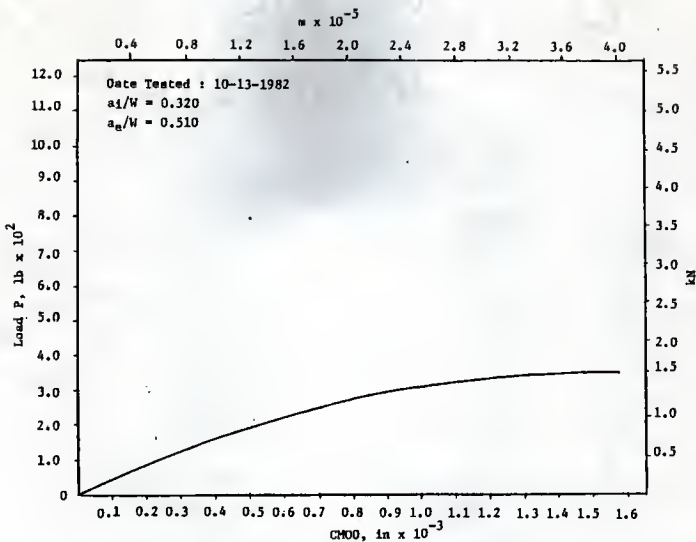


Fig. 133 P vs CHOD, 4 in Deep Beam (T7), Load Control, Go (4)

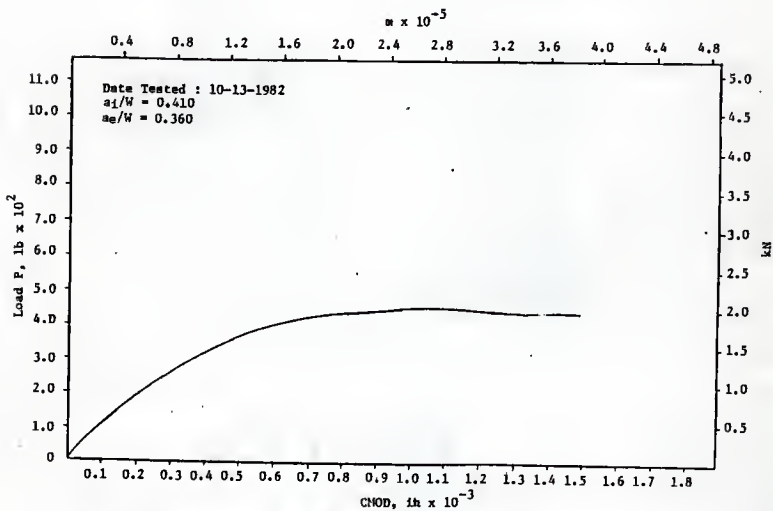


Fig. 134 P vs CHOD, 4 in Deep Beam (T8), Load Control, Go (4)

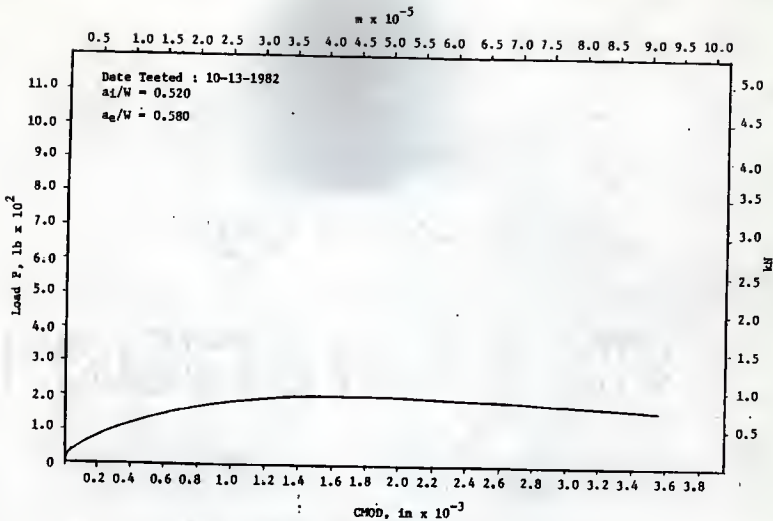


Fig. 135 P vs CMOD, 4 in Deep Beam (T9), Load Control, Go (4)

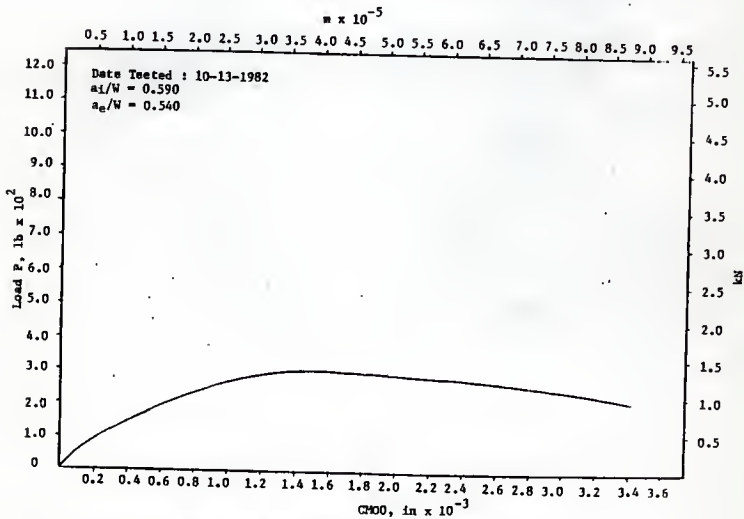


Fig. 136 P vs CMOD, 4 in Deep Beam (T10), Load Control, Go (4)

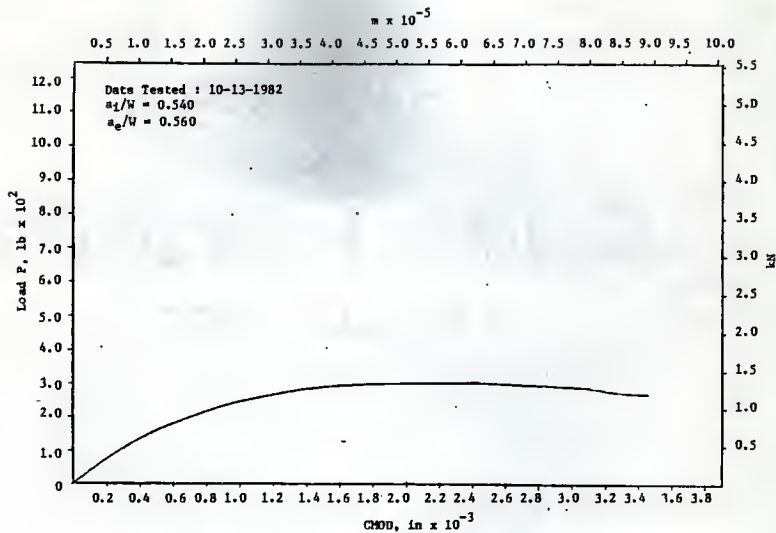


Fig. 137 P vs CMOD, 4 in Deep Beam (T11), Load Control, Go (4)

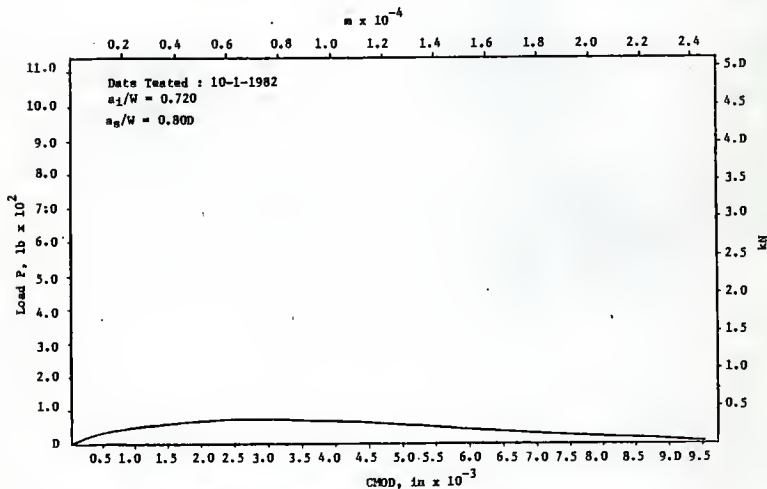


Fig. 138 P vs CMOD, 4 in Deep Beam (T12), Load Control, Go (4)

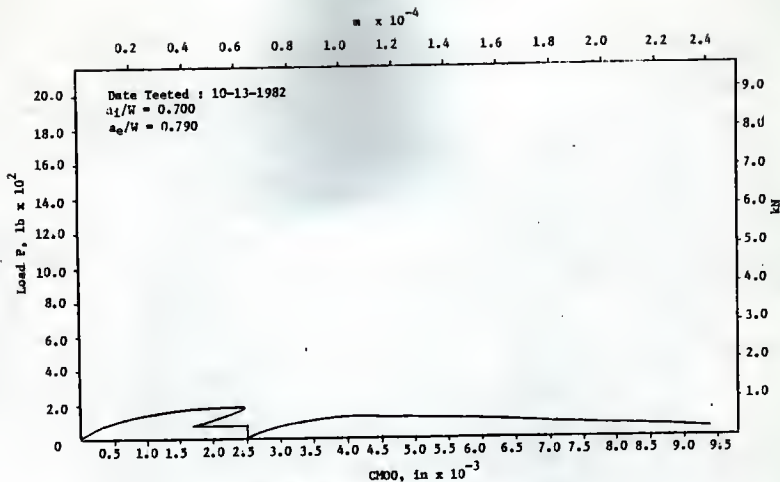


Fig. 139 P vs CHOD, 4 in Deep Beam (T13), Load Control, Go (4)

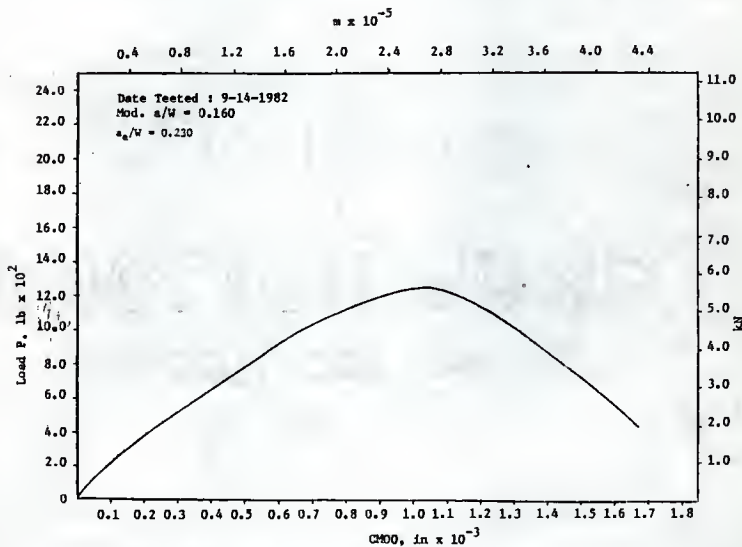


Fig. 140 P vs CHOD, 4 in Deep Beam (P2), Load Control, Go (4)

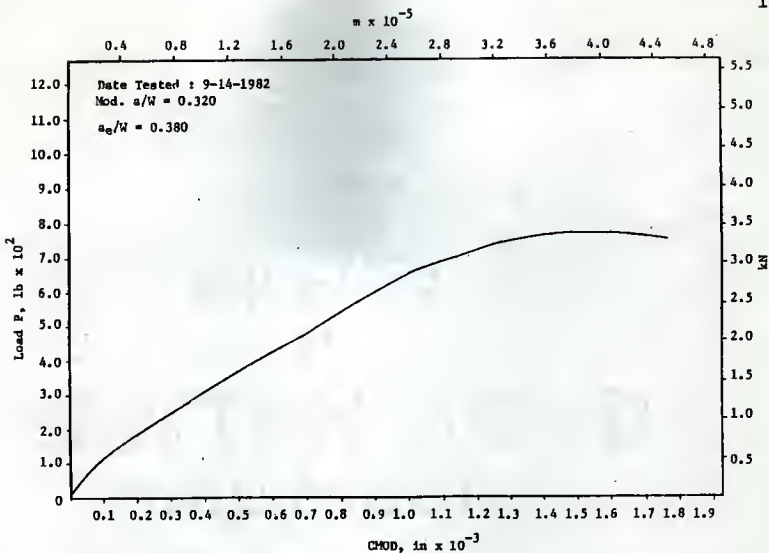


Fig. 141 P vs CHOD, 4 in Deep Beam (P3), Load Control, Go (4)

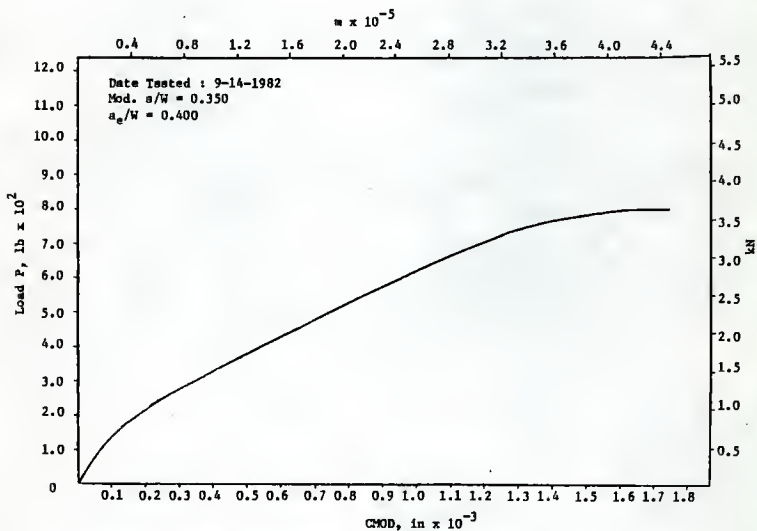


Fig. 142 P vs CHOD, 4 in Deep Beam (P4), Load Control, Go (4)

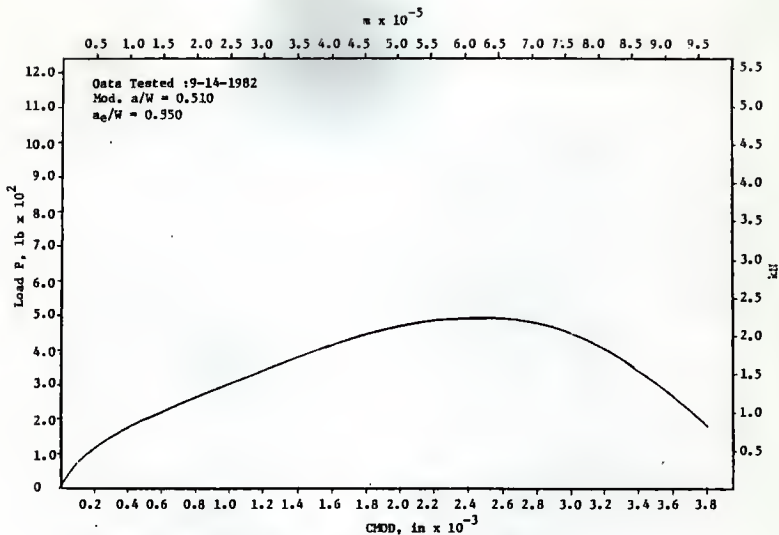


Fig. 143 P vs CHDD, 4 in Deep Beam (P5), Load Control, Go (4)

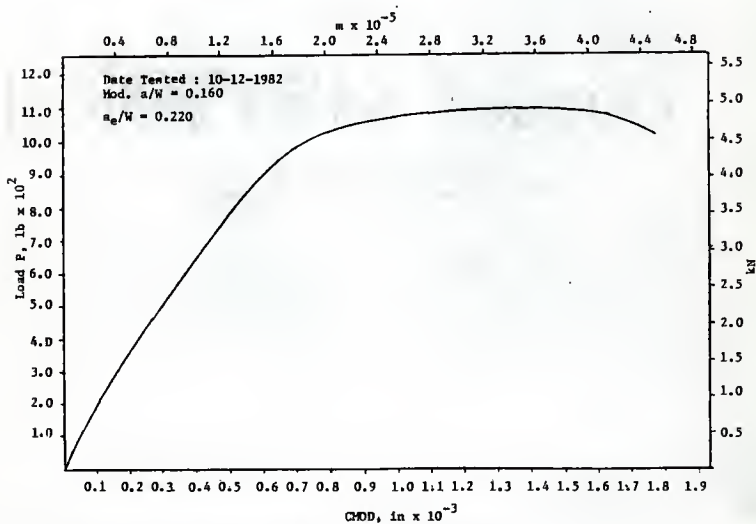


Fig. 144 P vs CHDD, 4 in Deep Beam (P7), Load Control, Go (4)

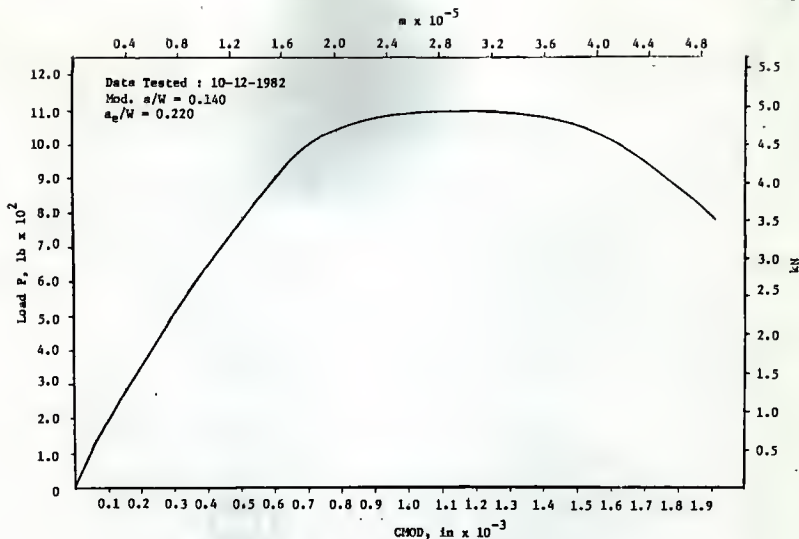


Fig. 145 P vs CHOD, 4 in Deep Beam (P8), Load Control, Go (4).

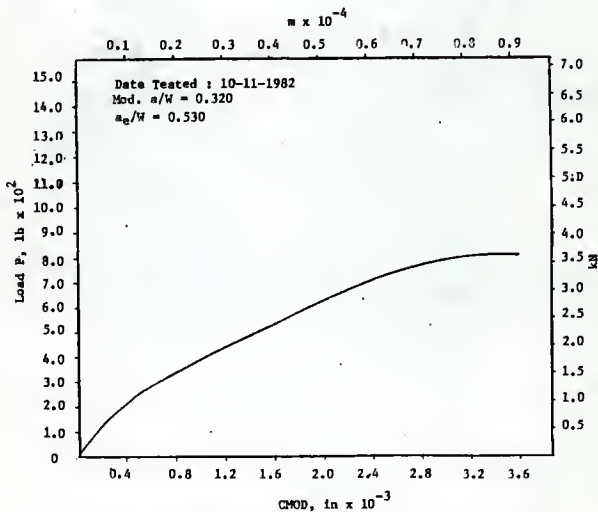


Fig. 146 P vs CHOD, 4 in Deep Beam (P9), Load Control, GO (4)

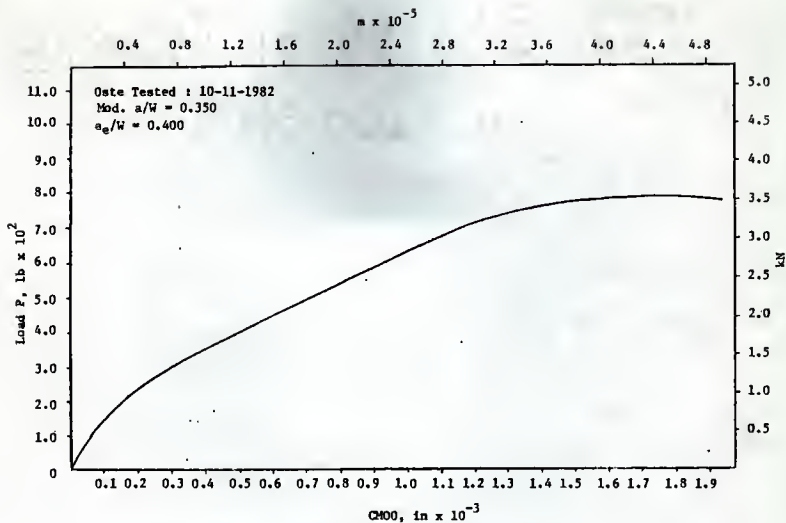


Fig. 147 P vs CHOO, 4 in Deep Beam (P10), Load Control, Go (4)

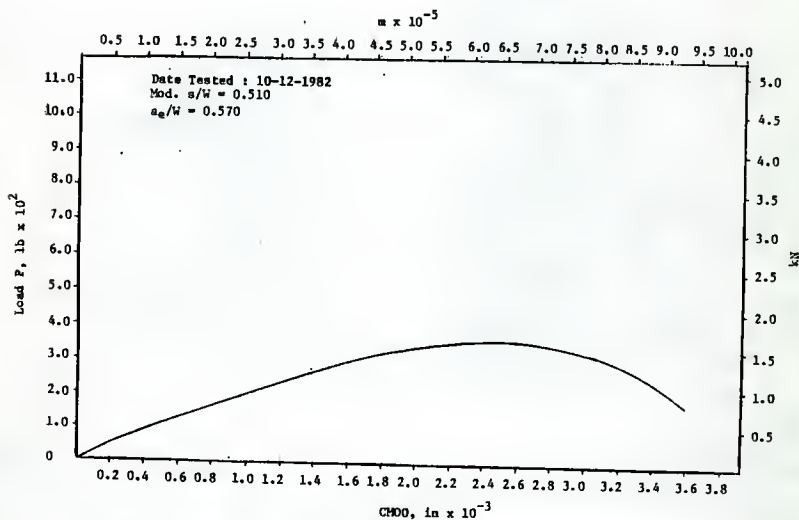


Fig. 148 P vs CHOO, 4 in Deep Beam (P11), Load Control, Go (4)

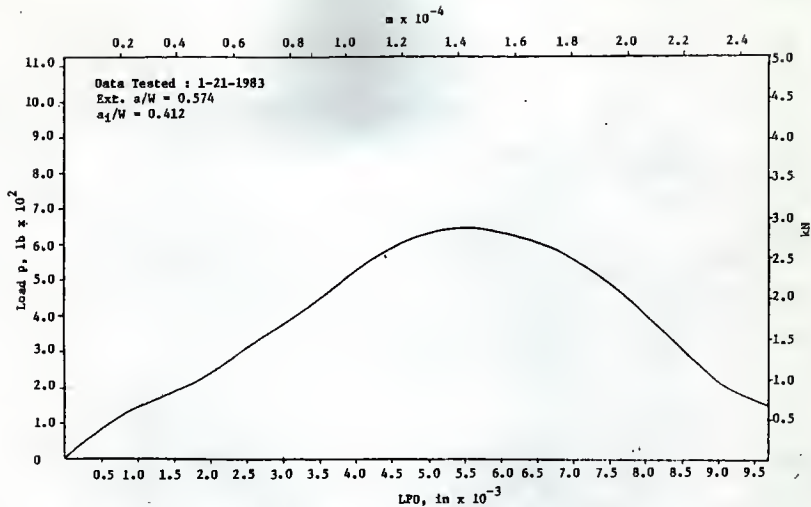


Fig. 149 P vs LPO, 4 in Deep Beam (N1), Load Control, Go (4)

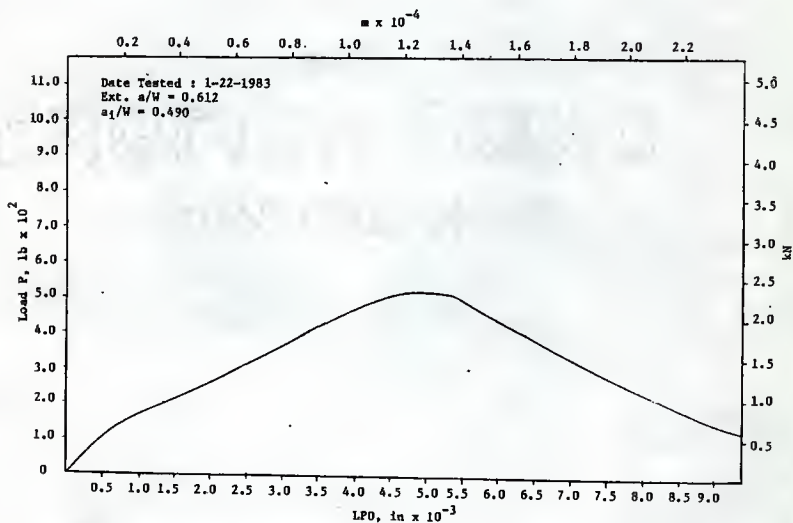


Fig. 150 P vs LPO, 4 in Deep Beam (N2), Load Control, Go (4)

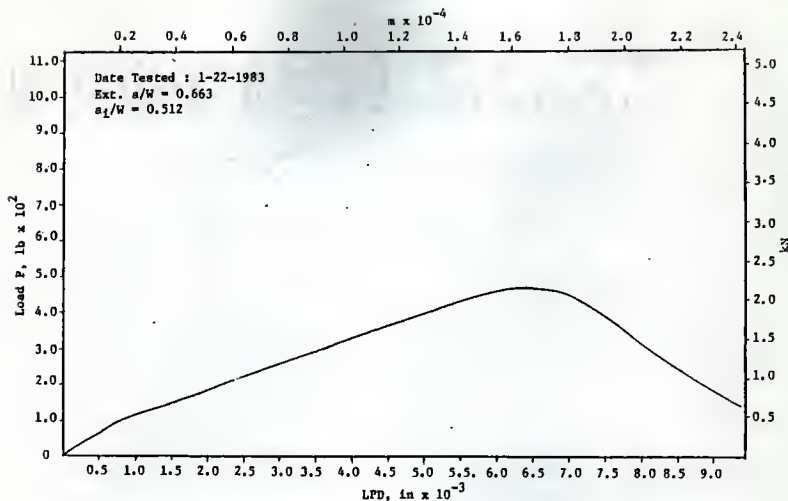


Fig. 151 P vs LPD, Deep Beam (N3), Load Control, Co (4)

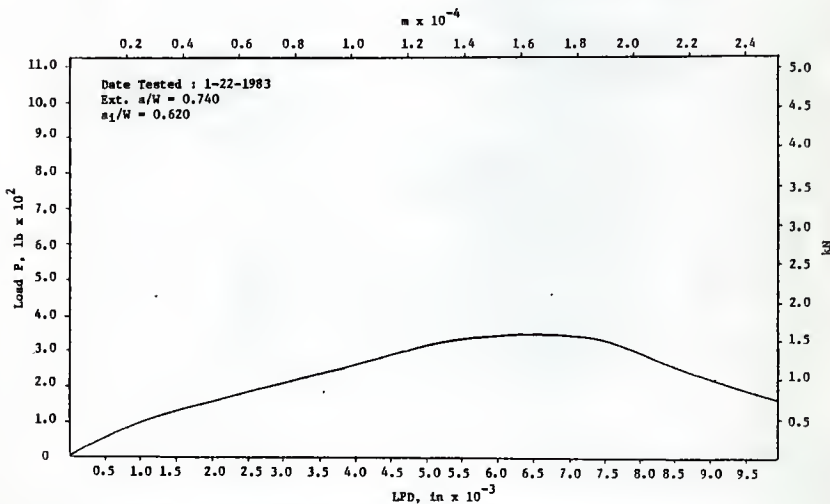


Fig. 152 P vs LPD, 4 in Deep Beam (N4), Load Control, Co (4)

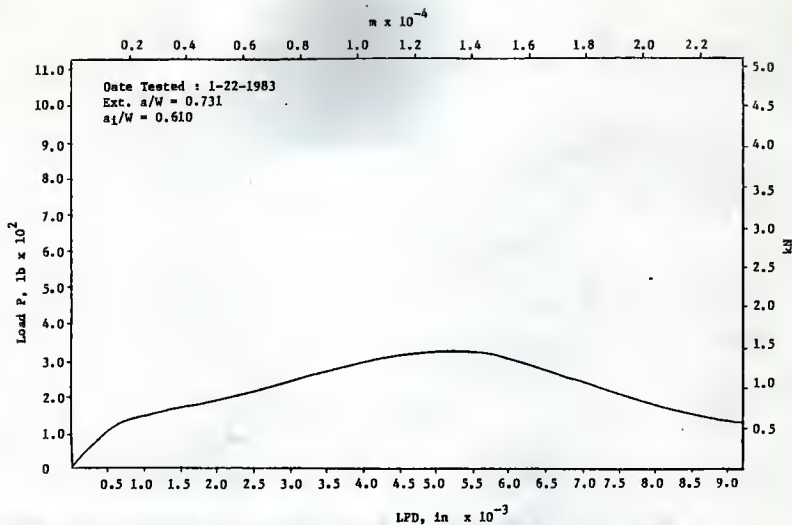


Fig. 153 P vs LPD, 4 in Deep Beam (N5), Load Control, Go (4)

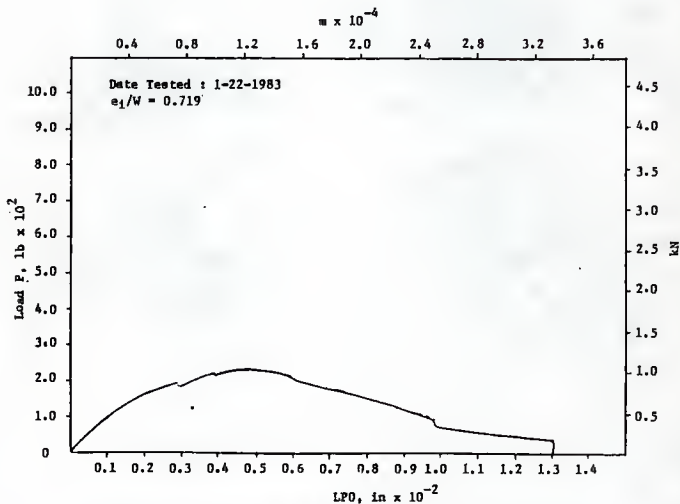


Fig. 154 P vs LPD, 4 in Deep Beam (N6), Load Control, Go (4)

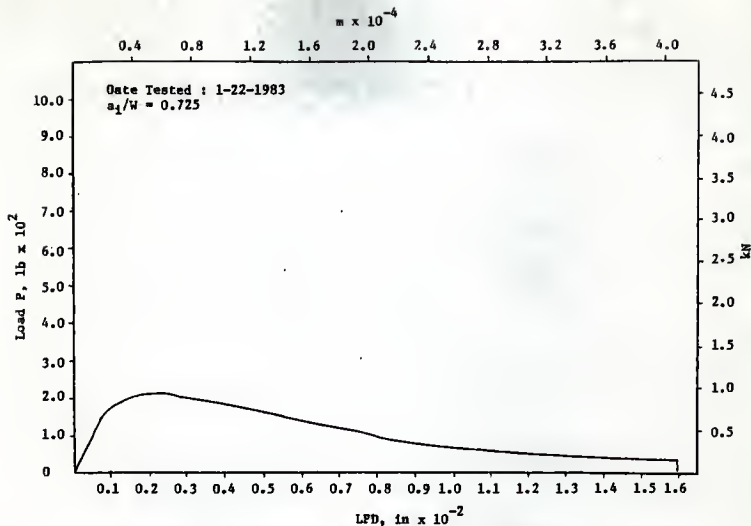


Fig. 155 P vs LFD, 4 in Deep Beam (N7), Load Control, Go (4)

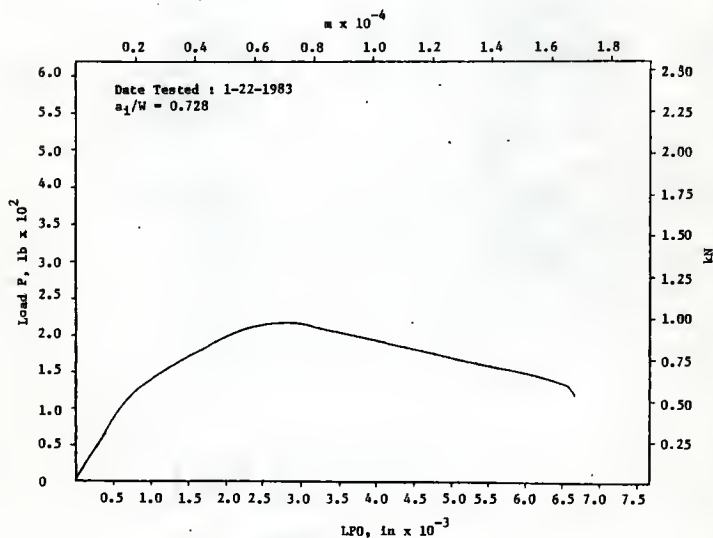


Fig. 156 P vs LFD, 4 in Deep Beam (N8), Load Control, Go (4)

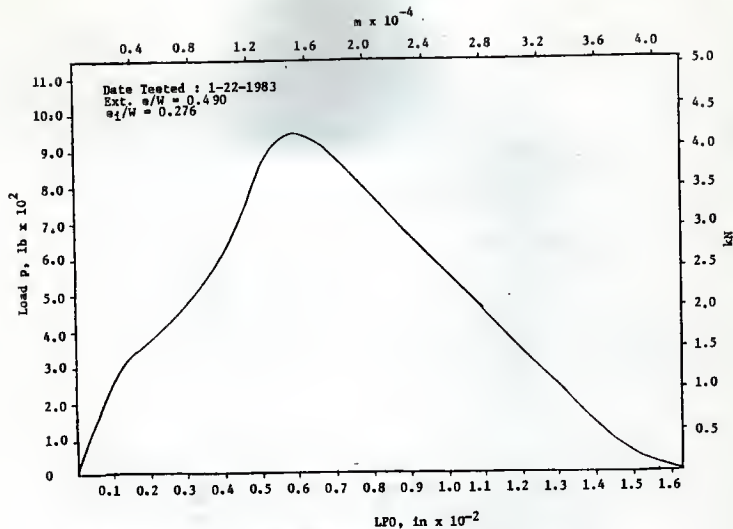


Fig. 157 P vs LPO, 4 in Deep Beam (N9), Load Control, Go (4)

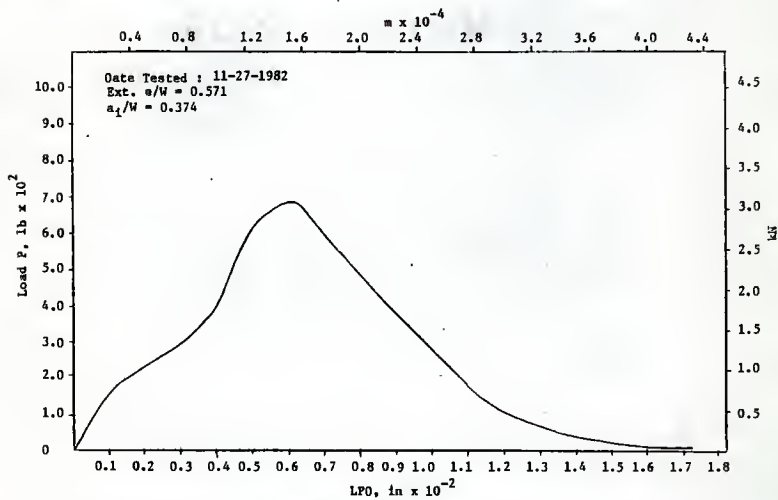


Fig. 158 P vs LPO, 4 in Deep Beam (N10), Load Control, Go (4)

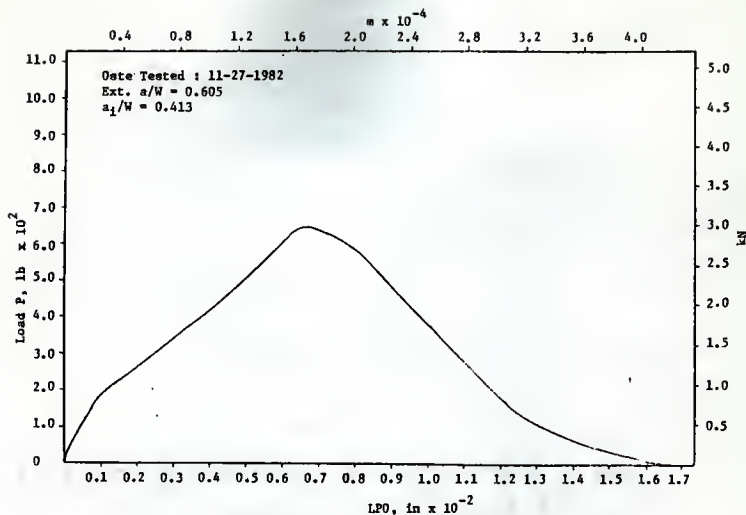


Fig. 159 P vs LPO, 4 in Deep Beam (N11), Load Control, Go (4)

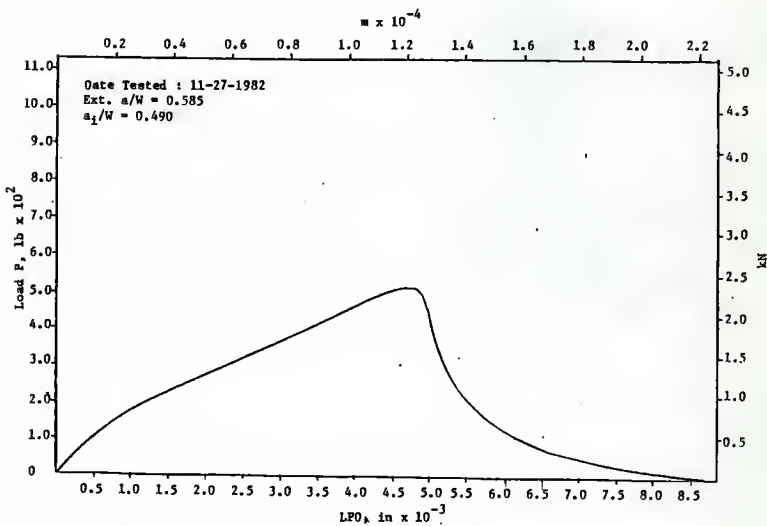


Fig. 160 P vs LPD, 4 in Deep Beam (N12), Load Control, Go (4)

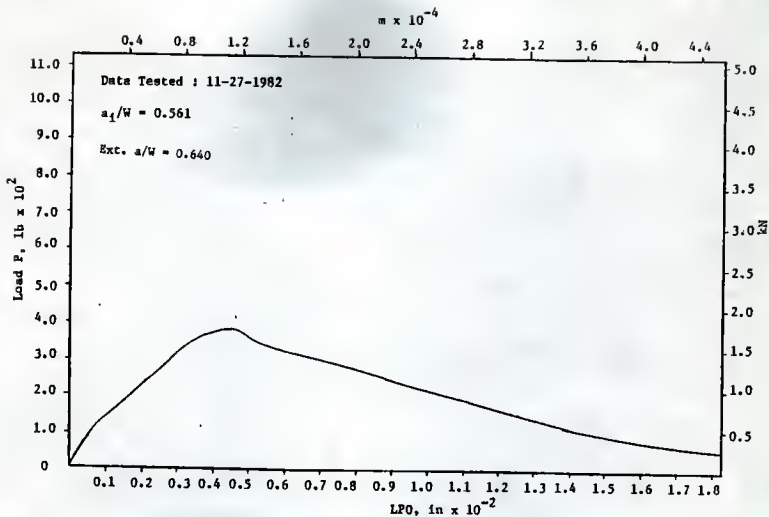


Fig. 161 P vs LPD, 4 in Deep Beam (N13), Load Control, Go (4)

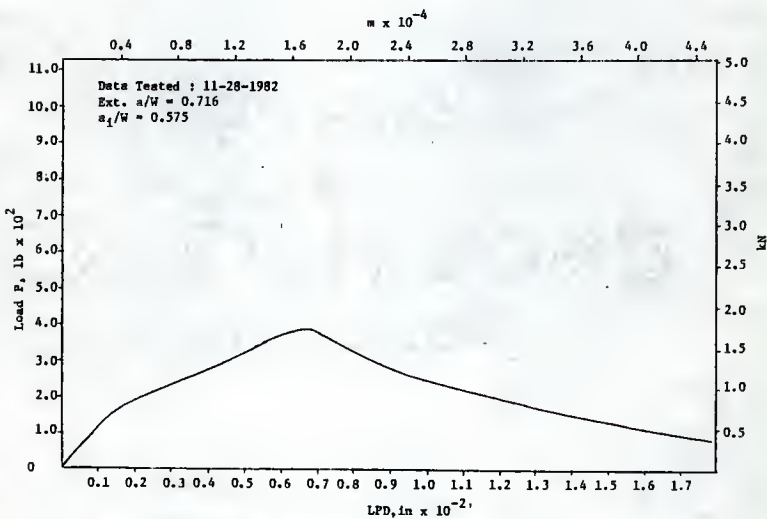


Fig. 162 P vs LPD, 4 in Deep Beam (N14), Load Control, Go (4)

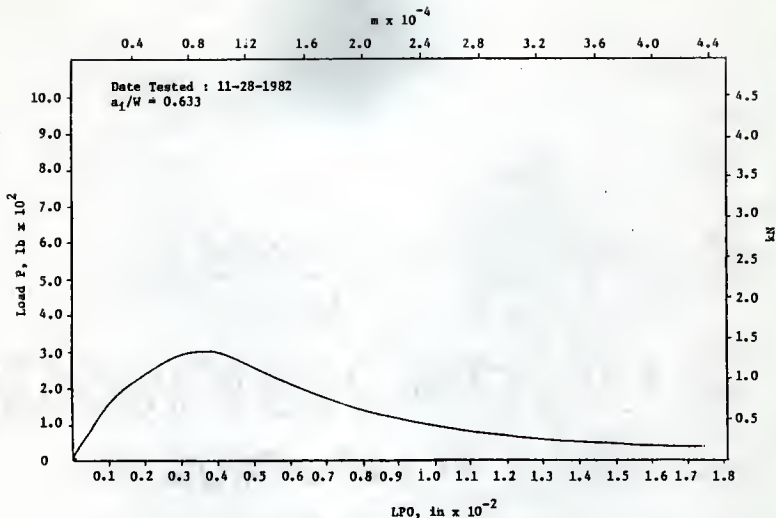


Fig. 163 P vs LPD, 4 in Deep Beam (N15), Load Control, Go (4)

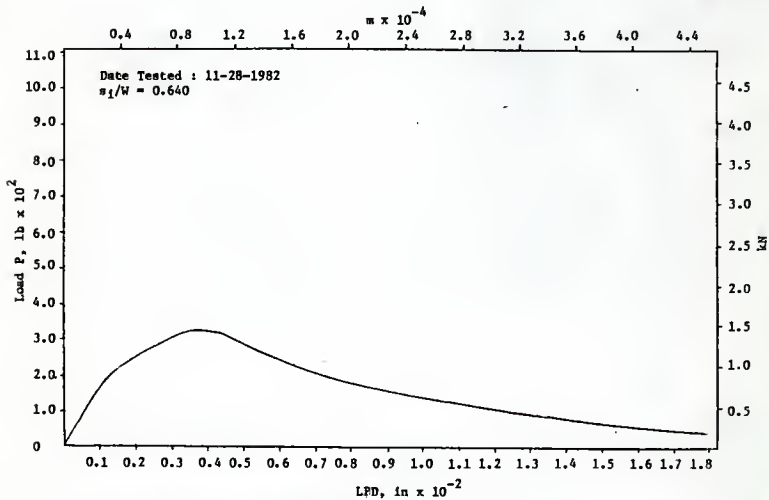


Fig. 164 P vs LPD, 4 in Deep Beam (N16), Load Control, Go (4)

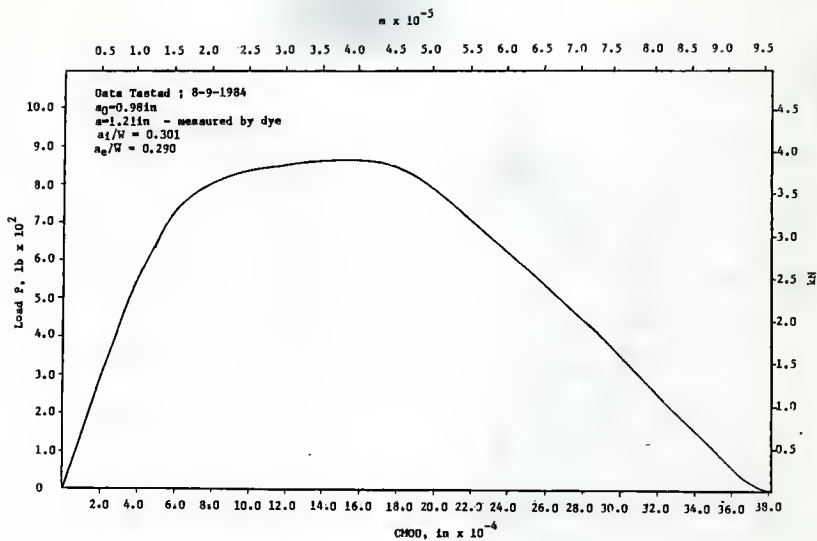


Fig. 165 P vs CMOD, 4 in Deep Beam (B1), Load Control, Rod (12)

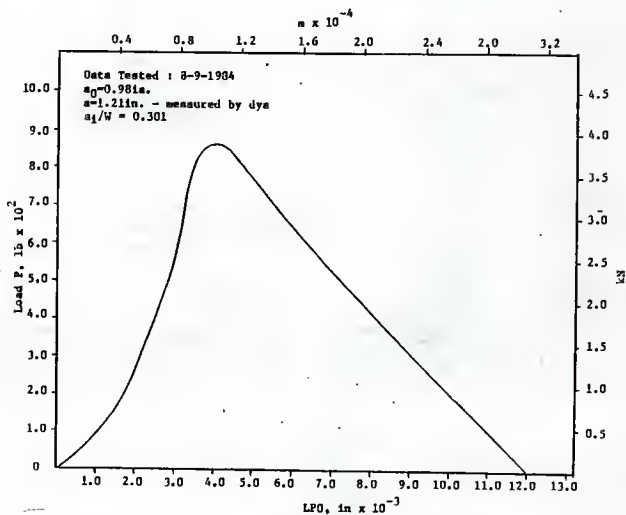


Fig. 166 P vs LPO, 4 in Deep Beam (B1), Load Control, Rod (12)

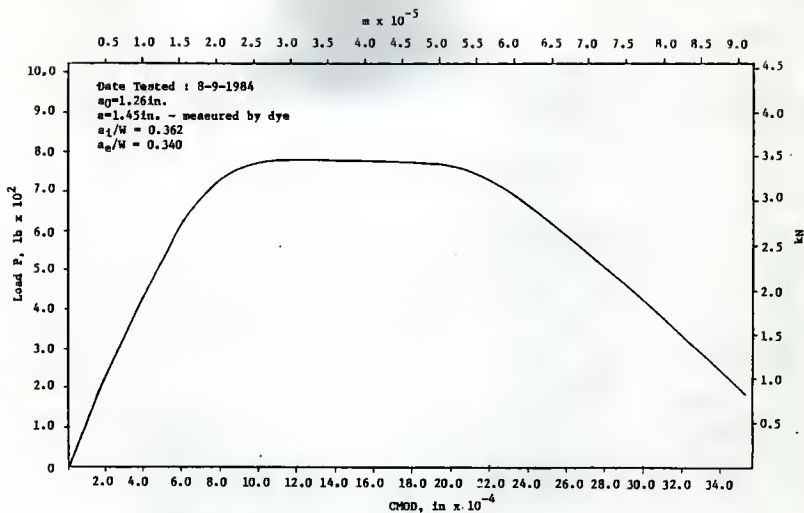


Fig. 167 P vs CMOD, 4 in Deep Beam (B2), Load Control, Road (12)

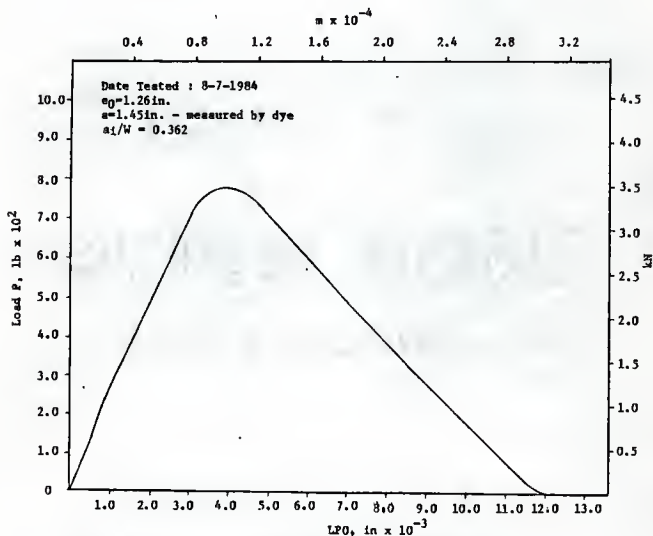


Fig. 168 P vs LPO, 4 in Deep Beam (B2), Load Control, Road (12)

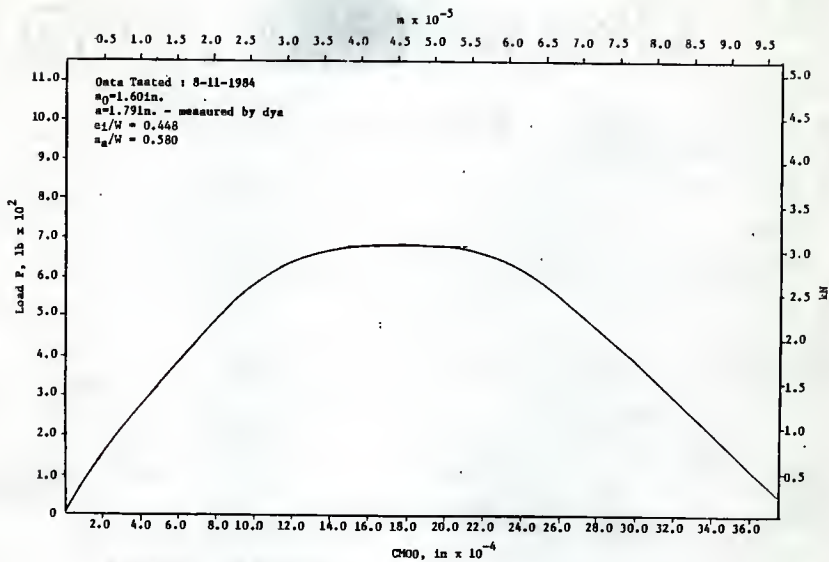


Fig. 169 P vs CMOD, 4 in Deep Beam (B3), Load Control, Rood (12)

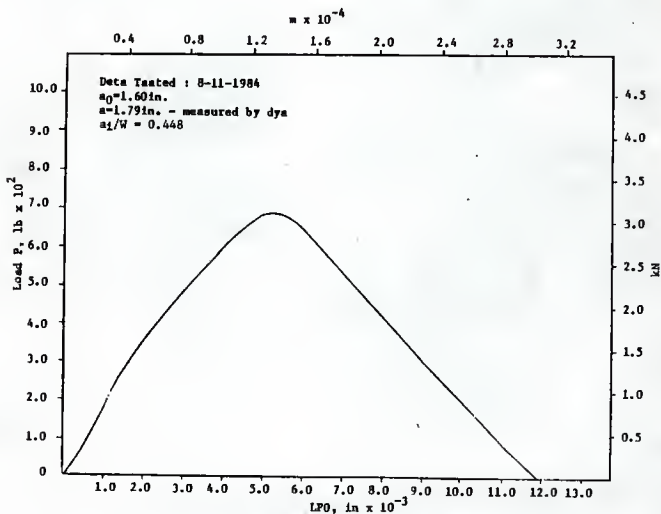


Fig. 170 P vs LPO, 4 in Deep Beam (B3), Load Control, Rood(12)

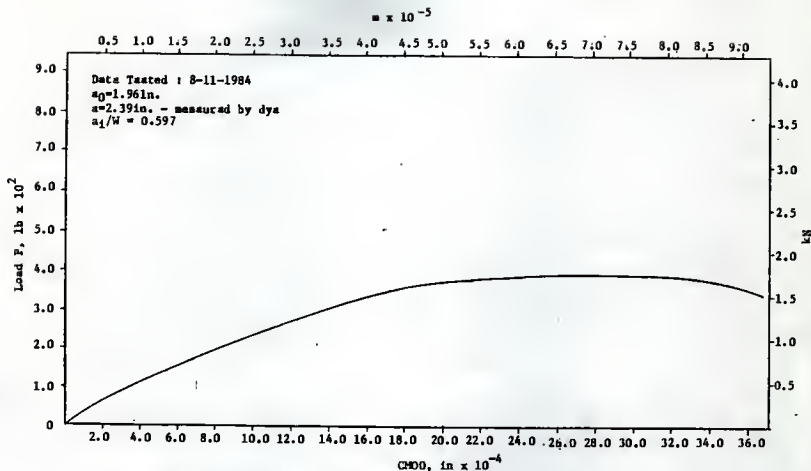


Fig. 171 P vs CMDO, 4 in Deep Beam (B4), Load Control, Rood, (12)

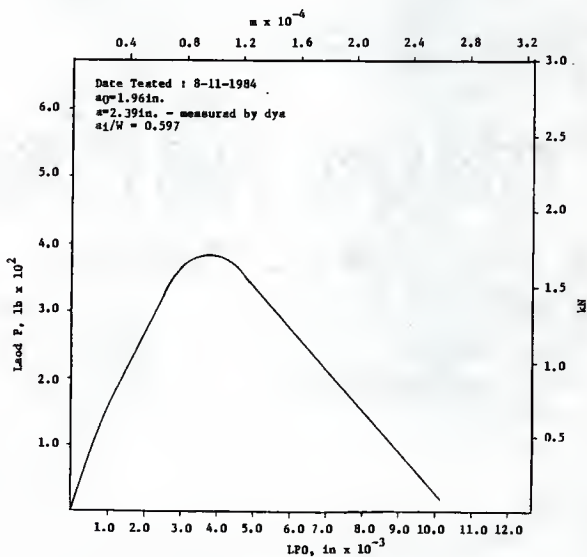


Fig. 172 P vs LPD, 4 in deep Beam (B4), Load Control, Rood (12)

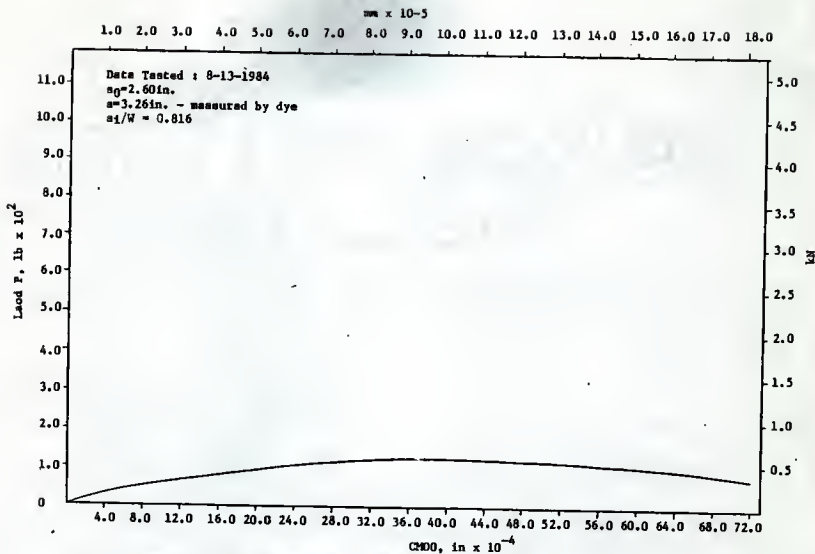


Fig. 173 P vs CHD0, 4 in Deep Seam (B6), Load Control, Rood (12)

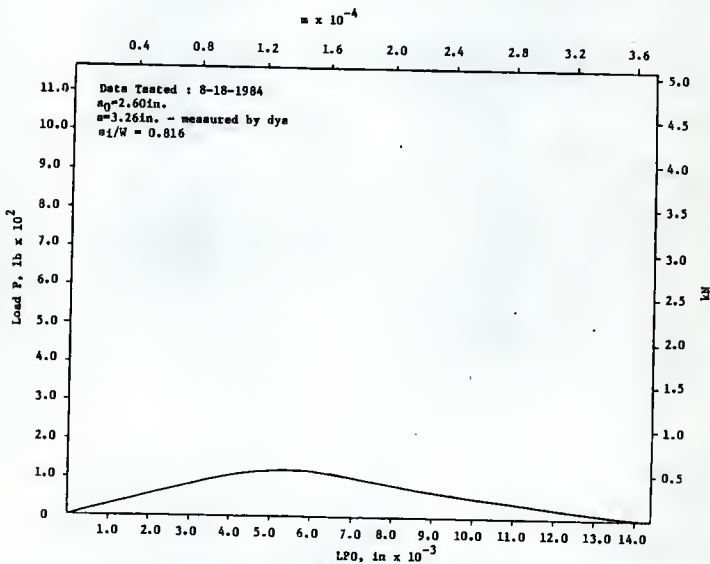


Fig. 174 P vs LPO, 4 in Deep Seam (B6), Load Control, Rood (12)

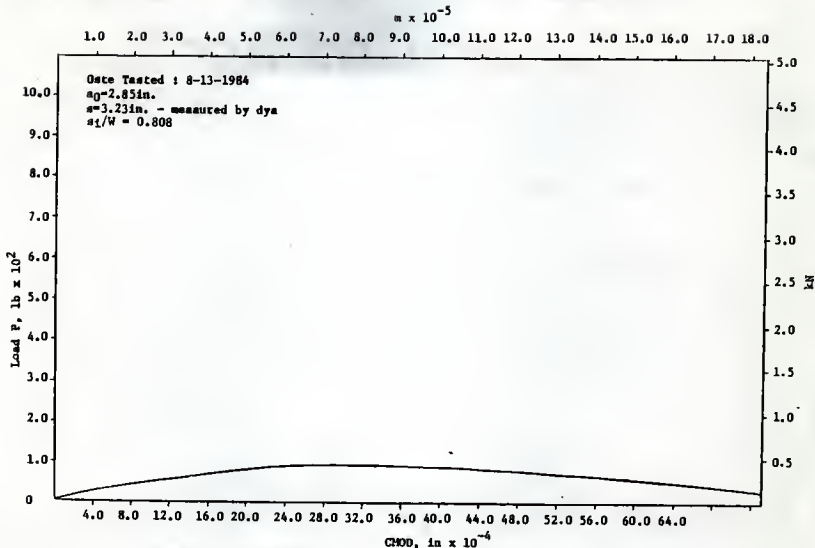


Fig. 175 P vs CHDD, 4 in Deep Beam (87), Load Control, Rod (12)

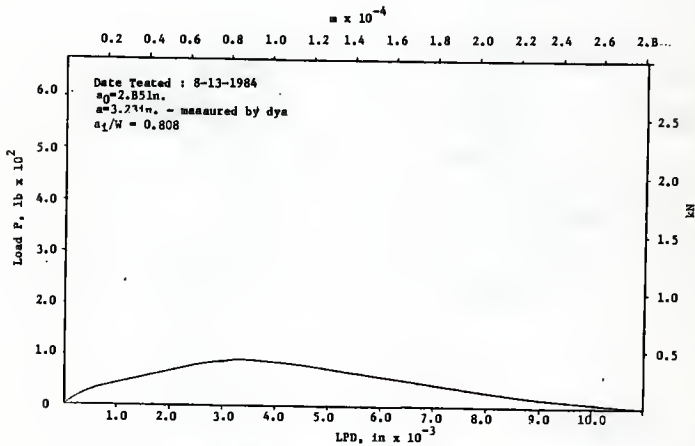


Fig. 176 P vs LPD, 4 in Deep Beam (87), Load Control, Rod (12)

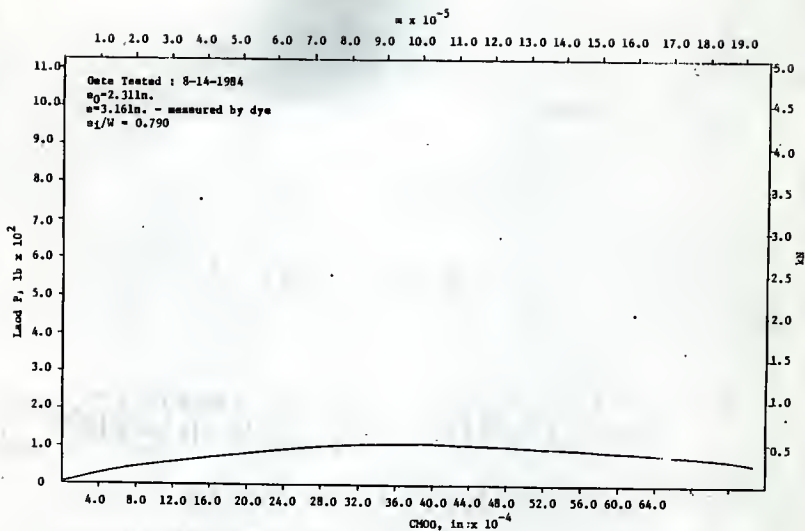


Fig. 177 P vs CHOD, 4 in Deep Beam (B8), Load Control, Road (12)

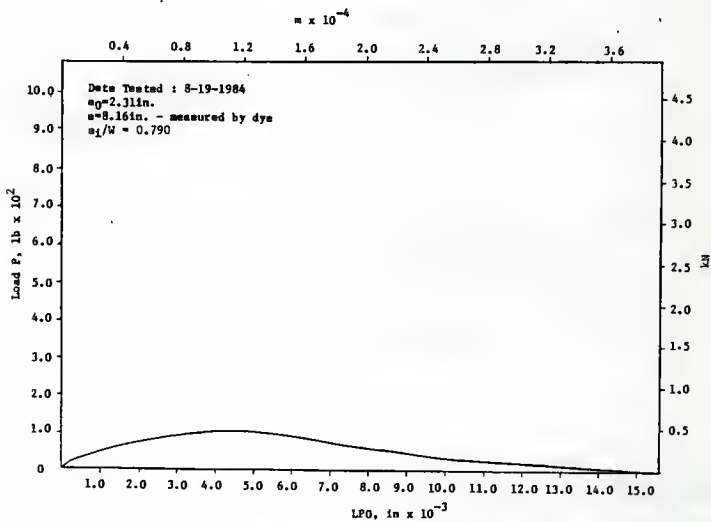


Fig. 178 P vs LPO, 4 in Deep Beam (B8), Load Control, Road (12)

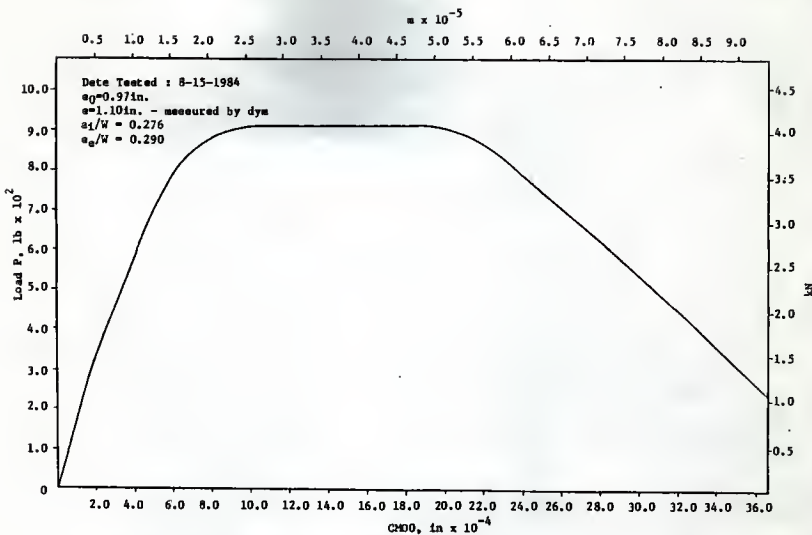


Fig. 179 P vs CHDD, 4 in Deep Beam (89), Load Control, Rood (12)

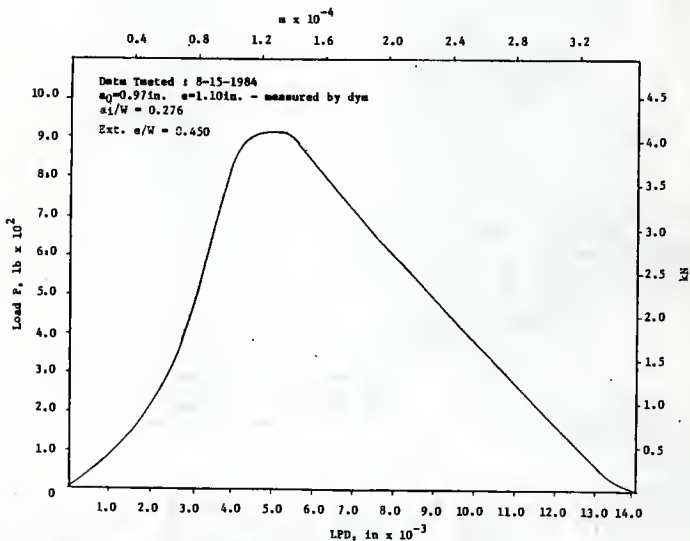


Fig. 180 P vs LPD, 4 in Deep Beam (89), Load Control, Rood (12)

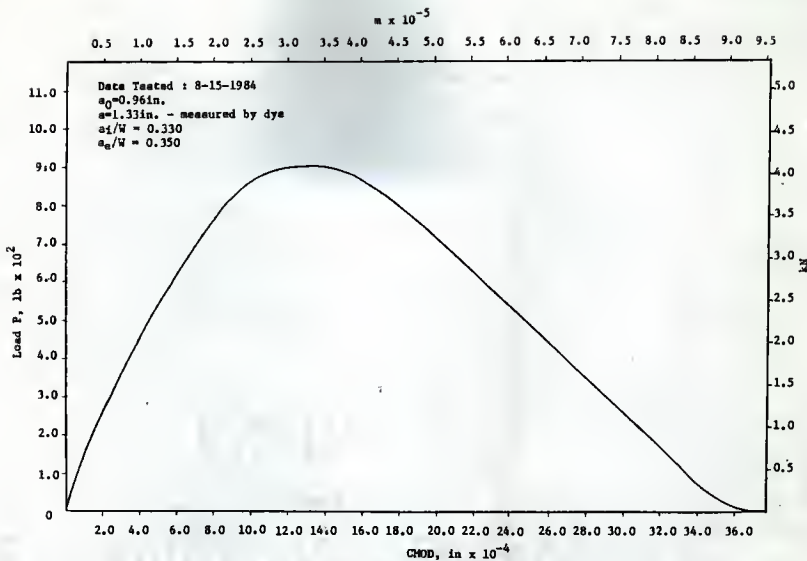


Fig. 181 P vs CHOD, 4 in Deep Beam (B10), Load Control, Rood (12)

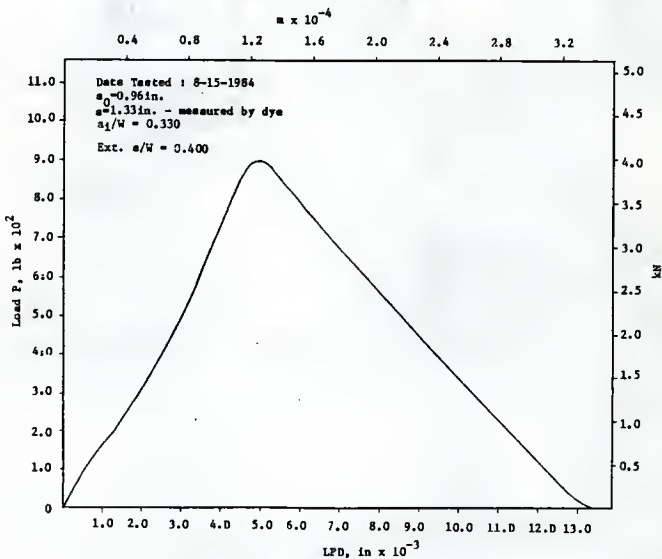


Fig. 182 P vs LFD, 4 in Deep Beam (B10), Load Control, Rood (12)

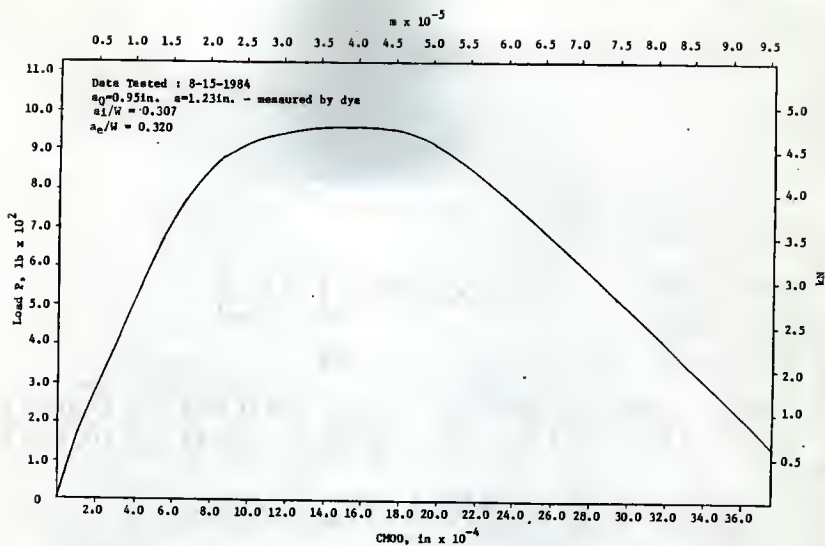


Fig. 183 P vs CMOD, 4 in Deep Beam (B11), Load Control, Rood (12)

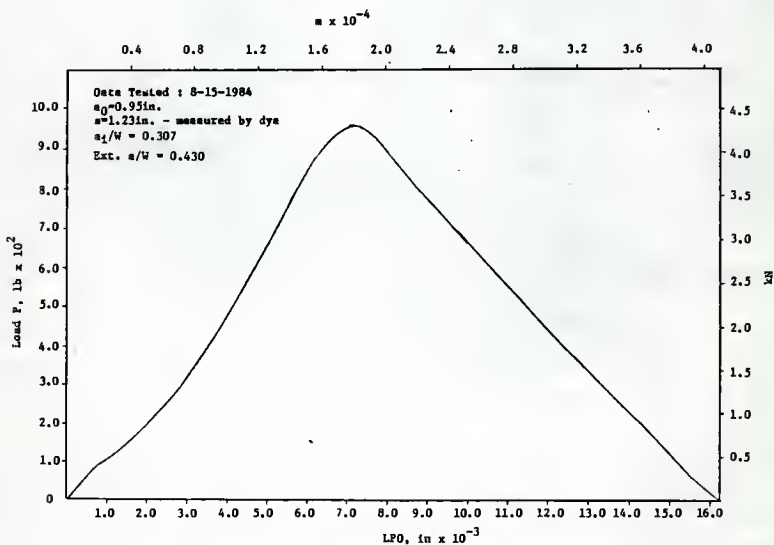


Fig. 184 P vs LPO, 4 in Deep Beam (B11), Load Control, Rood (12)

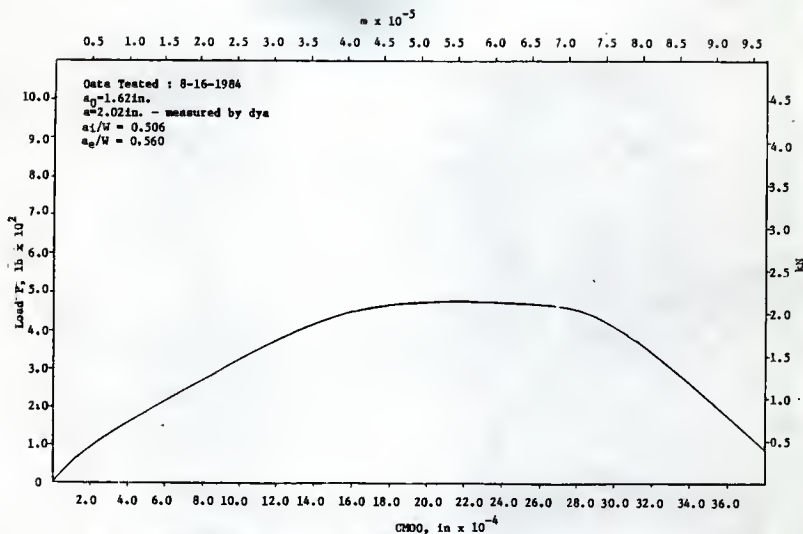


Fig. 185 P vs CHDO, 4 in Deep Beam (B14), Load Control, Road (12)

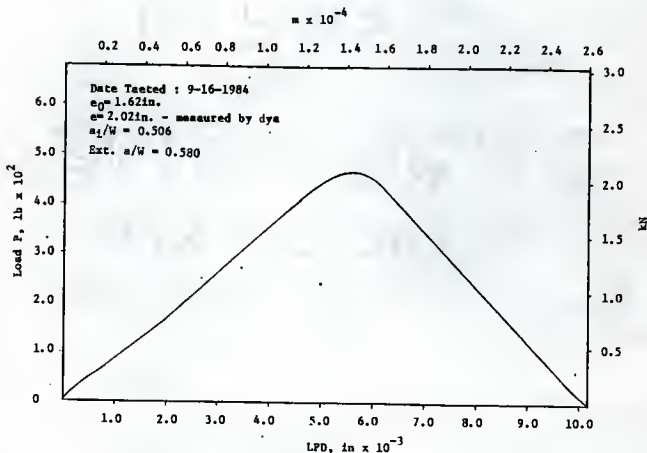


Fig. 186 P vs LPD, 4 in Deep Beam (B14), Load Control, Road (12)

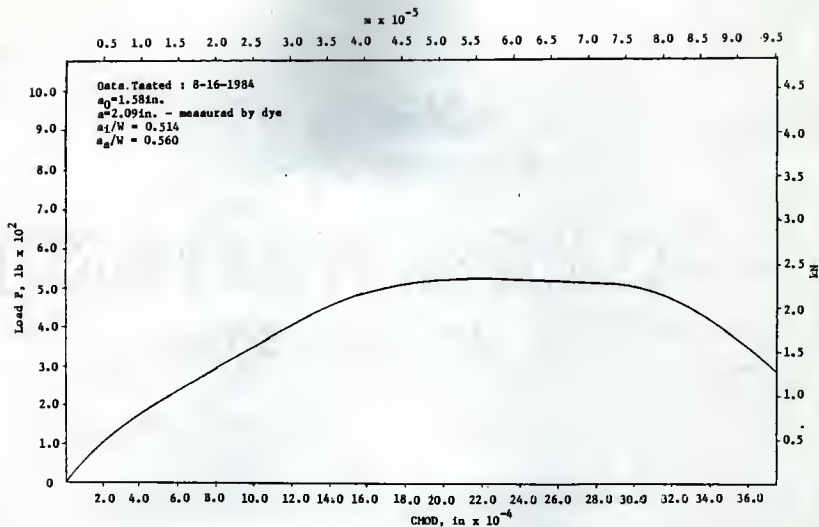


Fig. 187 P vs CMOD, 4 in Deep Beam (B16), Load Control, Road (12)

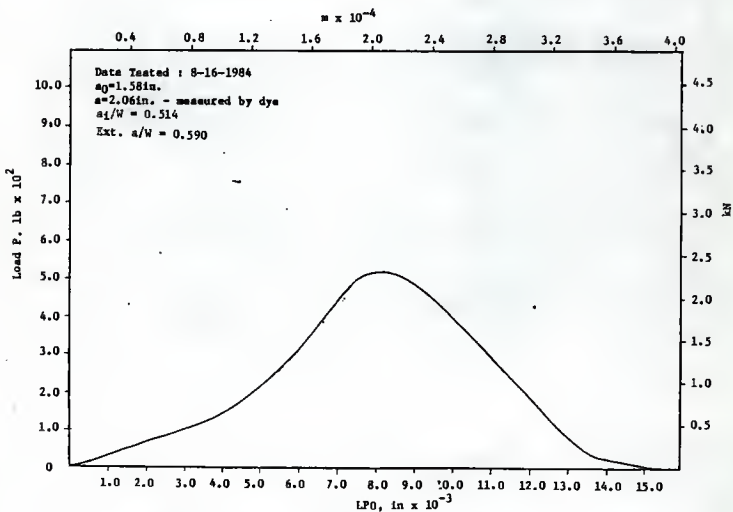


Fig. 188 P vs LPO, 4 in Deep Beam (B16), Load Control, Road (12)

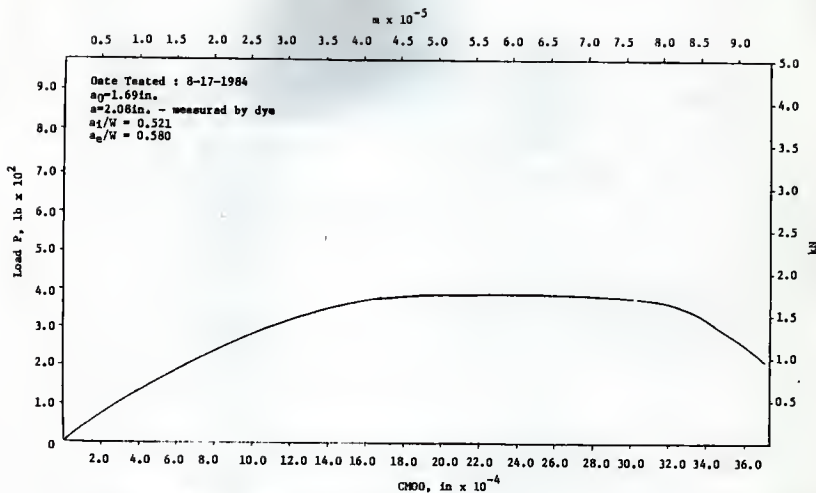


Fig. 189 P vs CHOD, 4 in Deep Beam (B17), Load Control, Rood (12)

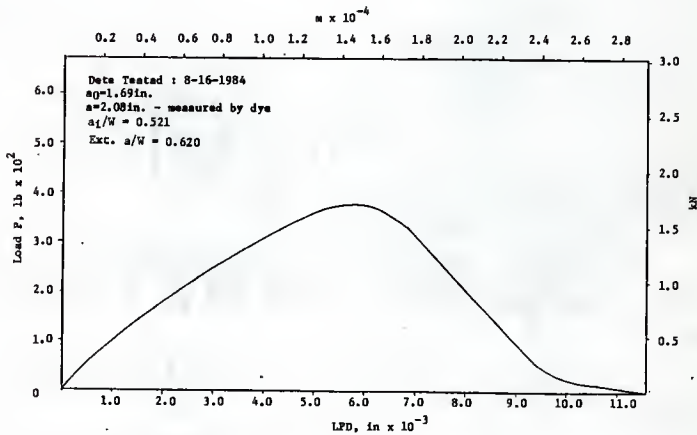


Fig. 190 P vs LPD, 4 in Deep Beam (B17), Load Control, Rood (12)

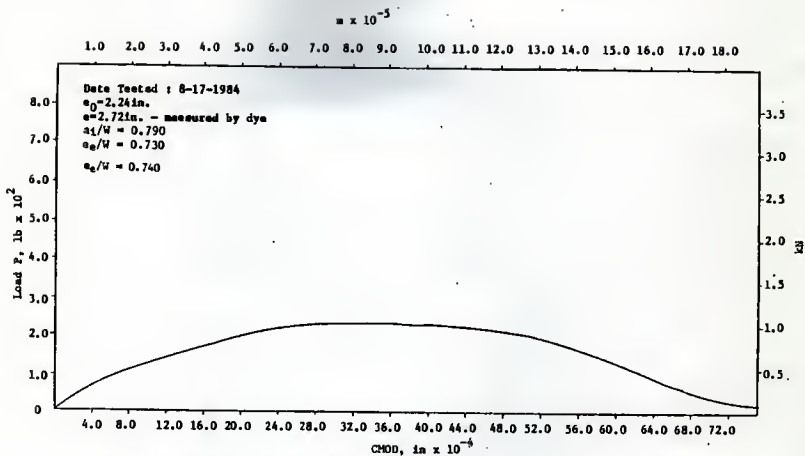


Fig. 191 P vs CHOD, 4 in Deep Beam (B18), Load Control, Rood (12)

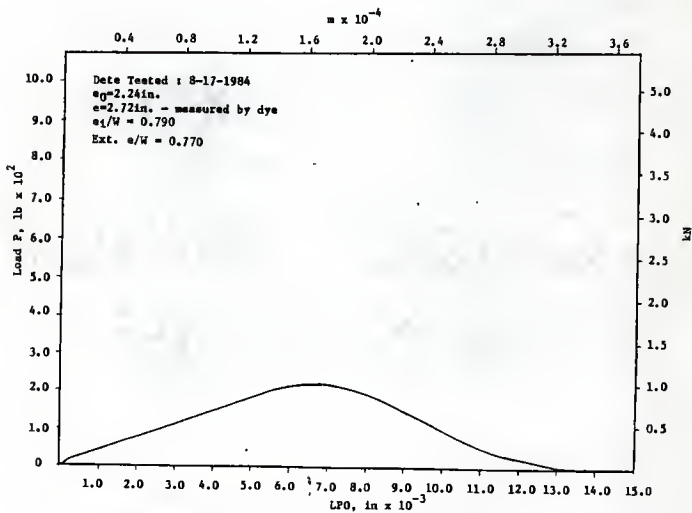


Fig. 192 P vs LFO, 4 in Deep Beam (B18), Load Control, Rood (12)

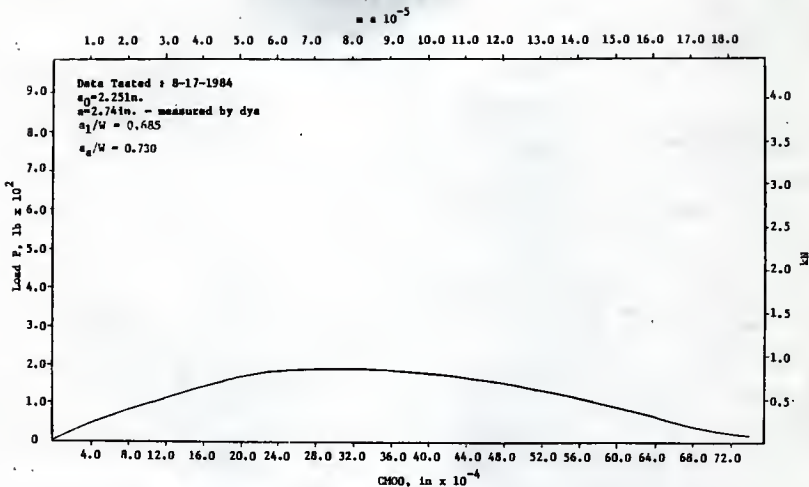


Fig. 193 P vs CM00, 4 in Deep Beam (B19), Load Control, Rood (12)

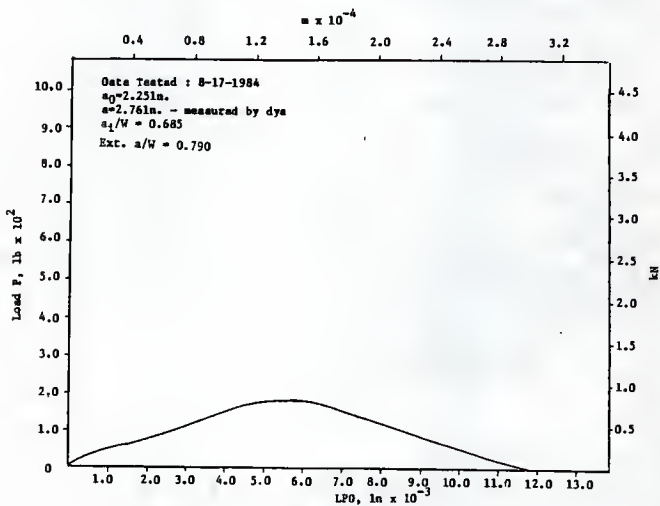


Fig. 194 P vs LP0, 4 in Deep Beam (B19), Load Control, Rood (12)

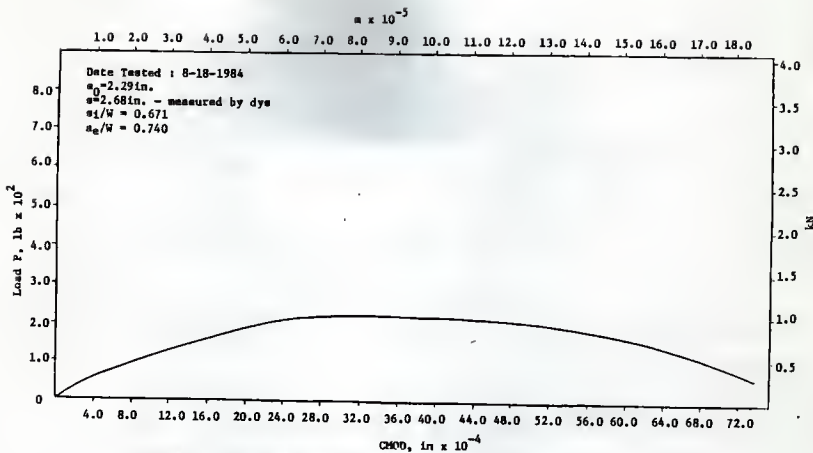


Fig. 195 P vs CMOD, 4 in Deep Beam (B20), Load Control, Rood (12)

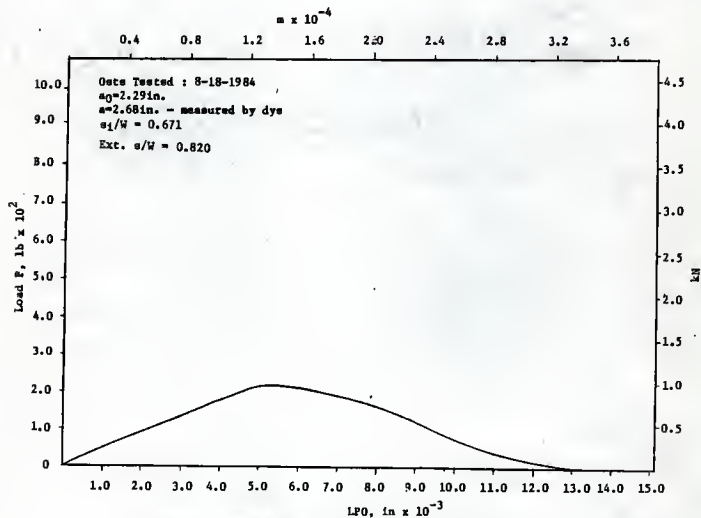


Fig. 196 P vs LPO, 4 in Deep Beam (B20), Load Control, Rood (12)

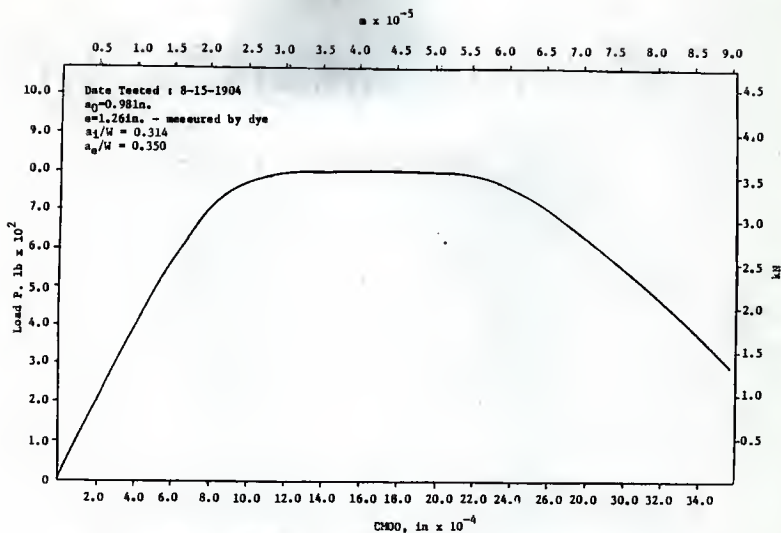


Fig. 197 P vs CMDO, 4 in Deep Beam (C1), Load Control, Rood (12)

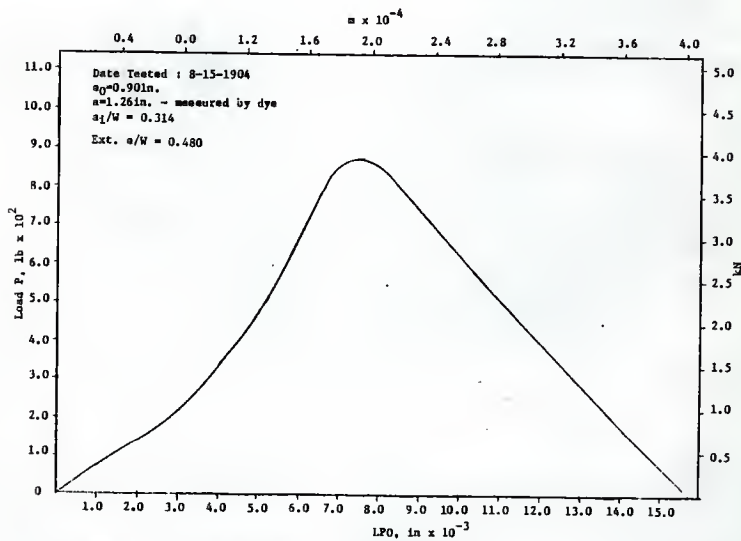


Fig. 198 P vs LPO, 4 in Deep Beam (C1), Load Control, Rood (12)

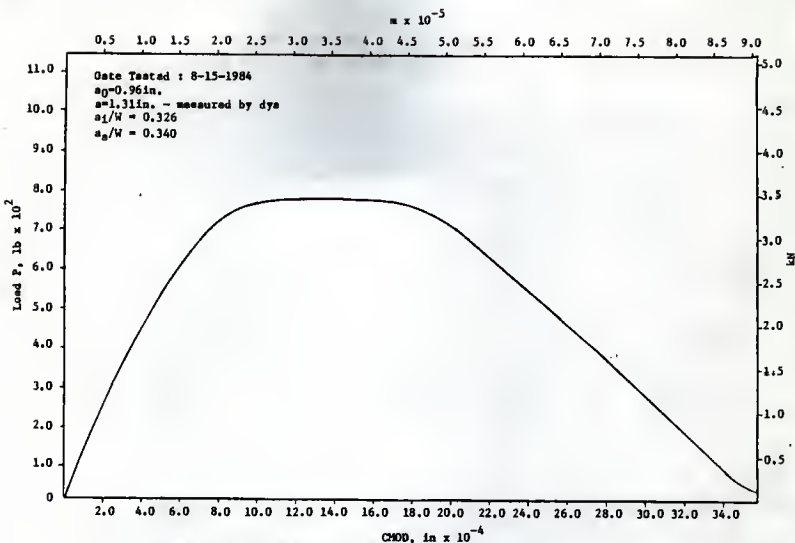


Fig. 199 P vs CMDO, 4 in Deep Beam (C2), Load Control, Rood (12)

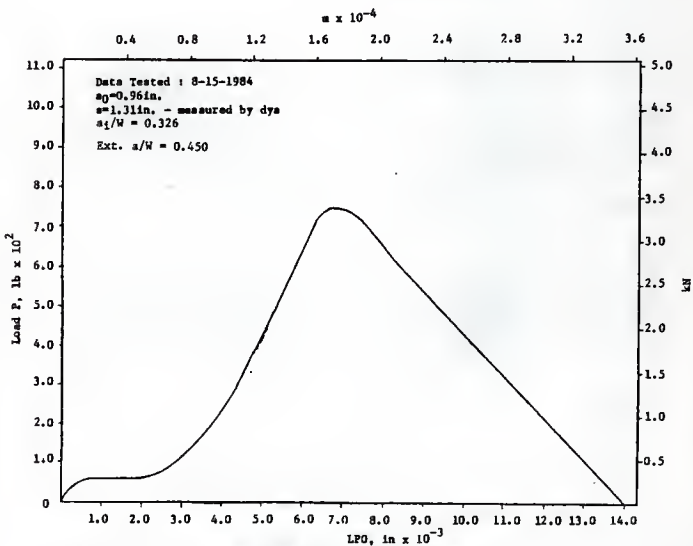


Fig. 200 P vs LPG, 4 in Deep Beam (C2), Load Control, Rood (12)

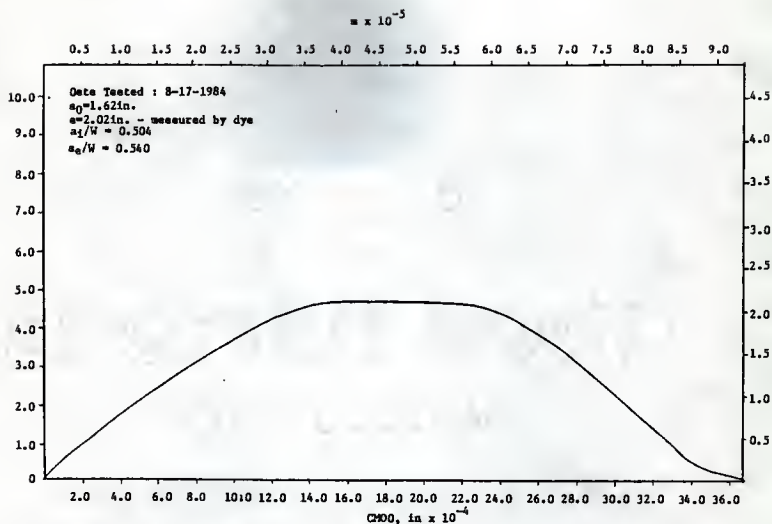


Fig. 201 P vs CM00, 4 in Deep Beam (C3), Load Control, Road (12)

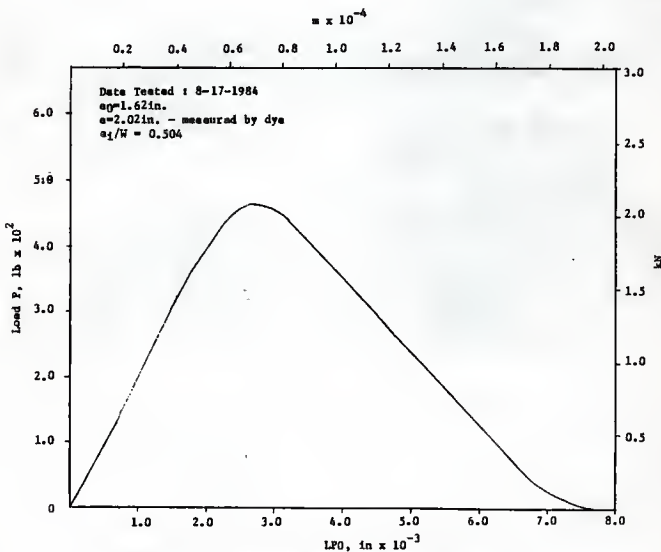


Fig. 202 P vs LP0, 4 in Deep Beam (C3), Load Control, Road (12)

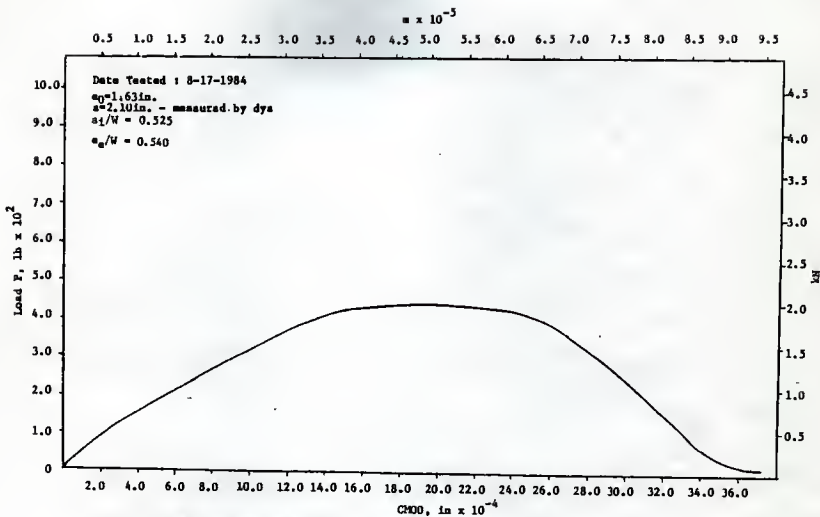


Fig. 203 P vs CHOD, 4 in Deep Beam (C4), Load Control, Road (12)

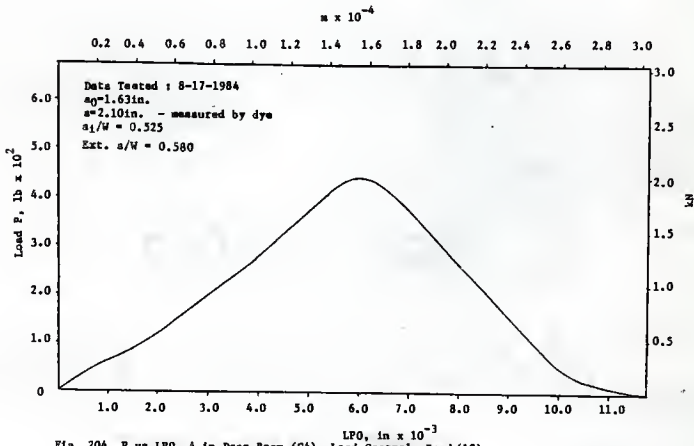


Fig. 204 P vs LPO, 4 in Deep Beam (C4), Load Control, Road (12)

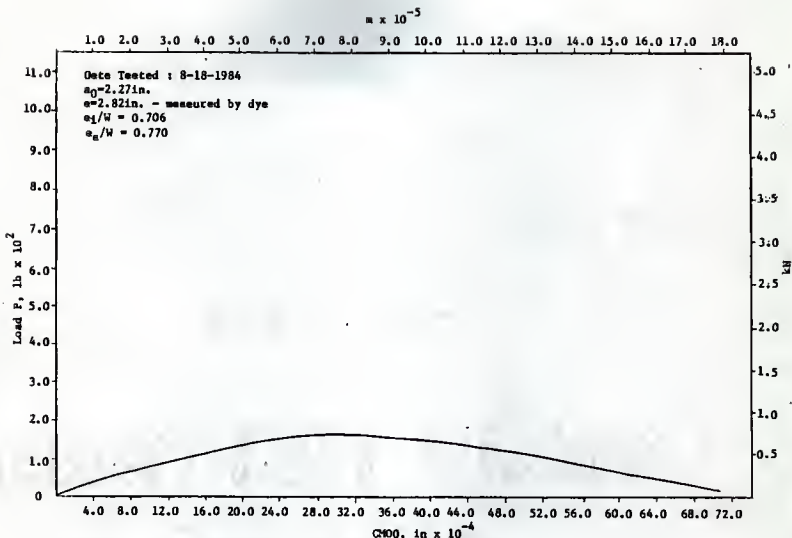


Fig. 205 P vs CHDD, 4 in Deep Beam (C5), Load Control, Rood (12)

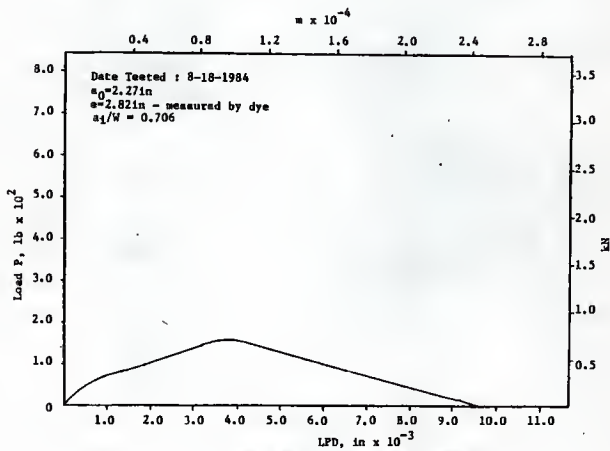
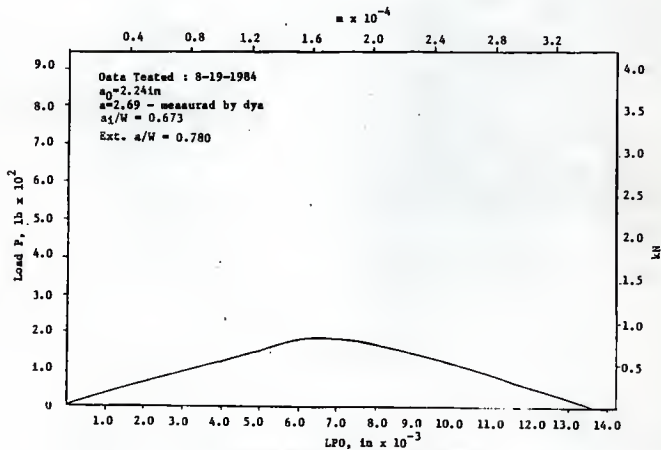
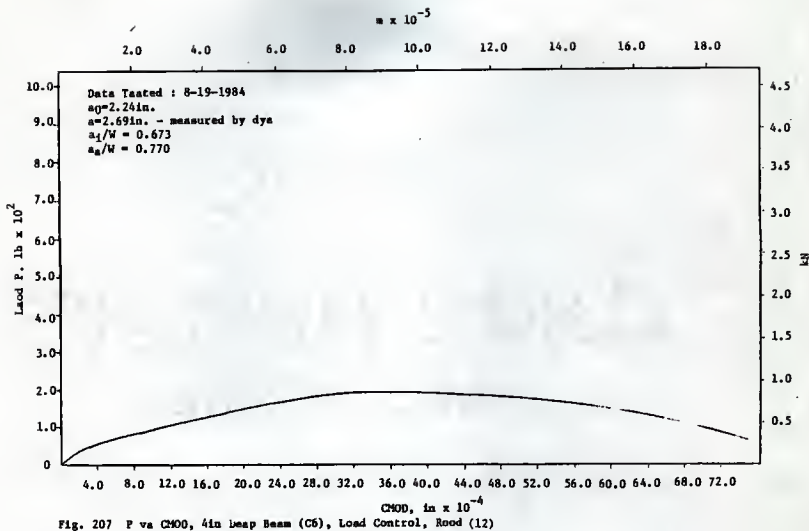
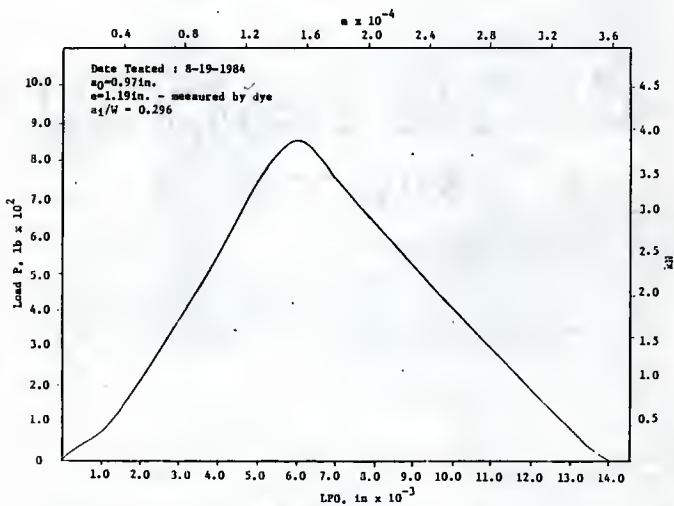
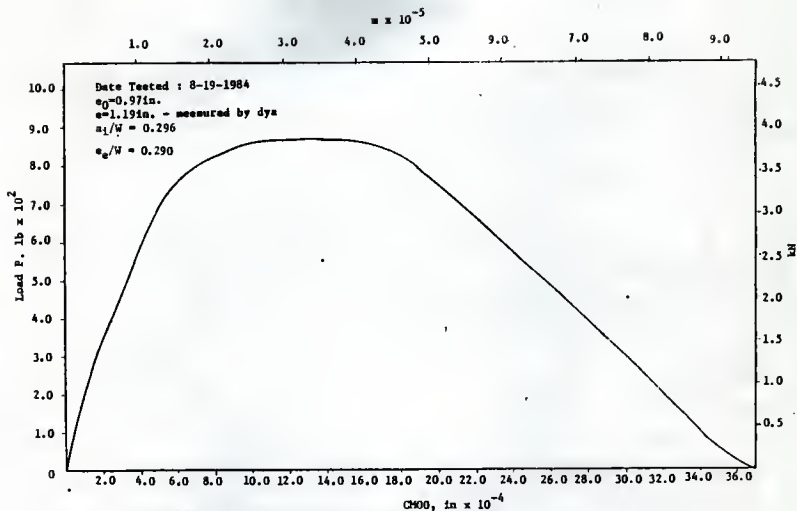


Fig. 206 P vs LPD, 4 in Deep Beam (C5), Load Control, Rood (12)





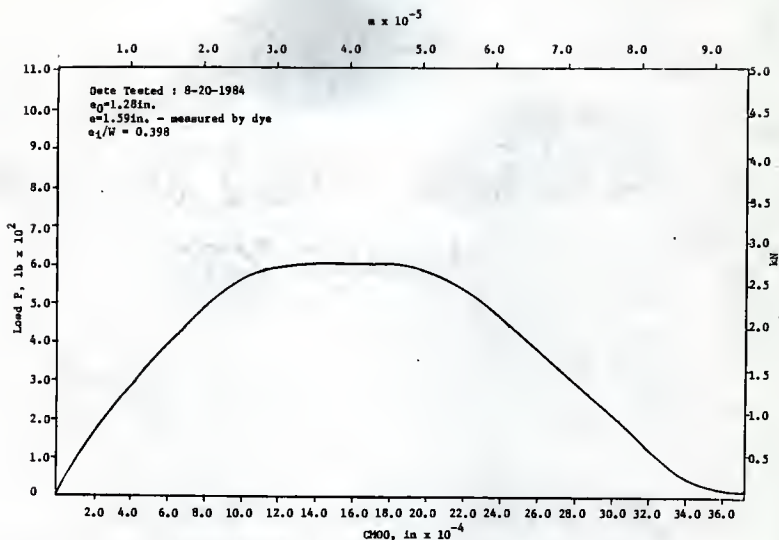


Fig. 211 P vs CM00, 4 in Deep Beam (CB), Load Control, Road (12)

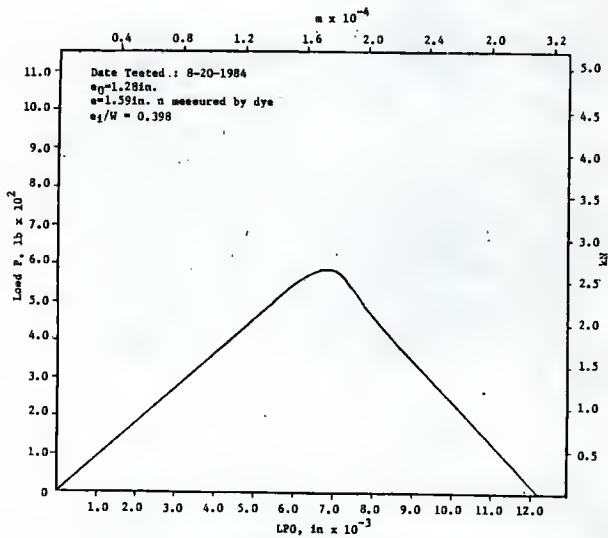


Fig. 212 P vs LPD, 4 in deep Beam (CB), Load Control, Road (12)

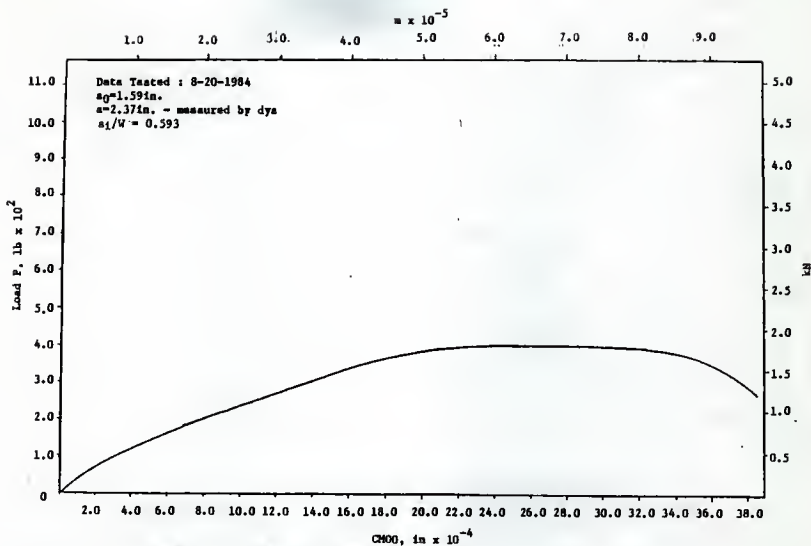


Fig. 213 P vs CH00, 4 in Deep Beam (C9), Load Control, Road (12)

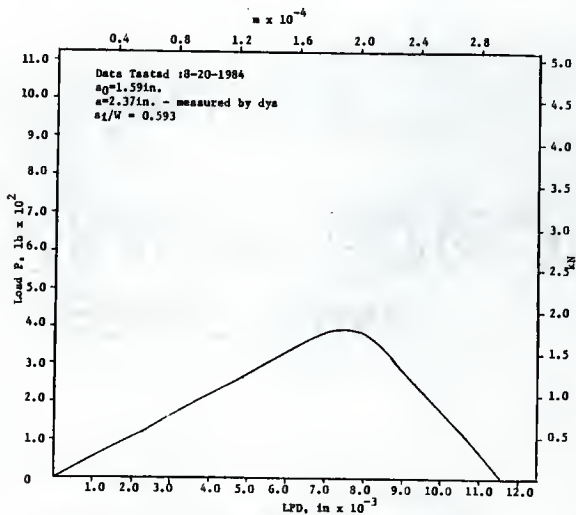


Fig. 214 P vs LFD, 4 in Deep Beam (C9), Load Control, Road (12)

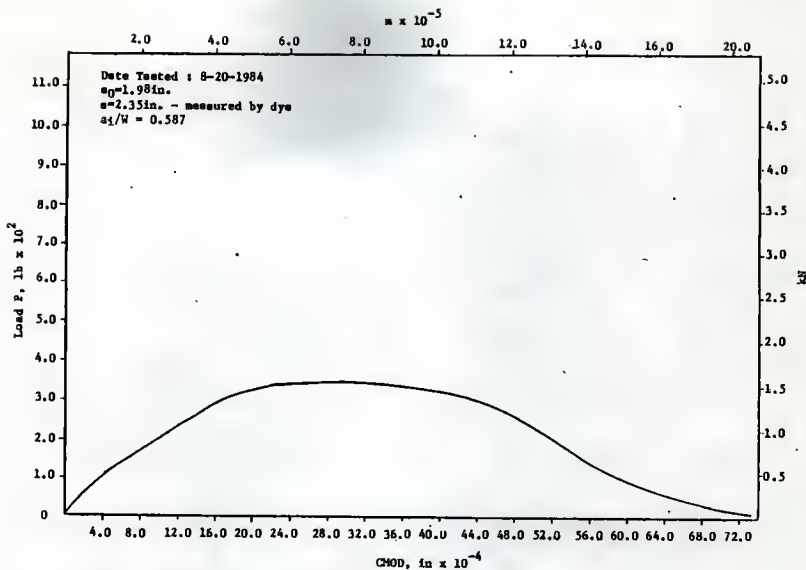


Fig. 215 P vs CMOD, 4 in Deep Beam (C10), Load Control, Rood (12)

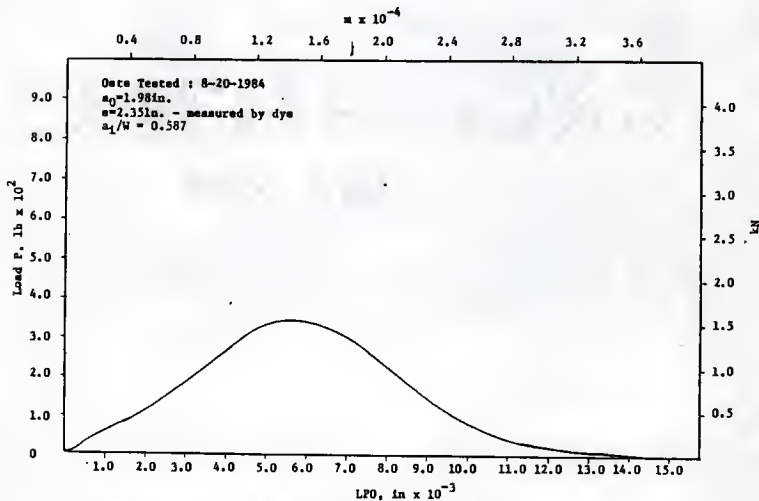


Fig. 216 P vs LFD, 4 in Deep Beam (C10), Load Control, Rood (12)

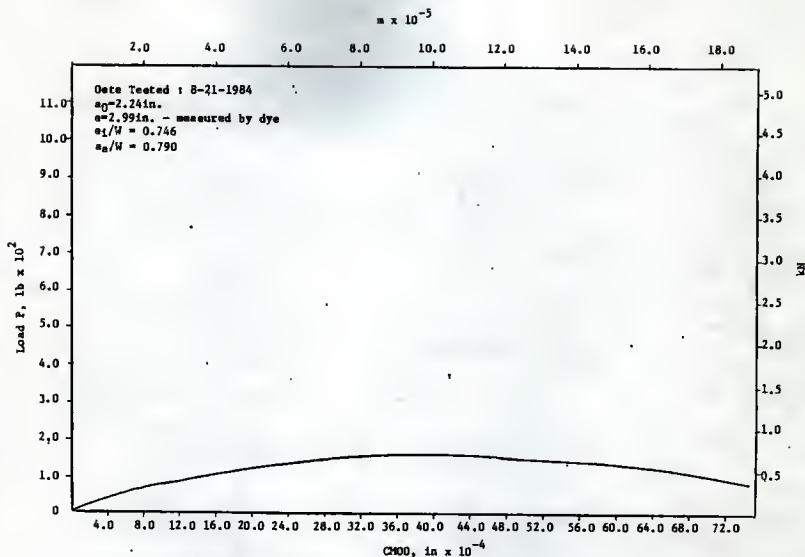


Fig. 217 P vs CMOD, 4 in Deep Beam (C11), Load Control, Rood (12)

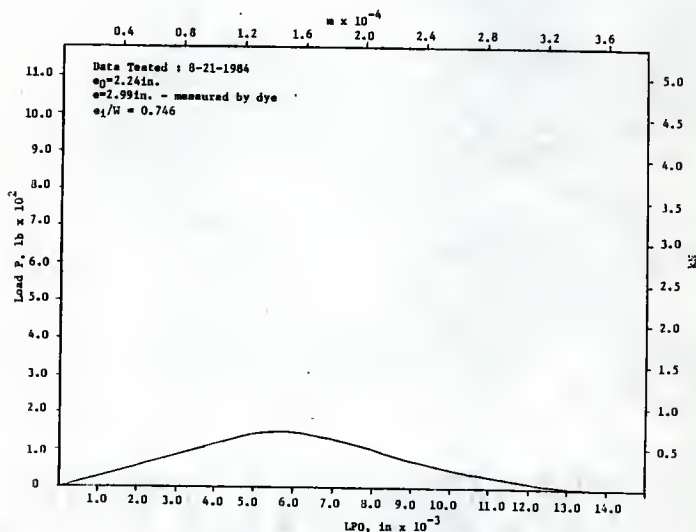


Fig. 218 P vs LPO, 4 in Deep Beam (C11), Load Control, Rood (12)

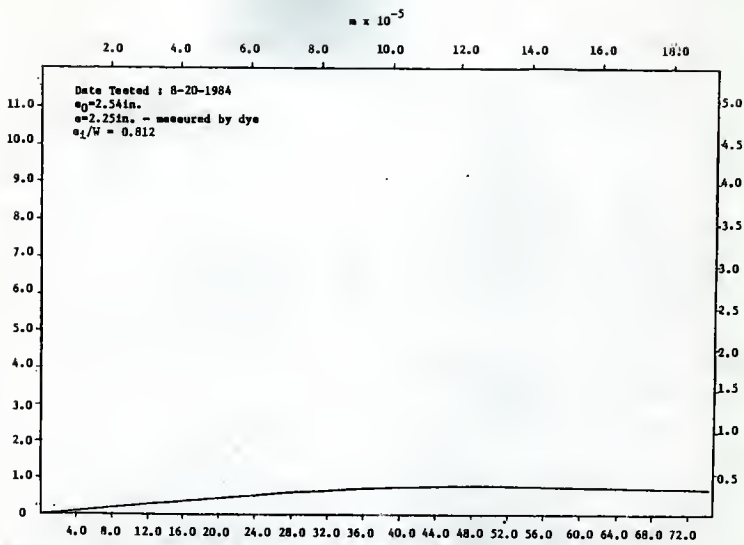


Fig. 219 P vs CM00, 4 in Deep Beam (C12), Load Control, Road (12)

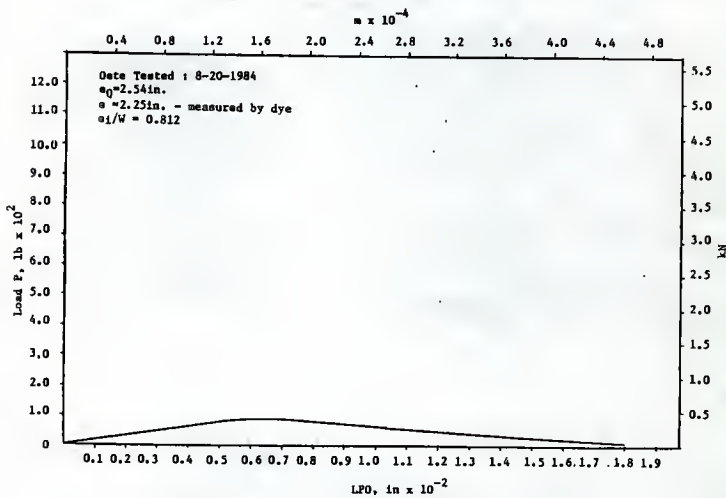


Fig. 220 P vs LPO, 4 in Deep Beam (C12), Load Control, Road (12)

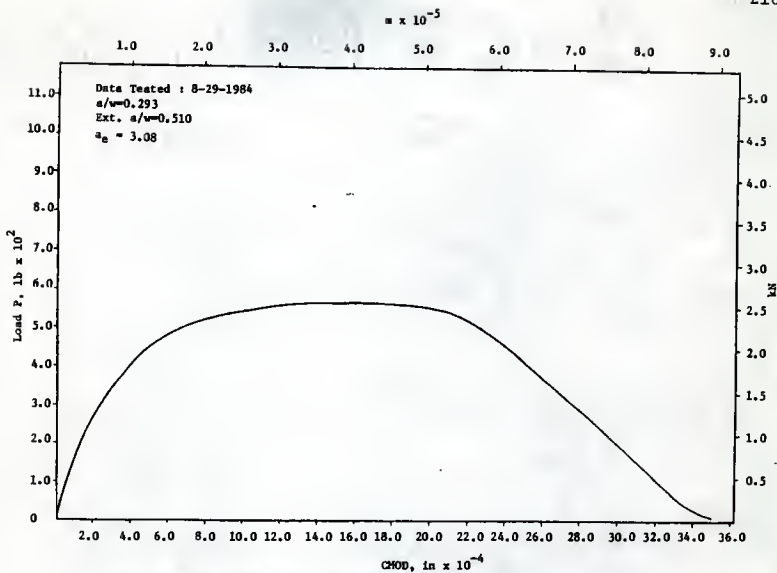


Fig. 221 P vs CHOD, 4 in Deep Beam (C15), Load Control, Rood (12)

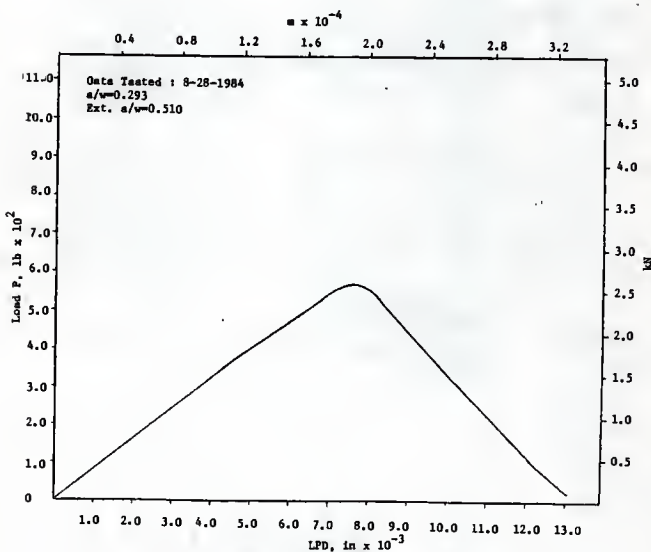


Fig. 222 P vs LFD, 4 in Deep Beam (C15), Load Control, Rood (12)

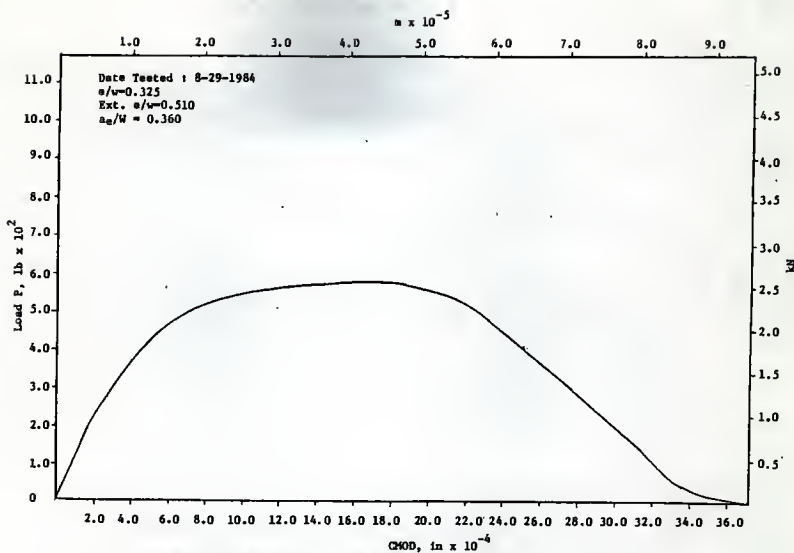


Fig. 223 P vs CHD0, 4 in Deep Beam (C16), Load Control, Rod (12)

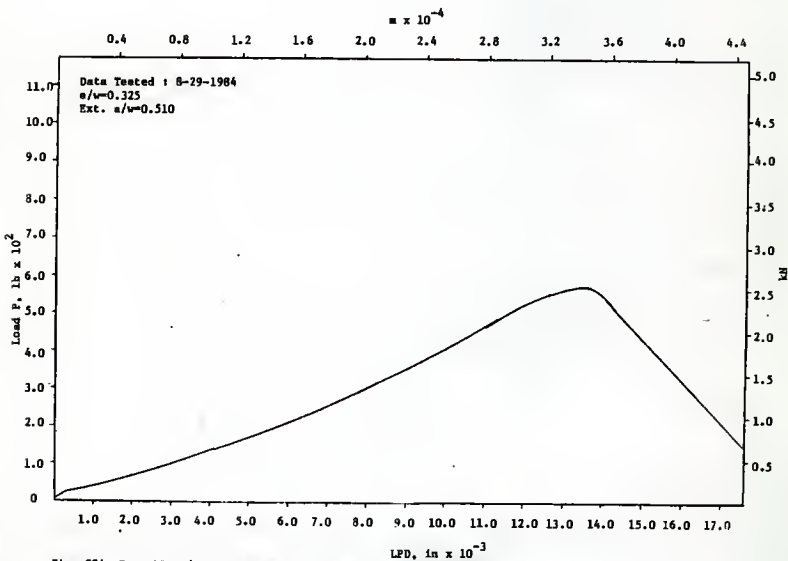


Fig. 224 P vs LPD, 4 in Deep Beam (C16), Load Control, Rod (12)

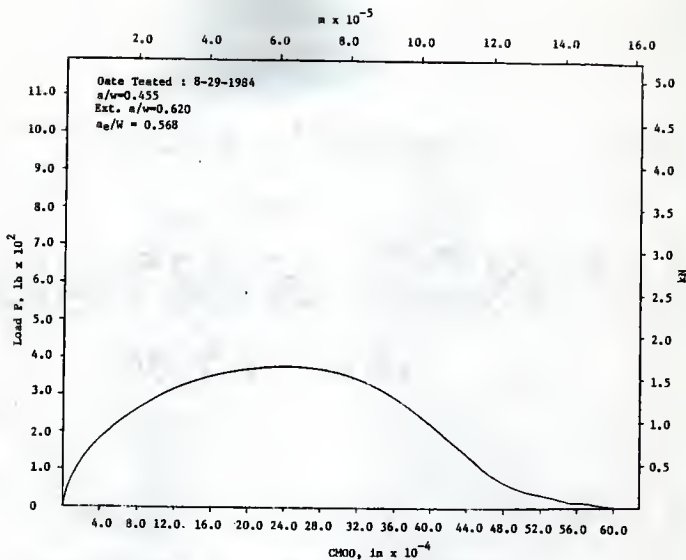


Fig. 225 P vs CH00, 4 in Deep Beam (C17), Load Control, Rood (12)

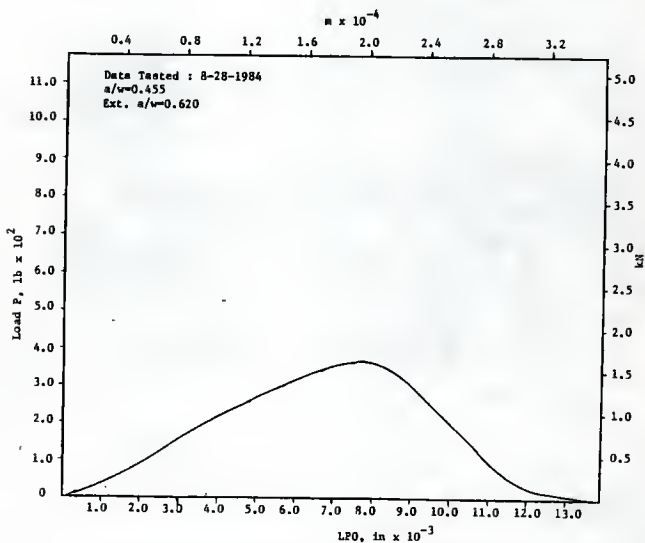


Fig. 226 P vs LPO, 4 in Deep Beam (C17), Load Control, Rood (12)

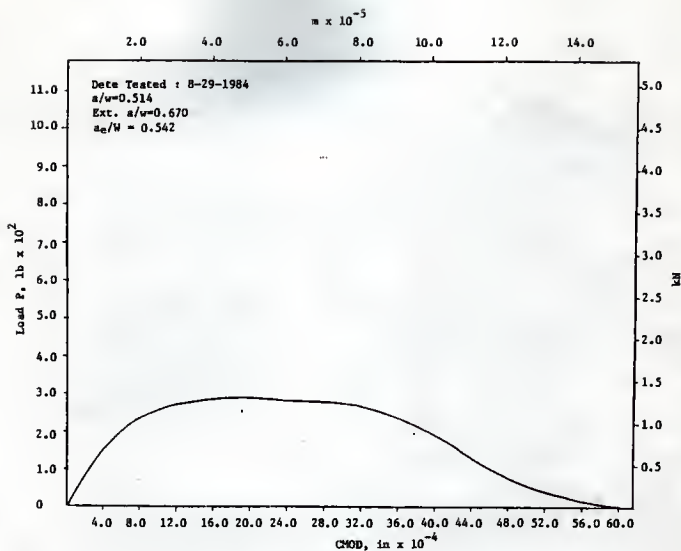


Fig. 227 P vs CMOD, 4 in Deep Beam (C18), Load Control, Rood (12)

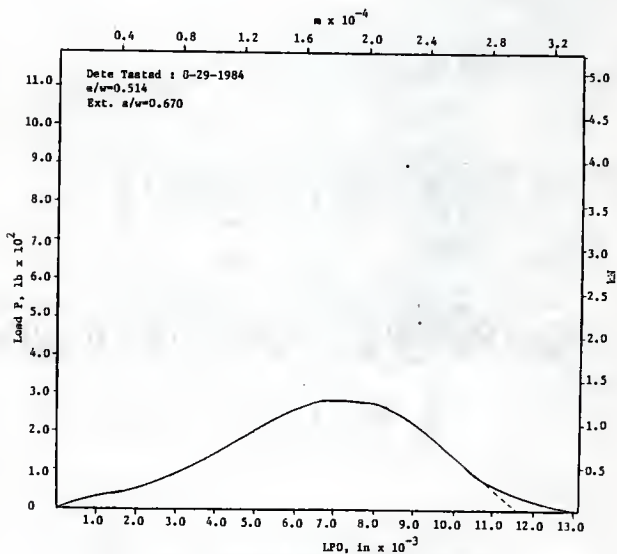
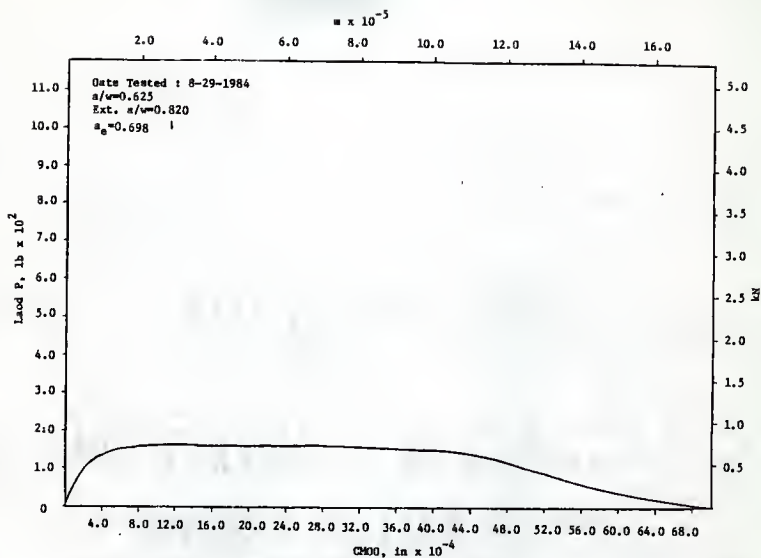
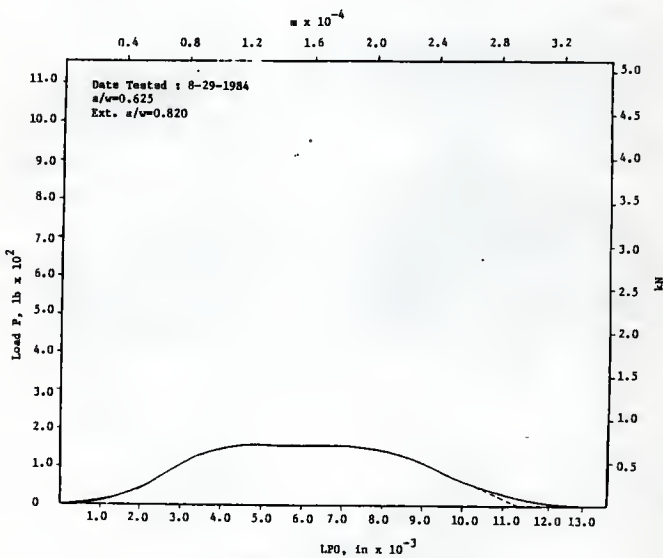


Fig. 228 P vs LPD, 4 in Deep Beam (C18), Load Control, Rood (12)

Fig. 229 P vs CHOD, 4 in Deep Beam (C19), Load Control, Rood (12)Fig. 230 P vs LPO, 4 in Deep Beam (C19), Load Control, Rood (12)

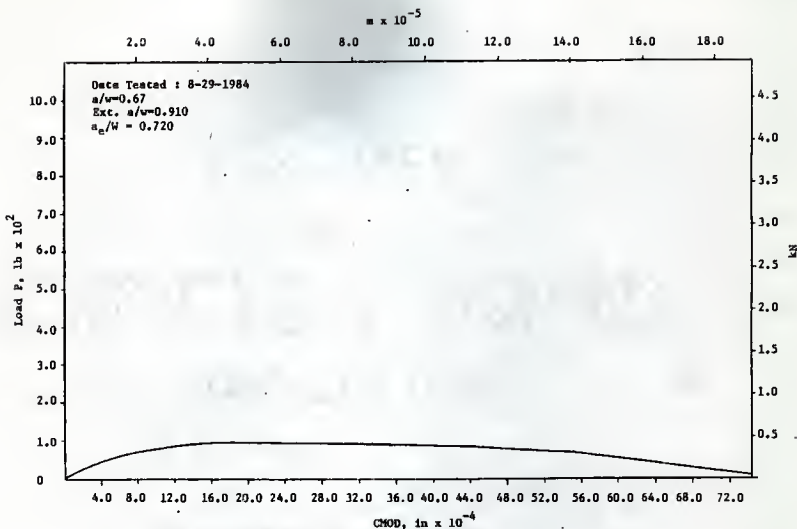


Fig. 231 P vs CH00, 4 in Deep Beam (C20), Load Control, Road (12)

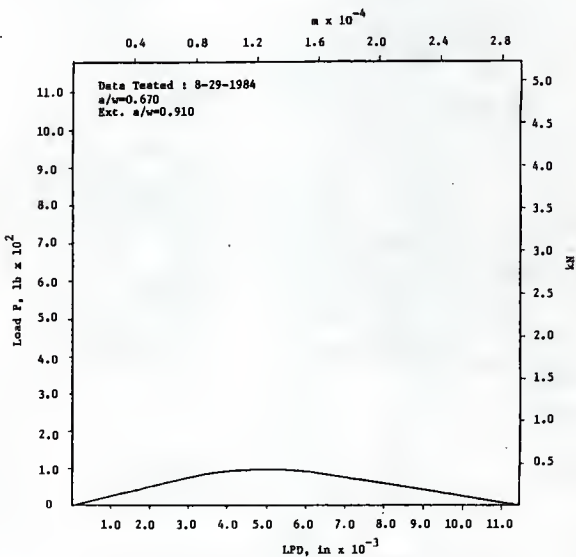
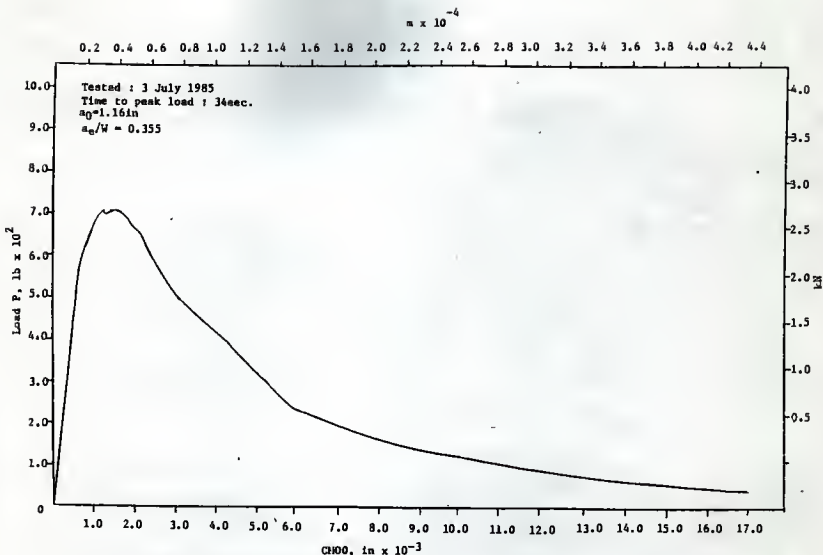
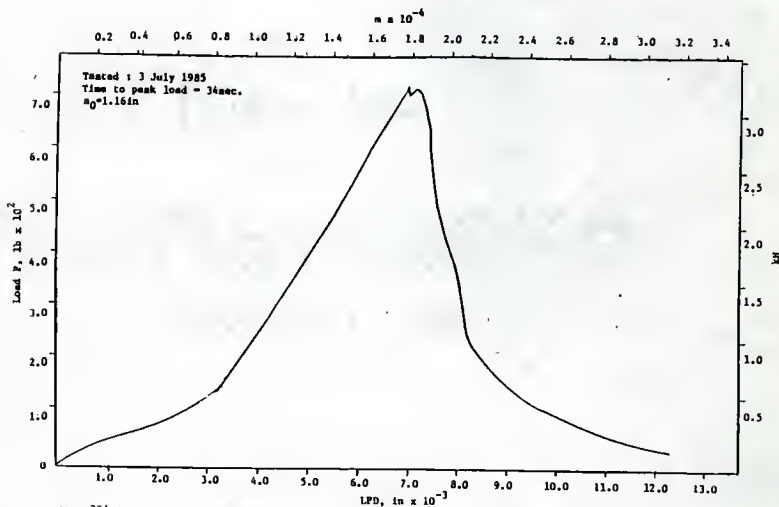


Fig. 232 P vs LPD, 4 in Deep Beam (C20), Load Control, Road (12)

Fig. 233 P vs CM00, 4 in Oesp Beam (LS.3), strain Control, Tested July 1985Fig. 234 P vs LPD, 4 in Deep Beam (LS.3), Strain Control, Tested July 1985

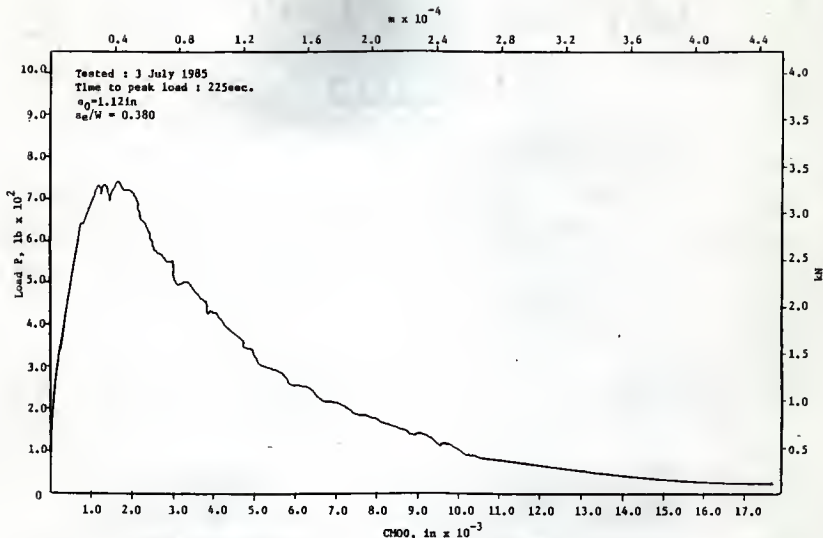


Fig. 235 P vs CHOO, 4 in Deep Beam (28.3), Strain Control, Tested July 1985

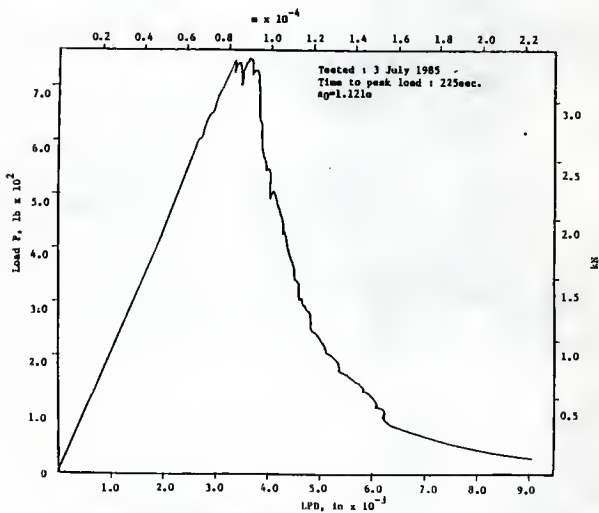


Fig. 236 P vs LPD, 4 in Deep Beam (28.3), Strain Control, Tested July 1985

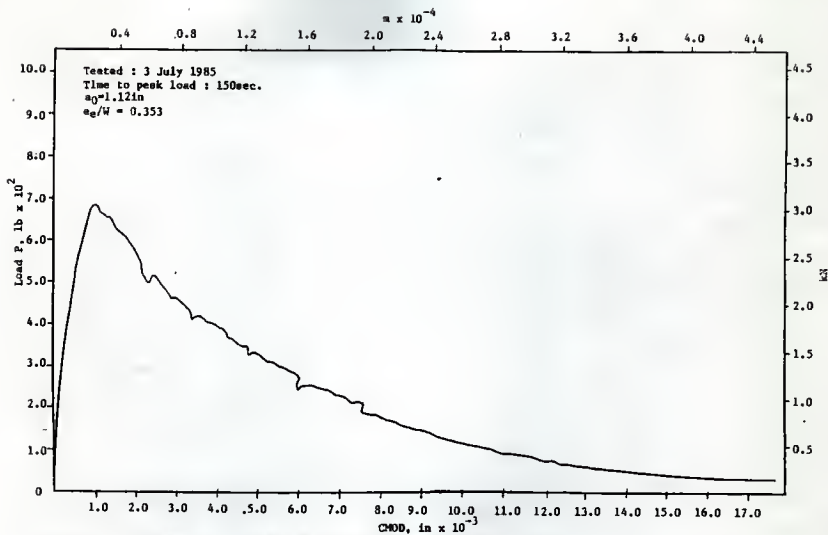


Fig. 237 P vs CMOD, 4 in Deep Seam (3S.3), Strain Control, Tested July 1985

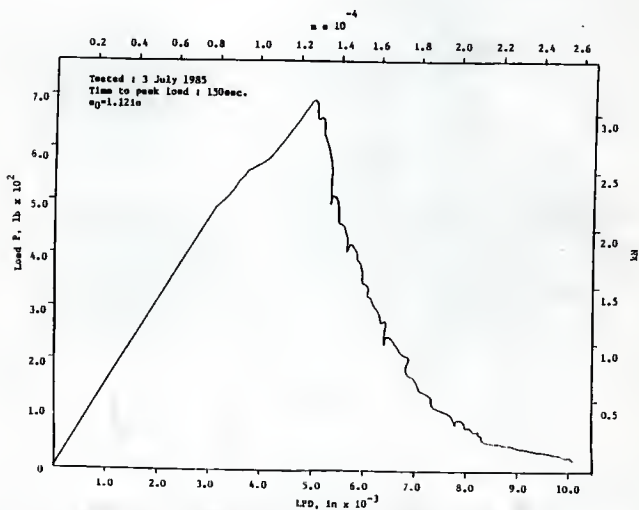


Fig. 238 P vs LFD, 4 in Deep Seam (3S.3), Strain Control, Tested July 1985

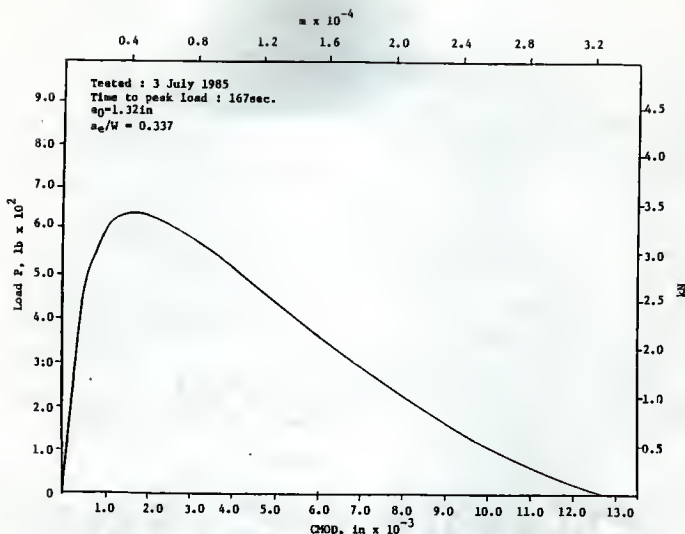


Fig. 239 P vs CHOD, 4 in Deep Beam (LL.3), Load Control, Tested July 1985

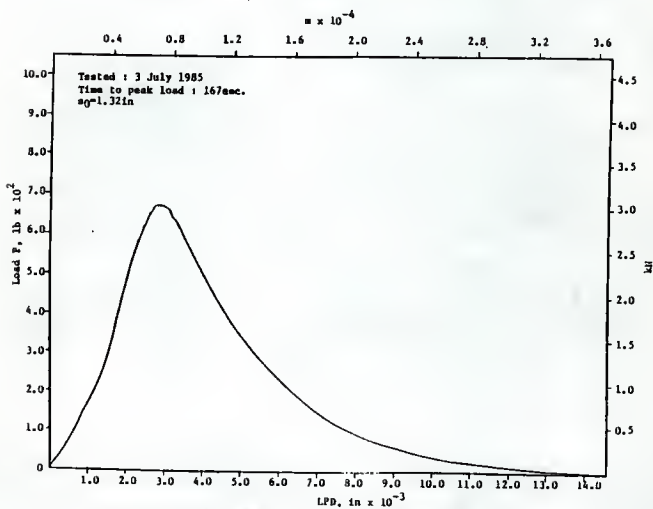


Fig. 240 P vs LPD, 4 in Deep Beam (LL.3), Load Control, Tested July 1985

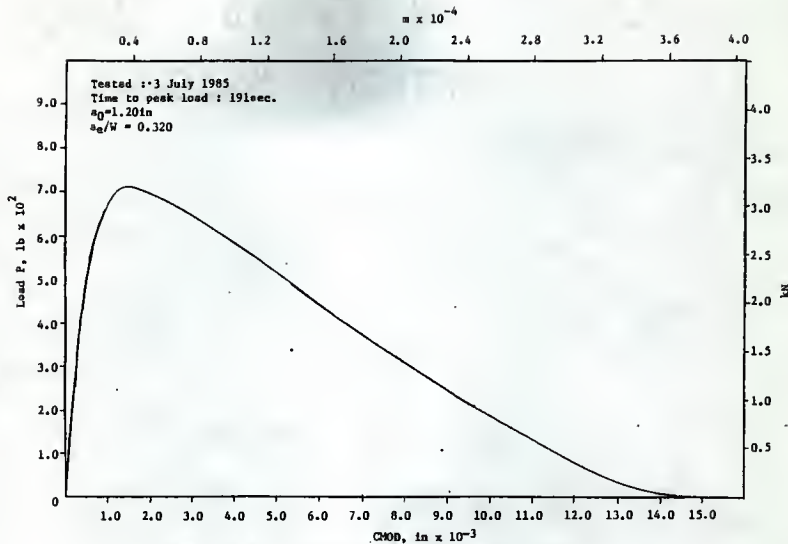


Fig. 241 P vs CMOD, 4 in Deep Beam (2L.3), Load Control, Tested July 1985

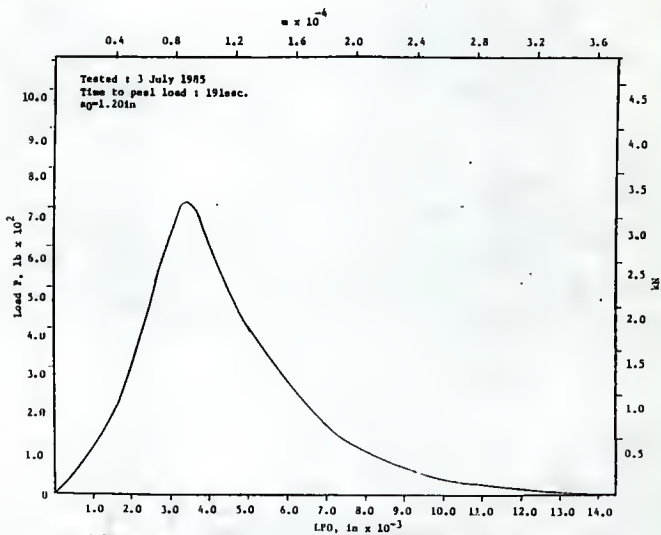


Fig. 242 P vs LFD, 4 in Deep Beam (2L.3), Load Control, Tested July 1985

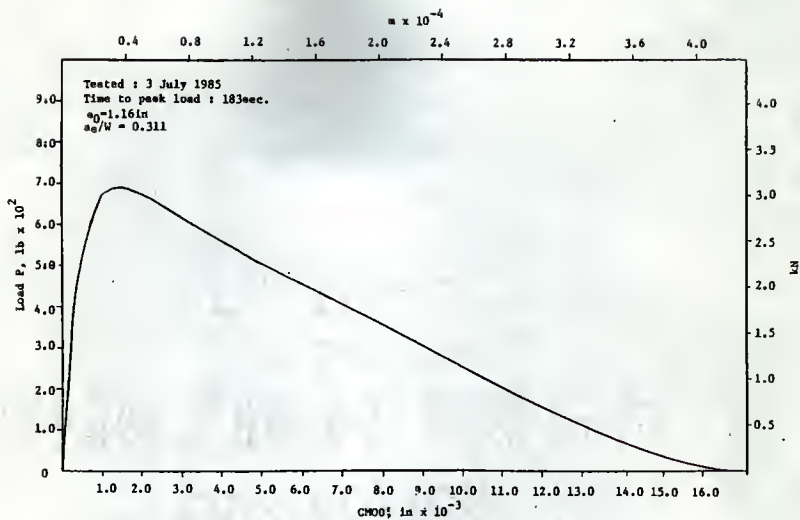


Fig. 243 P vs CMO0, 4 in Deep Beam (3L.3), Load Control, Tested July 1985

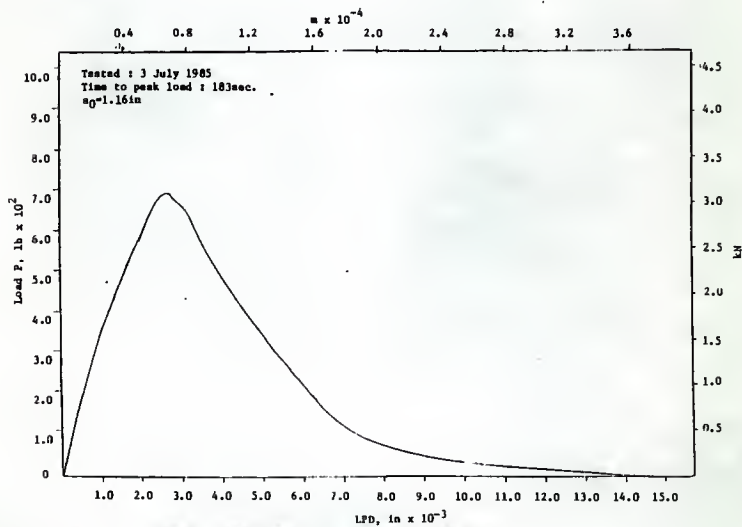


Fig. 244 p vs LFD, 4 in Deep Beam (3L.3), Load Control, Tested July 1985

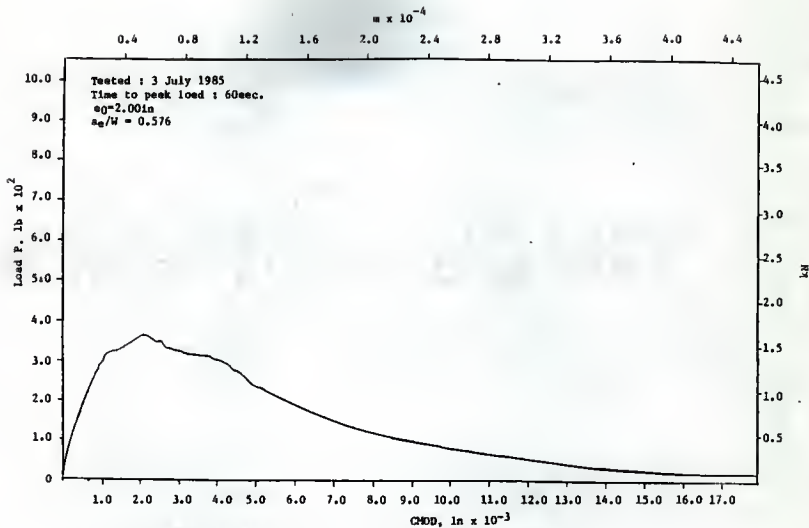


Fig. 245 P vs CHDD, 4 in Deep Beam (18.5), strain Control, Tested July 1985

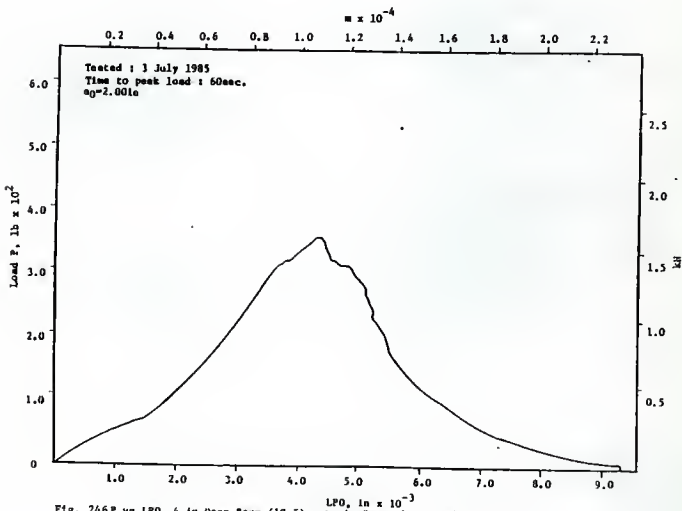
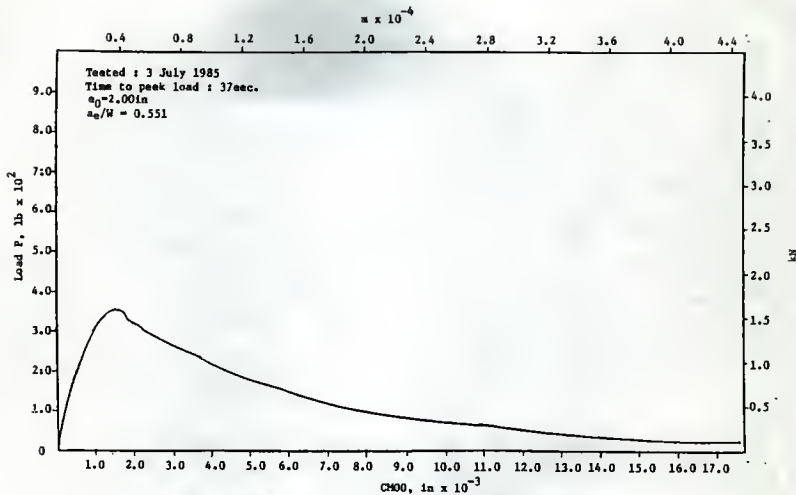
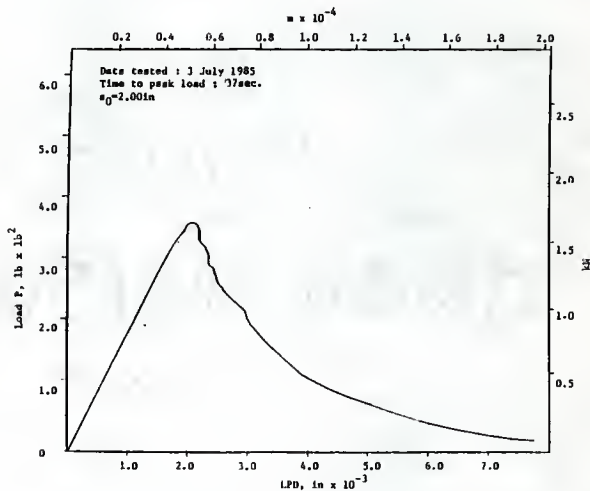


Fig. 246 P vs LPD, 4 in Deep Beam (18.5), strain Control, Tested July 1985

Fig. 247 P vs CH00, 4 in Deep Beam (2S.5), Strain Control, Tested July 1985Fig. 248 P vs LPD, 4 in Deep Beam (2S.5), Strain Control, Tested July 1985

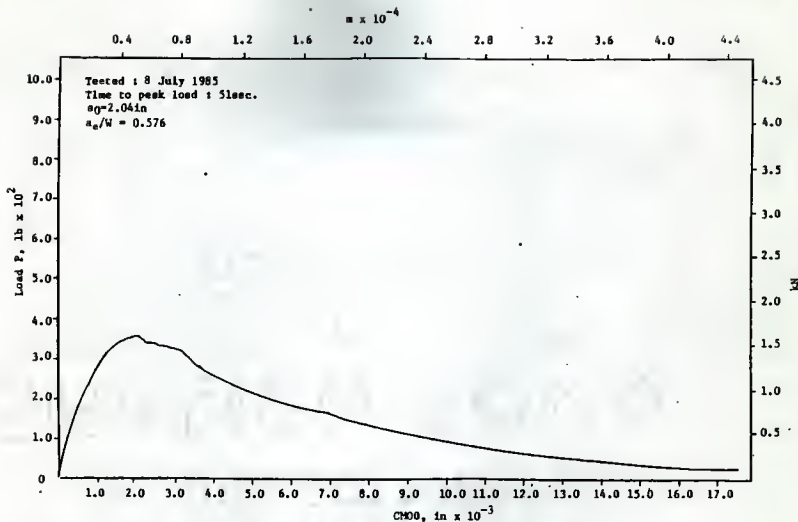


Fig. 249 P vs CHD0, 4 in Deep Beam (38.5), Strain Control, Tested July 1985

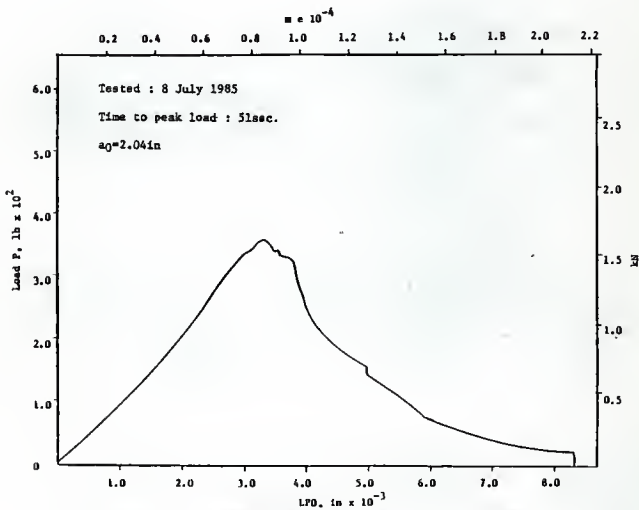


Fig. 250 P vs LFD0, 4 in Deep Beam (38.5), Strain Control, Tested July 1985

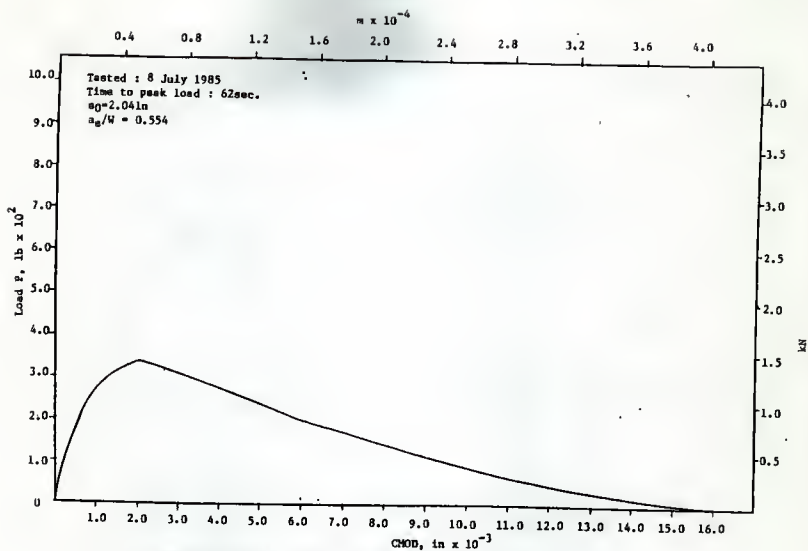


Fig. 251 P vs CHOD, 4 in Deep Beam (LL.5), Load Control, Tested July 1985

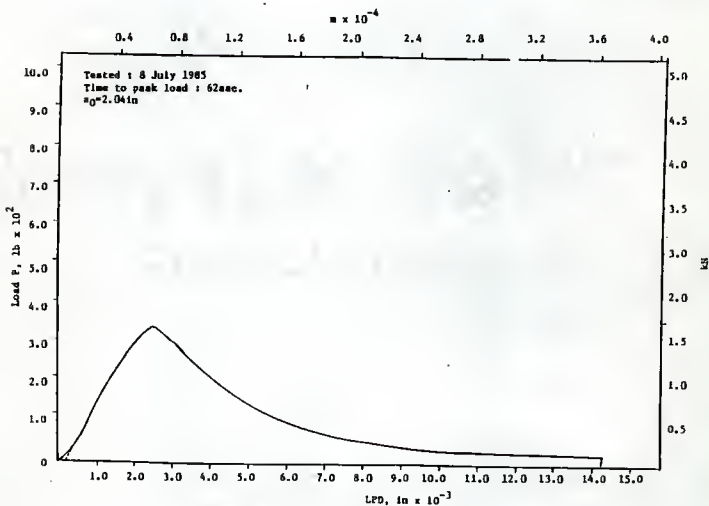


Fig. 252 P vs LFD, 4 in Deep Beam (LL.5), Load Control, Tested July 1985

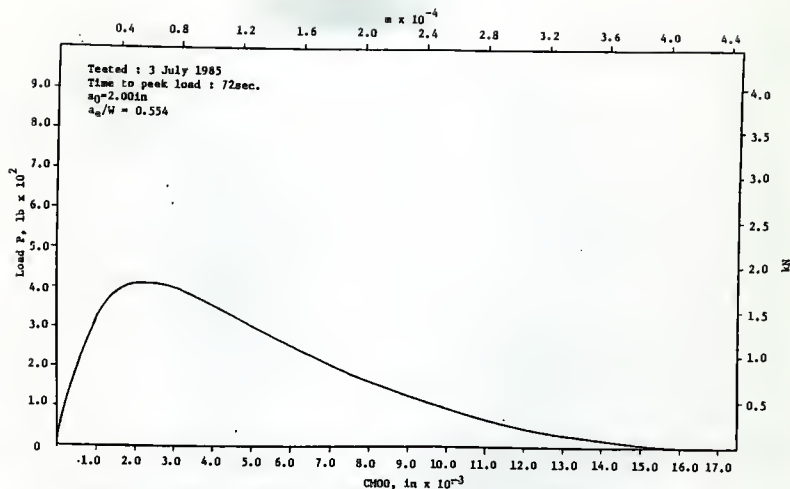


Fig. 253 P vs CH00, 4 in Deep Beam (2L.5), Load Control, Tested July 1985

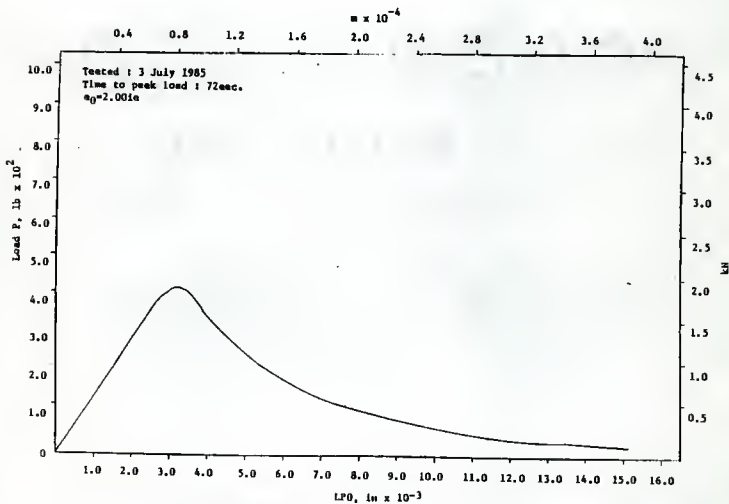
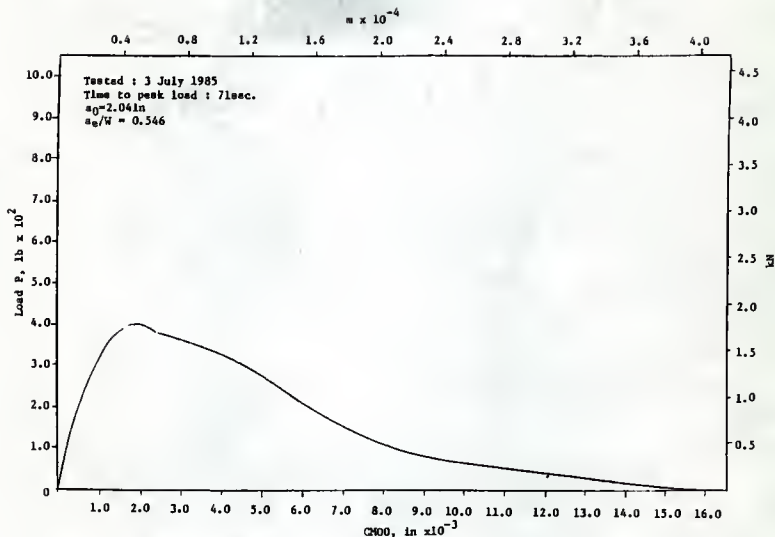
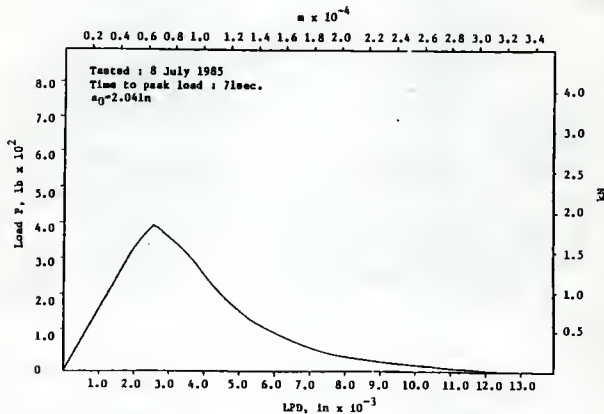


Fig. 254 P vs LP0, 4 in Deep Beam (2L.5), Load Control, Tested July 1985

Fig. 255 P vs CH00, 4 in Deep Beam (3L.5), Load Control, Tested July 1985Fig. 256 P vs LPD, 4 in Deep Beam (3L.5), Load Control, Tested July 1985

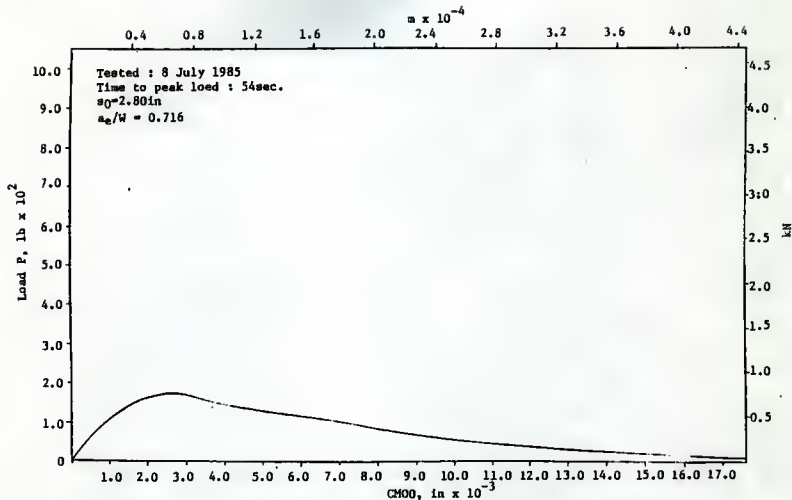


Fig. 257 P vs CM00, 4 in Deep Beam (18.7), Strain Control, Tested July 1985

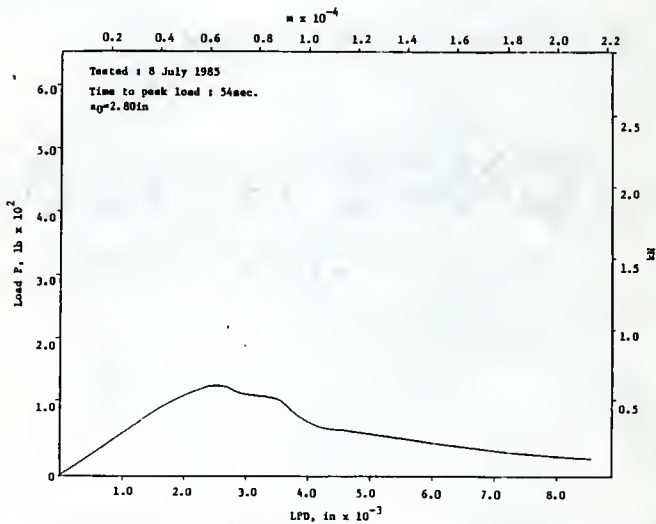
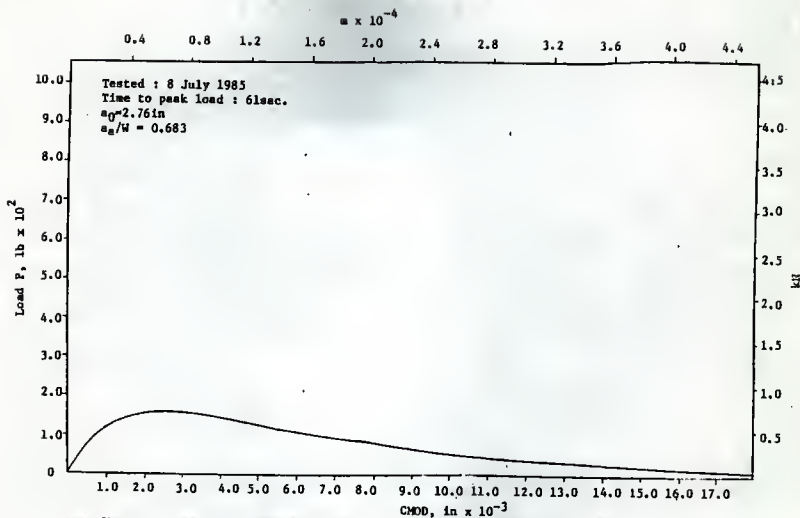
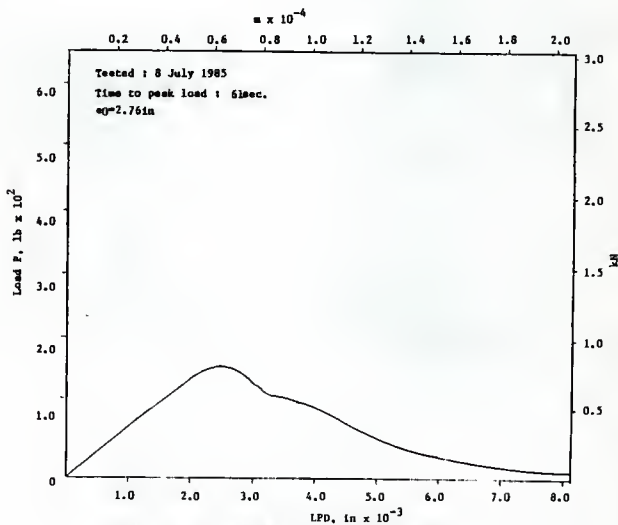


Fig. 258 P vs LPD, 4 in Deep Beam (18.7), Strain Control, Tested July 1985

Fig. 259 P vs CHOD, 4 in Deep Beam (3S.7), strain Control, Tested July 1985Fig. 260 P vs LPD, 4 in Deep Beam (3S.7), strain Control, Tested July 1985

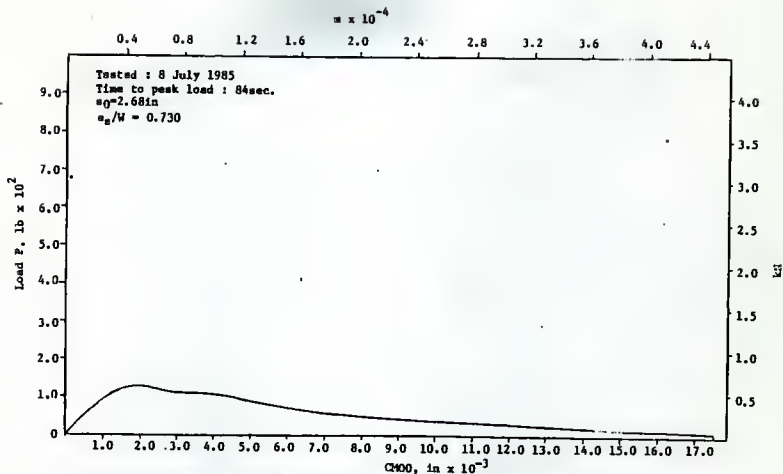


Fig. 261 P vs CHDO, 4 in Deep Beam (2L.7), Load Control, Tested July 1985

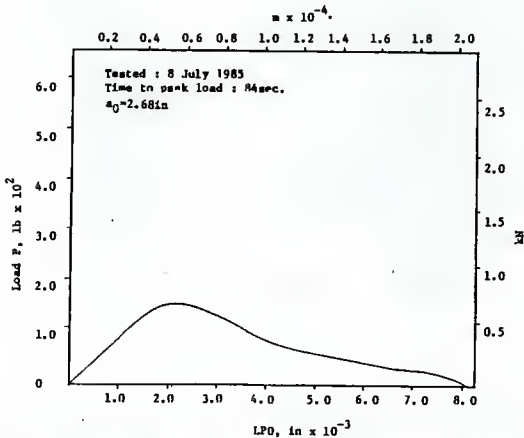


Fig. 262 P vs LPD, 4 in Deep Beam (2L.7), Load Control, Tested July 1985

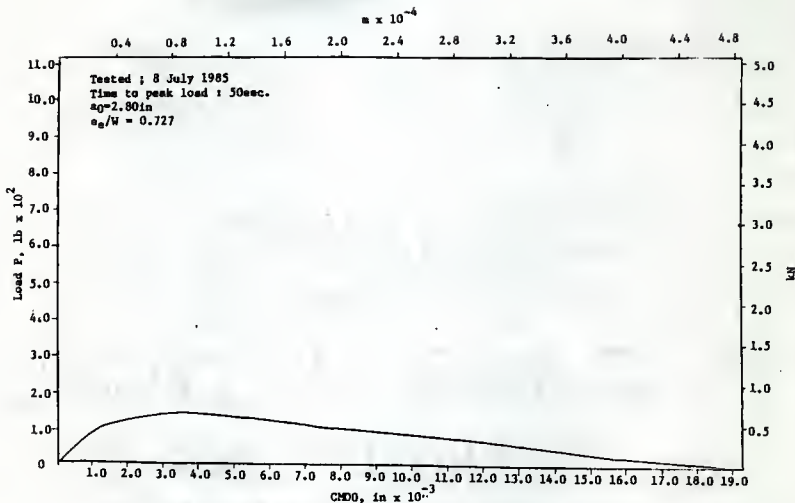


Fig. 263 P vs CHD0, 4 in Deep Beam (3L.7), Load Control, Tested July 1985

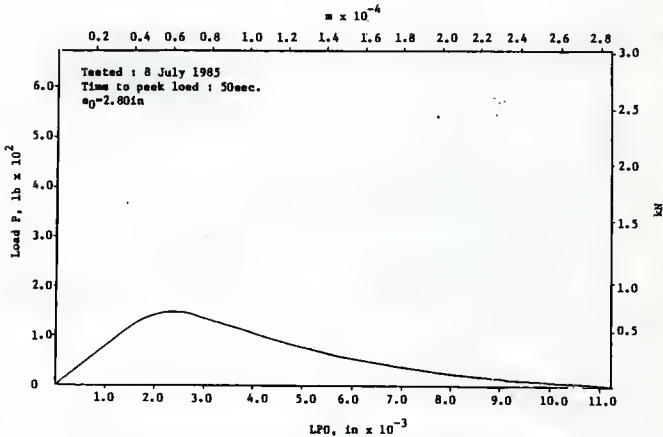


Fig. 264 P vs LPO, 4 in Deep Beam (3L.7), Load Control, Tested July 1985

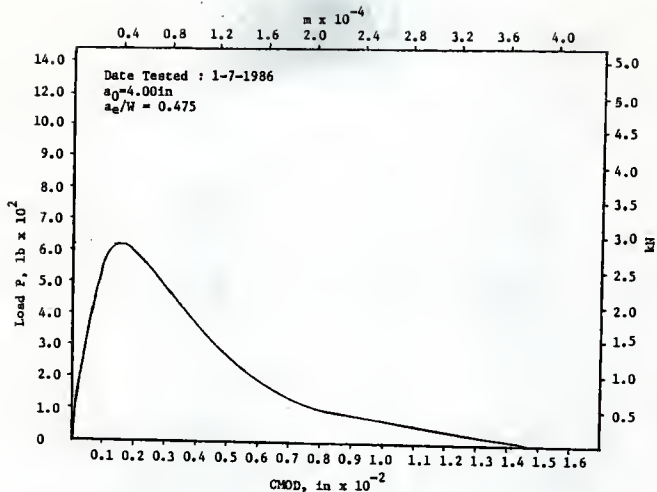


Fig. 265 P vs CMOD, 8 in Deep Beam (N-2-8), Load Control, Tested January 1986

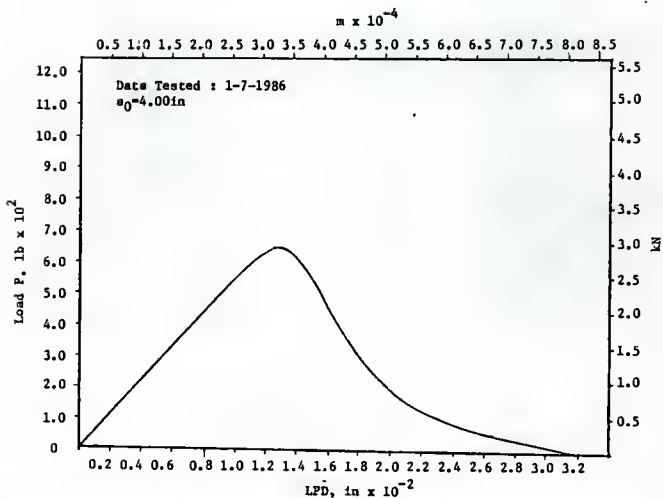


Fig. 266 P vs LPD, 8 in Deep Beam (N-2-8), Load Control, Tested January 1986

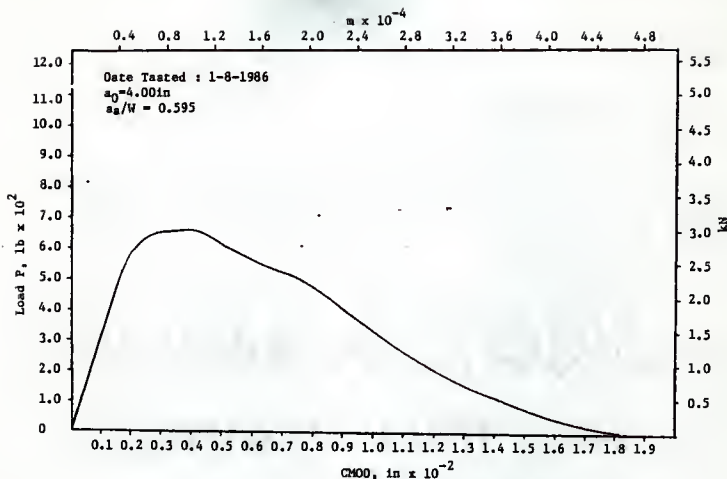


Fig. 267 P vs CMOD, 8 in Deep Beam (W-1-8), Load Control, Tested January 1986

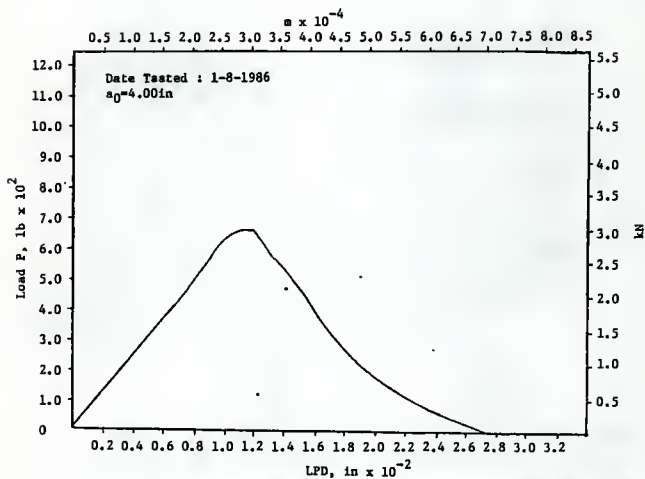


Fig. 268 P vs LPD, 8 in Deep Beam (W-1-8), Load Control, Tested January 1986

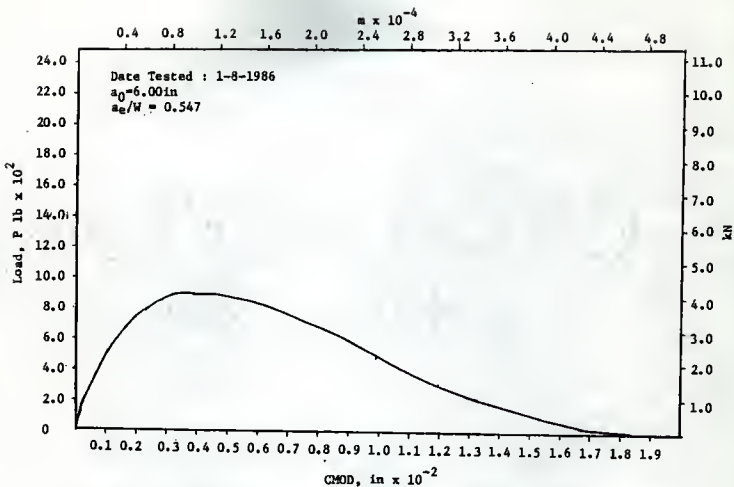


Fig. 269 P vs CMOD, 12 in Deep Beam (CB12), Load Control, Tested January 1986

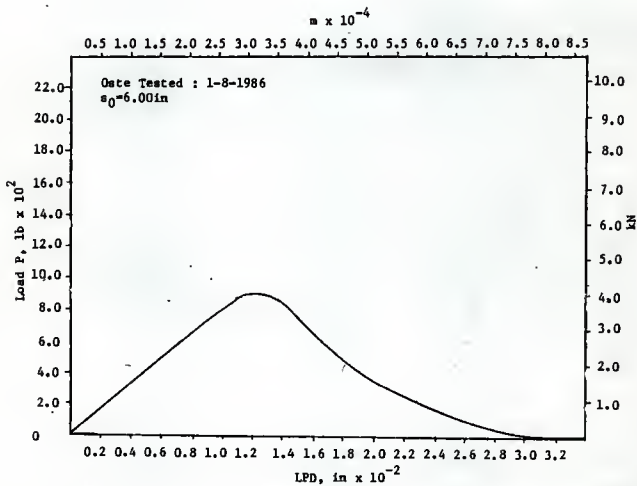


Fig. 270 P vs LPD, 12 in Deep Beam (CB12), Load Control, Tested January 1986

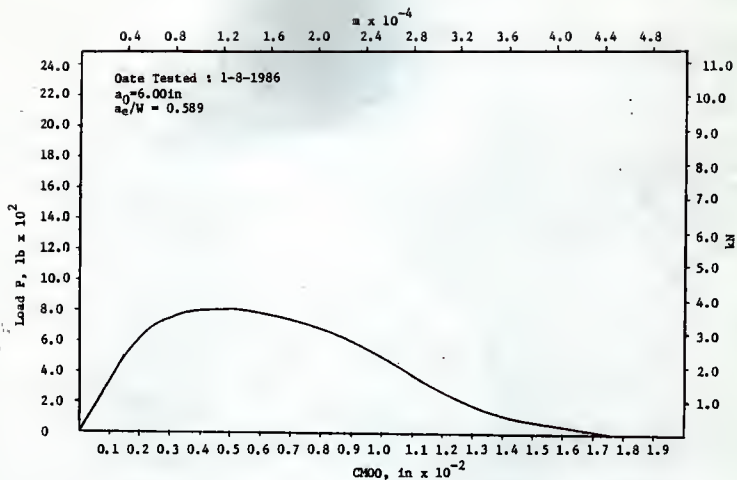


Fig. 271 P vs CHOD, 12 in Deep Beam (PW12), Load Control, Tested January 1986

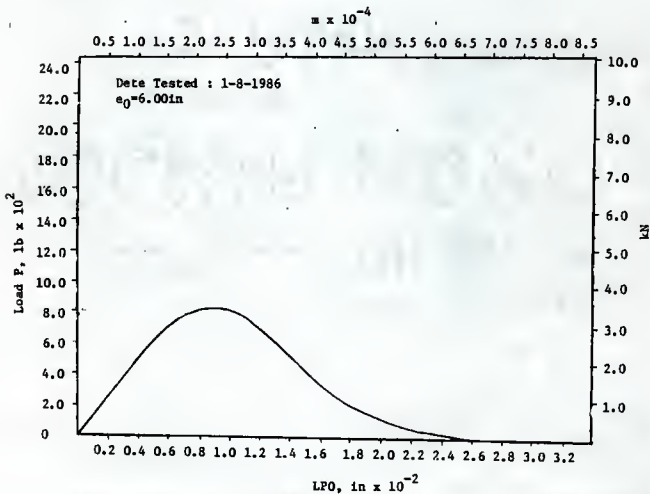


Fig. 272 P vs LPD, 12 in Deep Beam (PW12), Load Control, Tested January 1986

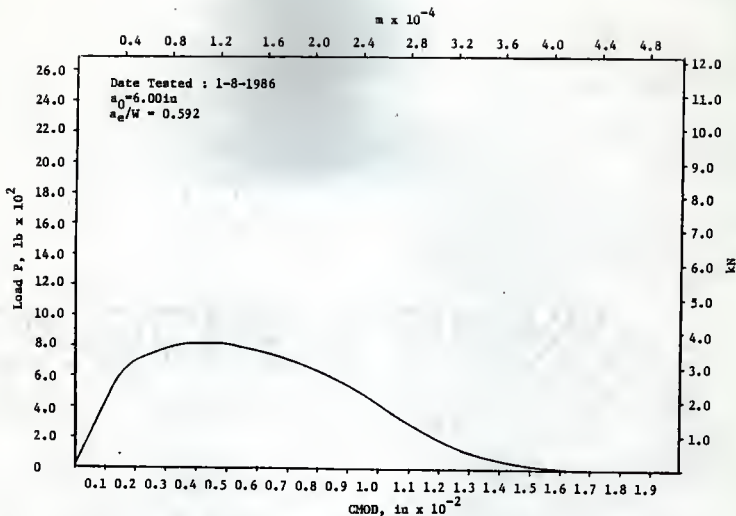


Fig. 273 P vs CMOD, 12 Deep Beam (W12), Load Control, Tested January 1986

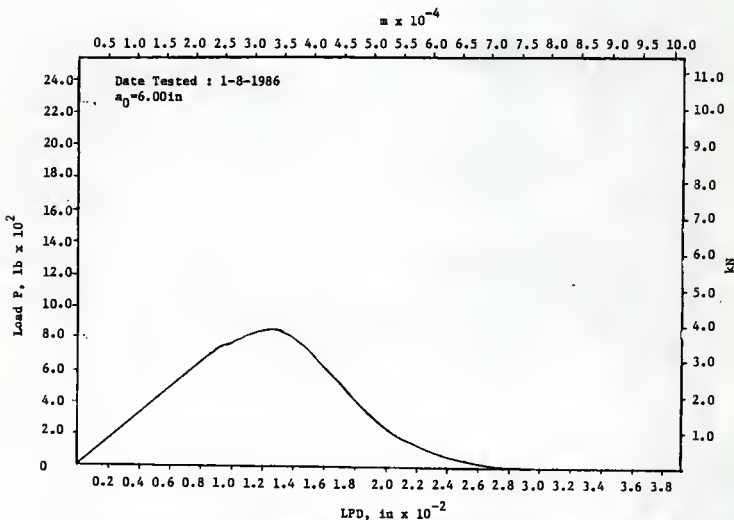


Fig. 274 P vs LPD, 12 in Deep Beam (W12), Load Control, Tested January 1986

EVALUATION OF PROPOSED METHODS TO DETERMINE
FRACTURE PARAMETERS FOR CONCRETE IN BENDING

by

Sze-Ting Yao

B.S., Kansas State University, 1984

AN ABSTRACT OF A MASTER'S THESIS

submitted in partial fulfillment of the
requirement for the degree of

MASTER OF SCIENCE

Department of Civil Engineering

Kansas State University

Manhattan, Kansas

1986

ABSTRACT

Many methods attempting to determine the fracture parameters K_{IC} , G_{IC} , G_F and J_{IC} of concrete using bending specimens have been proposed over the years. Results obtained by some of the earlier researchers indicated that concrete is a notch sensitive material, that is, it behaves differently when notched with teflon or sawcut, then it does when it is precracked. This study attempts to evaluate these proposed methods for the determination of fracture parameters for concrete in bending and also to provide recommendations.

The program presented here utilized the data obtained in the past seven years at Kansas State University. These beam sizes used include 3 in. (76 mm) wide, 4 in. (102 mm) deep with a 15 in. (381 mm) span, 4 in. (76 mm) wide, 8 in. (203 mm) deep with a 24 in. (610 mm) span, 3 in. (76 mm) wide, 8 in. (203 mm) deep with a 30 in. (762 mm) span and 3 in. (76 mm) wide, 12 in. (305 mm) with a 45 in. (1140 mm) span. Some of these beams were tested in three-point bending and others were tested in four-point bending. Beams used in this thesis were precracked beams and notched beams.

Results presented in include K_{IC} , G_{IC} , G_F and J_{IC} based on the methods that had been proposed. In addition, the results are calculated based on extended crack lengths and unextended crack lengths.